Ghent University
Faculty of Sciences
Department of Physiology

CHEMICAL GENETICS OF ETHYLENE SIGNALING AND CROSSTALK WITH OTHER SIGNALS IN *ARABIDOPSIS*

Yuming Hu
Promoter: Prof. dr. Dominique Van Der Straeten
Co-promoter: Prof. dr. Filip Vandenbussche
Laboratory of Functional Plant Biology

A thesis submitted in partial fulfillment of the requirements for the degree of
Doctor of Science, Biochemistry and Biotechnology
Ghent University
2016

If you have a garden and a library, you have everything you need.

-Marcus Tullius Cicero

Exam committee

Prof. dr. Geert De Jaeger (Chairman)
VIB Department of Plant Systems Biology
Ghent University

Dr. Dominique Audenaert (Secretary)
VIB Department of Plant Systems Biology
Ghent University

Prof. dr. Kris Audenaert
Department of Applied biosciences
Ghent University

Prof. dr. Bruno Cammue
Centre for Microbial & Plant Genetics
University of Leuven VIB Department of Plant Systems Biology

Prof. dr. Ann Cuypers
Centre for Environmental Sciences
Hasselt University

Prof. dr. Jan Petrášek
Laboratory of Hormonal Regulations in Plants
Institute of Experimental Botany AS CR, v. v. i., Czech Republic

Prof. dr. Dominique Van Der Straeten (Promoter)
Department of Physiology
Ghent University

Prof. dr. Filip Vandenbussche (Co-promoter)
Department of Physiology
Ghent University

Summary

The goal of this PhD project was to further understand the ethylene regulatory machinery and the crosstalk with other signals in *Arabidopsis* development using a chemical genetics approach.

In the first part, a general methodology of using a chemical genetics approach in ethylene biology research is presented in Chapter 1; and a general introduction of ethylene-auxin crosstalk in *Arabidopsis* seedling development is presented in Chapter 2. Chapter 3 describes a screen of 12,000 structurally diverse chemicals on *Arabidopsis* in the presence of the ethylene precursor 1-aminocyclopropane-1-carboxylic acid (ACC) to identify compounds altering the ACC-triggered triple response phenotype. 1313 (~11%) biologically active compounds which either enhanced or suppressed the phenotype in different tissues were picked up based on the primary screen. Information of all 12,000 chemicals and chemical-triggered phenotypes including negative hits were stored in the database (https://chaos.ugent.be/WE15/), and are freely accessible for the community. In the second part, characterization of the effect of a quinoline carboxamide compound exacerbating the triple response, named ACCERBATIN (AEX) is presented in detail in Chapter 4. Our studies suggest that AEX acts in parallel to ethylene signaling, affects auxin metabolism and transport as well as reactive oxygen species metabolism. Finally, a mutant screen based on EMS-mutagenesis, to search for potential target(s) of AEX was performed and its current results are presented in Chapter 5. The selected mutants will be characterized and the associated genes identified.

The investigation of such chemical compound and its analogs will be useful in plant hormone research and can offer potential use in agriculture. The conclusions from this study and perspectives are stated in Chapter 6.

Samenvatting

Het doel van dit doctoraatsonderzoek was om de regulatorische machinerie van het plantenhormoon ethyleen en de cross-talk met andere signalen in de ontwikkeling van Arabidopsis beter te begrijpen aan de hand van een chemisch-genetische benadering.
In het eerste deel wordt een algemene methodologie voor het gebruik van een chemisch-genetische aanpak voor ethyleen biologisch onderzoek voorgesteld in hoofdstuk 1, en een algemene inleiding over ethyleen-auxine interacties in de ontwikkeling van Arabidopsis zaailingen in hoofdstuk 2.
Hoofdstuk 3 beschrijft een screening van de respons van Arabidopsis zaailingen op 12.000 structureel diverse chemische verbindingen in aanwezigheid van de ethyleen precursor 1-aminocyclopropaan-1-carboxylzuur (ACC) om verbindingen te identificeren die het ACC-geïnduceerde triple respons fenotype wijzigen. 1313 (~11%) biologisch actieve verbindingen met een versterkt of onderdrukt fenotype in variërende weefsels werden opgepikt in de primaire screening. Van alle 12.000 moleculen, werden de chemische informatie en de chemisch geïnduceerde zaailingfenotypes, opgeslagen in de database (https://chaos.ugent.be/WE15/), inclusief de negatieve resultaten. Deze zijn vrij toegankelijk voor de wetenschappelijke gemeenschap.
In het tweede deel wordt de karakterisering van het effect van een chinoline-carboxamide verbinding die een overdrijving van de triple respons veroorzaakt, genaamd ACCERBATIN (AEX), gedetailleerd uiteengezet in Hoofdstuk 4. Onze studies suggereen dat AEX in parallel werkt met ethyleen signalering, auxine metabolisme en transport beïnvloedt, alsook het metabolisme van reactieve zuurstofspecies. Ten slotte is een screening voor mutanten op basis van EMS-mutagenese uitgevoerd om potentiële doelwitten van AEX te vinden. De huidige resultaten van dit onderzoek worden in hoofdstuk 5 weergegeven. De geselecteerde mutanten zullen worden gekarakteriseerd en de geassocieerde genen geïdentificeerd.
Het onderzoek naar een dergelijke chemische verbinding en haar analogen zal nuttig zijn in plantenhormoon onderzoek en heeft potentieel voor gebruik in de landbouw. De conclusies uit dit onderzoek en perspectieven zijn vermeld in hoofdstuk 6.

List of Abbreviations

1-MCP	1-Methylcyclopropene
1-NAA	1-naphthaleneacetic acid
1-NOA	1-naphthoxyacetic acid
2,4-D	2,4-dichloro-phenoxyacetic acid
2,5-NBD	2,5-norbornadiene
4-Cl-IAA	4-chloroindole-3-acetic acid
AA	amino acids
ABA	abscisic acid
ABC	ATP-BINDING CASSETTE
ABCB	ATP-BINDING CASSETTE B
ABP	AUXIN BINGING PROTEIN
ACC	1-aminocyclopropane-1-carboxylic acid
ACO	ACC oxidase
ACS	ACC synthase
AdoMet	S-adenosyl-methionine
AFB	AUXIN SIGNALING F-BOX PROTEIN
AIB	α-aminoisobutyric acid
AMT	ACC-N-malonyltransferase
AOA	aminooxyacetic acid
AOPP	L-2-aminooxy-3-phenylpropionic acid
APCI	atmospheric pressure chemical ionization
ARF	AUXIN RESPONSE FACTOR
ASA	ANTHRANILATE SYNTHASE α
ASB	ANTHRANILATE SYNTHASE β
Asp	aspartate
ATI	auxin transport inhibitor
auxinole	α-[2,4-dimethylphenylethyl-2-oxo]-IAA
AuxRE	Auxin Responsive-Element
AVG	Aminoethoxyvinylglycine
axr	*auxin resistant*
BBo	4-biphenylboronic acid
BC	backcrossed
BH-IAA	butoxycarbonylaminohexyl-IAA
BIN	BRASSINOSTEROID-INSENSITIVE
BRP	brassinopride
BRZ	brassinazole
BUM	2-[4-(diethylamino)-2-hydroxybenzoyl]benzoic acid
BY	Bright Yellow
bzr1-1D	*brassinazole-resistant 1-1D*
CDF	Compound Document Format
CEND	C terminus
CFM	methyl-2-chloro-9-hydroxyfluorene-9-carboxylate

CMT	cortical microtubules
CPD	2-carboxyphenyl-3-phenylpropane-1,2-dione
CTR	CONSTITUTIVE TRIPLE RESPONSE
CUL	Cullin
CYCB	CYCLIN-DEPENDENT PROTEIN KINASE B
DAB	diamino benzidine
dgt	*diageotropica*
DIC	Differential interference contrast
dicamba	2-methoxy-3,6-dichlorobenzoic acid
DII	domain II
DMSO	dimethyl sulfoxide
DZ	differentiation zone
EBF	EIN BINDING F-BOX PROTEINS
EBS	EIN3 BINDING SITE
ECH	ECHIDNA
EDFs	ETHYLENE RESPONSE DNA BINDING FACTORs
eer	*enhanced ethylene response*
EFE	ETHYLENE-FORMING ENZYME
EIL	EIN-Like
EIN	Ethylene Insensitive
EMS	Ethymethane sulphonate
EOL	ETO1-like proteins
ER	endoplasmic reticulum
ERF	ethylene response factor
ERS	Ethylene Response Sensor
ethephon	(2-chloroethyl)-phosphonic acid
eto	*ethylene overproducer*
ETP	EIN Targeting Proteins
ETR	Ethylene Resistant
EZ	elongation zone
FDR	false discovery rate
fer	*feronia*
FT-ICR-MS	Fourier transform-ion cyclotron resonance-mass spectrometer
GACC	γ-glutamyl-ACC
GFP	green fluorescent protein
GGT	ɣ-glutamyl-transpeptidase
GH3	Gretchen Hagen 3
Glu	glutamate
GSK	Glycogen synthase kinase
GUS	beta-glucuronidase
His	histidine
HLS	HOOKLESS
HOOKLESS	HLS
HY	LONG HYPOCOTYL

IAA	Indole-3-acetic acid
IAM	indole-3-acetamide
IAN	indole-3-acetonitrile
IAOx	indole-3-acetaldoxime
IBA	indole-3-butyric acid
IPA	indole-3-pyruvic acid
JA-ACC	jasmonyl-ACC
JAR	jasmonic acid resistance
KMBA	2-oxo-4-methylthiobutyric acid
Kyn	L-Kynurenine
LAX	LIKE-AUXs
LC-MS	Liquid chromatography-mass spectrometry
LRX	LEUCINE-RICH REPEAT/EXTENSIN
LUC	Luciferase gene
MACC	1-malonyl-ACC
MAPK	Mitogen-Activated Protein Kinase
MCPA	2-methyl-4-chlorophenoxyacetic acid
MDR	MULTIDRUG RESISTANCE
Met	methionine
MRL	maximum residue limits
MS	mass spectrometry
MTA	5’-methylthioadenosine
MW	molecular weight
MZ	meristematic zone
NBD	7-nitro-2,1,3-benzoxadiazole
NBT	nitroblue tetrazolium
NMR	Nuclear magnetic resonance
NPA	N-1-naphthylphthalamic acid
oxIAA	2-Oxindole-3-Acetic Acid
oxIAA-GE=oxIAA-Glc	1-O(2-oxoindol-3-ylacetyl)-beta-d-glucopyranose=oxIAA-Glucose
PAA	phenylacetic acid
PAT	polar auxin transport
P-body	processing body
pgm	*phosphoglucomutase*
PGP	P-GLYCOPROTEIN
picloram	4-amino-3,5,6-trichloropicolinic acid
PID	PINOID
PID-oex	overexpression line of PID
PIF	PHYTOCROME INTERACTING FACTORS
PIN	PIN-FORMED
PLP	pyridoxal 5'-phosphate
PLS	POLARIS
PM	plasma membrane

PPBo	4-phenoxyphenylboronic acid
PRP	PROLINE RICH PROTEIN
PYR	PYRABACTIN RESISTANCE
QC	quiescent center
qPCR	quantitative polymerase chain reaction
quinclorac	3,7-dichloroquinoline-8-carboxylic acid
quinmerac	7-chloro-3-methylquinoline-8-carboxylic acid
RCN	*ROOTS CURL IN NAPHTHYLPHTHALAMIC ACID*
rhd	*ROOT HAIR DEFECTIVE*
RMA	Robust Multichip Average
ROS	Reactive Oxygen Species
RP-UHPLC	reversed phase ultrahigh performance liquid chromatography
RTE	Reversion To Ethylene Sensitivity
SAM	shoot apical meristem
SAR	structure-activity relationships
SAUR	Small auxin-up RNA
SCF	SKP1-Cullin1-F-box
scr	*scarecrow*
sgr	*shoot gravitropism*
shr	*short root*
SHY	SHORT HYPOCOTYL
SLR	single-lens reflex
SKP2A	S-Phase Kinase-Associated Protein 2A
statoliths	starch granules
SUR	SUPERROOT
TAA	Trp Aminotransferase of *Arabidopsis*
TAM	tryptamine
TAR	TAA RELATED
TCO	trans-cyclooctene
TGN	trans-Golgi network
TIR	transport inhibitor response
Trp	Tryptophan
TWD	TWISTED DWARF
TZ	transition zone
WT	wild type
X-gluc	5-bromo-4-chloro-3-indolyl-glucuronide
Y3H	yeast-three-hybrid
yucasin	5–(4–chlorophenyl)-4H-1,2,4–triazole-3–thiol

Table of Contents

Chapter 1

Chemical Genetics as a tool to study ethylene biology in plants

Adapted from:

Hu Y, Vandenbussche F, Van Der Straeten D (2014) Chemical genetics as a tool to study ethylene biology in plants. Plant Chemical Biology**:** 184-201

Contribution:

YH, FV and DVDS **wrote the manuscript.**

Introduction

Ethylene (C_2H_4) is the only gaseous plant hormone with profound effects throughout plant growth and development. It affects seed germination, vegetative development, leaf and flower senescence, fruit ripening, stress and pathogen responses (De Vleesschauwer et al., 2014; Kazan, 2015; Klee and Giovannoni, 2011; Koyama, 2014; Linkies and Leubner-Metzger, 2012; Tripathi and Tuteja, 2007; Van de Poel et al., 2015). Morphological changes in dark-grown seedlings in the presence of ethylene or its metabolic precursor 1-aminocyclopropane-1-carboxylic acid (ACC), the so called "triple response", has been used to identify mutants defective in ethylene biosynthesis or response. In *Arabidopsis thaliana*, the triple response phenotype consists of a short hypocotyl and root, a radially swollen hypocotyl, and an exaggerated apical hook (Guzman and Ecker, 1990). Studies of ethylene mutants by conventional genetic and molecular approaches resulted in the cloning and characterization of genes in the ethylene pathway and have led to the elucidation of many aspects related to the regulation of ethylene synthesis and signal transduction. To further understand the role of ethylene in plant function, chemical genetics is emerging to support the discovery of novel bioactive molecules interfering with the ethylene response (He et al., 2011; Lin et al., 2010). The high throughput screening of small molecules as agonists or antagonists of hormones, represents a new approach at the interface of chemistry and biology (Blackwell and Zhao, 2003). In contrast to classical genetics, where mutations are introduced at the DNA or RNA level to disturb a biological process, chemical genetics is a ligand-based methodology to study gene or protein function, which uses low-molecular-mass organic compounds to modify or disrupt the function of specific proteins (Dobson, 2004; Lipinski and Hopkins, 2004; Stockwell, 2000). One of the major advantages over traditional genetic approaches is the possibility to overcome loss-of-function lethality (since the ligands only have an effect upon chemical treatment) and gene redundancy (since ligands may act as general antagonists inhibiting all isoforms of a protein, or as specific agonists activating a particular isoform). A second important advantage is that the chemical genetics approach allows reversible and conditional control of a phenotype by addition and subsequent removal of a compound, which enables a kinetic analysis of the *in vivo* consequences of protein function changes in a dose dependent manner. Last but not least, well-characterized bioactive chemicals and their targets identified in Arabidopsis can be used in non-model species to improve agronomic traits and increase crop value (Raikhel and Pirrung, 2005). Hence, chemical genetics allows the dissection of biological mechanisms and gene networks, in a way complementary to a classical, mutation-based approach.

Here, we describe approaches to screen libraries for bioactive chemicals that directly or indirectly affect ethylene-related processes in Arabidopsis. Considerations related to the characterization of these compounds and identification of their targets will be discussed. We also provide an overview of agonists and antagonists of ethylene biosynthesis, perception and signaling that have been identified previously, and are used to control ethylene effects in plants. Finally, we highlight the current issues and future perspectives of a chemical genetics approach to further elucidate the ethylene pathway and its crosstalk with other hormones.

Small molecules in ethylene biosynthesis and signaling

For a recent review of the ethylene pathway, we refer to (Vandenbussche et al., 2012; Yang et al., 2015; Zheng and Zhu, 2016).

Ethylene biosynthesis in plant tissues is initiated from methionine, which is converted to S-adenosyl-L-methionine (AdoMet) by AdoMet synthetase (Figure 1.1). Subsequently, the methionyl side chain of AdoMet undergoes cyclization to form ACC by ACC synthase (ACS), which is the major rate-limiting step in the pathway. The byproduct 5'-methylthioadenosine is recycled to methionine in the Yang cycle, feeding another round of ethylene synthesis (Yang and Hoffman, 1984). As the direct precursor of ethylene, ACC is further oxidized to ethylene by ACC oxidase (ACO), a reaction which is not proceeding under anaerobic conditions, resulting in ACC accumulation. It was hypothesized that ACC might act as a signal independently of ethylene receptors or the canonical pathway downstream thereof (Tsuchisaka et al., 2009; Xu et al., 2008b); a hypothesis which needs further investigation. *ACS* and *ACO* are encoded by multigene families that are differentially regulated (Johnson and Ecker, 1998). ACS belongs to pyridoxal 5'-phosphate (PLP)-dependent aminotransferases (Mehta et al., 1993), encoding eight functional genes (*ACS2, ACS4-9, ACS11*) and one nonfunctional gene (*ACS1*) in *Arabidopsis* (Rodriguespousada et al., 1993; Tsuchisaka and Theologis, 2004) (*ACS1/2* in Rodriguespousada et al., 1993 are called *ACS2/4* in Tsuchisaka and Theologis, 2004). *Ethylene overproducer mutants*, *eto1, eto2, eto3*, defective in the regulation of ethylene biosynthesis, emanate up to 50-fold more ethylene than the wild type by affecting ACS stability (Chae et al., 2003; Vogel et al., 1998; Woeste et al., 1999). *ETO2* and *ETO3* encode *ACS5* and *ACS9* respectively. Being part of an E3 ligase, ETO1 and ETO1-like proteins (EOL) regulate protein stability of ETO2 and ETO3 by the ubiquitin proteasome pathway (Christians et al., 2009; Wang et al., 2004a). Use of these mutants in chemical genetics studies, either as a control or to aim at phenotypic reversion, can help to relate the compound function to ethylene biosynthesis. Among the five genes which bear homology to *ACO*, *ACO1*, *ACO2* and *ACO4* (ethylene-forming enzyme) are ethylene related (Bovy et al., 1999; Gomezlim et al., 1993; Raz and Ecker, 1999).

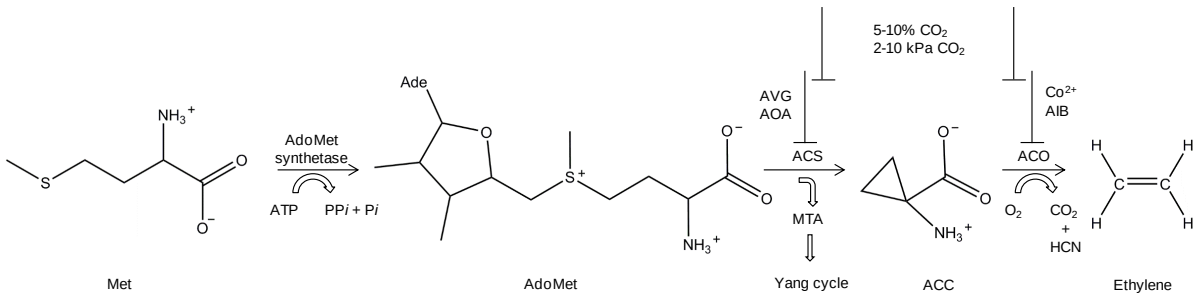

Figure 1.1 Central Points of Ethylene Biosynthesis including antagonists. The enzymes catalyzing steps are shown with the arrows. Met: L-methionine; AdoMet: S-adenosyl-L-methionine; MTA: 5'-methylthioadenosine; ACC: 1-amniocyclopropane-1-carboxylic acid. The antagonists are: Aminoethoxyvinylglycine (AVG); aminooxyacetic acid (AOA); Co^{2+}, α-aminoisobutyric acid (AIB); 5-10 % CO_2, 2-10 kPa.

Several small chemicals have been characterized as inhibitors of ethylene biosynthesis and have been tested for agricultural or horticultural applications. Aminoethoxyvinylglycine (AVG) is a widely used irreversible inhibitor of ACS that decreases ethylene production by

forming a conjugated enol ether with its cofactor, pyridoxal phosphate (PLP), blocking the active site of the enzyme (Rando, 1974). It is commercially named ReTain (containing 15% w/w AVG, Valent Biosciences Crop, USA), and is applied pre-harvest to slow down maturation and ripening of fruits and vegetables. The effectiveness is dose dependent and differs between species and cultivars (Baker et al., 1982; Byers, 1997) as is the case for application methods (Saltveit, 2004). On lab scale, the constitutive triple-response phenotype of the Arabidopsis *eto* mutants can be suppressed by 0.5 to 10 μM AVG (Lin et al., 2010). However, AVG is not specific to ACS, and likely inhibits most PLP-dependent enzymes. For example, AVG has been reported to be an inhibitor of auxin biosynthesis by blocking Tryptophan (Trp) aminotransferase activity (Soeno et al., 2010). This makes the need for a specific ethylene biosynthesis blocker more eminent. Another type of ACS inhibitors are hydroxylamine analogs, which react with PLP to form stable oximes. Aminooxyacetic acid (AOA) belongs to this group of inhibitors, which are applied in a concentration up to 375 μM (Bradford et al., 1982; Xu et al., 2008b). Cobalt ion (Co^{2+}) (Lau and Yang, 1976) and α-aminoisobutyric acid (AIB) (Satoh and Esashi, 1980) are also inhibitors of the ethylene biosynthesis, however, these compounds disrupt ACO activity. AIB is the only known ACC analog that significantly and competitively inhibits ACO. This inhibition is by far not as strong as the ACS inhibitors mentioned above. Carbon dioxide (CO_2) at higher pressure (2-10 kPa) and concentration (5-10%) inhibits ethylene effects in climacteric fruit (Bufler and Streif, 1986; Kerbel et al., 1988). It was suggested that inhibition by CO_2 is due to competition with ethylene at the ethylene receptor site (Burg and Burg, 1967; Gorny and Kader, 1996). However, CO_2 suppresses the expression of ethylene-independent and –dependent ripening genes (Rothan et al., 1997); while it does not inhibit wound-induced ethylene or autocatalytic ethylene via antagonizing ethylene perception (de Wild et al., 2003; de Wild et al., 1999; Mathooko et al., 2001), but rather before the conversion of ACC to ethylene.

In contrast to the use of antagonists of ethylene biosynthesis, ethylene itself can also be applied to accelerate (postharvest) ripening, for instance in tomato and banana, or to prevent lodging in grain crops (Abeles et al., 1992). However, as a gas it is difficult to apply in the field. Ethephon (2-chloroethylphosphonic acid) was discovered as an ethylene releasing compound that can be absorbed and transported within the plant and has been marketed by Bayer CropScience as Ethrel (Szyjewicz et al., 1984). In some cases, the effect of ethephon has been shown to be independent of ethylene generation (Lawton et al., 1994).

Current horticultural applications of inhibitors of ethylene action, such as inhibition of wilting or ripening largely rely on the interference with ethylene perception at the receptor level (Figure 1.2) (Sexton et al., 1995; Sisler and Serek, 1997). In *Arabidopsis*, ethylene is perceived by a family of transmembrane receptors Ethylene Resistant 1 and 2 (ETR1, ETR2), Ethylene Response Sensor 1 and 2 (ERS1, ERS2) and Ethylene Insensitive 4 (EIN4), residing at the ER membrane (Figure 1.2). The receptors are regulated by Reversion To Ethylene Sensitivity (RTE1) (Dong et al., 2008). The ethylene receptors require copper ions as a cofactor to bind ethylene (Rodriguez et al., 1999). Some amino acid residues (D25, Y32, I35 and P36 in Helix I and I62, C65 and H69 in Helix II) at the ligand-binding domain in the N-terminus of the receptors are important for ethylene binding (Wang et al., 2006). Many

ethylene antagonists interfere with the binding of ethylene to its copper-containing receptors. Even before the receptors were identified, silver ions, applied as silver nitrate ($AgNO_3$) or as silver thiosulfate ($Ag(S_2O_3)_2^{3-}$ (STS)) have been known as ethylene inhibitor (Beyer, 1976a). Beyer proposed that silver ions replaced another metal, at that time suggested to be copper or zinc, in the receptors, thus blocking ethylene perception by occupying the copper binding site of the receptors and interacting with ethylene, obviously inhibiting response (Rodriguez et al., 1999; Zhao et al., 2002a). Gold ions can substitute silver ions for ethylene binding, but do not block its action in plants, albeit that it can affect seedling growth independently of ethylene signaling (Binder et al., 2007). Silver ions have been demonstrated to promote IAA efflux independently of ethylene perception, in addition to block ethylene signaling, so that using silver ions to block ethylene signaling needs caution (Strader et al., 2009). Other antagonists of ethylene receptors are strained alkenes which have greater affinity to metal ion π-complexation than ethylene, including 2,5-norbornadiene (2,5-NBD), trans-cyclooctene (TCO) and 1-methylcyclopropene (1-MCP) (Hirayama et al., 1999; Sisler et al., 1990) (Figure 1.3). Some of these compounds have been used for basic research. The most ideal one is 1-MCP because of its effectiveness, stability, and its lack of odor and toxicity (Sisler, 2006). It has been marketed as EthylBloc to increase the shelf life of cut flowers and as SmartFresh to help preserve the freshness and quality of fruits; however, it is volatile and thus has limitations for some agricultural applications.

Possible Screens and recent findings in chemical genetics of ethylene

In a chemical genetics approach, the first essential step is the development of a robust bioassay that reports on the process of interest and can be downscaled to a 96-well plate format. A screening method based on reporter gene expression or a phenotype based assay can be defined as a forward chemical genetics screen, where thousands of compounds are tested for their ability to alter a biological process resulting in a phenotype change and an altered reporter expression. Alternatively, one can design a reverse chemical genetics screen, where small molecules are used to specifically inhibit or activate known selected targets in order to study the functional consequences (Blackwell and Zhao, 2003).

Lin et al. (2010) used a phenotype-based strategy based on suppression of the triple response phenotype in etiolated seedlings of the ethylene overproducer mutant *eto1-4*, on 10,000 structurally diverse compounds in the DIVERSet™ library (ChemBridge Corporation). This library represents a maximal chemical space with a minimal number of compounds chosen by a range of filtering methods. Moreover, the compounds are stable and non-toxic. The latter is important if compounds are to be used for agricultural purposes in the future. The primary screening was performed in 96-well micro-titer plates at a concentration of 50 µM of chemicals (dissolved in DMSO) in MS/2 agar medium to score the long hypocotyl phenotype. A picture database of the phenotypes of seedlings exposed to these 10,000 small molecules might be useful for future purposes. In fact, once publically available, such database could help researchers worldwide to determine characteristics and specificities of compounds of their interest.

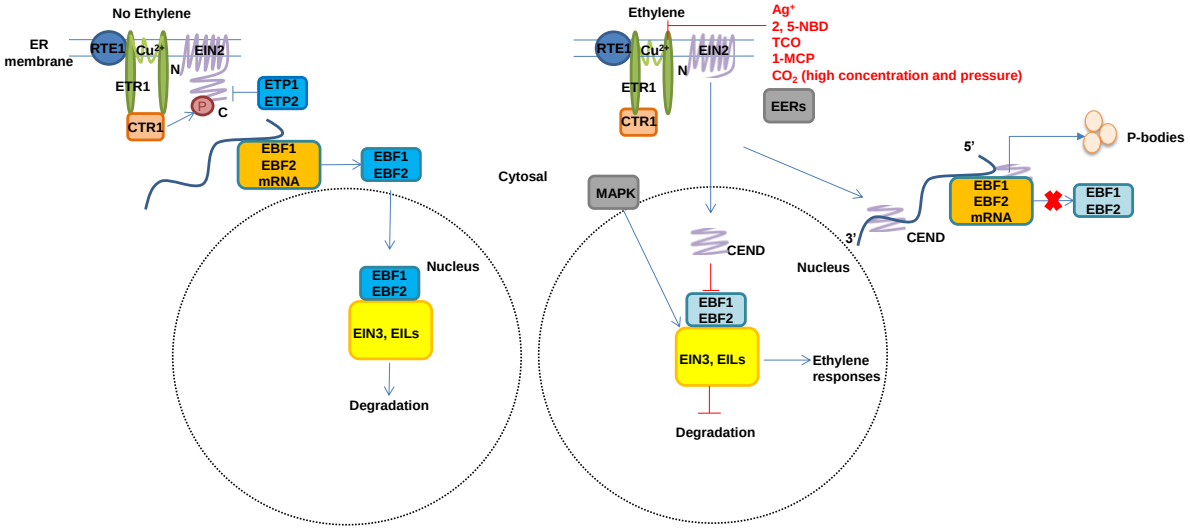

Figure 1.2 Central points of Ethylene Signaling including antagonists. In the absence of ethylene, CONSTITUTIVE TRIPLE RESPONSE 1 (CTR1) protein kinase is tightly associated with the receptor complex, phosphorylates the C-terminal domain (CEND) of ETHYLENE-INSENSITIVE 2 (EIN2), preventing signal transduction to the nucleus. The abundance of EIN2 is regulated by EIN2 targeting proteins 1 and 2 (ETP1and ETP2). In addition, the F-Box proteins EBF1 and EBF2 bind and degrade the transcription factors EIN3 and EIL1 in the nucleus via the ubiquitin proteasome system, preventing the ethylene response. Ethylene Resistant 1 and 2 (ETR1, ETR2), Ethylene Response Sensor 1 and 2 (ERS1, ERS2) and Ethylene Insensitive 4 (EIN4) are the receptors residing at the endoplasmic reticulum membrane, which are regulated by Reversion To Ethylene Sensitivity (RTE1). In the presence of ethylene, receptors and CTR1 are inactivated, leading EIN2 dephosphorylation, which results in its CEND cleaved and relocalized into nucleus, transfering the signal to the EIN3 and EIN3-LIKE (EIL) transcription factor family. EIN3 and EIL protein stability is regulated by EIN3 BINDING F-BOX PROTEINS (EBF1 and EBF2). Meanwhile in the cytosol, EIN2 CEND interacts with several cytoplasmic processing body (P-body) components and associates with the 3'UTR of *EBF1* and *EBF2* mRNAs, which inhibits their translation. The aforementioned route is the linear ethylene signaling pathway that is highly conserved in different plant species. Furthermore, mitogen-activated protein kinase (MAPK) cascades are involved in autocatalytic ethylene production under stress by enhancing ACS stability. Finally, some loci identified as *enhanced ethylene response (eer)* mutants showing an enhanced *ctr1* phenotype, are assumed to play a negative role in ethylene signaling. Antagonists are: Ag+; 2,5-norbornadiene (2,5-NBD); trans-cyclooctene (TCO); 1-methylcyclopropene (1-MCP); high concentration of CO_2 at high pressure.

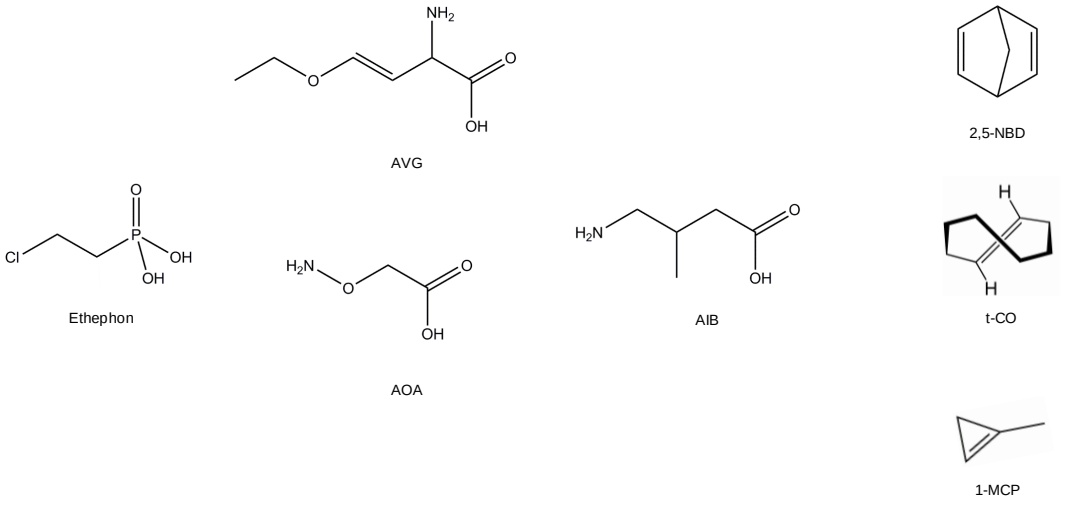

Figure 1.3 Structures of ethylene agonist and antagonists. Agonist: Ethephon (2-chloroethylphosphonic acid). Antagonists: ACC synthase inhibitors: Aminoethoxyvinylglycine (AVG) and Aminooxyacetic acid (AOA); ACC oxidase inhibitor: α-aminoisobutyric acid (AIB); ethylene perception inhibitors: 2,5-norbornadiene (2,5-NBD); trans-cyclooctene (TCO); 1-methylcyclopropene (1-MCP).

For the secondary and tertiary screen, the number of selected compounds can be narrowed down from around one hundred to about ten, by selecting highly active and specific compounds. Lin et al. (2010) finally selected two compounds the effectiveness of which is comparable with silver nitrate, therefore being potential suppressors of ethylene response. To determine whether they inhibit ethylene biosynthesis or a step upstream of ethylene signaling, they analyzed the effect of hit compounds in the constitutive ethylene mutant *ctr1* and mutants overexpressing *EIN3 (ETHYLENE INSENSITIVE 3)* under control of the cauliflower mosaic virus 35S promoter (Chao et al., 1997). However, any seedling with constitutive or enhanced ethylene response could serve the purpose, including 35S::EIN2 and mutants *ebf1-1 ebf2-1* (*ein3 binding f-box proteins*) (Potuschak et al., 2003), *eer(s)* (*enhanced ethylene response*) and the recently identified *sar1-7* (*suppressor of auxin resistance 1*) (Robles et al., 2012). Conversely, when looking for compounds that induce or enhance ethylene responses, ethylene resistant *etr1-1* (Chang et al., 1993), insensitive *ein2-1* (Alonso et al., 1999) and *ein3* or *ein3-1 eil1-1*(*eil: ein3-like*) (Alonso et al., 2003b) can be used. These compounds can be further tested for phenotypic reversal of the action of ethylene synthesis inhibitors or antagonists. In addition, Lin et al. used a reporter line of *eto1-4* harboring *5xEBS::LUC* to confirm the suppression of the ethylene response. Both luciferase gene (LUC) and beta-glucuronidase (GUS) reporter systems have been fused to the EIN3-binding-sequence, and report *EIN3* transcription factor activity, which acts as an indicator for the presence of an ethylene signal (Stepanova et al., 2007). The *LUC* activity or GUS-expression in the apical hook, hypocotyl and root can be scored in comparison with the ACC/non-ACC treated or ethylene inhibitor treated controls. Using an *EBS* reporter line in the primary screen can be a rewarding approach for rapidly selecting ethylene specific effects brought about by the compounds.

As an alternative to the use of ethylene overproducer mutants, the triple response phenotype can be induced by adding exogenous ACC to wild type plants, or applying ethylene in an open flow gassing system to prove that the observed phenotypes are truly ethylene-related.

Comparison of structural analogs is a valuable tool to discover novel active compounds. Lin et al. (2010) discovered a compound more effective than that identified in their initial screen. Structural comparison of compounds with similar biological effects or with known function can give further hints on their function (Kim et al., 2011b; Savaldi-Goldstein et al., 2008; Surpin et al., 2005; Tsuchiya et al., 2010). Ultimately, the selected compounds should be stable and effective at low concentrations to reduce off-target effects (De Rybel et al., 2009b; Grozinger et al., 2001). It is noteworthy that decreased signaling causes positive feedback on the biosynthesis, as in *etr1* or *ein2*, where the level of ethylene production is high, while in *ctr1-1* it is low compared to dark-grown wild type plants (Kieber et al., 1993; Vandenbussche et al., 2012). This overproduction can be referred to an increased ACS activity (octuple *acs* mutant has ethylene levels 10 times lower than the wild-type) (Tsuchisaka et al., 2009). Thus ethylene production can be measured to dissect the pathway and the function of the compound in a more detailed manner.

The aforementioned screen (Lin et al., 2010) identified a group of quinazolinones (Figure 1.4a) that function as novel ACS inhibitors. These novel inhibitors are non-competitive inhibitors of

ACS, albeit structurally and mechanistically unrelated to AVG according to in vitro activity assay and enzyme kinetics (Boller et al., 1979). However, a microarray analysis revealed that more than 40% of the genes in Arabidopsis are commonly regulated by the hit compounds and AVG, including possible factors required to establish the triple response during etiolated growth in elevated ethylene. Furthermore, it provides an alternative to investigate the role of ACC in ethylene independent processes (Tsang et al., 2011). It is worthwhile to point out that these compounds are different from naturally occurring quinazolinones (Mhaske and Argade, 2006).

Chemical genetics in ethylene- hormone interaction studies

Ethylene is known to functionally interact with various hormones (Dugardeyn and Van der Straeten, 2008). Reporter lines specific for these other hormonal pathways can assess the effect of chemicals identified in an ethylene-related screen, revealing hormonal crosstalk. The following reporters can be used, *DR5::GUS* (auxin responsive-element, AuxRE) for auxins (Ulmasov et al., 1997b)), *TCS::GUS* (two-component system) for cytokinins (Zhao et al., 2010), *CPD::GUS* (cytochrome P450) for brassinolide (Mathur et al., 1998), *RD29A::GUS* (responsive to dessication 29A) for abscisic acid (Yamaguchi-Shinozaki and Shinozaki, 1994) and *Thi2.1::GUS* (thionein 2.1) for jasmonic acid (Xie et al., 1998).

Interactions between ethylene and auxin are complex. Both agonist and antagonist effects have been reported. As agonists, they synergistically affect root elongation and root hair formation (Rahman et al., 2002; Swarup et al., 2007). As antagonists, they affect abscission of flower and fruits (Brown, 1997). With respect to auxin biosynthesis, loss of function of the weak ethylene insensitive *WEI2* and *WEI7* genes, which encode the α- and β-anthranilate synthases, are the key enzymes in Trp auxin biosynthesis (Stepanova et al., 2005; Stepanova et al., 2008); *WEI8*, which encodes *Trp aminotransferase of Arabidopsis 1* (*TAA1*), is the key enzyme catalyzing the indole-3-pyruvic acid (IPA) pathway for auxin biosynthesis. Its close relative TAR2 and the flavin monooxygenase YUC1 reporter lines can also link to ethylene through newly found L-Kynurenine (He et al., 2011; Stepanova et al., 2011). Defects in auxin biosynthesis or transport also result in ethylene insensitivity. For instance, mutation of the auxin transporters auxin resistant *AUX1* (Bennett et al., 1996) and ethylene-insensitive root *EIR1/PIN2* (Luschnig et al., 1998; Muller et al., 1998) both confer insensitivity to ethylene. Linking the aforementioned elements, a first step to monitor whether ethylene inhibits root growth by modulating auxin biosynthesis and transport, auxin reporter *DR5::GUS* in wild-type and ethylene mutant background can be used. The next step will be to determine which pathway of the auxin action is disturbed, biosynthesis or transport. Several reporter lines such as *WEI2*, *WEI7* or *TAR2* promoters driving *GUS* or GFP can be used to check whether the chemicals affect auxin biosynthesis; while reporter lines for auxin influx and efflux transporters AUX1 and PIN2 can be used to assess the effect on auxin transport. Moreover, the phenotypes of mutants treated with chemicals can be examined, and exogenous auxins can be applied in addition to the chemicals to further demonstrate the relations between auxin and ethylene.

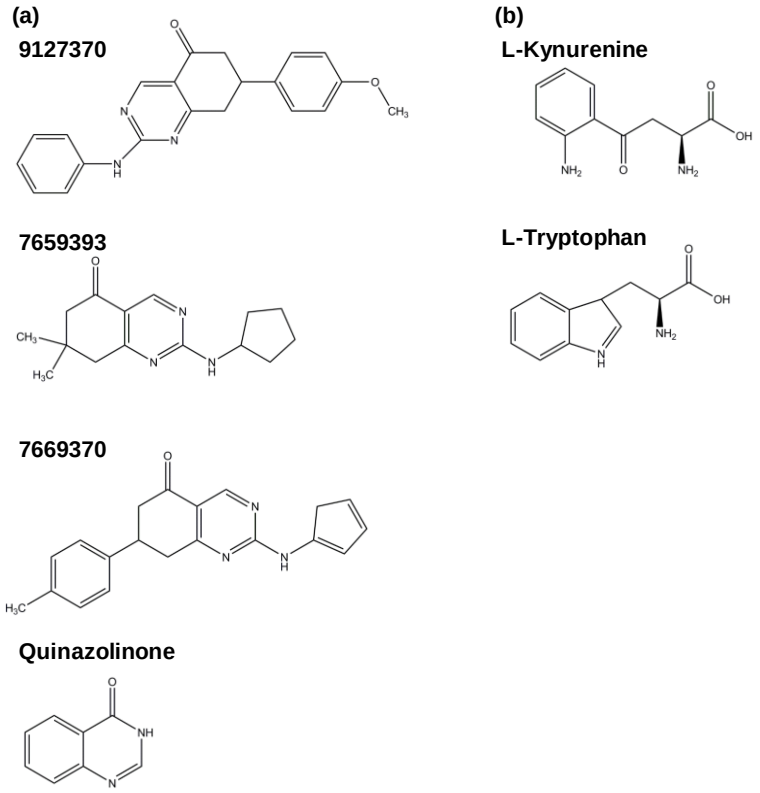

Figure 1.4 Recent chemical genetics findings in ethylene research. (a) Groups of quinazolinones that function as novel ACC synthase inhibitors: 9127303 (Chembridge^{TM} ID, 2-anilino-7-(4-methoxyphenyl)-7,8-dihydro-5(6H)-quinazolinone); 7659393 (2-(cyclopentylamino)-7,7-dimethyl-7,8-dihydro-5(6H)-quinazolinone); 7669370 (2-(cyclopentylamino)-7-(4-methylphenyl)-7,8-dihydro-5(6H)-quinazolinone). **(b)** L-Kynurenine is an analog of L-Trytophon that function as competitive inhibitor of TAA1/TARs-mediated auxin biosynthesis.

The work by He et al. (He et al., 2011) is a good example of how the search for ethylene-related compounds can lead to an auxin-ethylene link; in this case, that auxin positively regulates the ethylene signaling pathway to accelerate its own biosynthesis. The screen was initially done based on reversions of the ethylene related short-root phenotype of *eto1-2* and *ctr1-1* etiolated seedlings by compounds from a combinatorial SP2000 chemical library (www.msdiscovery.com). L-Kynurenine (Kyn) (Figure 1.4b) was identified as a new auxin biosynthetic inhibitor based on the suppression of the expression of a series of auxin biosynthesis reporters upon ACC treatment. Kyn selectively targets TAA1-like Trp aminotransferases, providing a new tool to explore TAA1/TAR-mediated auxin biosynthesis (Stepanova et al., 2011). These findings illustrate how strongly interwoven ethylene and auxin responses are. Secondary screens for auxin characteristics are therefore highly advisable when primary screens are based on ethylene-related phenotypes. Kyn is one of the few small molecules inhibitors with identified targets (Toth and van der Hoorn, 2010), the finding of which is based on the integration of the analysis of representative mutant lines and hormone marker gene, enzyme assays (if the potential target is an enzyme) and computational modeling. Structural analysis of the chemical in conjunction with the analysis of potential metabolites is also important in order to discover the direct target. Kyn is a natural product that has been reported in a non-plant species, and the metabolic pathway was investigated. Unlike Kyn, its derivatives such as quinolinic acid, NAD^+, nicotinamide and nicotinic acid (Katoh and Hashimoto, 2004) did not promote root elongation of *ctr1-1*.

In certain cases, compounds may also have double or multiple targets. For example, a BR inhibitor screen identified brassinopride (BRP), which besides inhibiting BR, also activates ethylene responses (Gendron et al., 2008). BRP activates expression of the BR-inhibited reporter gene *CPD::GUS*, inhibits hypocotyl length, and causes an exaggeration of the apical hook. The two latter features are characteristic of the triple response to ethylene in darkness, and were indicative for a double function of BRP. Further analysis using BR and ethylene mutants, treatment with ACC and an ethylene-perception inhibitor, support the view that BRP promotes ethylene action at the step of ethylene perception or upstream. The latter is consistent with the finding that ethylene controls the biosynthesis of BRs and establishes a gradient of BR in the apical hook to the hook formation (De Grauwe et al., 2005).

Target identification

Many techniques have been developed to facilitate chemical genetic screens, such as synthesis of various chemical libraries (Schreiber, 2000), automated preparation and phenotyping tools (Hicks and Raikhel, 2009), and the development of cell-based assays (Haggarty et al., 2000). However, in order to understand the mode-of-action of the ligands, the target identification remains the biggest challenge. Target identification can be roughly grouped into genetics-based (genetic), transcriptional profiling-based (molecular) and affinity-based (biochemical) (Cong et al., 2012). Here, we will discuss possible target identification for ethylene research in Arabidopsis.

Studies of structure-activity relationships (SAR) are a first step towards identification of possible target proteins. Structure-based clustering can be performed through the ChemMine interface using external or internal compounds or a combination of both (Girke et al., 2005). One can run a cluster analysis for all compounds identified, and test structurally related and unrelated compounds including functional cores in different bioassays. In some cases, SAR studies resulted in the discovery of antagonists or in uncoupling different targets of a given compound, as for brassinopride (BRP) derivatives (Gendron et al., 2008). Furthermore, there are several examples where the compounds are enzymatically converted to the actual bioactive molecules, for example by the action of amidases, esterases, aldehyde oxidases, or glucosyltransferases (Toth and van der Hoorn, 2010). This also may give a clue towards identification of the active principle. Thus, possible metabolization reactions of a given active compound should be investigated, using sensitive analytical methods such as liquid chromatography or gas chromatography combined with mass spectrometry (MS), in order to get a clue on the bioactive compounds.

To further identify the target protein, transcriptome analysis with either microarrays or RNA sequencing can be used. Genome wide transcriptome analysis of a wild type treated with the ligand, can help to diagnose which processes are affected by this compound, and thus help in identification of the targets. For example, transcriptional changes induced upon treatment with bikinin overlapped almost 90% with those induced by BR treatment, placing the bikinin targets in the BR signaling cascade (De Rybel et al., 2009b). Likewise, in a study of compounds affecting ethylene physiology, panoramic transcriptome analysis upon compound

treatment can be compared with the effect of either ethylene or AVG treatment, thus identifying whether the compound shows an agonist or antagonist action.

In parallel, EMS mutants resistant/hypersensitive to the compounds can be isolated, particularly if the aforementioned approaches have generated an interesting lead. As shown in the past, seedling responses to ethylene are extremely useful to identify mutants (Guzman and Ecker, 1990). T-DNA insertion mutants will be analyzed if there is an unequivocal indication for a particular gene. Next generation sequencing approaches will allow rapid and relatively low-cost identification of the mutations, and corresponding genes that are affected. The method mentioned above is genetics-based rather than biochemical-based. The genetics-based approach could lead to indirect target identification. A biochemical-based approach using affinity purification based on drug-affinity chromatography and high-resolution MS analysis can be applied to complement the genetic approach to discover the direct target (Zheng et al., 2004). Moreover, several strategies have been developed to optimize the biochemical-based approach, for instance yeast-three-hybrid (Y3H), protein microarrays and NMR-based metabolomics, allowing detection of low-abundant targets (Huang et al., 2004; Kim et al., 2010a; Kley, 2004). Another tool that has arisen in chemical genetics is "click chemistry", an organic synthesis method based on joining small units together with a covalent bond (Kolb, 2001). It offers promising possibilities to allow discovery of perfectly customized enzyme inhibitors. In this context, enzymes participate in the 'discovery' of their own inhibitors: by acting as a template that brings click reagents together, the binding pocket of a given target enzyme catalyses the in situ formation of its own, perfectly customized inhibitor. In plant research, click chemistry was used to identify targets of the cysteine protease inhibitor E-64 in Arabidopsis (Kaschani et al., 2009). Moreover, X-ray crystallography is an important tool to determine the interaction between small molecules and their targets, as for instance, for the auxin receptor transport inhibitor response 1 (TIR1) (Tan et al., 2007).

Future perspectives

The examples demonstrate the feasibility and power of chemical genetics in ethylene research. Inhibitors of ethylene biosynthesis and signaling and ethylene enhancing compounds are invaluable tools to further dissect the ethylene pathway or to distinguish between different hormones that have similar phenotypic effects. The control of ethylene production and action is also an important component in pre- and postharvest management of crops. For instance, discovery of specific inhibitors of ACS/ACO can reduce ethylene synthesis and thus help to control post-harvest losses, perhaps complementary to genetic modification approaches in countries where GMOs are withheld from commercialization. Thus, the discovery of novel chemical compounds will be useful in fundamental ethylene research and can offer potentially useful agrochemicals for quality improvement in both horticulture and agriculture.

Chapter 2

Regulation of seedling development by ethylene and the ethylene-auxin crosstalk

Contribution:

Yuming Hu, Filip Vandenbussche and Dominique Van Der Straeten wrote the chapter.

In dark-grown *Arabidopsis* seedlings, exogenous ethylene treatment triggers an exaggeration of the apical hook, the inhibition of both hypocotyl and root elongation, and radial swelling of the hypocotyl. These features are predominantly based on the differential cell elongation in different cells/tissues mediated by an auxin gradient. Interestingly, the physiological responses regulated by ethylene and auxin crosstalk can be either additive or synergistic, e.g. primary root and root hair elongation or antagonistic, e.g. hypocotyl elongation. This chapter focuses on the crosstalk of these two hormones in seedling development stage. Before illustrating the crosstalk, ethylene and auxin biosynthesis, metabolism, transport and signaling are briefly discussed.

Ethylene and auxin biosynthesis and metabolism

Ethylene in plants is derived from the amino acid L-Methionine (Met) (Figure 2.1). Nearly 80% of cellular Met is converted to S-adenosyl-L-methionine (AdoMet) by AdoMet synthetase with the expense of ATP (Giovanelli et al., 1985). AdoMet is subsequently converted to 1-aminocyclopropane-1-carboxylate (ACC) by ACC synthase (ACS), an aminotransferase requiring pyridoxal-5'-phosphate (PLP) as a cofactor, which catalyzes the rate-limiting step in most tissues. In addition to ACC, ACS also produces 5'-methylthioadenosine (MTA), which is recycled to Met in the Yang cycle (Yang and Hoffman, 1984). In the last step of the sequence, 2-oxo-4-methylthiobutyric acid (KMBA) is converted to Met via transamination. The reverse reaction is catalyzed by the (PLP)-dependent aminotransferase VAS1 (Zheng et al., 2013). Finally, ACC is oxidized by ACC oxidase (ACO) using ferrous ion (Fe^{2+}) as cofactor and ascorbate as co-substrate to form ethylene, carbon dioxide (CO_2) and cyanide (HCN), which is detoxified into β-cyanoalanine by β-cyanoalanine synthase. ACC can also be converted to 1-malonyl-ACC (MACC), γ-glutamyl-ACC (GACC) and jasmonyl-ACC (JA-ACC) by conjugation through ACC-N-malonyltransferase (AMT), ɣ-glutamyl-transpeptidase (GGT) and JA-amino synthetase (JAR1, jasmonic acid resistance 1) in the presence of malonyl CoA, glutathione and jasmonic acid (Amrhein et al., 1981; Martin et al., 1995; Staswick and Tiryaki, 2004). A homologue of the bacterial ACC deaminase can convert ACC to α-ketobutyrate and ammonia (McDonnell et al., 2009) (Figure 2.1). ACC conjugation can regulate ACC levels although the underlying regulatory mechanisms remain to be discovered. ACC can also function as a signaling molecule, independently from ethylene (Tsang et al., 2011; Tsuchisaka et al., 2009; Xu et al., 2008; Van de Poel and Van Der Straeten, 2014).

The experimental and practical uses of ethylene are limited by its gaseous nature. Alternatively, (2-chloroethyl)-phosphonic acid (ethephon), an ethylene-releasing chemical, is used in a wide variety of practical applications, e.g. stimulation of fruit ripening or counteracting lodging of wheat (Bondad, 1976; Simmons et al., 1988). However, the release of ethylene is not well controllable (Tucker and Wen, 2015).

Indole-3-acetic acid (IAA) has been recognized as the major auxin since its discovery in the 1930s (Went and Thimann, 1937). All plant tissues can synthesize IAA. The main source of auxin is the shoot apical meristem; the root apical meristem and young developing leaves also contribute to auxin synthesis (Ljung et al., 2005). A more recent study suggested that auxin

synthesized in roots by the YUCCA (YUC) flavin-containing monooxygenases is crucial in normal root elongation and root gravitropic responses, the shoot-derived auxin being insufficient (Chen et al., 2014).

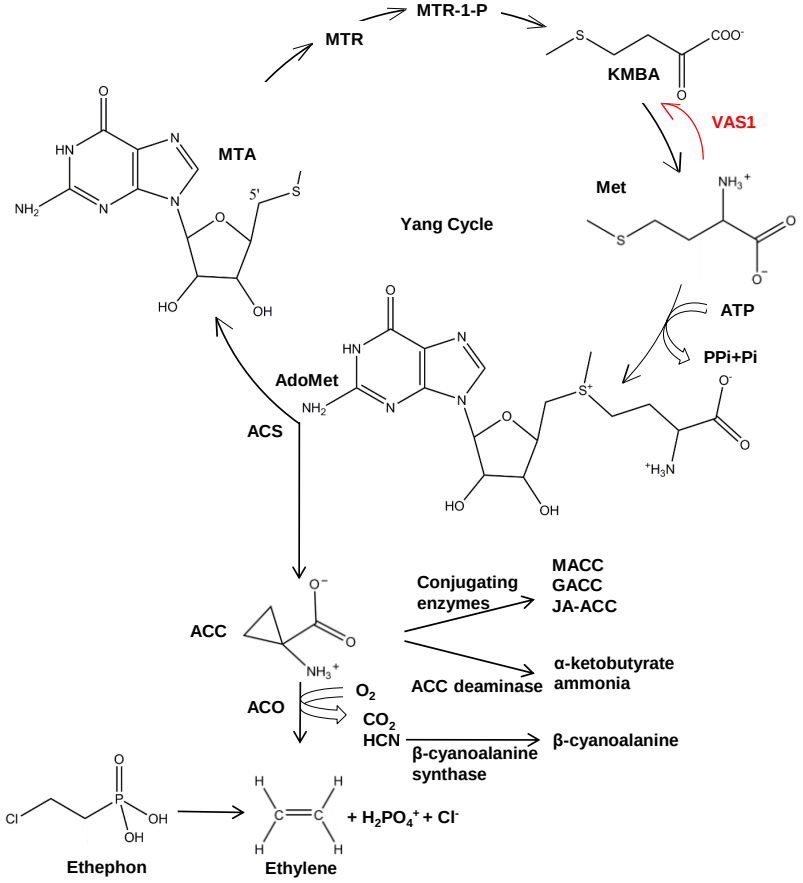

Figure 2.1 Ethylene biosynthesis and ACC metabolism. L-methionine (Met) is converted to S-adenosyl-methionine (AdoMet) by AdoMet synthetase with the requirement of ATP. AdoMet is converted to ethylene in two steps: Firstly, releasing 1-aminocyclopropane-1-carboxylic acid (ACC) by ACC synthase (ACS), with 5'-methylthioadenosine (MTA); Secondly, ACC is converted to ethylene by ACC oxidase (ACO), which requires oxygen (O_2) and releases carbon dioxide (CO_2) and hydrogen cyanide (HCN). HCN is detoxified to β-cyanoalanine. Met is recycled via the Yang cycle. The intermediates are: MTA: 5'-Methylthioadenosine; MTR: 5-methylthioribose; MTR-1-P: 5'-methylthioribose-1-phosphate; KMBA: 2-oxo-4-methylthiobutyric acid. ACC can be conjugated to 1-malonyl-ACC (MACC), γ-glutamyl-ACC (GACC) and jasmonyl-ACC (JA-ACC); ACC can also be converted to α-ketobutyrate and ammonia by the homologue of the bacterial ACC deaminase. Ethephon is an ethylene releasing compound.

It has been proposed that IAA can be synthesized through tryptophan (Trp)-dependent and Trp-independent pathways in plants (Figure 2.2). For reviews of auxin biosynthesis pathways, we refer to (Korasick et al., 2013; Tivendale et al., 2014; Zhao, 2014). Indole-3-glycerol phosphate and indole are likely precursors of IAA in Trp-independent pathways, but the mechanisms are largely unclear (Normanly et al., 1993; Ouyang et al., 2000). Four routes have been proposed as Trp-dependent pathways that convert indole precursors to Trp, and subsequently to IAA, via the following intermediates downstream of Trp: indole-3-acetamide (IAM), indole-3-pyruvic acid (IPA), tryptamine (TAM) and indole-3-acetaldoxime (IAOx); the IPA route being the most important pathway (Mano and Nemoto, 2012) (Figure 2.2a). Few genes coding for the predicted enzymes have been identified, such as TRYPTOPHAN

AMINOTRANSFERASE OF ARABIDOPSIS1/TRYPTOPHAN AMINOTRANSFERASE RELATED (TAA1/TARs) that convert Trp to IPA (Stepanova et al., 2008; Tao et al., 2008) and YUC flavin-monooxygenases that can convert IPA further into IAA (Mashiguchi et al., 2011; Stepanova et al., 2011; Won et al., 2011). YUC were previously identified to be involved in the TAM to N-hydroxyl-TAM conversion (Zhao et al., 2001), while more recent studies have questioned whether YUCs use TAM as substrate for auxin biosynthesis (Mashiguchi et al., 2011; Stepanova et al., 2011; Tivendale et al., 2010). Furthermore, cytochrome P450 enzymes, CYP79B2 and CYP79B3 that catalyze Trp conversion into IAOx, have been described (Zhao et al., 2002). So far, the IAOx pathway has only been found in *Brassicaceae*, including *Arabidopsis* (Mano and Nemoto, 2012). Inactivation of *SUPERROOT1* (*SUR1*) or *SUR2* blocks the indole glucosinolate (IG) biosynthesis, leading to auxin overproduction due to re-routing of IAOx to IAA (Bak et al., 2001; Mikkelsen et al., 2004), where IAM and indole-3-acetonitrile (IAN) were suggested as possible precursors (Sugawara et al., 2009). Because of redundancy in auxin biosynthesis, no loss-of-function auxin mutant has been isolated from genetic screens specific for auxin deficiency (Zhao, 2010).

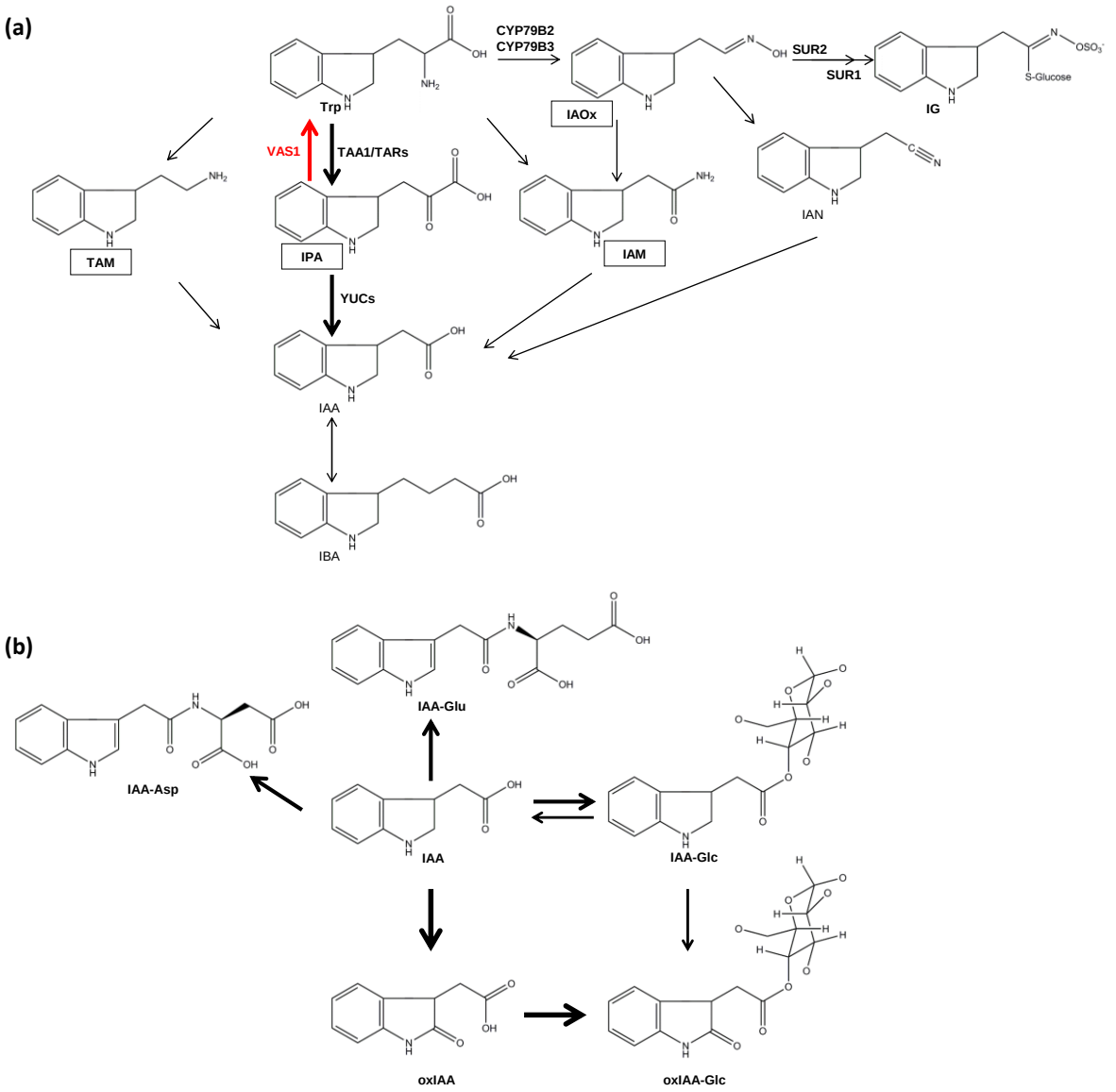

Figure 2.2 Auxin biosynthesis and metabolism.
(a) Four routes of Trp-dependent auxin biosynthesis: TAM, IPA, IAOx and IAM are the four primary intermediates; IPA is the most important one. Few enzymes have been identified, i.e. TAA1/TAR, YUCs, CYP79B, CYP79B3, SUR1 and SUR2. The reverse reaction of IPA to Trp is catalyzed by VAS1. IBA can be released from or converted back to IAA.
(b) Auxin metabolism: the most abundant amino acid conjugates in Arabidopsis seedlings are IAA-Asp and IAA-Glu. Oxidation of IAA to oxIAA, and subsequent conjugation with Glc to form oxIAA-Glc, is the major route for IAA catabolism.

Notably, VAS1, which employs Met as an amino donor, simultaneously uses the auxin biosynthetic intermediate IPA as an amino acceptor to produce Trp, suppressing both the levels of ethylene and auxin (Zheng et al., 2013) (Figure 2.1 and Figure 2.2a).

In addition, IAA can be released from indole-3-butyric acid (IBA) or IAA conjugates (reviewed in (Korasick et al., 2013; Ljung, 2013; Sauer et al., 2013)). IBA can be converted to IAA via peroxisomal β-oxidation (Zolman et al., 2000) (Figure 2.2a). Whether IBA itself has an auxin effect, is still subject of debate (Strader and Bartel, 2011), although it has been used as rooting agent.

Besides IAA, other endogenous auxins such as 4-chloroindole-3-acetic acid (4-Cl-IAA), and phenylacetic acid (PAA) (Figure 2.3a) have been identified in legumes, but their specific biological roles are less clear and they have not been identified in *Arabidopsis* (reviewed in (Simon and Petrasek, 2011)).

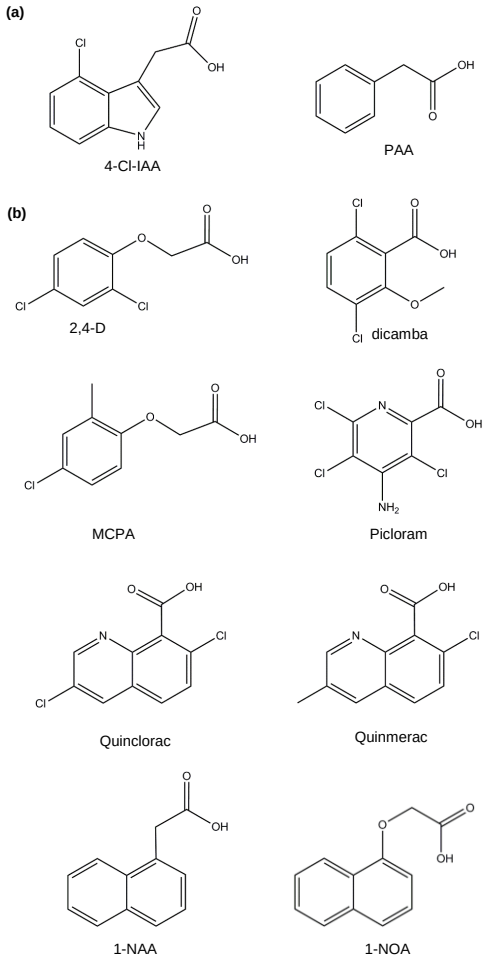

Figure 2.3 Auxin structure.
(a) Native auxins.
(b) Synthetic auxins including herbicides (2,4-D; MCPA; dicamba; picloram; Quinclorac and Quinmerac).

Many compounds with auxin-like activities have been characterized and are used in agricultural practice. Some are used as herbicides, for instance, phenoxyacetic acids, represented by 2,4-dichloro-phenoxyacetic acid (2,4-D) and 2-methyl-4-chlorophenoxyacetic acid (MCPA); benzoic acid derivatives 2-methoxy-3,6-dichlorobenzoic acid (dicamba); pyridine-carboxylic acids, represented by 4-amino-3,5,6-trichloropicolinic acid (picloram) and quinolinecarboxylic acids, represented by Quinclorac (3,7-Dichloro-8-quinolinecarboxylic acid) and Quinmerac (7-Chloro-3-methyl-8-quinolinecarboxylic acid) (Grossmann, 2003). Some are used as rooting agents for cuttings and in plant tissue culture, such as 1-Naphthaleneacetic acid (1-NAA) (Figure 2.3b). The exaggerated auxin responses triggered by these compounds are partly due to their higher stability compared to IAA (Dunlap et al., 1986). 2,4-D and 1-NAA can be used to follow auxin influx and efflux separately (Delbarre et al., 1998; Delbarre et al., 1996). 2,4-D is primarily uptaken by auxin influx carriers and its diffusion is very low; it is also quite bad substrate for auxin efflux. 1-

NAA easily enters cells by passive diffusion; after dissociation in the cytoplasm, it is a good substrate for auxin efflux carriers.

A major fraction of auxins is conjugated to amino acids (AA), sugars, peptides or proteins linked to IAA, which serve as biologically inactive and storage forms of IAA, either reversible or irreversible, and are believed to be essential for maintaining auxin homeostasis. The most abundant AA conjugates in *Arabidopsis* seedlings are IAA-aspartate (Asp) and IAA-glutamate (Glu) (Kai et al., 2007; Kowalczyk and Sandberg, 2001; Novak et al., 2012; Ostin et al., 1998; Tam et al., 2000) (Figure 2.2b). Genes involved in IAA conjugation and conjugate hydrolysis have been identified, including the auxin-inducible *GRETCHEN HAGEN 3 (GH3)* family of amido synthases and amido hydrolases, which can be promoted by elevated IAA levels (Ludwig-Muller, 2011). IAA-Trp is yet another auxin conjugate, which not only removes free IAA from the active auxin pool, but also acts as an antagonist of auxin-induced growth (Staswick, 2009). Furthermore, IAA can be irreversibly degraded by decarboxylation of the side chain or direct modification of the indole ring (non-decarboxylation pathway). IAA oxidases, such as peroxidases, have been proposed in oxidative IAA decarboxylation *in vitro* (Osswald et al., 1988; Vatulescu et al., 2004); however, little is known about the enzymes involved in IAA oxidation *in vivo*. In *Arabidopsis*, it has been shown that oxidation of IAA to 2-oxindole-3-acetic acid (oxIAA), and subsequent conjugation to oxIAA- glucose (Glc), is a major route for IAA catabolism, based on feeding experiments and mass spectrometry-based quantification of IAA metabolites (Figure 2.2b, adapted from (Pěnčík et al., 2013)). Localized IAA accumulation in roots or an increased shoot-derived auxin stream result in an increased oxIAA level in the root (Kubes et al., 2012; Ostin et al., 1998; Peer et al., 2013; Pěnčík et al., 2013). Peer et al. (2013) indicated that oxIAA is produced via a reactive oxygen species (ROS)– dependent pathway, as a consequence, IAA signaling is attenuated.

Ethylene and auxin transport

Hormones can exert influence at their site of synthesis or they can act at a distance (Williams, 2010). Ethylene is a gaseous molecule, which can be freely transported from one cell to another by diffusion. Aerenchyma and intercellular voids facilitate rapid long-distance ethylene transport. In addition, remote action can also be achieved by transport of ACC, the ethylene precursor (Van de Poel and Van Der Straeten, 2014). For instance, ACC can be transported from the root to the shoot under hypoxia (Bradford and Yang, 1980). ACC can also be transported intracellularly across the tonoplast, which can change the ACC concentration in cell compartments and have an impact on ethylene biosynthesis (Saftner and Martin, 1993).

Auxin transport essentially occurs via two distinct ways. One is a rapid, long-distance source-to-sink transport via the phloem from highly biosynthetically active apical shoot tissues to the roots by mass flow (Marchant et al., 2002). Another is over both short and long distances. It involves cell-to-cell transport via chemiosmosis or transport carrier proteins; and it is usually polar, commonly referred to as polar auxin transport (PAT). Since IAA is a weak acid with pKa of 4.75, a portion (~15%) is protonated (IAAH) in the acidic environment of the apoplast

(pH 5.5), thus becoming relatively lipophilic and able to diffuse through the cell membrane by passive movement (Vanneste and Friml, 2009). In addition, there are H^+-symporters that facilitate cellular auxin influx, such as AUXIN RESISTANT1 (AUX1), and LIKE-AUXs (LAX1, 2, 3) (Bennett et al., 1996; Marchant et al., 2002; Marchant et al., 1999; Swarup et al., 2008). When IAA enters the cytoplasm with pH 7.2, it is deprotonated, resulting in its anionic form (IAA^-). This form of auxins needs specific efflux carriers in the plasma membrane (PM) to leave the cell and direct the movement. Auxin efflux carriers include the ATP-binding cassette (ABC) superfamily, predominantly B type (ABCB/Multidrug Resistance/Phosphoglycoprotein, MDR-PGP) transporters and the PIN-FORMED (PIN) efflux carriers. The auxin long-distance stream from the shoot apical meristem to the root is loaded mainly by PIN1 and ABCB19 (Blakeslee et al., 2007; Friml et al., 2003; Gälweiler et al., 1998). ABCB19 might interact with PIN3 to mediate vascular auxin transport streams (Blakeslee et al., 2007). The strict polarization of some transporters such as PINs, AUX1, in specific cells is crucial for plant development and essential for differential auxin distribution in several physiological responses (Blilou et al., 2005; Friml et al., 2002; Luschnig et al., 1998; Swarup et al., 2001) (Figure 2.5).

Ethylene and auxin signaling

In *Arabidopsis*, ethylene signaling is initiated by the binding of a family of endoplasmic reticulum (ER)-localized receptors (ETHYLENE RESISTANT 1 (ETR1), ETR2, (ETHYLENE RESPONSE SENSOR 1 (ERS1), ERS2 and (ETHYLENE INSENSITIVE 4 (EIN4)) with sequence similarity to the bacterial two-component histidine kinases, which are the negative regulators of the signaling. Copper is a cofactor for ethylene binding, which is delivered to the receptors by the copper transporter RAN1. In addition, REVERSION TO ETHYLENE SENSITIVITY1 (RTE1) is associated with ETR1 and mediates the output of the receptor signal. In the absence of ethylene, the receptors activate CONSTITUTIVE TRIPLE RESPONSE 1 (CTR1), a rapidly accelerated fibrosarcoma (raf)-like Serine/Threonine protein kinase. CTR1 inactivates EIN2 by directly phosphorylating its C terminus (CEND). As a consequence, the master transcription factors EIN3/EIL1 are degraded in the nucleus. The stability of EIN2 is also negatively regulated by two F-box proteins, EIN2-TARGETING PROTEIN (ETP1) and ETP2 (Qiao et al., 2009). In the presence of ethylene, following ethylene perception by the ethylene receptors, CTR1 is inactivated, which leads to a reduction in the phosphorylation of the ER-localized transmembrane protein EIN2. Thus, the unphosphorylated EIN2 C-END is cleaved from the ER-anchored NRAMP domain (Ju et al., 2012; Qiao et al., 2012), and translocated to the nucleus. The transcriptional regulators of EIN3 and EIN3-LIKE 1 (EIL1) are consequently stabilized and regulate a transcriptional cascade involving hundreds of genes (Binder et al., 2004; Chang et al., 2013). On the other hand, a rapid ethylene response exits, which does not require EIN3 and EIL1 (Binder et al., 2004). In addition, EIN2 CEND directly or indirectly binds to 3'UTR of EBF1 and EBF2 mRNA molecules in cytoplasmic processing bodies (P-bodies) through interacting with EIN5 and several other P-body components to suppress EBF1 and 2 translation (Li et al., 2015; Merchante et al., 2015) (Figure 2.4).

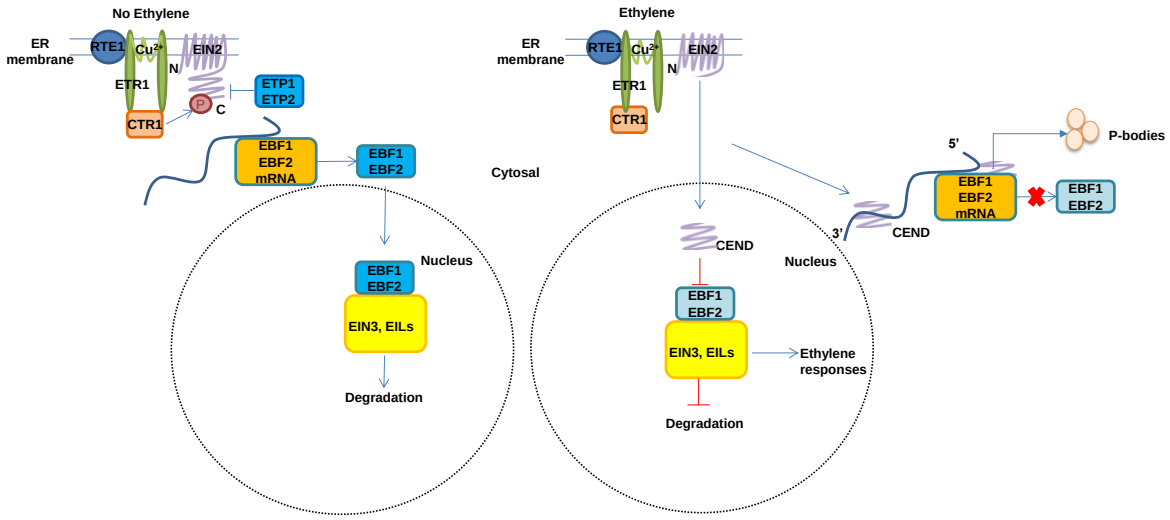

Figure 2.4 Ethylene signaling pathway. Without ethylene, ER-localized CTR1 phosphorylates EIN2 at its CEND, inhibiting EIN2 cleavage. EIN3 and EIL1 transcription factors are degraded by EBF1 and EBF2 in a 26S proteasome dependent pathway. When ethylene binds to the receptors (e.g. ETR1), CTR1 is inactivated; thus, EIN2 CEND is de-phosphorylated, resulting in the cleavage of the CEND. CEND subsequently moves to the nucleus to inhibit EBF1 and EBF2 E3 ligase activity, maintaining EIN3 and EIL1 protein accumulation, which leads to ethylene response. In addition, CEND inhibits EBF1 and EBF2 mRNA translation in the cytosol through association with their 3'UTR and other P-body components.

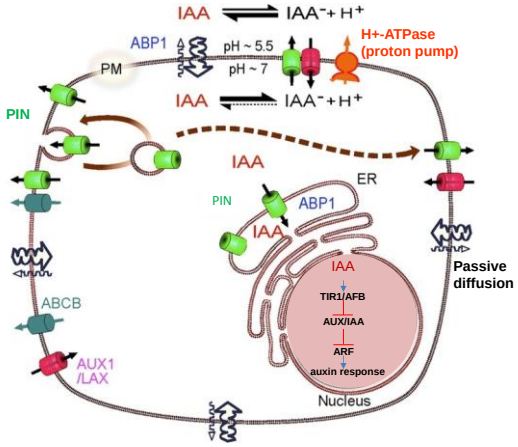

Figure 2.5 Auxin fluxes, perception and signaling in the plant cell. Adapted from (Friml and Jones, 2010). Auxin flux occurs via passive diffusion, influx carriers of AUX1/LAX type, and efflux carriers including the PINs and ABCBs. In the case of the PIN proteins, subcellular localization is important. The coordinated polar localization of the auxin-efflux carriers from the long PIN subfamily at the PM determines the direction of intercellular auxin flow and thus contributes to auxin distribution within tissues. The long PIN proteins undergo constitutive endocytic recycling, which allows dynamic changes of PIN polarity by transcytotic trafficking. In contrast, the short PINs (e.g.PIN5 and PIN8) have been shown to be localizedpredominantly to the ER. They mediate auxin flow between the cytoplasm and ER to regulate subcellular auxin homeostasis. The presumptive auxin receptor ABP1 is present both in the ER and in the PM. The receptor for the transcriptional auxin response pathway, TIR1/AFB, is found in the nucleus. PM: plasma membrane; ER: endoplasmic reticulum.

Auxin appears in three major pools in the cell: nuclear, cytosolic, and endoplasmic reticulum (ER), where it enables signaling events (Barbez and Kleine-Vehn, 2013) (Figure 2.5). Auxin is perceived both at the PM and in the nucleus (reviewed in (Hayashi, 2012; Wang and Estelle, 2014)). Perception of auxin at the nucleus is by TRANSPORT INHIBITOR RESPONSE 1 (TIR1) and AUXIN SIGNALING F-BOX PROTEIN 1-3 (AFB1, 2, 3). The TIR1/AFBs are the F-box subunit in SKP1-Cullin1-F-box (SCF)-type E3 ligases ($SCF^{TIR1/AFB}$). Auxin acts as

"molecular glue" enhancing the interaction of receptors with AUXIN/INDOLE-3-ACETIC ACID (AUX/IAA) repressors (Tan et al., 2007). Upon binding to auxin, the $SCF^{TIR/AFB}$ ubiquitin ligase complex is activated, resulting in degradation of the AUX/IAA repressors, which leads to the release of AUXIN RESPONSE FACTORs (ARFs) from AUX/IAA-ARF heterodimer complexes, thus activating early auxin responsive genes, including *AUX/IAA*, *SMALL AUXIN UP (SAUR)* and *GH3* gene families, that modulate development processes (Abel and Theologis, 1996; Hagen and Guilfoyle, 2002). In addition to this nuclear signaling pathway, rapid auxin responses involve another auxin receptor, termed AUXIN BINDING PROTEIN1 (ABP1). ABP1 is localized in the ER, but it is also associated with the PM (Henderson et al., 1997; Jones and Herman, 1993). Overexpression of ABP1 in tobacco BY-2 cells acts "auxin transport buffering role": with excessive PIN-dependent auxin transport action, ABP1 promotes PIN endocytosis to reduce undesirable auxin efflux (Čovanová et al., 2013). A third potential auxin receptor is the S-Phase Kinase-Associated Protein 2A (SKP2A), an F-box protein whose function has been found to be involved in the cell cycle regulation (Jurado et al., 2010).

Ethylene and auxin inhibitors

Aminoethoxyvinylglycine (AVG) was originally characterized as an inhibitor of ethylene biosynthesis, which irreversibly inhibits ACS, a PLP-dependent enzyme (Rando, 1974). Aminooxyacetic acid (AOA) is a hydroxylamine analog, also competing for binding of ACS catalytic site, but it is less effective than AVG (Bradford et al., 1982). However, it was demonstrated that AVG and AOA are general PLP enzyme inhibitors, inhibiting Trp-aminotransferase involved in auxin biosynthesis and transaminase in nitrogen metabolism as well (Leblanc et al., 2008; Soeno et al., 2010). α-aminoisobutyric acid (AIB) and Cobalt ions (Co^{2+}) are inhibitors of ACO activity (Lau and Yang, 1976; Satoh and Esashi, 1980). AIB can also compete with ACC, for instance by modifying ACC homeostasis through conjugation (Martin et al., 1995). Silver ions (Ag^{+}), applied as silver nitrate or silver thiosulfate, was assumed to interfere with ethylene receptors at the site occupied by copper ion (Cu^{2+}) (Beyer, 1976). Ag^{+} can also restore root elongation by promotion of IAA root efflux independently of ethylene perception. 1-Methylcyclopropene (1-MCP) is the most effective inhibitor of ethylene receptors, but it remains dependent on fumigation in a closed system, limiting its use. A specific ACS inhibitor, 2-anilino-7-(4-methoxyphenyl)-7,8-dihydro-5(6H)-quinazolinone (7303) has been identified from a chemical genetics screen (Lin et al., 2010) (Figure 2.6). The discovery of such chemical will be useful in ethylene research and may offer potential for agrochemicals, for example, in the quality improvement of post-harvest.

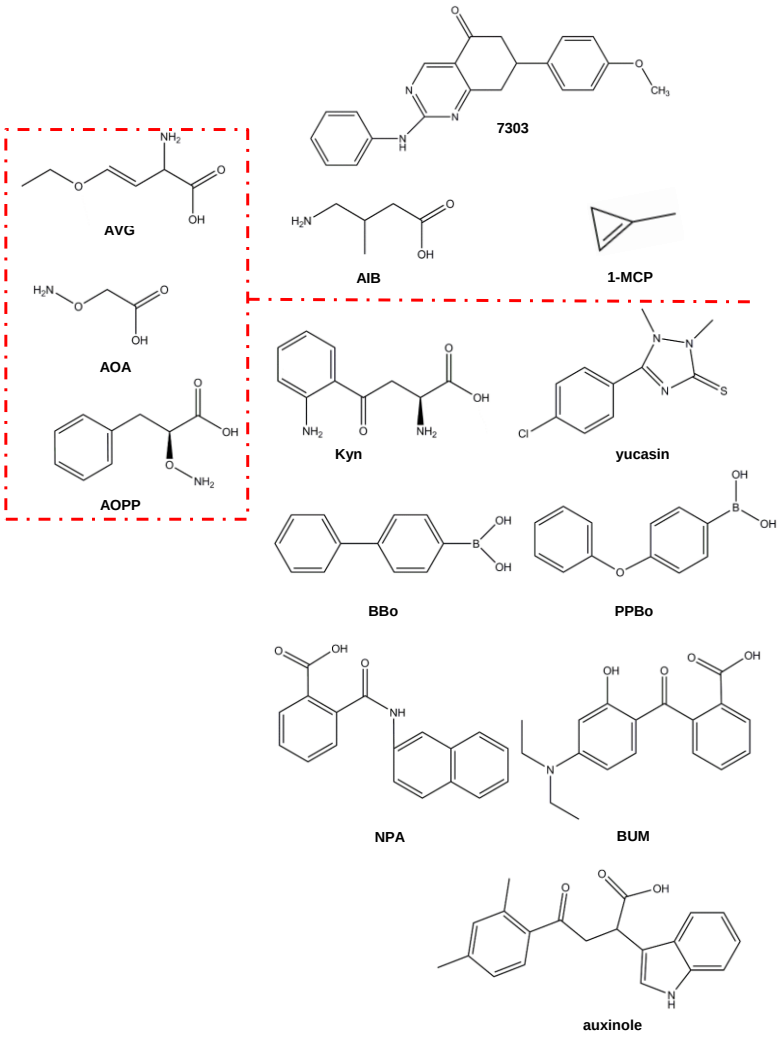

Figure 2.6 Inhibitors of ethylene and auxin. Aminoethoxyvinylglycine (AVG), aminooxyacetic acid (AOA) and L-2-aminooxy-3-phenylpropionic acid (AOPP) are used as ethylene inhibitors, which also inhibits auxin biosynthesis; 2-anilino-7-(4-methoxyphenyl)-7,8-dihydro-5(6H)-quinazolinone (7303), α-aminoisobutyric acid (AIB) and 1-Methylcyclopropene (1-MCP) are used as ethylene inhibitors; L-kynurenine (Kyn), 5–(4–chlorophenyl)-4H-1,2,4–triazole-3–thiol (yucassin), 4-biphenylboronic acid (BBo) 4-phenoxyphenylboronic acid (PPBo), N-1-naphthylphthalamic acid (NPA), BUM and auxinole are the auxin inhibitors.

Inhibitors of auxin biosynthesis, transport and signaling have been widely characterized (reviewed in (Hayashi and Overvoorde, 2013; Ma and Robert, 2013)). Aminoethoxyvinylglycine (AVG), aminooxyacetic acid (AOA) and L-2-aminooxy-3-phenylpropionic acid (AOPP) were characterized as auxin biosynthesis inhibitors, which reduce endogenous IAA levels by inhibiting Trp-aminotransferase, the first enzyme in the IPA-dependent pathway (Soeno et al., 2010) (Figure 2.6). However, these inhibitors are nonspecific, as they also affect other (PLP)-dependent enzymes. AVG and AOA were identified inhibiting ethylene biosynthesis by blocking ACS activity. Using a chemical genetics approach, other auxin biosynthesis inhibitors, L-kynurenine (Kyn), 5–(4–chlorophenyl)-4H-1,2,4–triazole-3–thiol (yucasin), 4-biphenylboronic acid (BBo) and 4-phenoxyphenylboronic acid (PPBo) were identified (Kakei et al., 2015). Kyn specifically

inhibits TAA1/TAR aminotransferases, while the others inhibit YUC. N-1-naphthylphthalamic acid (NPA) is the most widely used auxin transport inhibitor (ATI), which inhibits auxin efflux, thus limiting elongation and differential growth as well as lateral root development (Friml et al., 2002; Jensen et al., 1998; Reed et al., 1998; Thomson et al., 1973). ABCB1, 19 and the immunophilin-like protein, TWISTED DWARF1 (TWD1) are suggested NPA target proteins (Bailly et al., 2008; Nagashima et al., 2008; Noh et al., 2001; Rojas-Pierce et al., 2007). By chemical genetics screens, other ATIs were identified, such as 2-[4-(diethylamino)-2-hydroxybenzoyl]benzoic acid (BUM), which resembles NPA function, but is more effective on root PAT transport and root elongation (Kim et al., 2010). 1-naphthalene-oxy acetic acid (1-NOA) acts as an auxin influx inhibitor, possibly through AUX/LAXs (Parry et al., 2001; Yang et al., 2006). Thanks to the availability of TIR1-AUX/IAA structure information, a series of α-Alkyl IAAs were designed as antiauxins mediated by $SCF^{TIR1/AFB}$, such as butoxycarbonylaminohexyl-IAA (BH-IAA), while a weak auxin with a propyl chain (α-propyl-IAA) fits within the small cavity formed by Aux/IAA and does not block Aux/IAA binding (Hayashi et al., 2008). Based on the crystal structure of the TIR1-(BH-IAA) complex, auxinole (α-[2,4-dimethylphenylethyl-2-oxo]-IAA), an auxin antagonist with higher affinity for TIR1 was designed (Hayashi et al., 2012).

Tools to detect ethylene and auxin signals

The ethylene responses can be detected by *EBS:GUS*, in which the *β-glucuronidase* (*GUS*) reporter gene is driven by a synthetic EIN3-responsive promoter (Stepanova et al., 2007).

The most frequently used tools to monitor auxin distribution are *DR5*-based auxin-inducible reporters, which contains several ARF-binding sites, using TGTGTC as the auxin-responsive element fused to a constitutive promoter element (Ulmasov et al., 1997), driven the expression of a green fluorescent protein (GFP) or a reporter gene *GUS*, but it is adapted to measure auxin transcriptional output (Friml et al., 2003; Vernoux et al., 2011). To monitor directly the cellular auxin abundance, an AUX/IAA-based auxin-interaction domain II (DII) from IAA28 fused to the VENUS fast maturing yellow fluorescent protein under the constitutive 35S promoter, termed DII-VENUS, has been constructed; it is rapidly degraded in response to auxin (Brunoud et al., 2012). Alternatively, IAA can be quantified in whole tissues by liquid chromatography-mass spectrometry (Edlund et al., 1995; Kowalczyk and Sandberg, 2001) and isotope labeling (Cohen et al., 1986). In addition, a ratiometric luminescent biosensor that allows monitoring auxin dynamics in living cells was developed (Wend et al., 2013). Fluorescent auxin analogs 7-nitro-2,1,3-benzoxadiazole (NBD)-conjugated NAA (NBD-NAA) and NBD-IAA have been developed to visualize auxin distribution in both intercellular and subcellular levels (Hayashi et al., 2014).

Ethylene and auxin regulate seedling development

The crosstalk between ethylene and auxin in *Arabidopsis* seedling development is briefly reviewed for different tissues.

Regulation of primary root and root hair growth

Root growth is closely correlated with the root architecture (Brady et al., 2007; Dolan et al., 1993). Along the longitudinal axis, the primary root is characterized by a series of developmental zones: the meristematic zone (MZ), transition zone (TZ), elongation zone (EZ) and differentiation zone (DZ) (Jaillais and Chory, 2010; Verbelen et al., 2006). In the *Arabidopsis* root meristem, a small group of organized cells, the quiescent center (QC), surrounded by stem cells, form a stem cell niche (Sabatini et al., 2003), which continuously produces initial cells attributed to the root meristem after cell divisions. The TZ is wherein cell division rate slows and cell expansion starts (Nieuwland et al., 2009). In the EZ the cells undergo rapid longitudinal elongation. In the epidermal cell files, the first root hair bulge is marked as the start of DZ (Figure 2.7b).

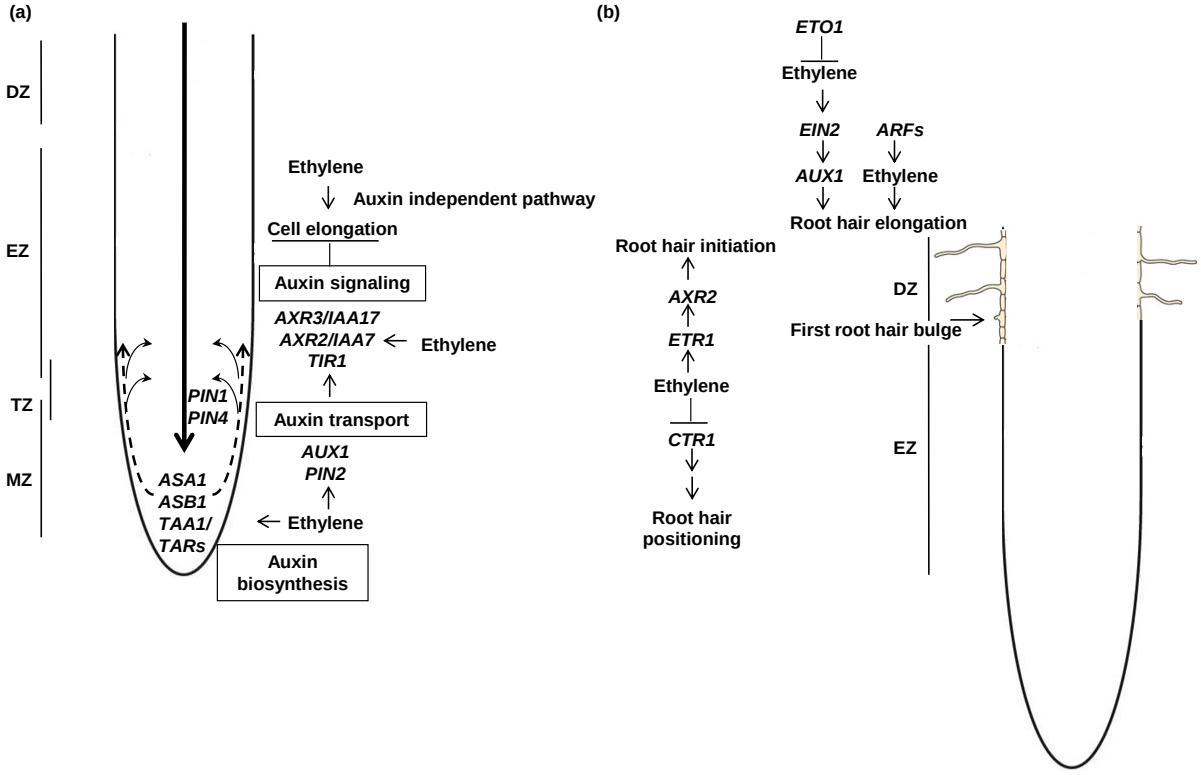

Figure 2.7 Auxin and ethylene synergistically inhibit root elongation and promote root hair emergence and elongation in etiolated seedlings (Ikeda et al., 2009; Masucci and Schiefelbein, 1996; Rahman et al., 2002; Růžička et al., 2007; Stepanova et al., 2005; Stepanova et al., 2008; Strader et al., 2010; Tanimoto et al., 1995). The growth zones in root apex, including meristematic zone (MZ), transition zone (TZ), elongation zone (EZ) and differentiation zone (DZ), where the root hair starts to initiate, are schematically depicted.
(a) Ethylene increases the capacity of local auxin biosynthesis in the root apex through *ASA1*, *ASB1*, *TAA1/TARs*, and affects auxin transport by regulating the transcription of acropetal auxin transporters *PIN1* and *PIN4*, as well as basipetal auxin transporters *AUX1* and *PIN2*. Subsequently, basipetal transported auxin activates auxin responses that is regulated by *TIR1* (auxin receptor), *AXR3/IAA17* and *AXR2/IAA7* (*AUX/IAAs*), inhibiting cell elongation. The selected components of the auxin responses are also required for ethylene inhibited root growth because mutants of *tir1*, *axr2-1* and *axr3-1* show an ethylene-insensitive root phenotype. Besides, an auxin independent pathway exists.
(b) Root hair initiation is inhibited in mutants defective in ethylene perception *(etr1)* while promoted in constitutive ethylene signaling (*ctr1*), which is attributed to the interruption of auxin signaling and biosynthesis; root hair elongation is most likely through modulation of the auxin levels mediated by auxin transporters (i.e. *AUX1/PIN2*).

Inhibition of root growth is one of the characteristic effects of ethylene or its precursor 1-aminocyclopropane-1-carboxylic acid (ACC). Mutants of *ETHYLENE OVERPRODUCER (eto(s))* and *CONSTITUTIVE ETHYLENE RESPONSE1 (ctr1)*, with an enhanced ethylene biosynthesis or signaling respectively, exhibit short roots (Guzman and Ecker, 1990; Kieber et al., 1993; Vogel et al., 1998; Woeste et al., 1999); in contrast, the inhibitory effect of ethylene on root growth is reduced in mutants with ethylene-insensitivity, such as *ETHYLENE RESISTANT1 (etr1)*, *ETHYLENE INSENSITIVE2 (ein2)*, *ein3, EIN3-like1 (eil1)* or in the presence of ethylene inhibitors, such as the biosynthesis inhibitor AVG and the perception inhibitor silver nitrate ($AgNO_3$) (Chao et al., 1997; Guzman and Ecker, 1990; Růžička et al., 2007).

Root growth rate is determined by the cell production in meristem and the cell elongation of cells leaving meristem. The reports of ethylene effects on cell division in roots are conflicting. Růžička et al., (2007) showed that ethylene does not affect mitotic activity in the root as evidenced by no changes of CYCLIN-DEPENDENT PROTEIN KINASE B1;1 (CYCB1;1) expression, a mitotic reporter. However, Ortega-Martínez et al. (2007) showed that ethylene can promote cell division in the QC. Later on, Thomann et al., (2009) showed that a *CULLIN3 (CUL3)* double loss-of-function mutant (*cul3a-3 cul3b-1*) displays a constitutive triple response and inhibits primary root growth by reducing root meristem size and cell number, which is ethylene-dependent. Recently, the role of ethylene in root meristem size through cell proliferation was confirmed by genetic and pharmacological analysis, where SHORT HYPOCOTYL 2 (SHY2/IAA3), a repressor of auxin signaling, acts as mediator of the ethylene response (Street et al., 2015).

It has been demonstrated that ethylene inhibits root growth primarily by inhibition of cell elongation in the root elongation zone (Le et al., 2001; Růžička et al., 2007; Swarup et al., 2007).

Auxins are also known to exert an inhibitory role on root growth, an effect that is most probably mediated in crosstalk with ethylene. An auxin gradient, established by local auxin biosynthesis and transport, is important for primary root growth. Increased auxin concentration and disrupted auxin transport negatively regulate primary root growth. For instance, treatment with exogenous auxins, *YUCCA* overexpressing plants, and auxin overproducing mutant *SUPERROOT2* (*sur2*) exhibit inhibited root growth (Delarue et al., 1998; Zhao et al., 2001). The boosted auxin levels in the EZ lead to induction of local auxin responses.

The mechanistic models of ethylene-auxin crosstalk in roots of *Arabidopsis* seedlings have been proposed based on several studies (Stepanova et al., 2007; Swarup et al., 2007). In summary, it is proposed that the inhibitory effect of root elongation by ethylene is in part mediated by stimulation of local auxin production and shootward auxin transport in the root apex and enhancing auxin response in the EZ (Figure 2.7a). Ethylene upregulates IAA biosynthesis in the *Arabidopsis* root tip as revealed by IAA measurements (Swarup et al., 2007). The transcription of *WEI2/ASA1/TIR7*, *WEI7/ASB1* and *TAA1/TARs*, enzymes involved in auxin biosynthesis, was upregulated by ethylene (Růžička et al., 2007; Stepanova et al.,

2005; Stepanova et al., 2008). Furthermore, the expression of *ACS(s)*, which catalyze the rate-limiting step in ethylene biosynthesis was positively regulated by auxin (Tsuchisaka and Theologis, 2004; Stepanova et al., 2007). This reveals a reciprocal regulation of auxin and ethylene biosynthesis. In addition, ethylene induces expression of *PIN1* and *PIN4*, the major acropetal auxin transporters towards root cap; as well as *AUX1* and *PIN2*, the major auxin transport carriers driving basipetal auxin transport from root cap to the EZ through the epidermal layers (Růžička et al., 2007). It was demonstrated that PIN1 and PIN2 levels are mediated by the POLARIS (PLS) peptide via ethylene signaling (Liu et al., 2013). Auxin response components are also required for ethylene inhibition of root growth in the EZ (Swarup et al., 2007). Mutants of auxin receptor *tir1* and auxin response *AUXIN RESISTANT axr2-1* and *axr3-1*, mutated in *IAA7* and *IAA17* respectively, show an ethylene-resistance root phenotype (Růžička et al., 2007; Stepanova et al., 2007);. The role of *ARF7* and *ARF19* was also tested but contradictory results are shown by different research groups. Li et al. (2006) claims an ethylene-resistant root growth in the etiolated *arf7* and *arf19* mutants, whereas Růžička et al. (2007) shows *arf7, arf19* and the corresponding double mutants exhibiting pronounced resistance to auxin but not to ethylene in the roots.

The ethylene-auxin crosstalk is further linked by flavonoids. Both ethylene and auxin can induce flavonol biosynthesis through distinct signaling pathways involving TIR1 and EIN2/ETR1, respectively, which converge on the MYB12 transcription factor (Lewis et al., 2011). Moreover, ethylene can inhibit root growth in an auxin-independent manner. One of the evidences is that ethylene can cause root length reduction in *aux1* (Swarup et al., 2007). A transcriptome analysis, including *aux1* and *ein2* mutants, suggested the existence of ethylene-regulated auxin-dependent and auxin-independent response gene sets, as well as auxin-regulated ethylene-dependent and independent gene sets (Stepanova et al., 2007).. The same transcriptional profiling study suggests the involvement of cell wall proteins as they are significantly enriched among genes co-regulated by auxin and ethylene (Stepanova et al., 2007). In this context, it has been shown that an elevated apoplastic ROS level in the EZ of Arabidopsis roots in response to ACC leads to callose deposition and cross-linking of hydroxyproline-rich glycoproteins in the cell wall, which is associated with the reduction in cell elongation (De Cnodder et al., 2005). Inhibition of cell elongation is associated with rearrangement of cortical microtubules (CMT), from transversal to longitudinal (Baluska et al., 1992; Steen and Chadwick, 1981). However, it is suggested that the reorientation may not be the cause of altered growth by ethylene since root cell elongation stops before the microtubule reorientation is established (Le et al., 2004). In addition, inhibition of wound-induced ethylene biosynthesis in pea roots does not affect wound-induced microtubule re-orientation (Geitmann et al., 1997). Similarly, it was recently demonstrated that auxin inhibits root cell expansion in a CMT-independent manner (Baskin, 2015).

Ethylene can also modulate differential root growth, as evidenced by its effects on gravitropism (Figure 2.8a). Exogenous ethylene or ACC can reduce or delay the root gravitropic response (Buer et al., 2006; Lee et al., 1990). It is proposed that gravity is sensed by starch granules (statoliths) in the statocytes, columella cells of the root cap. In vertically oriented roots, auxin transport sustains an equal distribution of auxin on both sides of the root.

When the root is horizontally oriented, auxin is redirected and transported more efficiently to the lower side of the root, resulting in an elevated auxin level at the lower side, inhibiting cell elongation, thus leading to downward growth (reviewed in (Geisler et al., 2014; Zadnikova et al., 2015)). Indeed, alteration of basipetal/shootwards auxin transport, either enhanced or reduced, abolishes root gravitropic curvature (Buer and Muday, 2004; Chen et al., 1998; Rashotte et al., 2000; Rashotte et al., 2001; Sukumar et al., 2009). Ethylene has been shown to downregulate auxin transport in root tips of maize and in epicotyls of pea (Lee et al., 1990; Suttle, 1988), while the role of ethylene is different in *Arabidopsis*, in which basipetal auxin transport was enhanced by ethylene through induction of *AUX1* and *PIN2* transcripts could explain the ethylene inhibitory effects on root gravitropism (Muday et al., 2012; Negi et al., 2008; Růžička et al., 2007). It could also be related to the elevated local auxin responses regulated by *AXR2/IAA7* and *AXR3/IAA17* since gain-of-function mutations in these loci display an altered gravitropic curvature and reduced ethylene sensitivity (Leyser et al., 1996; Lincoln et al., 1990; Timpte et al., 1995; Wilson et al., 1990). In the gravistimulated root of DR5-GFP, marker gene expression is enhanced on both sides of the roots upon ACC treatment, resulting in a reduced gravitropic curvature (Muday et al., 2012). Buer et al., (2006) suggested that ACC reduces gravitropism through ETR1 and EIN2; in addition, ethylene-enhanced flavonoid synthesis may cause reduced root gravitropism. Flavonoids are thought to act through ABCB4 to control basipetal auxin transport and gravitropism (Lewis et al., 2007), while ACC positively regulates basipetal auxin transport that is independent of flavonoid (Lewis et al., 2011).

In addition, ethylene affects root cell differentiation, which is represented by the initiation of root hairs from a subset of specialized epidermal cells called “trichoblasts (hair cells)”. It has been demonstrated that both ethylene and auxin positively regulate root hair development. For example, in the presence of exogenous ACC or in the *ctr1-1* mutant “non-hair” cells can develop into ectopic hair cells (Dolan et al., 1994; Tanimoto et al., 1995). The *ROOT HAIR DEFECTIVE6* (*rhd6*) mutant, displaying a reduction in the number of root hairs, an overall shift (towards the shoot) of the site of root hair emergence and a relatively high frequency of epidermal cells with multiple root hairs, can be rescued by exogenous ACC or IAA. Conversely, mutants of *axr2* and *etr1* have a similar phenotype as *rdh6* , as well as WT in the presence of hormone inhibitors (AVG) or transport inhibitors (NPA) (Masucci and Schiefelbein, 1994). In addition, *AXR2* gene is required for ethylene or auxin to induce root hairs (Masucci and Schiefelbein, 1996). Root hairs normally emerge from the apical end (towards the root tip) of a hair cell, which is based on the auxin influx- and efflux-carrier mediated auxin redistribution from a local auxin biosynthesis maximum in the root tip, referred to as planar polarity, i.e. the coordination of cell polarity within the plane of a single tissue layer (Grebe et al., 2002; Ikeda et al., 2009; Sabatini et al., 1999). Genetic evidence suggests that *AUX1*, showing impaired basipetal auxin transport from the root tip to elongating epidermal cells contributes to planar polarity, therefore *aux1* displays apical shifts of hair position and occasional formation of supernumerary hairs on single cells (Grebe et al., 2002). Mutation in *CTR1* leads to increased IAA synthesis in roots, and subsequently alters the proximal–distal placement of root hairs (Ikeda et al., 2009). In addition, the auxin biosynthesis mutants, *sur1* and *yuc1-D* which show elevated auxin levels, produce more

abundant and longer root hairs (Boerjan et al., 1995; Zhao et al., 2001). The major auxin signaling components, TRANSPORT INHIBITOR RESPONSE1 (TIR1), AUXIN SIGNALING F-BOX PROTEINs (AFBs) and the auxin signaling repressors Aux/IAAs have been involved in root hair growth as well (Dharmasiri et al., 2005; Leyser et al., 1996; Lincoln et al., 1990; Okada and Shimura, 1994; Wilson et al., 1990). In summary, the cross-talk between auxin and ethylene on root hair growth is complex, since the hormones impact reciprocally on one another. For instance, the root hair defective auxin signaling mutant *arf7arf19* can be rescued by ACC (Kapulnik et al., 2011), which suggests that ethylene works downstream of auxin on root hair growth. By contrast, decreased auxin transport (e.g. *aux1*) can suppress *eto1* promoted root hair elongation, which suggests auxin signaling acting downstream of ethylene signaling on root hair growth (Strader et al., 2010). The key interactive components between ethylene and auxin in root hair initiation and elongation are illustrated in Figure 2.7b.

Regulation of hypocotyl growth

Etiolated seedlings display a long hypocotyl in the dark, resulting from longitudinal cell expansion rather than cell division (Gendreau et al., 1997). Longitudinal cell expansion is correlated with a transversal orientation of CMT and changes in cell wall extensibility (Le et al., 2005; Refregier et al., 2004). CMT regulates the direction of cell expansion by directing the orientation of cellulose microfibrils (Paredez et al., 2006; Shibaoka, 1994; Wasteneys, 2004). Nevertheless, longitudinal CMT are predominant in the presence of ethylene in shoots of dark-grown seedlings (Le et al., 2005; Steen and Chadwick, 1981). The hypocotyl growth pattern upon ethylene exposure is different in light compared to darkness. Under white light, ethylene stimulates hypocotyl growth, while it inhibits in the dark (Smalle et al., 1997). The ethylene promoted hypocotyl elongation in the light was suggested regulated by the PHYTOCROME INTERACTING FACTORS 3 (PIF3)-dependent growth-promoting pathway and ERF1-mediated growth inhibiting pathway transcriptionally activated by EIN3 (Zhong et al., 2012). Moreover, ethylene regulates IAA biosynthesis, transport, and signaling during light-mediated hypocotyl growth, dependent on the effect of CONSTITUTIVE PHOTOMORPHOGENESIS1 (COP1) on downstream transcription of EIN3 (Liang et al., 2012). Another study suggested that ethylene enhances the movement of COP1 to the nucleus where it mediates the degradation of LONG HYPOCOTYL5 (HY5), a positive regulator of light signaling, contributing to the control of hypocotyl growth in the light (Yu et al., 2013). HY5 has also been shown regulating auxin response gene expression (Jing et al., 2013). Other genes were also shown mediating ethylene-auxin crosstalk, as for instance, *ROOTS CURL IN NAPHTYLPHTALAMIC ACID 1* (*RCN1)*, which encodes a protein phosphatase 2A regulatory subunit A that was found in a screen for mutants with altered responses to NPA. *rcn1* mutant has an enhanced ethylene production and an altered auxin transport combined with inhibition of hypocotyl elongation (Muday et al., 2006; Skottke et al., 2011).

It was reported that auxin transport plays a more important role in light-grown hypocotyl elongation than in etiolated seedlings (Jensen et al., 1998). Auxin can promote or inhibit hypocotyl growth depending on the conditions (temperature, light intensity and nutrient medium) (Chao et al., 1997; Smalle et al., 1997). A threshold level exists to keep normal

hypocotyl growth; while a raise in auxin level would lead to inhibitory effects (Chao et al., 1997).

The seedling response to gravity is essential to survive underground germination. The upward growth of the shoot is triggered by gravity perception by the starch-filled amyloplasts in the hypocotyl endodermis cells. Mutants with reduced levels of starch, such as *phosphoglucomutase* (*pgm*), as well as mutants lacking endodermal tissue (e.g. *shoot gravitropism 1/scarecrow* (*sgr1/scr*) and *sgr7/short root* (*shr*)), have an agravitropic shoot phenotype, suggesting the importance of endodermal statoliths (Caspar and Pickard, 1989; Fukaki et al., 1998). Contrasting to the root and apical hook, lateral auxin redistribution leads to an auxin maximum at the more elongating (lower) side of the gravistimulated hypocotyl (Esmon et al., 2005). PIN3 is supposed to transport auxin laterally to the vasculature; upon gravistimulation, PIN3 is relocated to the new basal side of endodermal cells, where auxin is redirected to the outer cell layers along the new gravity vector (Ding et al., 2011; Friml et al., 2002). Lateral auxin redistribution also involves interruption of PIN1 and PGP19-mediated basipetal auxin transport in the hypocotyl (Figure 2.8a) (Blakeslee et al., 2004; Noh et al., 2003). Furthermore, the auxin signaling mutants *iaa3/shy2*, *iaa7/axr2*, *iaa14/slr*, *iaa17/axr3*, *iaa19/msg2*, *nph4/arf7* and *arf19* are defective in hypocotyl gravitropism (Harper et al., 2000; Okushima et al., 2005; Tatematsu et al., 2004). It was suggested that MSG2/IAA19 and NPH4/ARF7 may constitute a negative feedback loop to regulate differential growth responses of hypocotyls (Tatematsu et al., 2004). Ethylene can stimulate negative shoot gravitropism in darkness, which is dependent on AUX/IAA because of the complete resistance of axr3/iaa17 to ACC; alternatively, ARF7 and ARF19 regulate negative gravitropic growth by ethylene, however, since higher level of ACC can rescue phenotype of *arf7arf19*, other ARFs may be involved, or an ARF independent pathway exists (Vandenbussche et al., 2013). In the end, the output of the hormonal signaling cascades relies in part on modifications of the cell walls (Chen et al., 1999; Hoson et al., 2005). Not surprisingly, defects in the cell wall can change gravitropism and the cell wall strength is necessary to support the plant's own weight and the capacity of orientation is also essential for the negative gravitropism (Hoson et al., 2005).

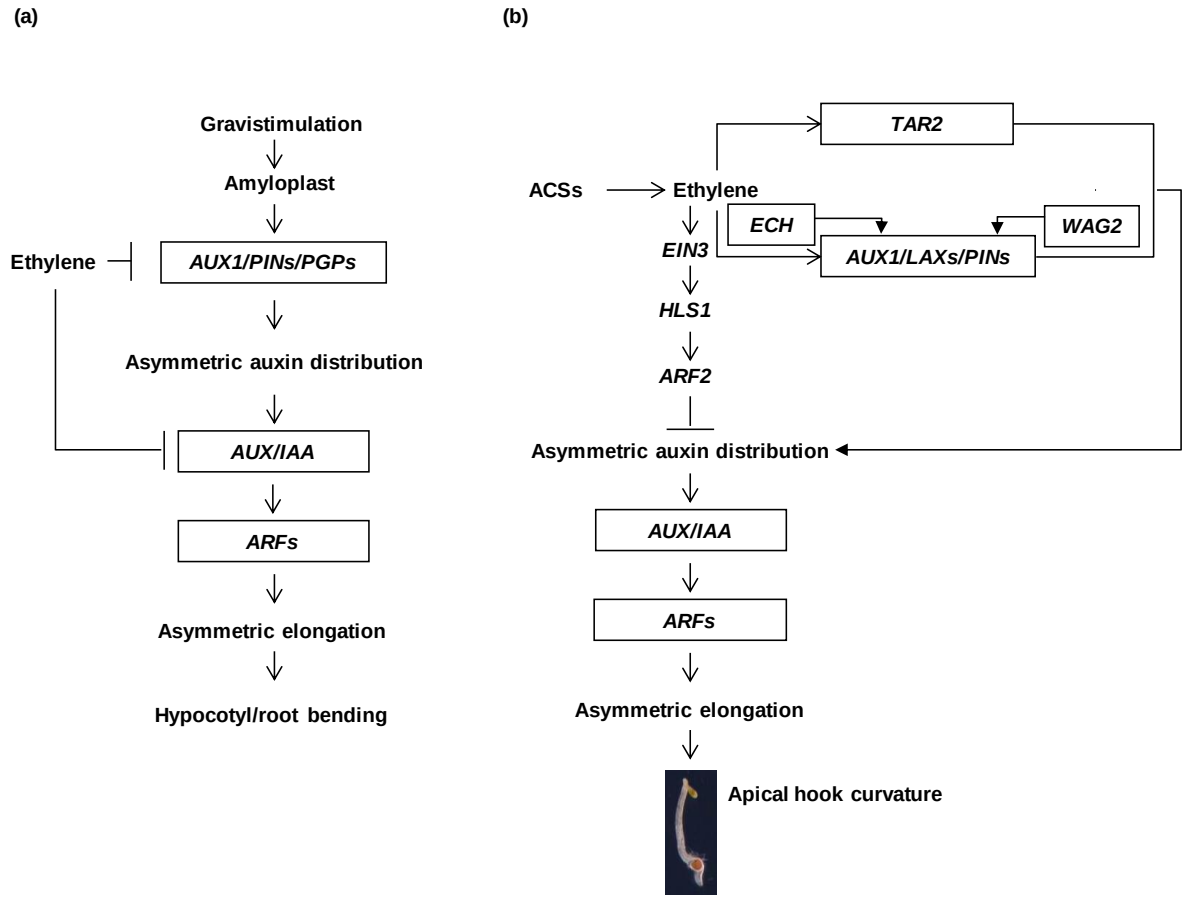

Figure 2.8 Model of the interaction between ethylene and auxin in differential growth of gravitropism and apical hook development of etiolated seedlings.
(a) Ethylene negatively regulates the gravity response in hypocotyl and root (Muday et al., 2012; Zadnikova et al., 2015).
(b) Ethylene induces asymmetric accumulation of auxin at the concave side of the hook through auxin biosynthesis (i.e. TAR2), polar auxin transport (i.e. *AUX1/LAX3/PINs*) and auxin signaling (*AUX/IAAs* and *ARFs*). Through *EIN3*, ethylene inhibits ARF2 protein accumulation in an *HLS1*-dependent manner to control the asymmetric auxin accumulation (An et al., 2012; Li et al., 2004; Vandenbussche et al., 2010; Zadnikova et al., 2010).

Regulation of apical hook development

The apical hook of dicotyledonous plants is developed upon underground germination, when the seedlings emerge from the soil. It protects the shoot apical meristem and cotyledons from damage. Hook development consists of three phases: formation, maintenance and opening (Raz and Ecker, 1999), which can be visualized by a time-lapse infrared imaging system (Smet et al., 2014). The hook is formed by the coordination of differential cell division and cell elongation (Raz and Ecker, 1999; Raz and Koornneef, 2001). Cell division is contributing mainly during the first 24 h of hook formation, where more dividing subepidermal cells are seen in the apical as compared to the basal part of the hook (Raz and Koornneef, 2001). Both hook formation and maintenance are contributed by differential cell elongation between opposite sides of the apical portion of the hypocotyl (Raz and Ecker, 1999), driven by a local auxin accumulation at the concave side, that inhibits cell elongation (Lehman et al., 1996; Schwark and Schierle, 1992). The auxin gradient disappears during hook opening, which is represented by the auxin response reporter DR5::GUS (Vandenbussche et al., 2010;

Zadnikova et al., 2010). The asymmetric auxin gradient during hook development requires normal auxin synthesis, transport and signaling. Exogenous auxin (Lehman et al., 1996; Vandenbussche et al., 2010) or auxin biosynthesis mutants, with more auxin, such as *sur1* (*superroot1*), *sur2* (Boerjan et al., 1995; Delarue et al., 1998), *yuc1-D* (yucca flavin monooxygenase dominant mutant) (Zhao et al., 2001), or less auxin such as *wei8-1 tar2-1* (*tryptophan aminotransferase 1/ tryptophan aminotransferase related 2*), have impaired hook formation or are hookless (Stepanova et al., 2008). Besides, blocking auxin transport using 1-NOA and NPA, lead to a hook deficient or hookless phenotype, indicating the importance of auxin transport in hook development (Lehman et al., 1996; Vandenbussche et al., 2010). As to the auxin transport proteins involved, auxin influx carriers AUX1, LAXs (Vandenbussche et al., 2010), the efflux carriers PIN1, PIN3, PIN4 and PIN7 (Friml et al., 2002; Zadnikova et al., 2010) as well as the ATP-BINDING CASSETTE (ABC) transporters, ABCB1 and ABCB19 (Wu et al., 2010), have been reported as key players. An AGC kinase, WAG2, was proposed to phosphorylate PIN3 to regulate auxin maximum required for apical hook maintenance (Willige et al., 2012). Besides, a trans-Golgi network (TGN)-localized protein ECHIDNA (ECH) was reported to be required for AUX1 exocytosis to the plasma membrane, which mediates the differential cell elongation in apical hook (Boutte et al., 2013). In addition, several mutants regulating the auxin dependent transcription machinery have been characterized showing defective hook formation, such as *axr1* (*auxin resistant1*) (Lehman et al., 1996; Leyser et al., 1993), *iaa1/axr5* (Yang et al., 2004), *iaa3/shy2* (Tian and Reed, 1999), *iaa17/axr3* (Leyser et al., 1996; Vandenbussche et al., 2010), *iaa19/msg2* (Tatematsu et al., 2004), *nph4 /arf7* and *arf19* (Harper et al., 2000). Moreover, plants expressing stabilized SAUR19-24 fusion proteins have impaired apical hook maintenance (Spartz et al., 2012). Time-lapse imaging of apical hook development shows that ethylene prolongs the formation phase of hook development, triggering exaggeration of the hook (Vandenbussche et al., 2010; Zadnikova et al., 2010). Notably, the sensitivity window for ethylene is restricted to 2 to 3 days after germination (Raz and Ecker, 1999). ACC synthase 5 (ACS5/ETO2) and ACS8-mediated ethylene production contributes to hook development (Tsuchisaka et al., 2009; Vogel et al., 1998). Through EIN3, ethylene activates HLS1 (HOOKLESS1) transcription, whereas it inhibits ARF2 protein accumulation in an HLS-dependent manner to control the asymmetric accumulation of auxin for hook formation and maintenance (An et al., 2012; Li et al., 2004). Upon ACC treatment, the auxin reporter DR5::GUS shows increased expression on the concave side of the hook (Li et al., 2004; Zadnikova et al., 2010). In addition, auxin transport mediates the effects of ethylene since NPA blocks hook formation of *eto1* and *ctr1*, which display exaggerated hook curvature (Lehman et al., 1996); while exogenous auxin can restore the hook formation of ethylene-insensitive mutants (Vandenbussche et al., 2010). Furthermore, ACC treatment increases the expression of PIN3::GFP and AUX1::GUS, which suggests that ethylene can affect auxin transport by up-regulation of auxin transporter genes (Vandenbussche et al., 2010; Zadnikova et al., 2010). Ethylene can also enhance the expression of TAR2::GUS as well as IAA3::GUS, IAA12::GUS, IAA13::GUS at the concave side of hook (Vandenbussche et al., 2010; Zadnikova et al., 2010). Together it is suggested that a threshold level of auxin is necessary for hook curvature; ethylene signaling is necessary to achieve this threshold by altering auxin synthesis, transport, and signaling. The interaction between ethylene and auxin in apical hook development was schematically shown in Figure

2.8b. Yet a larger hormonal network appears to affect apical hook development, reviewed in (Abbas et al., 2013; Mazzella et al., 2014; Zadnikova et al., 2015).

Conclusions and perspectives

This chapter summarized the role of ethylene and its crosstalk with auxins in the early stage of seedling development. Many aspects of seedling growth regulated by ethylene are auxin-dependent throughout alterations of auxin biosynthesis, transport and signaling. It highlighted the importance of an auxin gradient, established by local auxin biosynthesis and transport that can be controlled by ethylene. The increased ethylene biosynthesis caused by high auxin levels support a bi-directional control mechanism for ethylene-auxin interactions.

Current studies are focusing on a certain developmental stage. Since a hormonal physiological response is a dynamic process affected by time and space, therefore, a study of temporal aspects of ethylene-auxin transcriptional regulation will provide more insight in this crosstalk.

In addition, information about the interaction between ethylene and auxin is limited in crop species, for example in tomato (Solanum lycopersicum) (Santisree et al., 2012). However, it has been suggested that ethylene signaling could modulates auxin synthesis and/or transport to trigger the pathway responsible for the penetration of roots in the soil. One the other hand, some aspects are not conserved. For example, ethylene has been shown to downregulate auxin transport in root tips of maize (*Zea may*s) and in epicotyls of pea (Pisum sativum) (Lee et al., 1990; Suttle, 1988), but the role of ethylene is opposite in *Arabidopsis*. We can always compare the results between *Arabidopsis* and crop species, and use the research tools from *Arabidopsis* to investigate the crop species.

Chapter 3

TR-DB: An open-access database of compounds affecting the ethylene-induced triple response in *Arabidopsis*

Adapted from:

Hu Y, Callebert P, Vandemoortel I, Nguyen L, Audenaert D, Verschraegen L, Vandenbussche F, Van Der Straeten D (2014) TR-DB: An open-access database of compounds affecting the ethylene-induced triple response in *Arabidopsis*. Plant Physiol Biochem 75C: 128-137

Contribution:

YH performed experiments; analyzed the data and wrote the manuscript; DVDS and FV designed experiments, analyzed data and wrote the manuscript; PC created the original TR-DB in Access; IV and LV created the TR-DB web Application; LN and DA set up the primary screening; DVDS coordinated the project. All authors read and commented on the manuscript.

Abstract

Small molecules which act as hormone agonists or antagonists represent useful tools in fundamental research and are widely applied in agriculture to control hormone effects. High-throughput screening of large chemical compound libraries has yielded new findings in plant biology, with possible future applications in agriculture and horticulture. To further understand ethylene biosynthesis/signaling and its crosstalk with other hormones, we screened a 12,000 compound chemical library based on an ethylene-related bioassay of dark-grown *Arabidopsis thaliana* (L.) Heynh. seedlings. From the initial screening, 1313 (~11%) biologically active small molecules altering the phenotype triggered by the ethylene precursor 1-aminocyclopropane-1-carboxylic acid (ACC), were identified. Selection and sorting in classes were based on the angle of curvature of the apical hook, the length and width of the hypocotyl and the root. A MySQL-database was constructed (https://chaos.ugent.be/WE15/) including basic chemical information on the compounds, images illustrating the phenotypes, phenotype descriptions and classification. The research perspectives for different classes of hit compounds will be evaluated, and some general screening tips for customized high-throughput screening and pitfalls will be discussed.

Introduction

Ethylene (C_2H_4) is a gaseous plant hormone with profound effects throughout plant growth and development as well as in stress responses. Morphological changes in etiolated *Arabidopsis* seedlings grown in the presence of ethylene or its precursor 1-aminocyclopropane-1-carboxylic acid (ACC), referred to as "triple response" (an exaggerated apical hook, a radially swollen short hypocotyl and a short root, have been used to identify mutants defective in ethylene metabolism, cornerstones in the elucidation of the pathway (Dugardeyn and Van der Straeten, 2008). Figure 3.1 shows the typical triple response phenotype of 4 days old etiolated seedlings in the presence of 20 μM ACC in liquid (Figure 3.1a–c) or on agar containing medium (Figure 3.1d) compared to the mock-treated control. The major rate-limiting step in ethylene biosynthesis is ACC synthase (ACS), which converts the methionyl side chain of S-adenosylmethionine (AdoMet) to ACC. ACC is further oxidized to ethylene by ACC oxidase (ACO) under aerobic conditions. ACS and ACO are encoded by multigene families that are differentially regulated. In *Arabidopsis* there are eight functional ACS genes (ACS2, ACS4-9, ACS11). The ethylene overproducer mutants *eto* can emanate up to 50-fold more ethylene than the wild type by affecting ACS stability (Dugardeyn and Van Der Straeten, 2008). ACO is encoded by a multigene family of five members in *Arabidopsis*. ACO1, ACO2 and ACO4 are ethylene-related; the role of ACO AT1G12010 and AT1G77330 remains to be clarified. Furthermore, autocatalytic stress ethylene production is controlled by MAPK (mitogen-activated protein kinase) phosphorylation cascades, stabilizing ACS2/6 (Takahashi et al., 2007).

It was hypothesized that ACC might act as a signal independently of ethylene receptors or the canonical pathway downstream thereof (Xu et al., 2008). The ethylene biosynthesis inhibitors aminooxyacetic acid (AOA) and α-aminoisobutyric acid (AIB) reverted root cell expansion

defects in *fei1fei2* double mutants, while this was not the case when ethylene perception or signaling was disrupted, suggesting that ACC plays a distinct role in these processes.

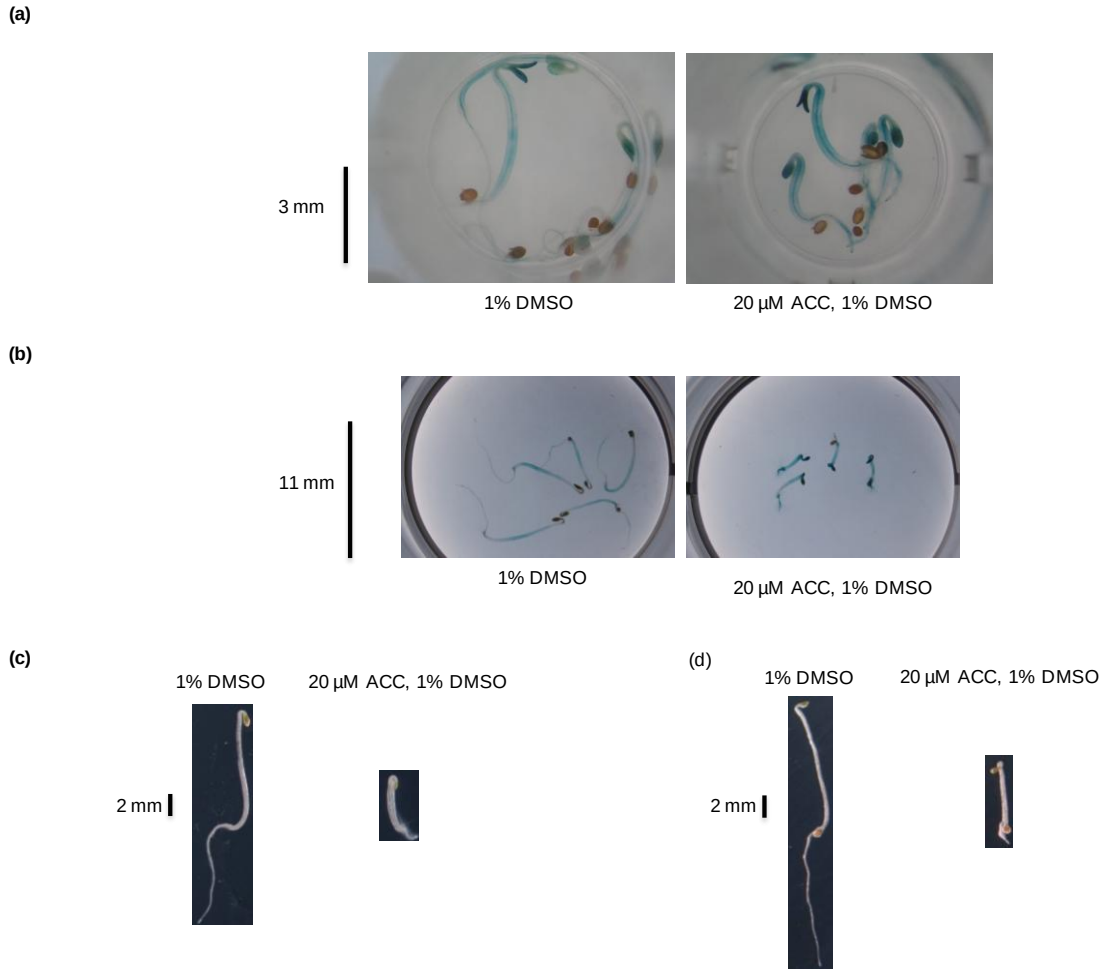

Figure. 3.1 Morphological features of 4-day old dark-grown seedlings in the presence of 20 µM ACC. EBS:GUS (Col-0) plants were grown in liquid medium in **(a)** 96-well plates (well diameter = 6 mm); **(b)** 12-well plates (well diameter = 22 mm). Col-0 seedlings grown in 12-well plates with **(c)** liquid medium or **(d)** agar containing medium.

In *Arabidopsis*, ethylene is perceived by a family of ER-transmembrane receptors, Ethylene Resistant 1 and 2 (ETR1, ETR2), Ethylene Response Sensor 1 and 2 (ERS1, ERS2) and Ethylene Insensitive 4 (EIN4), which require copper ions as a cofactor to bind ethylene (Rodriguez et al., 1999).

The mechanism of ethylene signaling is based on derepression. Essentially, in the absence of ethylene, the receptors activate CONSTITUTIVE TRIPLE RESPONSE (CTR1; (Kieber et al., 1993), which represses ETHYLENE-INSENSITIVE 2 (EIN2). In the presence of ethylene, receptor and CTR1 functions are blocked, activating EIN2 by dephosphorylation, leading to cleavage of its C-terminal end, which is translocated to the nucleus (Ju et al., 2012). This triggers a transcription cascade involving EIN3/EIN3-Like1 (EIL1) and ethylene response factors (ERFs), which act as activators or repressors (Alonso et al., 2003) of target genes such as HLS1 (HOOKLESS1), (Li et al., 2004), a factor linking auxin and ethylene pathways. While stability of EIN2 is controlled by EIN2 targeting proteins (ETP1-2; (Qiao et al., 2009)),

EIN3/EIL1 protein stability is regulated by EIN3 BINDING F-BOX PROTEINS (EBF1/2). Small molecules have proven their importance in agronomy as blockers or activators of ethylene action, albeit that none show specific action (Hu et al., 2013). Ethylene gassing is still used to accelerate (postharvest) ripening of climacteric fruit. Ethephon (2-chloroethylphosphonic acid, marketed as Ethrel) was discovered as an ethylene releasing compound that can be absorbed by, and transported within the plant. In addition, several small chemicals have been characterized as inhibitors of ethylene biosynthesis and binding, and are used in agri-/horticultural applications. Aminoethoxyvinylglycine (AVG, commercialized as Retain), an inhibitor of pyridoxal phosphate-mediated reactions, decreases ethylene production by inhibiting ACS activity. However, AVG is likely inhibiting most PLP-dependent enzymes, and has recently been reported to inhibit auxin biosynthesis by blocking Tryptophan (Trp) aminotransferase activity. Another type of ACS inhibitors are hydroxylamine analogs, which react with PLP to form stable oximes, such as AOA; again however, lacking specificity. AIB is the only known ACC analog that significantly and competitively inhibits ACO, albeit less effective than the ACS inhibitors mentioned above. Silver ions, applied as silver nitrate ($AgNO_3$) or as silver thiosulfate ($Ag_2(S_2O_3)$- (STS)), can substitute for copper as a cofactor for ethylene binding activity in the ETR1 ethylene receptor, yet also inhibit ethylene responses in plants. Moreover, silver was recently demonstrated to promote IAA efflux indicating that the use of silver ions to block ethylene signaling needs caution. Other antagonists of ethylene receptors are strained alkenes that have greater affinity to metal ion π-complexation than ethylene, including 2,5-norbornadiene (2,5-NBD), trans-cyclooctene (TCO) and 1-methylcyclopropene (1-MCP, marketed as EthylBloc and SmartFresh). Altogether, it is clear that there is a prominent need for specific ethylene biosynthesis/action blockers.

Chemical genetics recently emerged as a powerful tool to support the discovery of novel bioactive molecules interfering with ethylene response (Lin et al., 2010 and He et al., 2011). Chemical genetics can complement the classical mutation-based approach in the dissection of gene networks (Raikhel and Pirrung, 2005). Major advantages over traditional genetic approaches are the possibility to overcome loss-of-function lethality and gene redundancy, and the fact that it allows reversible and conditional control of a phenotype. In addition, the knowledge from studies of well-characterized bioactive chemicals and their targets identified in model systems can be translated to agronomical applications in non-genetically tractable species. Plants offer a perfect objective for phenotypic screening in chemical genetics since plant roots easily take-up small molecules (Walsh and Chang, 2006). In the past decade, over 50 papers have been published describing small compound screens which led to the identification of molecules that affect plant growth (for a review, see (Hicks and Raikhel, 2012; Sadhukhan et al., 2012); for screening tips, we refer to the website of the Cutler LAB (http://cutlerlab.blogspot.com/), for screening procedures, see (Norambuena et al., 2009; Zhao, 2012); for general methodology in the field, see (Bocobza et al., 2012; Cong et al., 2012; Rojas-Ruiz et al., 2011). However, only in few cases screening results have been released in the public domain. In plant research, two efforts were made to disseminate screening and bioactivity information in searchable databases: ChemMine (http://chemminedb.ucr.edu/ (Girke et al., 2005) and Library of AcTive Compounds in Arabidopsis

(LATCA, cutlerlab.blogspot.com/2008/05/latca.html). LATCA provides approximately 3600 compounds known to be bioactive based on their ability to influence etiolated hypocotyl growth in *Arabidopsis*, identified from combinatorial libraries. The compounds have been systematically characterized and classified in phenoclusters. Access to the database is provided upon request. ChemMine, now available in a new version, ChemMineV2, is a compound mining portal that facilitates drug and agrochemical discovery and chemical genomics screens. It covers seven databases including structure and phenotype data from specific screens, focusing on the auxin transport-regulated endomembrane system and the plant-specific Rop subfamily of Rho GTPases. Here we report on an open access database containing phenotypic information on the effects of 12,000 compounds on etiolated *Arabidopsis* seedlings grown in the presence of ACC. The compounds altering the phenotype triggered by ACC were sorted in classes, based on the angle of curvature of the apical hook, and on the length and width of the hypocotyl and the root. The primary purpose of this paper is to disseminate our findings to the plant hormone and the ethylene community in particular. Pitfalls of a high throughput approach are discussed, to help optimal design of a chemical library screening.

Results and discussion

Chemical genetics screening for interference with ethylene responses: design considerations

Essentially, screening of a library of chemical compounds can either be done based on a conspicuous phenotype related to the signal, or based on a reporter which is induced or repressed by the signal, or combining both approaches in confirmation of one another. Phenotypic screening is a rapid and direct way to analyze the effect of a chemical (Surpin et al., 2005, De Rybel et al., 2009 and De Rybel et al., 2012). Generally, a chemical genetics approach consists of a test-screening with a limited number of compounds, followed by the primary screening and further confirmatory experiments. Given that large libraries of compounds need a high throughput approach, at least in the primary screening phase, the assay has to be conceived in 96-well plates in liquid medium, with the chemicals dissolved in dimethyl sulfoxide (DMSO). Since ethylene is a gas, its application is not straightforward. Therefore, the ethylene precursor ACC was administered, which results in an increase of endogenous ethylene levels and induces the well-known triple response. We screened the chemical library for compounds that alter the triple response in ACC-treated dark-grown wild-type *Arabidopsis* seedlings. In principle, the absence of the triple response hints at compound-induced reduction in ethylene levels or inhibition of ethylene sensitivity or signaling. An exaggerated response indicates that the compound activates ethylene signaling by triggering higher ethylene levels or sensitising the ethylene signaling cascade. In addition to the phenotypic read-out, we used a reporter line of Col-0 harboring *EBS::GUS* (*EIN3 BINDING SITE::β-GLUCURONIDASE*) (Stepanova et al., 2007) to confirm the effect on ethylene response. With ACC, the *EBS::GUS* line shows an ethylene-induced expression in cotyledons, apical hook, root elongation zone and the root cap, whereas the non-treated control shows only a weak signal at the cotyledons, lower hypocotyl, and root elongation zone (Figure 3.1).

Once a biological assay suitable for rapid analysis is established, a chemical library can be chosen. We used a pre-plated DIVERSet™ library from ChemBridge™ (http://www.chembridge.com/index.php), which contains 12,000 chemicals with broad structural diversity. In principle, to improve solubility and membrane permeability, chemicals in the compound collection are selected based upon "druglike" physicochemical properties: MW (molecular weight) ≤ 500, logP (logarithm of the partition coefficient between n-octanol and water) ≤ 5, tPSA (topological polar surface area) ≤ 100, rotatable bonds ≤ 8, hydrogen bond acceptors ≤ 10 and hydrogen bond donors ≤ 5 (Lipinski et al., 2001). The availability of hit compounds and its analogues for follow-up studies after the initial screening is also an important point to be considered (Irwin, 2006). Out of 12,000 compounds in the DIVERSet™ library, 9881 are still available (searched on 07/08/2013). Thus, it is advisable to get information about restocking policies, resupply pricing, the prices charged for customized synthesis, and other vendors of compounds in advance.

For large-scale screening, automation of the system is essential. We performed the screening in 96-well plate format using the screening platform at the VIB Compound Screening Facility (CSF, Belgium). Due to technical reasons, the use of robotic handling platforms requires that the primary screening is performed in liquid medium. This increases the surface area between compounds and plantlet, which improves compound uptake compared to agar-based medium. However, the volume is critical, because plantlets may not be submerged completely to avoid water stress and allow oxygenation for the conversion of ACC to ethylene. In order to maximize the contact surface, avoid inhibitory effects of the ethylene effect, and to be applicable in the robotic system, 100 μL of medium was selected as the optimal volume in the primary assay.

The concentrations of chemicals during screening vary from case to case. In plant research, screenings have been done between 20 and 100 μM (Kim et al., 2011b; Surpin et al., 2005), which is in the same concentration range as for most precursors and antagonists of plant hormones (e.g. ACC works at 0.1–20 μM; ethylene antagonists AVG at 0.5–10 μM (Lin et al., 2010) and AOA up to 375 μM (Bradford et al., 1982; Xu et al., 2008a)). DMSO is generally used as a solvent. For *Arabidopsis* seedlings, DMSO needs to be kept at or below 1% (v/v) to prevent growth inhibition.

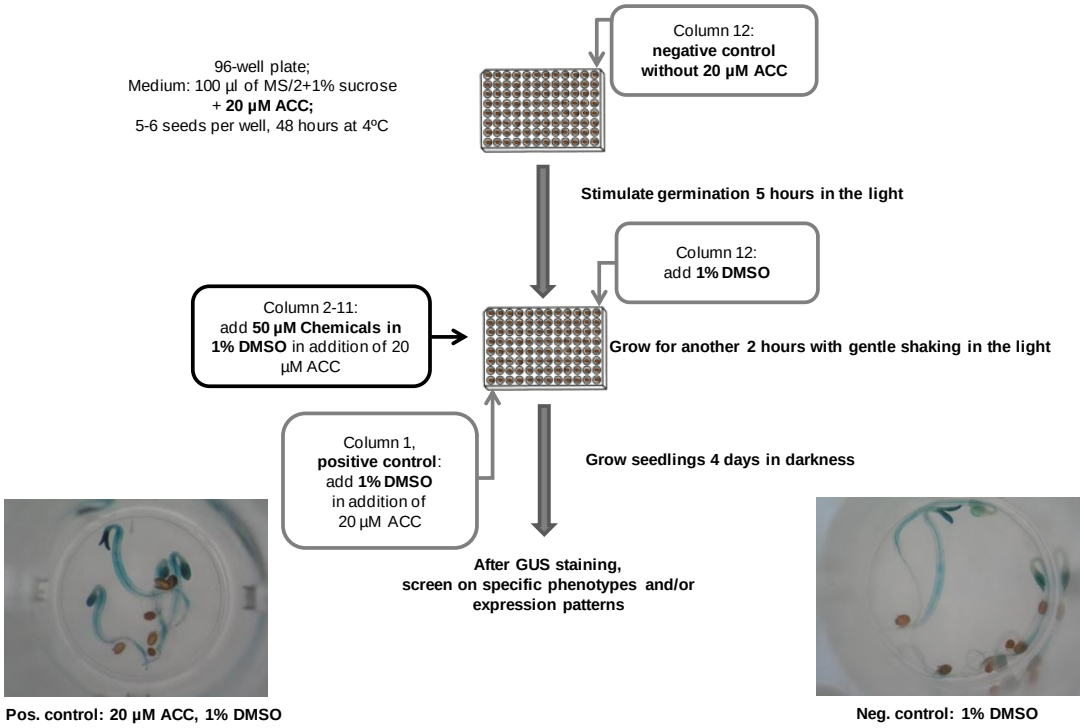

Figure. 3.2 Overview of the screening procedure used to establish TR-DB.

Phenotype-based screen and database assembly

To validate the automated screening procedure, we performed a pre-screen using a small library containing 480 DIVERSet™ compounds. The screening procedure is shown in Figure 3.2. Notably, the triple response phenotypes on 96-well plates differ from when it is done in other conditions, for example, in the same liquid medium but using a bigger plate (the diameter of the well is 22 mm (Figure 3.1b) instead of 6 mm (Figure 3.1a)), or using the medium containing agar (Figure 3.1d). The differences might due to the additive effects of spatially restricted and semi-submerged condition, in which the oxygen is less than in air. In addition, the batchwise variability exists as seen from controls on all the plates. Therefore, to correct for batchwise variability and normalization of the readout, proper controls were added to each plate. Plants incubated in 1% (v/v) DMSO were used as a negative control (column 12, 96-well plate), while plants treated with 20 µM ACC (1% (v/v) DMSO) were set as a positive control (column 1, 96-well plate). Phenotypes and expression patterns were scored after GUS staining. A complete screening of 12,000 diverse synthetic molecules (DIVERSetTM) was performed using the previously established assay (Figure 3.2). After GUS staining, the effects of the compounds were digitally recorded with a camera attached to a binocular. The phenotypes and staining patterns of the apical hook, hypocotyl and root were scored by comparing to the ACC and non-ACC treated controls on the same plate. Ten out of 150 plates (7%) were discarded because the phenotypes of the control plants deviated from the expected phenotypes. Moreover, due to robotized seed distribution, there is some variability in the number of seeds per well. When a minimum of 2 seeds were germinated and all seedlings showed similar effects of the compound, they were scored. Single seedlings were scored only if the phenotype was very pronounced.

A wide spectrum of biological activities was recorded. 1,313 out of 12,000 compounds were selected and classified under the 10 subclasses, 9 of which are based on the major morphogenic changes of the apical hook, hypocotyl and root compared to ACC-treated controls. These include hookless (121 compounds), hook deficient (466 compounds), exaggerated hook (134 compounds), short hypocotyl (308 compounds), fat hypocotyl (140 compounds), long root (122 compounds), short root (301 compounds), fat root (37 compounds) and 2,4-D (2,4-Dichlorophenoxyacetic acid)-like (114 compounds). Finally, one subclass compiles compounds which induce the changes in the GUS expression pattern (139 compounds). An example of the phenotype characteristic for each subclass is shown in Figure 3.3a. The hook angle of curvature was defined as previously described (Vandenbussche et al., 2010). When the apical part of the hypocotyl retained the same growth direction as the basal part, as is the case for the *hls1-1* mutant, seedlings were classified as "hookless" (Lehman et al., 1996); "hook deficient" was accredited to seedlings with a clear angle albeit smaller than that of the ACC-treated control). An example of a known "hook deficient" mutant is *aux1lax3* (Vandenbussche et al., 2010); "exaggerated hook" represents a bending exceeding that of the ACC-treated control (>180°). "Short" and "long" represent changes in length as compared to the ACC-treated control. "Fat" refers to radial expansion (Xu et al., 2008). The 2,4-D subclass corresponds to the phenotype mimicking 2,4-D treatment on Col-0 (Lehman et al., 1996). Compounds within this subclass are possibly linked to ethylene–auxin interactions. A number of compounds were classified under multiple subclasses (phenotypic categories). Two examples from the "exaggerated hook" subclass presented in Figure 3.3b, show that compounds may occur in common but also different phenotypic subclasses, suggesting that they have a different mode of action and may affect distinct pathways ultimately leading to hook exaggeration. Further molecular and/or genetic analysis is required to pinpoint the target of individual compound.

Figure 3.3 Examples of the different phenotype/staining pattern based categories in the database (see next page). (a) Information including total number of compounds in each subclass, an exemplary picture of the phenotype, the relative library ID & chemical structure, additional phenotypic features, and an estimation of possible function/pathway involved. **(b)** Two examples from the "exaggerated hook" subclass, showing that compounds within one subclass can affect other exhibit different other phenotypes, which are not necessarily shared.

(a)

Category in the database	Hookless	Hook deficient	Exaggerated hook	Short hypocotyl	Fat hypocotyl	Long root	Short root	Fat root	2,4-D like	Altered staining pattern
Total number in the subclass	121	466	134	308	140	122	301	37	114	139
Example	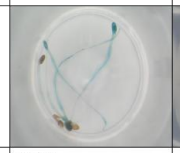	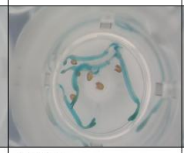	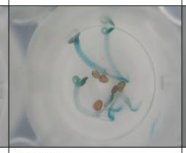			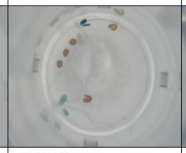	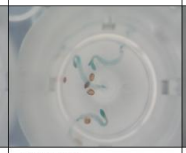			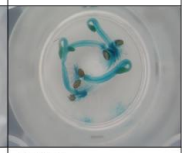
Library ID & Chemical structure	6825783 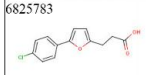	5219795 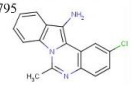	5194436 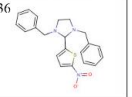	6368291 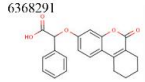	6284499 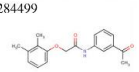	6537590 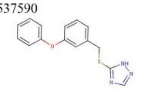	5226461 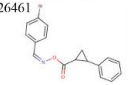	5233173 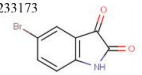	5200863 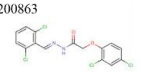	7569614 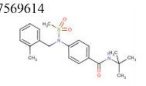
Other phenotypic categories	Long root	Altered staining pattern	-	Hookless	Hookless, short hypocotyl, short root	-	-	Short hypocotyl, fat hypocotyl, short root	-	-
Possible function/related pathway	Ethylene/auxin	Auxin-ethylene, gibberellins, brassinosteroids and light	Auxin-ethylene, gibberellins, brassinosteroids	Ethylene/auxin/ photomorphogenesis	Ethylene/ auxin/cell wall	Ethylene/ auxin/brassinosteroids	Ethylene/auxin/gibberellins	Ethylene/ cell wall biosynthesis	Ethylene-auxin interaction	Enhanced ethylene signaling

(b)

Category in the database	Exaggerated hook	
Other phenotypic categories	Long root	Altered staining
Phenotype	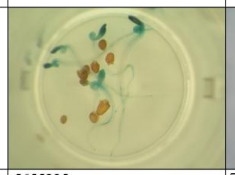	
Library ID & Chemical structure	5655235 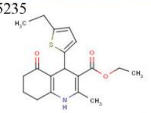	7545217 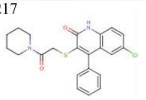

An image database including the phenotypes of seedlings exposed to the 12,000 small molecules was constructed (https://chaos.ugent.be/WE15/). Figure 3.4 illustrates the interface with 4 main parts:

1) Photographs (Figure S3.1a): a picture of the chemical-triggered phenotype is shown on the right; controls in the presence or absence of ACC are on the left. When clicking a picture, it can be viewed in the original format. Users can click the navigation button next to the control images to check images of all control seedlings on the same plate. The navigation button under the image of the chemical-triggered phenotype leads the user through all the photos of the selected subclass;

2) Control panel (Figure S3.1b): there are two drop-down menus and four navigation buttons. On the right, different subclasses, including the altered staining subclass and 9 phenotypic subclasses can be selected from the drop-down menu of the classification filter; on the left, different screening plates can be chosen from the plate drop-down menu or the navigation buttons "Prev(ious)" and "Next". The chemical-triggered phenotypes can be browsed by category throughout the plates. The navigation button "List" leads the user to the chemical information page. The "Home" button leads the user to the introduction page;

3) Staining pattern/phenotypic description (Figure S3.1c): on the right side of the chemical-triggered phenotype picture, a list of phenotypic characteristics is shown (green tick symbol indicates presence of a given phenotypic feature, red cross indicates absence);

4) Chemical information (Figure S3.1d): the full name of the compound can be seen. By clicking the chemical name, the user navigates to the Chembridge™ online chemical store (www.hit2lead.com), where more detailed information including LibraryID, chemical structure and other relevant information can be found. An example is shown in Figure S3.2a.

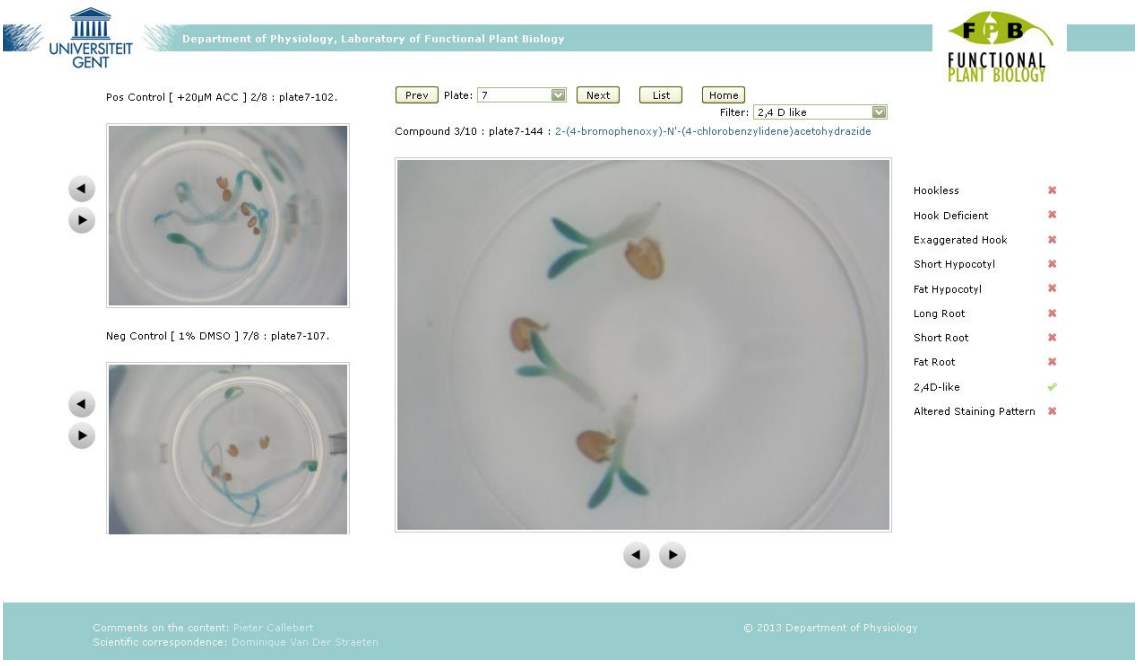

Figure 3.4 Example of a page on the TR-DB website, showing screening results.

To use the database, the users can browse a given subclass and find phenotypes relevant to their interests. Changes in the GUS expression pattern provide additional information. Promising compounds can be selected for further investigation at a glance. Alternatively, the compounds in one subclass can be screened in another condition, to see whether the phenotypes remain visible, suggesting an interaction between the two biological processes. For instance, a group of sulfonamides (folate biosynthesis inhibitors) originally selected from LATCA was recently rescreened on high sucrose medium, showing a synergistically inhibited hypocotyl elongation, indicating an interaction between sucrose and folates to regulate auxin signaling (Stokes et al., 2013). In TR-DB, 20 out of 308 compounds (Highlighted in yellow in Tab "short hypocotyl",Supplemental Table S3.1) in the "short hypocotyl" subclass showing inhibitory effects on hypocotyl elongation contain a sulfonamide core, supporting rationality and practicality of TR-DB.

Chemical analysis of candidate compounds

Bioactive compounds identified in the primary phenotypic screening are rarely the best candidates to use as research tools, but rather represent leads towards more active analogs. Structure–activity relationship (SAR) studies to reveal the correlation between biological effects of compound derivatives and their structure are important for further optimization towards possible future applications. Structural comparison of compounds can sometimes provide hints on their function, based on biological effects or known function of analogs (Surpin et al., 2005). For instance, the effect of a compound showing a phenotype similar to that of a known hormone but having a distinct structure, could be a promising lead for further analysis. A structurally related compound, substructure or derivative of the compound may also have more pronounced biological effects. Based on such search for structural analogs, Lin et al. discovered a quinazolinone more effective than the ethylene inhibitor initially identified in their screen. The chemical analogues or derivatives can either be found in the same library or from other sources, or an extended structure-related drug design can be applied. Some online databases like PubChem (http://pubchem.ncbi.nlm.nih.gov/) and ChemMine (http://chemminedb.ucr.edu/) can access chemicals from both academic and commercial sources, where compounds similar to the one of interest can be found. Information on metabolism of the compound can be searched from online sources, such as Scifinder (https://www.cas.org/products/scifinder), but often remains an open question.

Ultimately, the selected compounds should be stable and effective in a short-term response assay at low concentrations to avoid possible undesired effects of metabolites. This also bypasses complications upon target identification, since secondary effects can be avoided.

Confirmation of hit compounds and further research: case study on fat root phenotypes

An integral part of a chemical genetics screen is the validation and a mode-of-action study of hit compounds. Depending on the number of candidates, robotized or manual screening can be chosen for further confirmation of compound effects. Our secondary screen was performed on 12-well cell culture plates (well diameter, 22 mm) under the same condition as in the primary screen, albeit on solid medium. Dose-response measurements were performed to determine the optimal concentration for future experiments. In order to prove that the

observed phenotypes in our screening are genuinely ethylene-related, and not affecting ACC oxidation, it is necessary to confirm the phenotypes with exogenous ethylene in an open flow gassing system. Moreover, ethylene agonists or antagonists can be added to support that the effects of compounds are indeed ethylene-dependent. To dissect the function of compounds, their effect on mutants with constitutive or enhanced ethylene response, or causing ethylene insensitivity can be analyzed, as well as mutants related to other hormones which interact with ethylene. The level of ethylene production triggered by the compound can provide further indications to pursue the target. Furthermore, as the ethylene pathway interacts in an organ-dependent manner, with various other signaling pathways, the database could be used to identify compounds to investigate seedling development in general. Since the triple response is a very characteristic ethylene response, commonly found in etiolated dicot seedlings (albeit with some variants), the use of the compounds is not limited to *Arabidopsis* research, and may be informative in studies on other species. Moreover, the compounds have the potential to be used in fundamental and applied studies on ethylene regulation of postharvest physiology. For example, compounds causing ethylene insensitivity, could be further studied for their impact on climacteric or non-climacteric fruits, vegetables and cut-flowers, in comparison with currently available chemicals (e.g. STS, 1-MCP).

Two out of 37 compounds, 7579232 (Chembridge™ chemical access code) and 5233173, which showing the strongest "fat roots" phenotypes were chosen to confirm the effects in a manual screen. This "fat root" phenotype resembles the phenotype of *fei1 fei2* shown in Xu et al. (2008); the FEI proteins defined a novel ACC-mediated signal that regulates cell wall function. The root-swelling phenotypes were consistent with the primary screen (Figure 3.5). For compound 7579232, the typical swollen root phenotype appears at 50 μM, while compound 5233173 shows a swollen root phenotype at 10 μM. Interestingly, both compounds can induce a swollen root phenotype in the absence of ACC as shown in Figure 3.5b, indicating that addition of ACC is not essential to induce the fat root phenotype. However, as for *fei* fat root mutants, the endogenous ACC level may play an important role. Since *fei1fei2* mutants can be rescued by application of ethylene biosynthesis but not signaling inhibitors (Xu et al., 2008), AIB, a competitive inhibitor of ACC oxidase, was applied. Two mM of AIB largely reverted the swollen-root phenotype (Figure 3.5c and 3.5d), indicating that the endogenous level of ACC is important for the observed fat root phenotypes. Since a high salt or high sucrose condition is required to trigger the fat root phenotype in the *fei1fei2* double mutant, the role of the compounds identified here might be distinct from the pathway involving FEI1/2. More experiments need to be designed to find out the relation with ACC and other possible mechanisms, such as cellulose biosynthesis.

Towards target identification

The short-term effect of the compounds on the biosynthesis and signal transduction of ethylene can be assessed at the molecular level by in quantitative polymerase chain reaction (qPCR) of marker genes. To this end, the expression of EFE (ETHYLENE-FORMING ENZYME), EBF2 (EIN3-binding F-box protein 2), ETR2 (ETHYLENE RESPONSE 2) and other components related to the ethylene pathway can be evaluated (Alonso and Stepanova, 2003; De Paepe et al., 2004; Nemhauser et al., 2004). However, in order to identify the target

of the chemical compound, a broader insight into its effects can be provided by global gene-expression analysis using microarrays or RNA sequencing.

If the approaches mentioned above have generated an interesting lead, a screen can be designed to isolate either EMS or insertion mutants with altered responses to the compound (De Rybel et al., 2012). Next generation sequencing approaches allow swift and relatively low-cost identification of the corresponding genes that are affected (Egan et al., 2012). Moreover, a biochemical-based approach using affinity chromatography and high-resolution mass spectrometry analysis can be applied to complement the genetic approach to discover the direct target (Zheng et al., 2004). Several strategies have been developed to optimize the biochemical-based approach, for instance yeast-three-hybrid (Licitra and Liu, 1996), protein microarrays (Gong et al., 2008) and NMR-based metabolomics, allowing detection of low-abundant targets (Kim et al., 2011a).

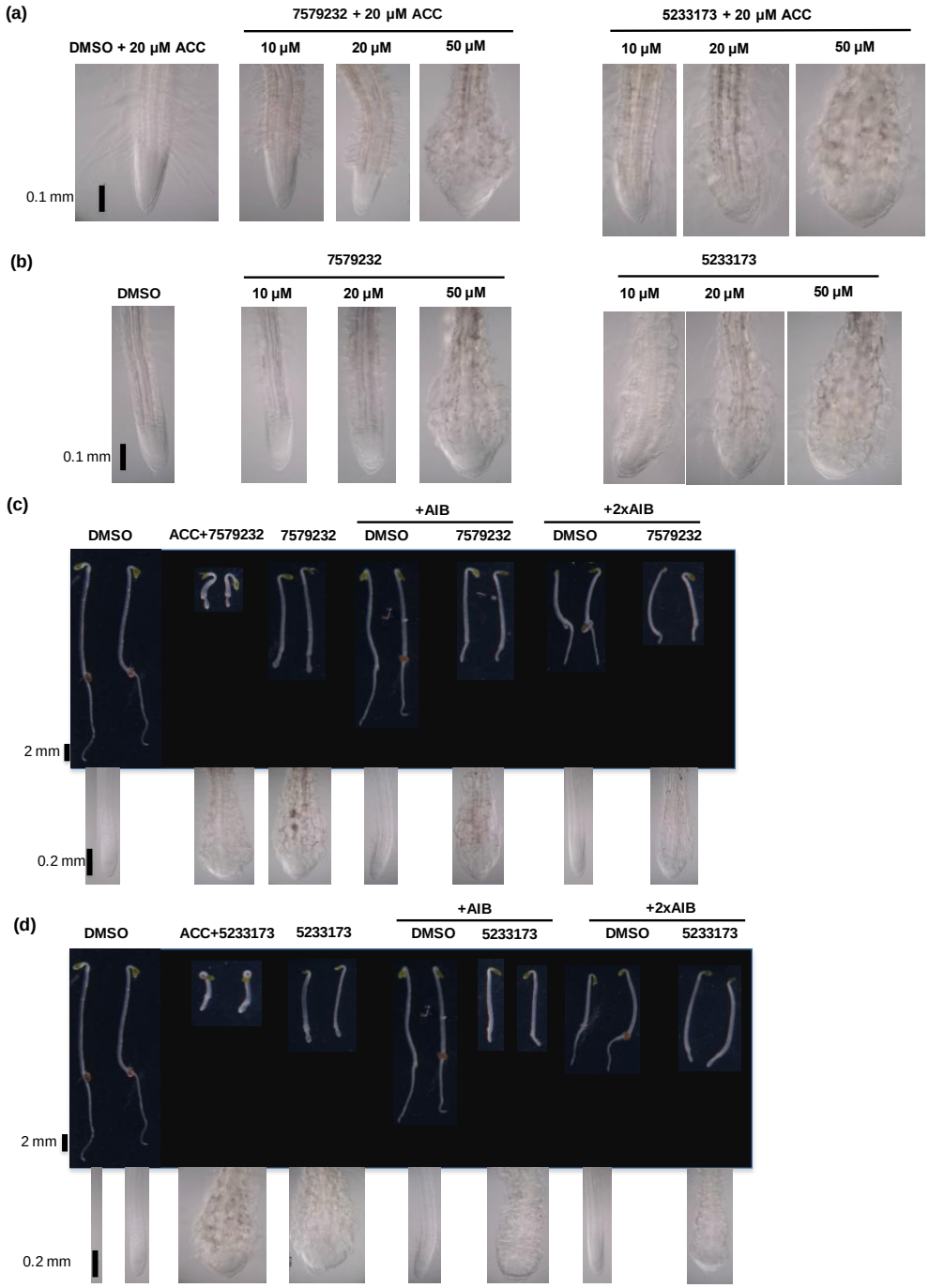

Figure 3.5 Combinatorial effect of ACC and the compounds triggering "fat root" phenotypes. Numbers indicate the ChemBridge™ chemical access code. Dose response assay of the two compounds in the presence **(a)** and **(b)** absence of 20 µM ACC. Wild type seedlings were grown on 1/2MS medium containing 1% sucrose supplemented with different amounts of the chemicals for 4 days in the dark; **(c)** Reversion of the fat root phenotype with α-AIB. Wild type seedlings were grown on 1/2 MS medium containing 1% sucrose plus DMSO, 20 µM ACC and chemical (at 10, 20 and 50 µM), chemical only, AIB (1 mM) or 2 mM AIB (2xAIB), as indicated. Beneath the respective panels, close-ups of the root tip are shown.

Conclusion

Because of the availability of huge chemical collections and the increasing number of screens performed, the development of databases covering bioactive molecules by phenotypic clustering is of primordial importance to serve the scientific community. We have presented

an open-access database on a high throughput chemical genetics screen on ethylene related traits, including a detailed manual (https://chaos.ugent.be/WE15/). It can be used for assay validation as the responses of the compounds are visible in the database. For instance, a small collection of bioactive compounds could be screened prior to a large scale screen using one of the compounds listed in TR-DB as a control to optimize the assay. In addition, the compounds in one subclass can be rescreened in an independent condition, to reveal interactions between the two biological processes. A phenotype-based clustering including screening results and related compounds from this database can help to interpret the results and to seek analogs based on initial hits as long as the clusters contain highly similar compounds. In addition, the compounds in the database or their related analogs can be used directly to identify known and novel targets of a process of interest, and thus can save time and investment for a primary screen.

Materials and Methods

High-throughput chemical screen and growth conditions

A DIVERSet™ library (ChemBridge Corporation, USA) containing 12,000 compounds was screened based on phenotypic changes of the *Arabidopsis thaliana* (L.) Heynh. Col-0 *EBS::GUS* (*EIN3 BINDING SITE::β-GLUCURONIDASE*) 1–11 reporter line at the Compound Screening Facility (VIB-UGent, Belgium). Chemicals were distributed into 384-well plates, at a stock concentration of 5 mM in dimethyl sulfoxide (DMSO). To preserve quality, stocks were kept in a 100% nitrogen atmosphere in order to avoid water uptake and oxidation (PlateStable™ conditioned storage system). Surface-sterilized seeds (5–6 per well) of the reporter line were robotically sown in 96-well filter plates (Multiscreen HTS MSBVS1210; Millipore, USA) in liquid medium (half strength Murashige and Skoog (1/2 MS) and 1% sucrose at pH 5.7), supplemented with 20 μM ACC, and cold treated for 48 h at 4 °C. Then, the plates were transferred to a growth chamber under continuous light (110 μmol m^{-2} s^{-1} photosynthetically active radiation, supplied by cool-white fluorescent tungsten tubes; Osram) at 22 °C to stimulate germination. After 5 h, the chemicals were added to a final concentration of 50 μM in 1% (v/v) DMSO and the plates were incubated for another 2 h with gentle shaking. Plants incubated with or without 20 μM ACC, in the absence of chemical compounds, were used as positive and negative controls, respectively. After that, the plates were removed from the shaker, wrapped with two layers of aluminium foil and incubated at 22 °C. Plant phenotypes and GUS staining patterns were analyzed 3 days after germination.

The secondary screen and small-scale experiments were performed on 22 mm (diameter) 12-well cell culture plates (Greiner Bio-one, Austria).

Analysis of the reporter line

For histochemical analysis of GUS expression, samples were treated with 90% ice-cold acetone for 30 min after removal of the liquid medium, washed with 0.1 M phosphate buffer (pH 7.2) for 15 min at room temperature and incubated at 37 °C overnight in GUS staining buffer containing 2 mM 5-bromo-4-chloro-3-indolyl-glucuronide (X-gluc, Duchefa, The

Netherlands), 0.1 M sodium phosphate buffer (pH 7.2), 0.5 mM potassium ferricyanide and 0.5 mM potassium ferrocyanide. Subsequently, the seedlings were kept in 70% ethanol until analysis. The analysis was done using a Zeiss Stemi SV11 binocular. An Olympus camera (CAMEDIA C5050zoom) attached to the binocular was used to make the pictures.

Differential interference contrast (DIC) Microscopy

To take close-up photos of the root tips, seedlings were mounted on the microscope slide in a solution containing 2.5 g of Chloral hydrate (Acros, USA) in 1 mL of 30% glycerol (Sigma–Aldrich, USA). DIC Microscopy images was captured with an AxioCam ICc3 camera attached to the Zeiss Axiovert 200 microscopy using AxioVision. Rel. 4.6 software (Carl Zeiss, Germany). A objective Plan Apochromat 10× was used.

Database setup

A MySQL™-database (http://www.mysql.com/) was constructed to store the results. Photos are managed using MediaMosa Open Source media management software (http://www.mediamosa.org/).

Supplementary data

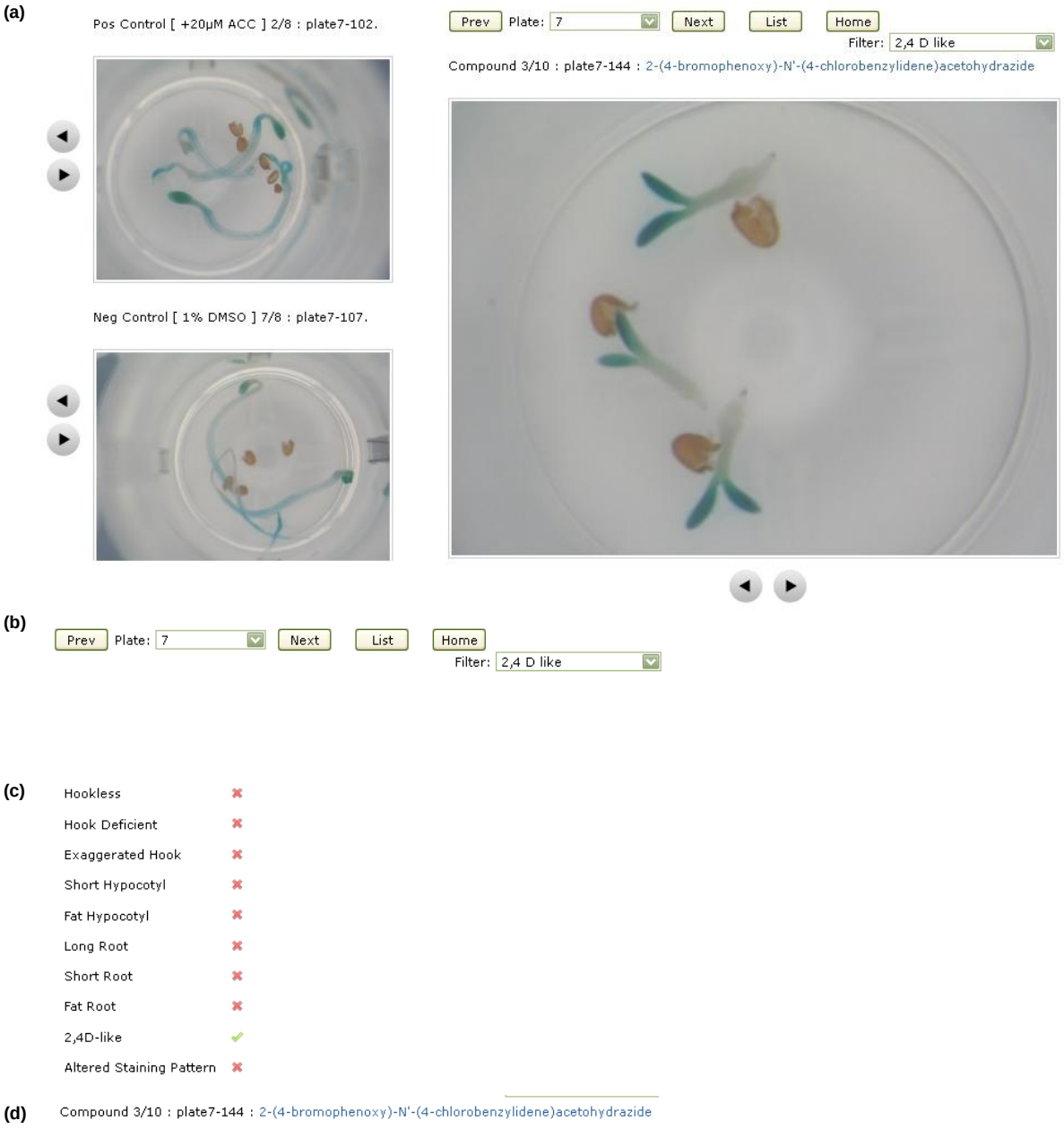

Figure. S3.1 Illustration of 4 main parts in TR-DB screening results page. (a) A photograph of the chemical-triggered phenotype is on the right, and controls in the presence (positive control) or absence (negative control) of ACC are on the left; navigation buttons are next to the photos. **(b)** Control panel including 2 drop-down menus and 4 navigation buttons. Drop-down menu on the right is a classification filter, including 1 altered staining subclass and 9 phenotypic subclasses; drop-down menu on the left is to navigate from plate to plate; alternatively, the two navigation buttons "Prev" and "Next" can be used; the navigation button "List" leads the user to the chemical information page; The "Home" button leads the user to the introduction page. **(c)** A complete staining pattern and additional phenotypic features are indicated on the right side of the chemical-triggered phenotype picture. **(d)** Chemical information: by clicking the chemical's name, the user navigate to the ChemBridge™ online chemical store (www.hit2lead.com).

(a)

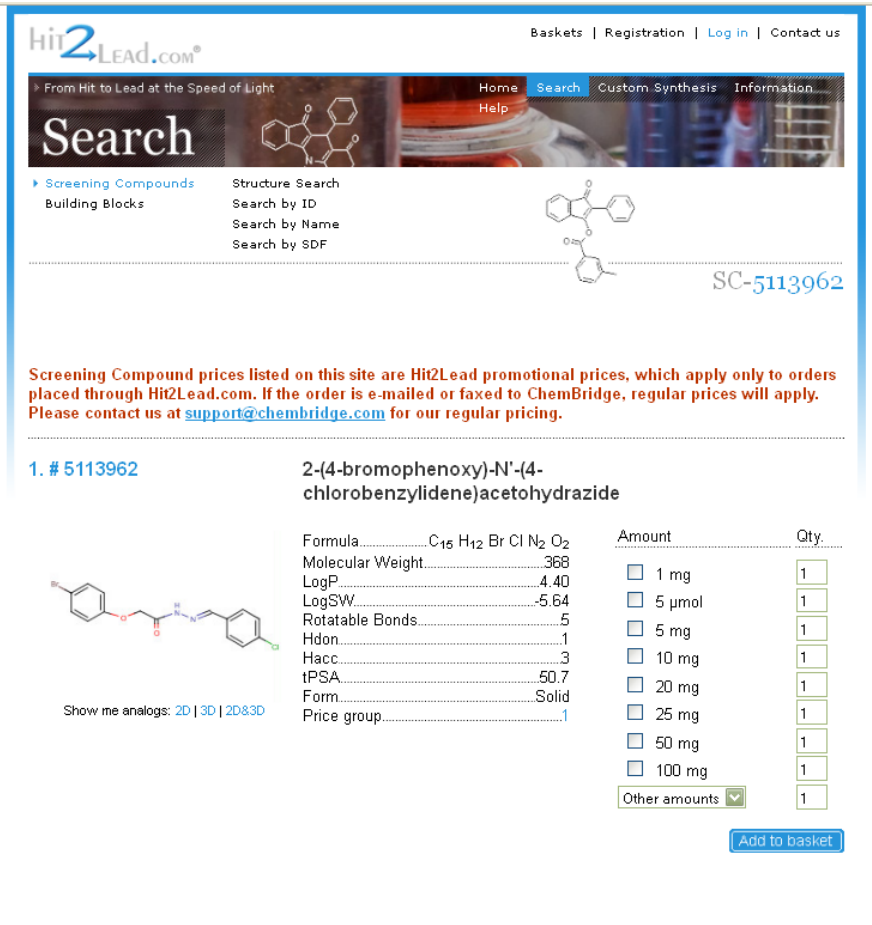

(b)

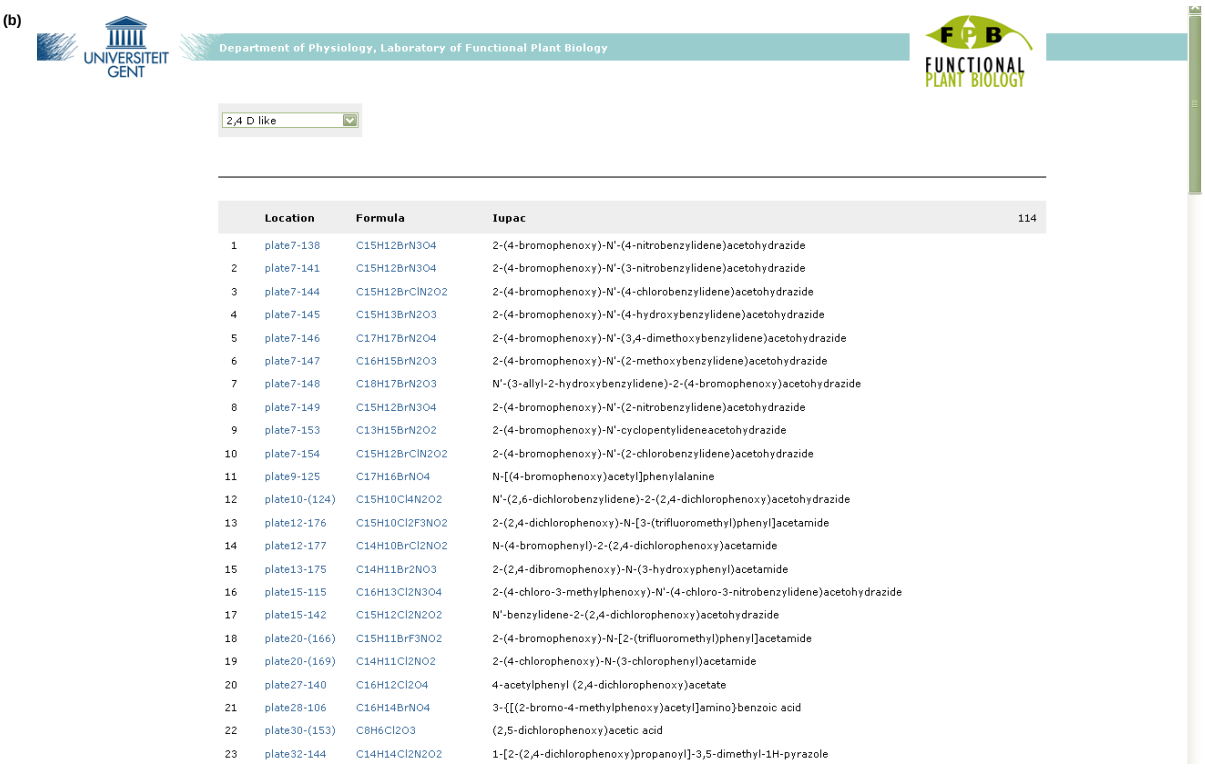

	Location	Formula	Iupac	114
1	plate7-138	C15H12BrN3O4	2-(4-bromophenoxy)-N'-(4-nitrobenzylidene)acetohydrazide	
2	plate7-141	C15H12BrN3O4	2-(4-bromophenoxy)-N'-(3-nitrobenzylidene)acetohydrazide	
3	plate7-144	C15H12BrClN2O2	2-(4-bromophenoxy)-N'-(4-chlorobenzylidene)acetohydrazide	
4	plate7-145	C15H13BrN2O3	2-(4-bromophenoxy)-N'-(4-hydroxybenzylidene)acetohydrazide	
5	plate7-146	C17H17BrN2O4	2-(4-bromophenoxy)-N'-(3,4-dimethoxybenzylidene)acetohydrazide	
6	plate7-147	C16H15BrN2O3	2-(4-bromophenoxy)-N'-(2-methoxybenzylidene)acetohydrazide	
7	plate7-148	C18H17BrN2O3	N'-(3-allyl-2-hydroxybenzylidene)-2-(4-bromophenoxy)acetohydrazide	
8	plate7-149	C15H12BrN3O4	2-(4-bromophenoxy)-N'-(2-nitrobenzylidene)acetohydrazide	
9	plate7-153	C13H15BrN2O2	2-(4-bromophenoxy)-N'-cyclopentylideneacetohydrazide	
10	plate7-154	C15H12BrClN2O2	2-(4-bromophenoxy)-N'-(2-chlorobenzylidene)acetohydrazide	
11	plate9-125	C17H16BrNO4	N-[(4-bromophenoxy)acetyl]phenylalanine	
12	plate10-(124)	C15H10Cl4N2O2	N'-(2,6-dichlorobenzylidene)-2-(2,4-dichlorophenoxy)acetohydrazide	
13	plate12-176	C15H10Cl2F3NO2	2-(2,4-dichlorophenoxy)-N-[3-(trifluoromethyl)phenyl]acetamide	
14	plate12-177	C14H10BrCl2NO2	N-(4-bromophenyl)-2-(2,4-dichlorophenoxy)acetamide	
15	plate13-175	C14H11Br2NO3	2-(2,4-dibromophenoxy)-N-(3-hydroxyphenyl)acetamide	
16	plate15-115	C16H13Cl2N3O4	2-(4-chloro-3-methylphenoxy)-N'-(4-chloro-3-nitrobenzylidene)acetohydrazide	
17	plate15-142	C15H12Cl2N2O2	N'-benzylidene-2-(2,4-dichlorophenoxy)acetohydrazide	
18	plate20-(166)	C15H11BrF3NO2	2-(4-bromophenoxy)-N-[2-(trifluoromethyl)phenyl]acetamide	
19	plate20-(169)	C14H11Cl2NO2	2-(4-chlorophenoxy)-N-(3-chlorophenyl)acetamide	
20	plate27-140	C16H12Cl2O4	4-acetylphenyl (2,4-dichlorophenoxy)acetate	
21	plate28-106	C16H14BrNO4	3-{[(2-bromo-4-methylphenoxy)acetyl]amino}benzoic acid	
22	plate30-(153)	C8H6Cl2O3	(2,5-dichlorophenoxy)acetic acid	
23	plate32-144	C14H14Cl2N2O2	1-[2-(2,4-dichlorophenoxy)propanoyl]-3,5-dimethyl-1H-pyrazole	

(c)

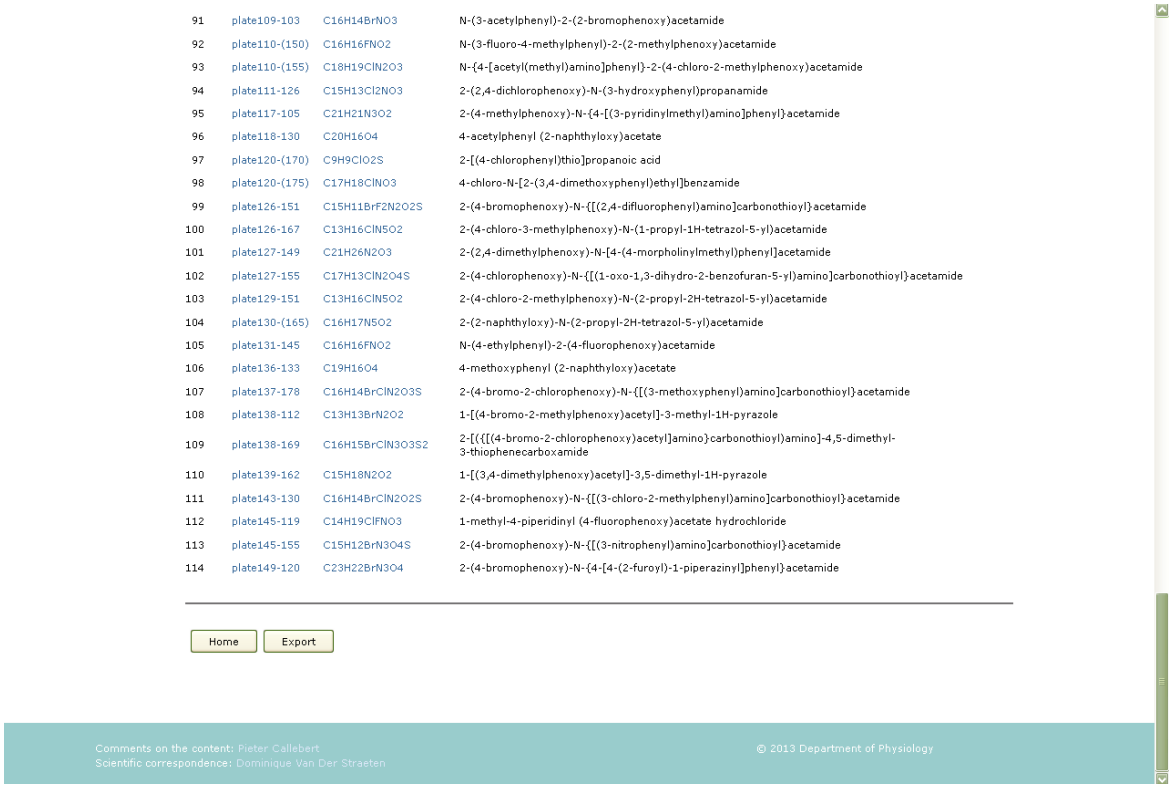

91	plate109-103	C16H14BrNO3	N-(3-acetylphenyl)-2-(2-bromophenoxy)acetamide
92	plate110-(150)	C16H16FNO2	N-(3-fluoro-4-methylphenyl)-2-(2-methylphenoxy)acetamide
93	plate110-(155)	C18H19ClN2O3	N-{4-[acetyl(methyl)amino]phenyl}-2-(4-chloro-2-methylphenoxy)acetamide
94	plate111-126	C15H13Cl2NO3	2-(2,4-dichlorophenoxy)-N-(3-hydroxyphenyl)propanamide
95	plate117-105	C21H21N3O2	2-(4-methylphenoxy)-N-{4-[(3-pyridinylmethyl)amino]phenyl}acetamide
96	plate118-130	C20H16O4	4-acetylphenyl (2-naphthyloxy)acetate
97	plate120-(170)	C9H9ClO2S	2-[(4-chlorophenyl)thio]propanoic acid
98	plate120-(175)	C17H18ClNO3	4-chloro-N-[2-(3,4-dimethoxyphenyl)ethyl]benzamide
99	plate126-151	C15H11BrF2N2O2S	2-(4-bromophenoxy)-N-{[(2,4-difluorophenyl)amino]carbonothioyl}acetamide
100	plate126-167	C13H16ClN5O2	2-(4-chloro-3-methylphenoxy)-N-(1-propyl-1H-tetrazol-5-yl)acetamide
101	plate127-149	C21H26N2O3	2-(2,4-dimethylphenoxy)-N-[4-(4-morpholinylmethyl)phenyl]acetamide
102	plate127-155	C17H13ClN2O4S	2-(4-chlorophenoxy)-N-{[(1-oxo-1,3-dihydro-2-benzofuran-5-yl)amino]carbonothioyl}acetamide
103	plate129-151	C13H16ClN5O2	2-(4-chloro-2-methylphenoxy)-N-(2-propyl-2H-tetrazol-5-yl)acetamide
104	plate130-(165)	C16H17N5O2	2-(2-naphthyloxy)-N-(2-propyl-2H-tetrazol-5-yl)acetamide
105	plate131-145	C16H16FNO2	N-(4-ethylphenyl)-2-(4-fluorophenoxy)acetamide
106	plate136-133	C19H16O4	4-methoxyphenyl (2-naphthyloxy)acetate
107	plate137-178	C16H14BrClN2O3S	2-(4-bromo-2-chlorophenoxy)-N-{[(3-methoxyphenyl)amino]carbonothioyl}acetamide
108	plate138-112	C13H13BrN2O2	1-[(4-bromo-2-methylphenoxy)acetyl]-3-methyl-1H-pyrazole
109	plate138-169	C16H15BrClN3O3S2	2-[({[(4-bromo-2-chlorophenoxy)acetyl]amino}carbonothioyl)amino]-4,5-dimethyl-3-thiophenecarboxamide
110	plate139-162	C15H18N2O2	1-[(3,4-dimethylphenoxy)acetyl]-3,5-dimethyl-1H-pyrazole
111	plate143-130	C16H14BrClN2O2S	2-(4-bromophenoxy)-N-{[(3-chloro-2-methylphenyl)amino]carbonothioyl}acetamide
112	plate145-119	C14H19ClFNO3	1-methyl-4-piperidinyl (4-fluorophenoxy)acetate hydrochloride
113	plate145-155	C15H12BrN3O4S	2-(4-bromophenoxy)-N-{[(3-nitrophenyl)amino]carbonothioyl}acetamide
114	plate149-120	C23H22BrN3O4	2-(4-bromophenoxy)-N-{4-[4-(2-furoyl)-1-piperazinyl]phenyl}acetamide

Figure. S3.2 Chemical information of the screened compounds. (a) An example of a chemical information page from the ChemBridge™ online chemical store (www.hit2lead.com). **(b)** and **(c)** Webpage of the screened compounds: Full list of compounds or a certain subclass can be selected from the drop-down menu on the top of the webpage **(b)**; the selected list can be exported as an excel file using the "export" button at the bottom of the webpage **(c)**.

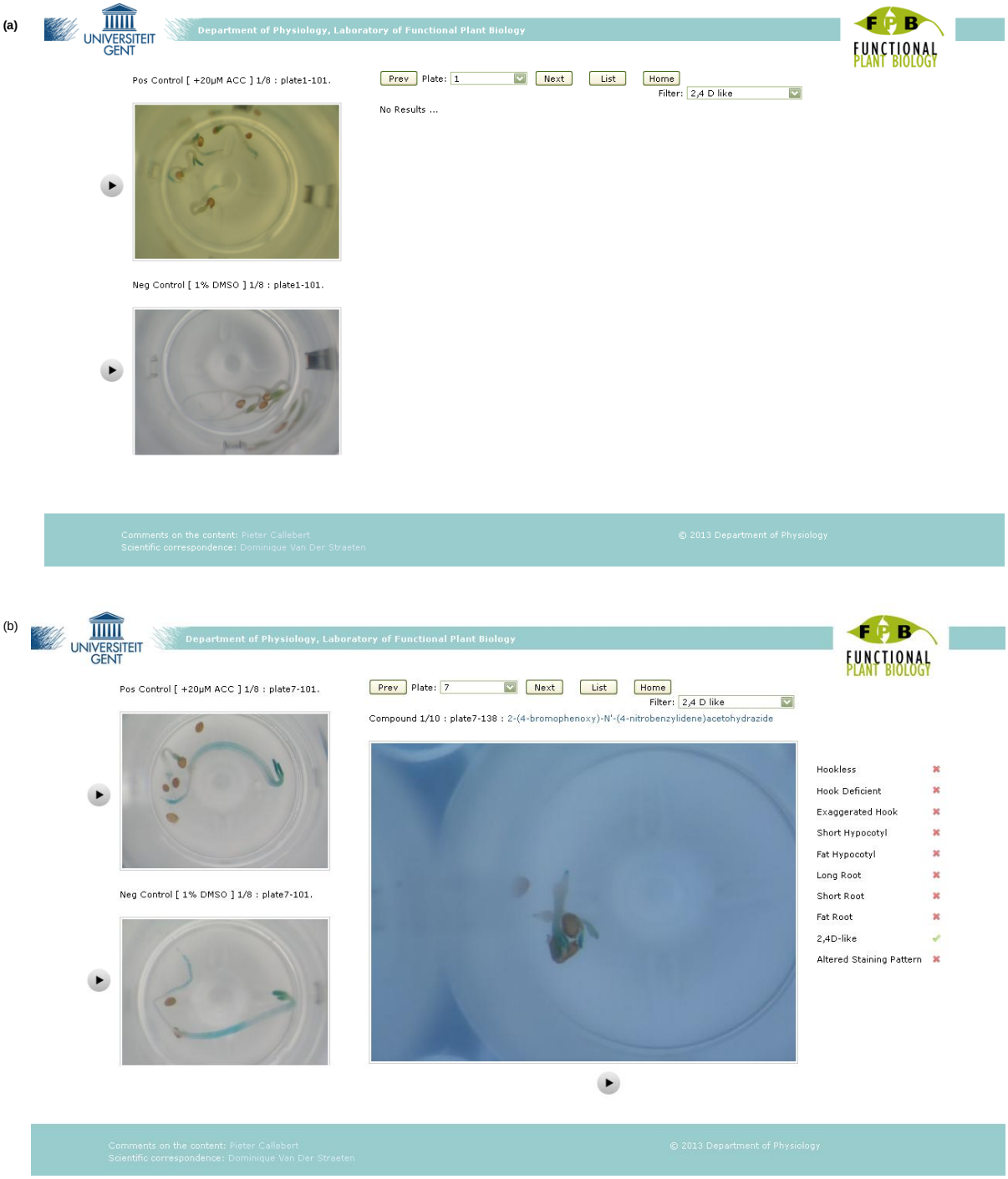

Figure S3.3 An example of how to use TR-DB. (a) The 2,4-D like subclass is chosen from the subclass filter; subsequently, the phenotypes are browsed plate by plate. Selecting Plate "1" in the drop-down menu yields "no results", indicating that plate 1 does not contain seedlings with a 2,4-D like phenotype, **(b)** Selecting Plate "7" in the drop-down menu yields photographs from the first well on that plate, containing a compound that induces a 2,4-D phenotype.

More supplementary data related to this article can be found at dx.doi.org/10.1016/j.plaphy.2013.12.008

Chapter 4

The quinoline carboxamide ACCERBATIN mimicking triple response in darkness, affects auxin metabolism and reactive oxygen species accumulation

In preparation

Hu Y, Depaepe T, Smet D, Hoyerova K, Klíma P, Cuypers A, Cutler S, Buyst D, Morreel K, Boerjan W, Martins J, Petrášek J, Vandenbussche F, Van Der Straeten D (2015) The quinoline carboxamide ACCERBATIN mimicking triple response in darkness, affects auxin metabolism and reactive oxygen species accumulation.

Contributions

YH designed the experiments, performed the phenotypic, physiological and genetic characterizations (TDP: experiments in Figure 4.3a-e, Fig.4a-h, Figure S4.2a-c, Figure S4.7; DS (experiments in Figure 4.6) **and wrote the manuscript**; TDP update the statistical analysis; KH and JP performed the analysis of auxin and auxin metabolites; PK and JP were responsible for auxin accumulation experiments on BY-2 cell-suspension culture; AC assisted with interpretation of the oxidative stress response; SC provided essential research materials; DB and JM performed the NMR analysis; KM and WB performed metabolite profiling; FV designed the experiments; DVDS designed the experiments, coordinated the research and wrote the manuscript; all authors commented on the manuscript.

Summary

1. Ethylene acts in concert with an array of signals to affect etiolated seedling development. Here we report on a quinoline carboxamide compound designated ACCERBATIN (AEX), that exacerbated the 1-aminocyclopropane-1-carboxylic acid (ACC)-induced triple response in a chemical screen.

2. A detailed study on the effects of AEX on the cellular and whole plant level and subsequent chemical, genetic and molecular analyses were conducted to gain insight in its mode of action.

AEX mimicked the ethylene response in etiolated Arabidopsis seedlings, though lacking radial expansion of the hypocotyl, while inhibiting root hair development and resulting in a shortened root meristem. Mutant and reporter studies confirmed that AEX most probably acts in parallel to ethylene signaling and affects auxin metabolism. AEX inhibited 1-naphthaleneacetic acid (1-NAA) efflux in Bright Yellow (BY)-2 cells. In addition, 2-oxindole-3-acetic acid-glucoside (oxIAA) accumulation was observed in the shoot apical meristem and cotyledons of etiolated seedlings. Distorted auxin homeostasis was accompanied by oxidative stress, supported by microarray analysis and superoxide/hydrogen peroxide staining.

3. It is proposed that AEX interferes with auxin transport from its major biosynthesis sites, shoot apical meristems (SAMs) and cotyledons, either as a direct consequence of poor basipetal transport from the meristematic region, or indirectly, through excessive IAA oxidation and reactive oxygen species (ROS) accumulation.

Key words: auxin homeostasis, chemical genetics, ethylene signaling, reactive oxygen species, triple response

Introduction

Ethylene is a gaseous plant hormone regulating many aspects in plant development and responses to stress (Abeles *et al.*, 1992). Ethylene effects on dark-grown pea seedlings were described as the triple response (Neljubov, 1901; Knight *et al.*, 1910). In *Arabidopsis*, the triple response phenotype includes exaggerated curvature of the apical hook, reduced hypocotyl and the root length, and increased radial expansion of the hypocotyl (Bleecker et al., 1988).

Ethylene is synthesized by almost all plant tissues from methionine, over S-adenosylmethionine (AdoMet) and 1-aminocyclopropane-1-carboxylic acid (ACC) (Yang & Hoffman, 1984; Van de Poel & Van Der Straeten, 2014). ACC is oxidized to ethylene by ACC oxidase (ACO). Several *ethylene overproducing* mutants *eto1*, *eto2* and *eto3*, that fail to regulate ACC synthase (ACS) stability, resulting in increased ethylene production, have been identified (Chae et al., 2003).

Ethylene signaling is initiated by inactivation of copper containing ethylene receptors, ETHYLENE RESPONSE 1 (ETR1), ETHYLENE RESPONSE SENSOR 1 (ERS1), ETR2, ETHYLENE-INSENSITIVE 4 (EIN4), and ERS2, located at the endoplasmic reticulum (ER)

membrane and Golgi apparatus (Dong *et al.*, 2010). Upon ethylene binding to its receptors, the CONSTITUTIVE TRIPLE RESPONSE (CTR1) kinase is inactivated, preventing phosphorylation of the EIN2 C-terminal domain, which results in its proteolytic cleavage and movement to the nucleus (Ju *et al.*, 2012). Subsequently, the EIN2 C-terminus activates the downstream transcriptional factors, EIN3 and EIN3-LIKE (EILs), which in turn switch on transcription of ETHYLENE RESPONSE FACTORs (ERFs) and ETHYLENE RESPONSE DNA BINDING FACTOR (EDFs) (Alonso *et al.*, 2003).

Many ethylene effects on growth and development of young seedlings in darkness are auxin-mediated and vice versa (Muday *et al.*, 2012). Ethylene and auxin act synergistically in root elongation and root hair formation (Masucci & Schiefelbein, 1994; Pitts *et al.*, 1998; Rahman *et al.*, 2002), while working antagonistically or independent in controlling hypocotyl elongation (Burg & Burg, 1966; Suttle, 1988; Collett *et al.*, 2000; Vandenbussche et al., 2003). Recent research on auxin-ethylene crosstalk in hypocotyl growth focused on apical hook development. Hook formation results from differential cell elongation (Raz & Ecker, 1999), driven by an auxin maximum at the concave side (Lehman *et al.*, 1996).

Exogenous auxins and polar auxin transport (PAT) inhibitors, suppress hook curvature. Likewise, some mutants with defective auxin synthesis, transport or signaling, display a hook deficient or hookless phenotype (Harper *et al.*, 2000; Stepanova *et al.*, 2008; Vandenbussche *et al.*, 2010; Zadnikova *et al.*, 2010). Further evidence for an auxin-ethylene interaction comes from *HOOKLESS1* (*HLS1*), the transcription of which can be activated through *EIN3* (Lehman *et al.*, 1996; An *et al.*, 2012). HLS1 inhibits accumulation of AUXIN RESPONSE FACTOR2 (ARF2), a repressor controlling differential auxin responses (Li *et al.*, 2004).

Chemical genetics has led to the identification of new compounds to help dissecting plant hormone pathways (e.g.bikinin (De Rybel *et al.*, 2009); pyrabactin (Park *et al.*, 2009)). Ethylene relevant chemicals include quinazolinone inhibitors of ACS (Lin *et al.*, 2010), L-kynurenine, an inhibitor of TRYPTOPHAN AMINOTRANSFERASE OF *ARABIDOPSIS*1/TAA RELATED (TAA1/TAR), key enzymes in ethylene-mediated auxin biosynthesis (He *et al.*, 2011), as well as brassinopride, an inhibitor of brassinosteroid action which also promotes ethylene response (Gendron *et al.*, 2008). In addition, the use of small molecules discovered in *Arabidopsis* can be translated to crop species (Schreiber *et al.*, 2011). We previously screened a 12,000 compound chemical library for molecules that altered the triple response phenotype triggered by ACC in etiolated *Arabidopsis* seedlings (Hu *et al.*, 2014). Here, we report follow-up work on the quinoline carboxamide compound ACCERBATIN (AEX), which was selected based on its exacerbation of the triple response.

Results

Identification of ACCERBATIN (AEX), a compound exacerbating the triple response

Recently, a series of chemicals altering the ACC-induced triple response phenotype of etiolated *Arabidopsis* seedlings were identified from a high-throughput chemical genetics screen (Hu *et al.*, 2014). A quinoline carboxamide compound, called AEX, was chosen for further investigation (Figure 4.1a). Four-day-old etiolated seedlings treated with AEX display

a phenotype mimicking the triple response, including an exaggerated apical hook, as well as shortening of the hypocotyl and the root, but without conspicuous lateral expansion of the hypocotyl (Figure 4.1b). Combined treatment with 50 µM AEX and either 10 µM ACC, or 5 ppm ethylene, enhanced the effect of ethylene or its precursor. The exacerbated triple response phenotype was characterized by an even stronger apical hook curvature, and a more severe shortening of both the hypocotyl and the root (Figure 4.1b).

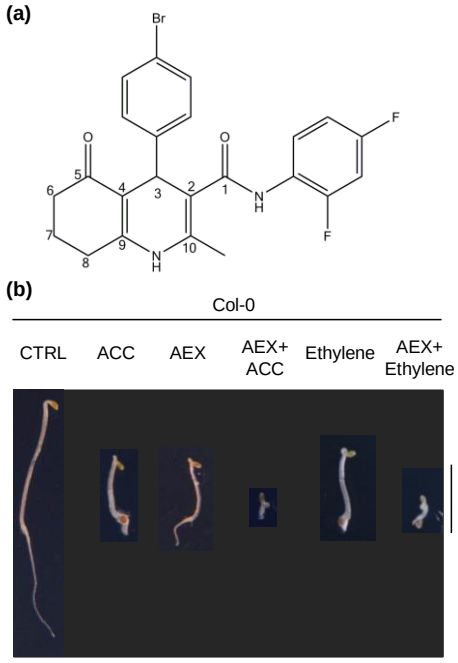

Figure 4.1 AEX enhances the triple response phenotype. (a) Chemical structure of AEX. IUPAC name: (4-(4-bromophenyl)-N-(2,4-difluorophenyl)-2-methyl-5-oxo-1,4,5,6,7,8-hexahydro-3-quinolinecarboxamide. Chembridge ID: 6527749. The carbon atoms of the quinoline carboxamide core are numbered. **(b)** Four-day etiolated seedlings of wild-type (Col-0) were grown on horizontal plates using half-strength MS (1/2 MS) medium containing 1% sucrose supplemented with 0.05% DMSO (CTRL), 10 µM ACC, 50 µM AEX, 10 µM ACC + 50 µM AEX, or placed in air supplied with 5 ppm of ethylene or treated with the combination of 50 µM AEX + 5 ppm ethylene. All treatments contained 0.05% DMSO. Individual photographs were cropped without changing the scale; the black background was post-added. Scale bar = 5 mm.

In order to determine the minimal concentration at which AEX affects seedling growth, a dose response assay was performed. Fifty µM AEX was necessary to quantitatively mimic the apical hook exaggeration and inhibition of root and hypocotyl elongation induced by 10 µM ACC (Figure 4.2a-c). In combination with 10 µM ACC, the effects of AEX on apical hook development, hypocotyl and root were additive in all concentrations tested. Based on the above-mentioned findings, 50 µM of AEX was mostly used for further investigations to explore its function.

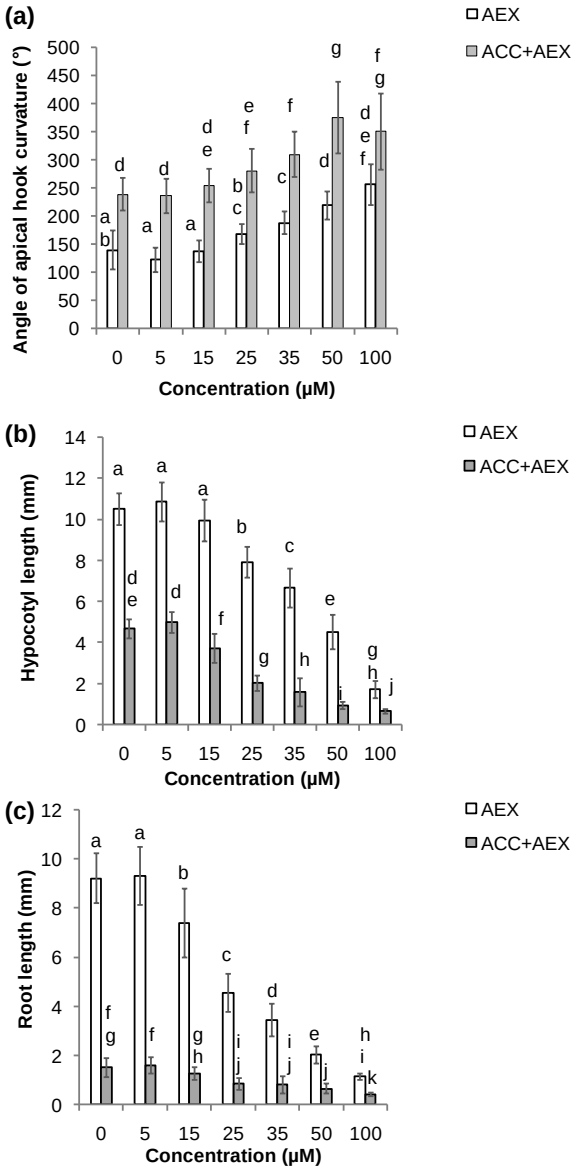

Figure 4.2 Dose-response of 4-day etiolated seedlings exposed to AEX concentrations ranging from 0 to 100 µM, grown on horizontal plates. The apical hook angle **(a)**, hypocotyl **(b)** and root **(c)** lengths were measured. White bars represent dose-response effects of AEX alone (at 0 µM AEX, growth medium is supplied with 0.05% of DMSO); grey bars represent AEX dose-response effects in the presence of 10 µM ACC. Data are presented as mean ± SD. Statistical analysis was performed by means of the Scheirer-Ray-Hare extension of the non-parametric Kruskal-Wallis rank sum test. The dependent variables (rank-transformed) (Supplemental Table S4.6). Multiple pairwise comparisons were performed with post-hoc Wilcoxon rank sum tests (P<0.05) and P-values were adjusted with Bonferroni correction. Bars with at least one letter in common are not significantly different.

AEX stability in planta

Many chemicals act *in planta* indirectly, i.e. through the action of a breakdown product (e.g. pro-auxins, (Savaldi-Goldstein *et al.*, 2008)). Therefore, we assessed whether AEX can be metabolized. Liquid chromatography–mass spectrometry (LC-MS) spectra of etiolated AEX-treated seedlings, which were continuously treated for 4 days or only 6 hours on day 3, revealed the presence of intact AEX (Supplemental Data S4.1). In addition, a compound with chemical formula $C_{19}H_{17}O_2NBr$ was found, corresponding to the loss of a $C_4H_2NF_2$ fragment from AEX ($C_{23}H_{19}O_2N_2BrF_2$), possibly formed by cleavage of the amide bond followed by

addition of an ethyn moiety, since the amide cleavage would have resulted in the loss of 6 carbons and 4 hydrogens (Supplemental Data S4.1). To assess temperature and pH stability, AEX was analyzed by ^{1}H NMR spectroscopy after heating (up to 80^{o}) or acid treatment (pH 4) by hydrogen chloride (HCl). Neither one of these experiments revealed notable differences, leading to the conclusion that AEX is both thermally and pH stable *in vitro* (Supplemental Data S4.2 and Figure S4.1).

Effects of AEX on the shoot: hypocotyl growth and apical hook curvature

To investigate how AEX affects hypocotyl growth at the cellular level, cortex cell dimensions were quantified (Figure 4.3). Fifty µM AEX alone inhibited hypocotyl elongation of 4-day-old etiolated seedlings compared to control seedlings, although less than 10 µM ACC, while combining AEX and ACC had an additive inhibitory effect (Figure 4.3a). These data were largely supported by a significant decrease in cortex cell length for AEX and ACC (Figure 4.3b,d). However, in contrast to 10 µM ACC, which increased radial expansion by 1.5-fold compared to the control, AEX alone did not significantly alter the hypocotyl diameter. In combination with ACC hypocotyl diameter was weakly increased compared to control indicating a negative effect of AEX on ACC-mediated lateral expansion (Figure 4.3c,d).

Apical hook formation in etiolated seedlings is dependent on cell division and differential elongation of hypocotyl cells (Raz & Ecker, 1999; Raz & Koornneef, 2001). The *pCYCB1;1::DB-GUS* construct with a destruction box (DB) was used as a marker for cell division, indicating the number of cells in G2-M transition (DiDonato *et al.*, 2004). This number was significantly enhanced in the apical hook in the presence of AEX compared to the control (Figure S4.2a). The total number of cells along the cortex cell file at the convex side of the apical hook and the basal portion of the hypocotyl were identical in AEX-treated and in control seedlings (31 cells) (Figure 4.3e). However, the cortex cell distribution in the apical versus basal part of the hypocotyl differed between AEX-treated and control seedlings. Upon AEX treatment there were more cortex cells in the apical region (17 cells) as compared to the lower hypocotyl (14 cells) (number of cells in the apical hook divided by the number of cells in the lower hypocotyl = 1.2), while the distribution in control seedlings was opposite (ratio= 0.4). Upon ACC treatment, there were less cortex cells in the apical hook compared to the lower hypocotyl, but the ratio was enhanced to 0.9 compared to the control. An additive effect was observed upon the combination of AEX and ACC (ratio=2). This differential cell distribution along the shoot indicated that AEX might affect cell fate within the hypocotyl.

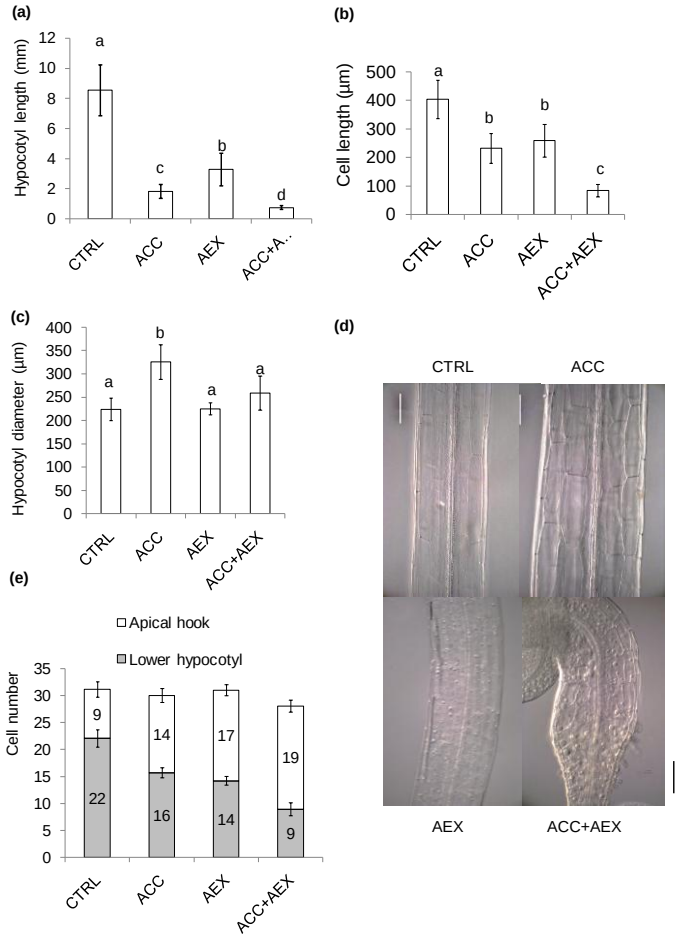

Figure 4.3 Effect of AEX on apical hook and hypocotyl growth of 4-day etiolated Col-0 seedlings, grown on horizontal plates. Length **(a)** and diameter **(c)** (of the middle part) of hypocotyls; and the corresponding length **(b)** of cortex cells from the middle part of the hypocotyl were measured. **(d)** DIC images of the middle part of the hypocotyl of 4-day old etiolated seedlings. From left to right and top to bottom: CTRL, ACC, AEX, AEX+ACC. **(e)** Numbers of cortex cells along the convex side of the apical hook and the lower part of the hypocotyl. Data are presented as mean ± SD. Statistical analysis was performed by means of a Kruskal-Wallis rank sum test (Supplemental Table S4.6). Multiple pairwise comparisons were performed with post-hoc Wilcoxon rank sum tests (P<0.05); P-values were corrected with Bonferroni correction. Bars with at least one letter in common are not significantly different. Scale bar = 100 µm.

Effects of AEX on root growth

Root growth depends both on cell division rates in the root meristem and on longitudinal cell expansion in the elongation zone. Thus, the effects of AEX on primary root length, meristem size and activity, as well as epidermal cell length were investigated. Seedlings grown on 50 µM AEX displayed a more severe reduction of root elongation as compared to those grown on 10 µM of ACC (Figure 4.4a), while being even more pronounced on the combination of AEX and ACC. In contrast to the reduction upon ACC treatment, the inhibition of root length induced by AEX correlated with a shortening of the root meristem (Figure 4.4b,c). Combining AEX and ACC had an additive effect on root shortening as compared to AEX alone, but the root meristem length was comparable to that of AEX-treated seedlings. Furthermore, cortex cell number was significantly reduced by AEX, either alone or combined with ACC, suggesting a suppressive effect on mitotic activity of root meristem cells (Figure 4.4d). The latter was supported by a reduced expression of cell cycle marker *pCYCB1;1::DB-GUS*

(Figure S4.2a). ACC alone did not affect cell cycle activity, supporting a differential action of ACC and AEX on root elongation. In addition, AEX restricted elongation of epidermal cells that leave the root meristem although the extent of inhibition varied among seedlings (Figure 4.4e,f), an effect that was also observed upon ACC or ethylene treatment (Le *et al.*, 2001). Altogether, these results indicate that AEX inhibits both cell division and elongation, as manifested by root shortening.

Another key feature in root growth, related to ethylene/ACC response is root hair emergence and elongation (Tanimoto *et al.*, 1995). Both root hair length and number were negatively affected by AEX as compared to the control, while ACC exhibited a positive effect (Figure 4.4g,h), and combined treatment resulted in an intermediate effect (Figure 4.4g,h). Thus, AEX represses both the ethylene-mediated root hair emergence and growth.

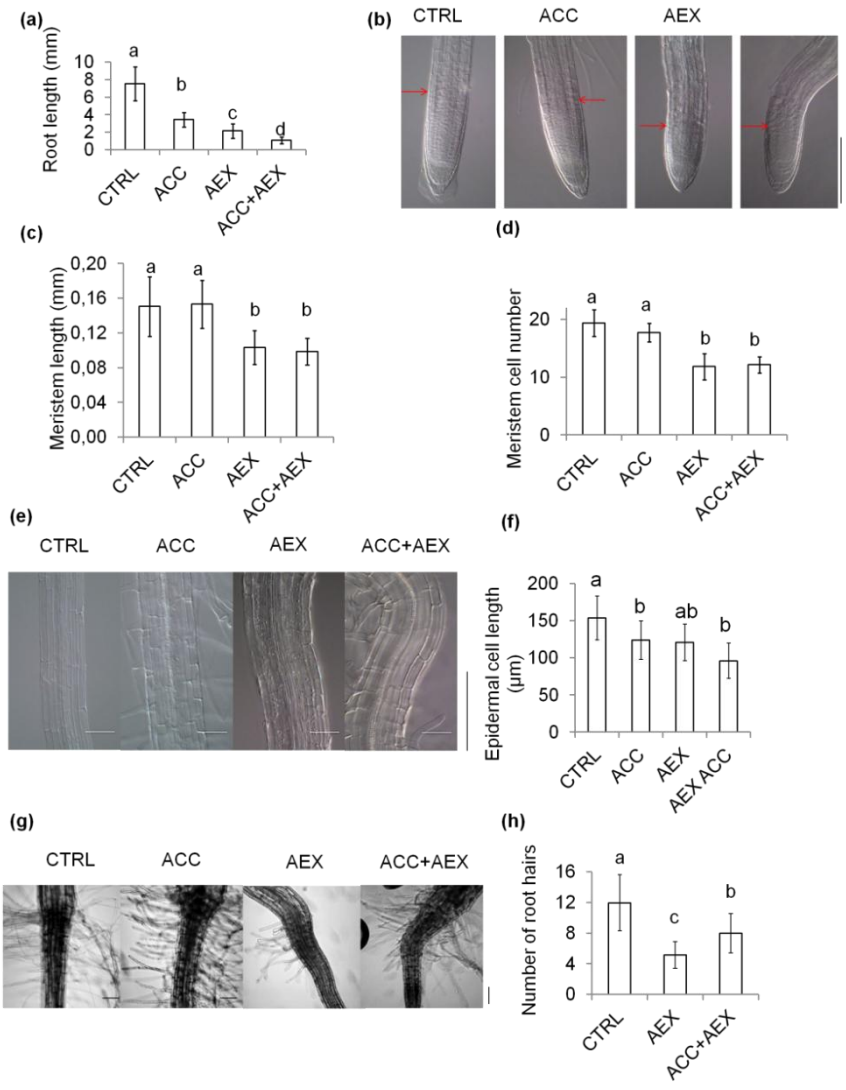

Figure 4.4 Inhibitory effect of AEX on root growth of 4-day etiolated Col-0 seedlings grown on vertically standing plates. (a) Root length. **(b)** DIC microscopy images of the root tip. The last cortex cells of the root meristem are marked with a red arrowhead. Individual photographs were cropped without changing the scale. **(c)** Meristem length. **(d)** Meristem cell number. **(e)** DIC microscopy images of the root elongation zone. **(f)** Epidermal cell length in the root elongation zone. **(g)** Bright-field microscopy images near the hypocotyl-root junction. **(h)** Total number of root hairs from a single epidermal cell file. Seedlings were grown on half-strength MS (1/2 MS) medium containing 1% sucrose supplemented with 0.05% DMSO (CTRL), 10 µM ACC, 50 µM AEX, 10 µM ACC + 50 µM AEX. Data are presented as mean ± SD. Statistical analysis was performed by means of a Kruskal-Wallis test (Supplemental Table S4.6). Multiple pairwise comparisons were performed with post-hoc Wilcoxon rank sum tests (P<0.05); P-values were adjusted with Bonferroni correction. Bars with at least one letter in common are not significantly different. Scale bar = 100 µm.

AEX most likely acts in parallel with ethylene signaling

To determine whether the effect of AEX is dependent on ethylene biosynthesis, ethylene emanation of etiolated Col-0 seedlings grown in the presence of AEX was measured, using laser photo-acoustic spectroscopy. No significant effect was registered, indicating that the effect of AEX on growth is most probably independent of ethylene biosynthesis (Figure 4.5a).

To further dissect a possible site of action of AEX, a series of ethylene-related mutants were tested (Figure 4.5b). , Mutants exhibiting a constitutive ethylene response phenotype (*eto2-1* and *ctr1-1*) showed an exacerbated triple response phenotype in the presence of AEX. Interestingly, AEX triggered an enhanced apical hook curvature in the ethylene insensitive mutants *etr1-1, ein2-1,* and *ein3-1eil1-1* double mutant, while inhibiting elongation of both hypocotyl and root. Altogether, these data suggest that AEX acts downstream or, more likely, independent of ethylene signaling. The latter was strengthened by the fact that some phenotypes of AEX-treated seedlings are distinct from those typically observed in ACC-treated seedlings, as the absence of lateral expansion of the hypocotyl and the reduction of root hairs (vide supra). Moreover, AEX did not enhance expression of the ethylene reporter *EBS::GUS* (*GUS* gene driven by a synthetic *EIN3*-responsive promoter) (Stepanova *et al.*, 2007) in either shoots or roots, compared to control seedlings (Figure S4.2b). In conclusion, the action of AEX most probably occurs in parallel to ethylene signaling.

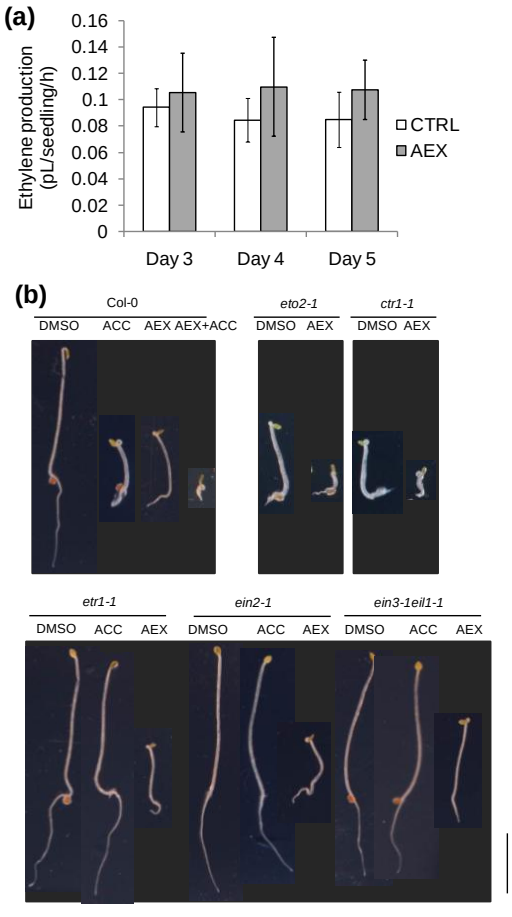

Figure 4.5 AEX effects on ethylene production and ethylene mutants. (a) Ethylene production of etiolated Col-0 seedlings in the presence of 50 µM AEX was not affected as compared to 0.05% DMSO control. Data are presented as mean ± SD. The experiments were performed twice with 3 replicates per condition with highly similar results; results of a representative experiment are shown. Statistical analysis did not detect significant differences between AEX and CTRL. **(b)** Four-day-old etiolated seedlings of Col-0, *eto2-1, etr1-1, ein2-1* and *ein3-1eil1-1* grown on medium supplemented with 0.05% DMSO (CTRL), 10 µM ACC, 50 µM AEX, 10 µM ACC + 50 µM AEX, 10 µM $AgNO_3$ (horizontal plates) All treatments contained 0.05% DMSO. The individual photographs were cropped without changing the scale; the black background was post-added. Scale bar = 5 mm.

Effects of AEX on auxin responsiveness in shoot and root

Since etiolated seedling growth depends on auxin, DR5::GUS (Ulmasov *et al.*, 1997) expression was visualized (Figure S4.2c). The auxin maximum appeared at the concave side of the hook in all conditions. However, when combining AEX with ACC, more cells were stained at the concave side and toward the basal end of the hypocotyl, rather than being restricted to the hook as in seedlings treated with ACC alone. This result confirmed that the effect of AEX on the apical hook is probably parallel to ethylene signaling, and is auxin dependent. In root tips, DR5::GUS was expressed in the quiescent center and columella both in AEX and in control roots, while ACC expanded the area of staining, particularly in the vascular tissue. Remarkably, combining AEX with ACC reduced the signal compared to ACC alone, which was opposite to the effect seen in the apical hook.

Kinematic and genetic analysis of the effect of AEX on hook development

The exaggerated apical hook curvature is one of the key features of AEX (Figure 4.1b, Figure 4.6a). To know when AEX starts to act in hook development, a kinematic analysis was performed. The apical hook of etiolated Col-0 seedlings displayed three constitutive phases of development, consistent with previous results: the formation (0~36 hours), maintenance (36~48 hours) and opening phase (48~144 hours) (Fig 6B) (Vandenbussche *et al*., 2010; Smet *et al*., 2014). ACC-treated WT seedlings exhibited a significant hook exaggeration (~235° during maintenance phase), and were characterized by an extended formation phase (0~48 hours) and prolonged opening phase (252 hours after germination), while the rate of opening was similar to control. AEX-treated Col-0 seedlings also showed three distinct phases of hook development, but exhibited a formation phase lasting 3.5 days and a prolonged maintenance phase (84~132 hours; 258°) compared to control seedlings. The hook opening rate was slower, and not even completed after 360 hours post germination. Finally, when AEX and ACC were combined, effects on all three phases of apical hook development were even more pronounced. Hence, the combined treatment led to a significantly more exaggerated curvature than that of AEX or ACC-treated seedlings.

Hook development in *Arabidopsis* is strongly controlled by the *HOOKLESS 1 (HLS1)* gene (An *et al.*, 2012). Kinetic analysis of *hls1-1* hook development revealed that both control and ACC-treated seedlings immediately entered into the opening phase and reached an angle of 0° at 48 hours after germination (Figure 4.6a,c). Upon AEX treatment however, *hls1-1* seedlings formed a conspicuous hook structure (until 132° at 24 hours after germination), and subsequently started opening, which was completed at 90 hours after germination. Thus, AEX is likely acting downstream of HLS1.

As auxin is involved downstream of ethylene signaling and also acts in parallel to the ethylene pathway (Stepanova *et al*., 2007), selected auxin signaling (*arf2-6*; *nph4-1arf19-1*; *axr3-1* (Okushima *et al.*, 2005a; Vandenbussche *et al.*, 2010; Zadnikova *et al.*, 2010)) and transport mutants (*aux(s)lax3*; *aux1-7*; 35S::PIN1; *pin3-3*; *rcn1-1*; *pid(s)*; *wag(s)*; *pgp4-1*; *abcb1abcb19* (Friml *et al.*, 2002; Vandenbussche *et al.*, 2010; Wu *et al.*, 2010; Zadnikova *et al.*, 2010; Chen *et al.*, 2013)) were screened in the presence of 50 µM AEX (Figure S4.3a). Apical hook development was enhanced by AEX in all lines. In the presence of exogenous auxin (IAA or

2,4-D) or the auxin efflux inhibitor NPA, no hook was observed at day 4 in seedlings treated with AEX (Figure S4.3b). In contrast, a hook was still seen when 1-NOA, an auxin influx inhibitor, was applied. Thus, AEX required a threshold level of auxin to induce a full response of apical hook curvature, as seen in Col-0.

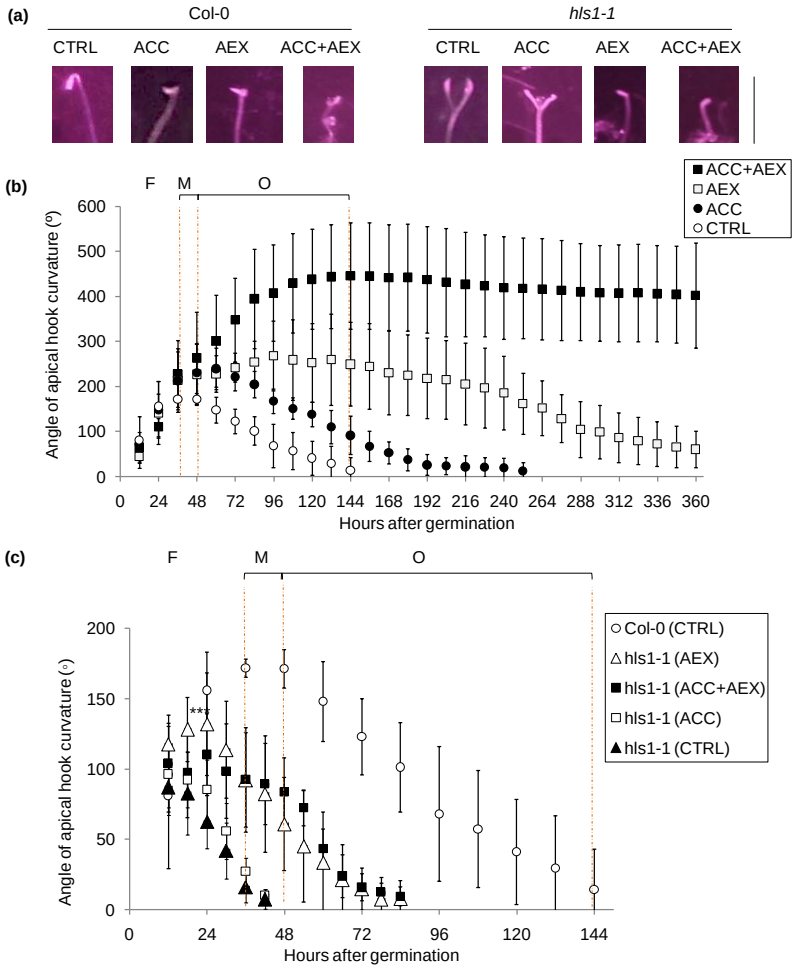

Figure 4.6 AEX-regulated apical hook development of etiolated seedlings grown on vertical plates. (a) Phenotypic effects of 0.05% DMSO (CTRL), 10 µM ACC, 50 µM AEX or/and 10 µM ACC on the apical hook curvature of etiolated seedlings at 60 hours after germination. The individual photographs were cropped without changing the scale. Scale bar = 5 mm. Kinetics of hook development in Col-0 **(b)** and *hls1-1* **(c)** seedlings grown on 0.05% DMSO (CTRL), 10 µM ACC, 50 µM AEX, 10 µM ACC + 50 µM AEX. Dotted vertical lines represent the transition between developmental phases. The apical hook of WT in control medium forms shortly after germination, until bending reaches a plateau around 170° corresponding to the formation phase (F); the maintenance phase (M) spans a period of 30-60 hours (at day 2 and day 3); subsequently, the apical hook starts opening (opening phase (O)). All treatments contained 0.05% DMSO. Data are presented as mean ± SD. Angle of AEX-treated *hls1-1* was compared to CTRL *hls1-1* at timepoint 24h (Wilcoxon rank sum test W (16) = 78; P=0.004 (**); 6 > n > 10). Experiments were performed twice, with comparable kinetics.

AEX enhances shoot gravitropism in darkness

Given the common mechanisms of differential growth in hook development and gravitropism (Zadnikova *et al.*, 2015), the effect of AEX on shoot gravitropism was determined by a reorientation assay (Nakamoto *et al.*, 2006). Consistent with previous reports (Nagashima *et al.*, 2008; Vandenbussche *et al.*, 2013) control seedlings and seedlings treated with ACC

showed similar kinetics, and reoriented to an angle of 45° after 24 hours, while NPA treated seedlings did not react (Figure 4.7). By contrast, AEX enhanced the rate of reorientation of wild type (WT) seedlings significantly compared to control at as early as 4 hours, reaching an angle of 70° after 24 hours. Proper auxin signaling contributed to the stimulatory effects of AEX on asymmetric elongation in gravistimulated hypocotyls as the rate of reorientation in *msg2-1* (mutant in IAA19) and *nph4-1arf19-1* (carrying mutations in *ARF7* and *ARF19*) was not enhanced upon AEX (Figure S4.4).

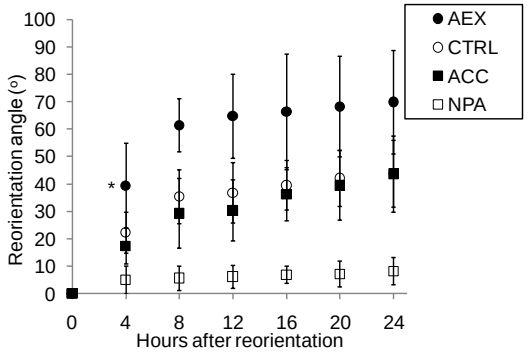

Figure 4.7 Response of etiolated Col-0 seedlings after growth and reorientation on vertically standing plates. Seedlings were grown in the presence of 0.05% DMSO (CTRL), 10 µM ACC, 50 µM AEX or 10 µM NPA. All treatments contained 0.05% DMSO. On day 2 after germination, plates were rotated by 90°, plants laying close to the horizontal axis were analyzed and the average reorientation angle of the hypocotyl was calculated. 90° corresponds with the new direction of the gravity vector. Data are presented as mean ± SD. Reorientation angle of AEX-treated seedlings at timepoint 4 hours was compared to CTRL seedlings (Wilcoxon rank sum test W (18) = 50; P=0,.0235 (*); 8 > n > 10). Experiments were performed twice with highly similar results; results of a representative experiment are shown. Results of a reorientation assay on selected mutants are shown in Figure S4.4.

AEX limits movement of free IAA produced from the shoot apical meristem and enhances auxin catabolism

Since altered hypocotyl gravitropic response and apical hook formation result from asymmetric auxin distribution, which largely depends on altered auxin transport (Muday *et al.*, 2006; Vandenbussche *et al.*, 2010; Zadnikova *et al.*, 2010; Rakusova *et al.*, 2011), we aimed to verify whether AEX affects the auxin transport machinery. Auxin efflux was measured by cellular changes in accumulation of radioactively labeled NAA ([^{3}H]NAA) in Tobacco Bright Yellow (BY)-2 cells. 1-NAA is a good substrate for active efflux but a weak substrate for active influx because it enters cells easily by diffusion (Delbarre *et al.*, 1996). An AEX dose-dependent effect was reflected in [^{3}H]NAA accumulation kinetics, indicating inhibitory effects on auxin efflux (Figure 4.8). The effective concentration (50 µM) fits to AEX dose-dependent effects for triple response-like phenotypes. Interestingly, simultaneous application of 100 µM ACC had no additive effect combined with 100 µM AEX, even though 100 µM ACC alone raised the accumulation slightly (Figure S4.5).

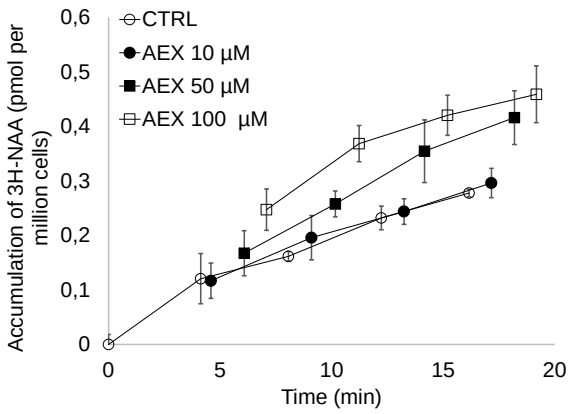

Figure 4.8 AEX inhibits auxin efflux in BY-2 cells. [^{3}H]NAA accumulation kinetics in tobacco BY-2 cells upon treatment with 10, 50 and 100 µM AEX. Error bars indicate SD (n=4).

Next, we investigated whether AEX affects auxin metabolism and transport in planta. Since auxin conjugation and degradation are also essential for the establishment and maintenance of cellular auxin gradients, auxin content and the primary IAA catabolites and conjugates, such as 2-Oxindole-3-Acetic Acid (oxIAA), oxIAA-glucose ester (GE), IAA-aspartate (Asp), IAA-glutamate (Glu) and IAA-GE (Ostin *et al.*, 1998; Kowalczyk & Sandberg, 2001; Kai *et al.*, 2007; Hošek *et al.*, 2012) were measured in cotyledons together with shoot apical meristems (SAMs) and in hypocotyls of 4-day old dark-grown seedlings. In control seedlings, a substantial amount of free IAA produced in meristems was possibly transported to the hypocotyls, where it was predominantly conjugated into IAA-Glu or metabolized to oxIAA, and subsequently to its non-active stable derivative, 1-O(2-oxoindol-3-ylacetyl)-beta-d-glucopyranose (oxIAA-GE) (Figure 4.9; Figure S4.6). Upon 50 µM AEX treatment, the amount of free IAA in meristems was maintained, but dropped in hypocotyls to about 30% compared to the control (Figure S4.6a,b); in addition, a strong reduction of the IAA conjugates IAA-Asp and IAA-GE was seen, particularly in hypocotyls (Figure S4.6c). Moreover, while the total amount of OxIAA-GE did not differ from that of control seedlings the largest fraction accumulated in meristems (85%), and only a small portion in hypocotyls (15%) (Figure 4.9; Figure S4.6). Since auxin catabolites are not transported across the plasma membrane (Pencik *et al.*, 2013), it is suggested that AEX limits the movement of free IAA produced in meristems, resulting in an apical accumulation of IAA, subsequently oxidized into ox-IAA, and converted to oxIAA-GE. Interestingly, the effect of ACC on the spatial distribution of IAA and its catabolites and conjugates was reminiscent of that seen upon AEX treatment (Figure 4.9; Figure S4.6).

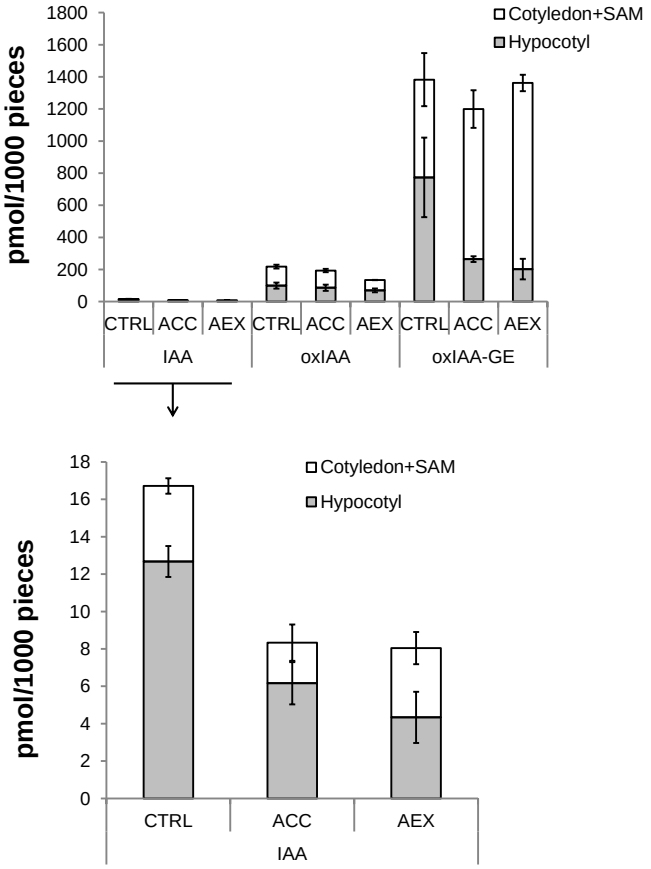

Figure 4.9 Endogenous auxin content in apices (including cotyledons and shoot apical meristems, SAMs) and hypocotyls treated with AEX. IAA, oxIAA and oxIAA-GE contents are shown for Col-0 treated with 0.05% DMSO (CTRL), 10 µM ACC and 50 µM AEX. All treatments contained 0.05% DMSO. Analyses were performed by GC-MS/MS on 4-day etiolated seedlings. Error bars indicate SD. Statistical analyses were performed by means of a two-way ANOVA comparing mean IAA, oxIAA or oxIAA-GE content (measurement variable) among treatments and tissues (nominal variables) with $F(5,14)= 80,49$ and $P<0.05$ (IAA); $F(5,14)= 5,80$ and $P<0.05$ (oxIAA); $F(5,14)= 12,14$ and $P<0.05$ (oxIAA-GE). Pairwise comparisons were performed with post-hoc Tukey-Kramer tests ($P<0.05$). Different letters represent means that are significantly different. IAA, oxIAA and oxIAA-GE content in cotyledons (including SAMs) and hypocotyls are presented separately in supplemental Figure S4.6.

Changes in Global Gene Expression upon short-term AEX treatment

To assess direct effects of AEX, a genome-wide transcript analysis after short-term AEX treatment was performed. RNA was extracted from entire Col-0 seedlings grown for 2.5 days in darkness, treated for 6 hours with 100 µM AEX compared to an untreated control. 539 and 579 genes were identified as up- or down-regulated by AEX compared to the control (Table S4.1). The Biological Networks Gene Ontology tool (BiNGO) analysis (Maere *et al.*, 2005) showed that genes responding to stimuli and metabolic processes were significantly enriched (Table S4.2). Comparison of the data with publicly available datasets revealed a link with Reactive Oxygen Species (ROS). Notably, four out of five previously identified hallmarks for the general oxidative stress response (AT1G19020, AT1G05340, AT2G21640 and AT1G57630) (Gadjev *et al.*, 2006) were represented in the AEX induced set of transcripts. Furthermore, 32% of genes differentially regulated by H_2O_2 are shared with AEX, suggesting a strong overlap in response (Figure 4.10a; Table S4.3a). Large transcript overlaps were also found when comparing AEX down-regulated genes to genes down-regulated by UPBEAT1

(UPB1) (Tsukagoshi *et al.*, 2010). More than 38% of genes down-regulated by AEX were shared with those down-regulated by UPB1, while 10% shared up-regulated genes were found (Figure 4.10b; Table S4.3b). UPB1 is a transcription factor that negatively regulates root meristem size by repression of a set of class III peroxidases that modulate the balance of ROS at the boundary between the meristematic and elongation zone. In *Arabidopsis*, there are 73 Class III peroxidase genes (Tognolli *et al.*, 2002), 25 of which were down-regulated by AEX; the majority (70%) overlapped with UPB1 down-regulated peroxidases. Moreover, class III peroxidases are known to modify cell wall structure resulting in cell elongation, through consumption or release of ROS (Passardi *et al.*, 2004). Many Class III peroxidases appear in the top 135 of AEX down-regulated genes with a minimal change of 4-fold along with other cell wall related genes and genes encoding cell wall remodeling enzymes (Table S4.4), some of which have clear effects on cell elongation in a tissue-specific manner (LEUCINE-RICH REPEAT/EXTENSIN1 (LRX1), EXPA7, EXPA18). In order to characterize how AEX may affect auxin response, publicly available microarray data from auxin experiments (Zhao *et al.*, 2003; Okushima *et al.*, 2005b; Nemhauser *et al.*, 2006) were analyzed. Nearly 25% of auxin-responsive genes were also regulated by AEX, with the majority (102 genes) regulated in the same sense (increased or decreased expression), whereas 39 genes showed an inverse regulatory pattern (Figure 4.10c, Table S4.3c). Notably, early auxin-responsive gene families of Aux/IAA, GretchenHagen-3 (GH3), and Small auxin-up RNA (SAUR) (Abel & Theologis, 1996; Hagen & Guilfoyle, 2002) appeared down-regulated by AEX. Comparison between AEX and transcriptional profiles of ethylene datasets (Alonso et al., 2003; Olmedo et al., 2006) illustrates that the overlap in genes repressed by ethylene and AEX (24%) is larger than the overlap in induced ones (13%); in addition, only 51 genes were regulated in the same sense by AEX and ethylene, indicating that the overlap with ethylene is less than with the signals mentioned above (Figure 10d, Table 4.3d). Overall, the microarray data indicate a global redox imbalance leading to a ROS induction signature as a prime effect of AEX. The significant overlap of transcripts induced/suppressed by AEX and H_2O_2, as well as between AEX and UPB1, suggest that AEX altererd ROS homeostasis.

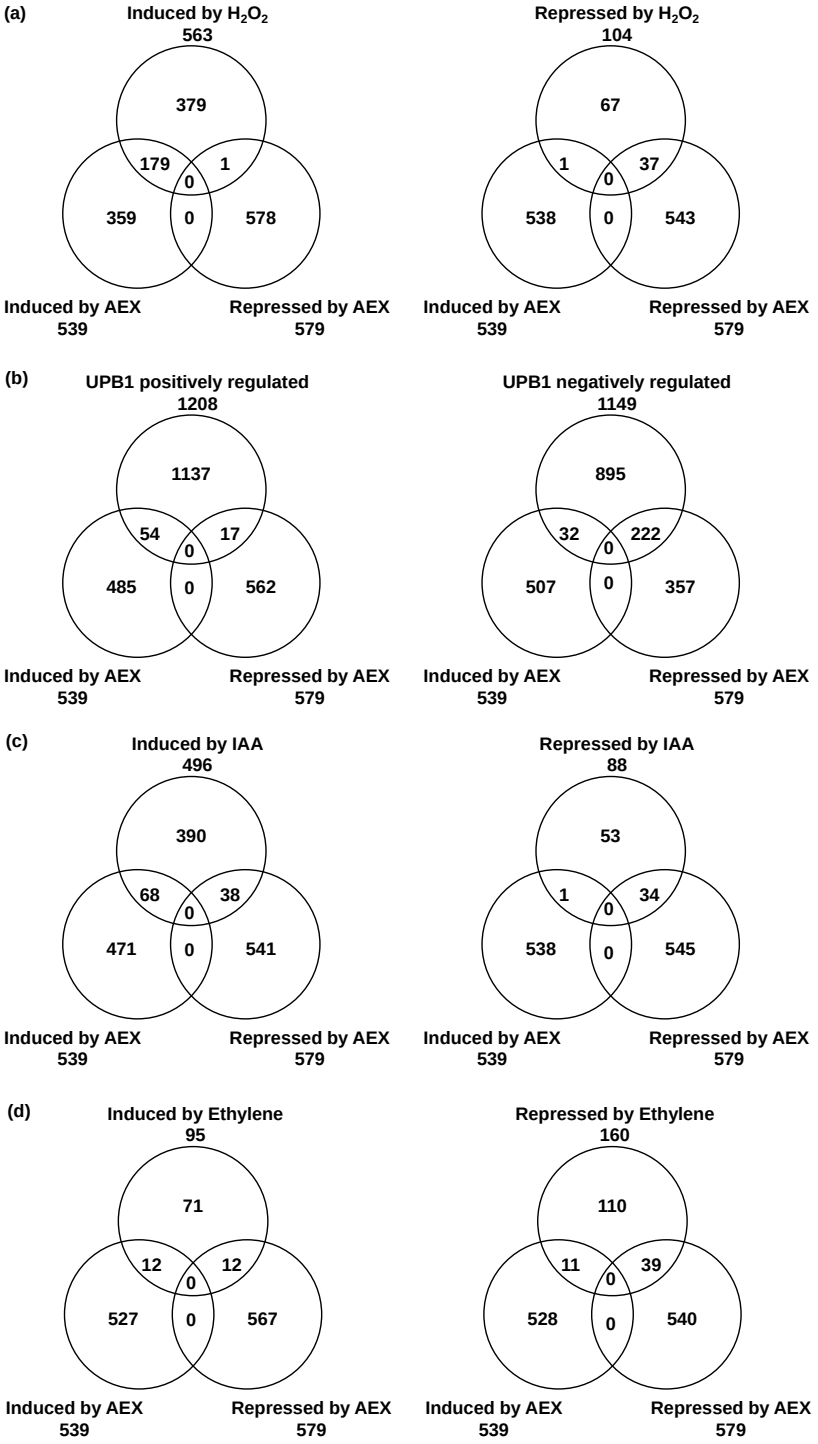

Figure 4.10 Changes in global gene expression upon short-term AEX treatment. Venn diagrams showing the overlap between transcript dynamics upon AEX treatment (from microarray analysis performed on 3 independent biological repeats) and published microarray data. Details in Supplemental Table 4.1-4. **(a)** Induced/suppressed by AEX and H_2O_2; the transcriptional profile (>2-fold) of 5-day-old light-grown Col-0 plants treated with H_2O_2 (20 mM, 1h) was from Davletova et al., 2005. **(b)** Induced/suppressed by AEX and UPB1 transcription factor; transcriptional profile of UPB1 regulated genes was from Tsukagoshi *et al.*, 2010. **(c)** Induced/suppressed by AEX and IAA; transcriptional profiles of IAA regulated genes were from Zhao et al., 2003; Okushima et al., 2005b; Nemhauser et al., 2006. **(d)** Induced/suppressed by AEX and ethylene; transcriptional profiles of ethylene regulated genes were from Alonso et al., 2003 and Olmedo et al., 2006. The data processing of the transcriptional profiles are shown in Supplemental Experimental Procedures.

Induction of reactive oxygen species by AEX

In order to obtain direct proof that the ROS balance was distorted by AEX, both nitroblue tetrazolium (NBT) and diamino benzidine (DAB) staining was performed on 4-day-old seedlings, reflecting endogenous levels of superoxide (O_2^-) and H_2O_2, respectively. NBT staining was mainly detected in the apical regions of hypocotyl and root (Figure 4.11a). The fraction of seedlings stained in the apical part of the hypocotyl was significantly larger in AEX-treated seedlings as compared to the control (AEX: sum of strong+ medium= 0.84; control: 0.54) (Figure 4.11b). ACC treatment resulted in staining patterns comparable to AEX (0.79). Furthermore, both ACC and AEX induced the O_2^- level in the root, particularly in the root tip and the vasculature (Figure 4.11a). In contrast, the DAB staining did not result in significant differences in the apical region of hypocotyls, while being significantly increased in roots treated with AEX compared to both untreated and ACC-treated seedlings (Figure 4.11b). In accordance with the microarray data, these results demonstrate that the ROS level is enhanced by AEX. Moreover, DAB staining of AEX-treated seedlings was stronger in the elongation zone than in the meristem; while being significantly weaker in the epidermis of the elongation zone as compared to inner cell types.

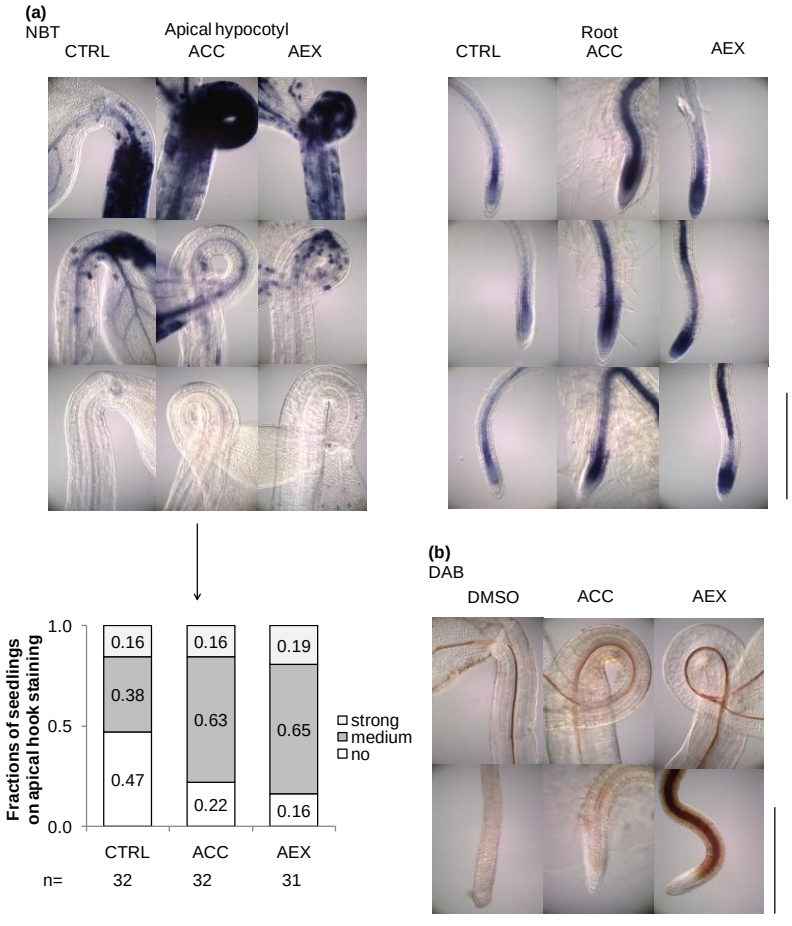

Figure 4.11 ROS levels are induced by AEX treatment. Col-0 seedlings were continuously grown on medium containing 50 µM AEX for 4 days in darkness compared to untreated (0.05% DMSO) and ACC (10 µM ACC, 0.05% DMSO) treated seedlings. **(a)** Images of 4-day etiolated seedlings stained for O_2^- using NBT and summary of frequencies of staining intensity. The degree of staining in the apical part of the hypocotyl was classified as strong, medium, or no staining. Fractions of seedling staining on the apical hook is shown with sample sizes indicated under the graph. **(b)** Images of 4-day etiolated seedlings stained for H_2O_2 using DAB. Scale bar = 0.5 mm.

Discussion

ACCERBATIN (AEX), a quinoline carboxamide which exacerbates ethylene effects in etiolated seedlings, acts in parallel to the ethylene pathway

We recently screened the DIVERSet™ library from ChemBridge™ (http://www.chembridge.com/index.php), which contains 12,000 chemicals with broad structural diversity, for compounds altering the ACC-induced triple response phenotype of etiolated *Arabidopsis* seedlings (Hu *et al.*, 2014). A number of compounds including a quinoline carboxamide compound called Accerbatin for its ACC exacerbating effect (hence the acronym AEX) (Figure 4.1a), were chosen for further investigation. Here, we present a detailed study of the effects of AEX at the cellular and whole plant level, and propose a mechanism of action, based on a number of chemical, genetic, molecular and physiological analyses.

Since application through the medium resulted in a conspicuous shoot phenotype, AEX or a metabolite thereof appeared to be effectively taken up and transported throughout the plant body. An LC-MS-based global metabolomics study in etiolated seedlings and an NMR analysis of the compound *in vitro*, indicated that AEX probably remains stable *in planta* (Supplemental Data S4.1 and S4.2). The only cleavage compound found (the prevalence of which could not be assessed precisely, but which was assumed to be very low, as also suggested by NMR analysis) resulted from loss of the C4H2NF2 fragment of AEX through hydrolysis of the amide bond, essentially leaving the quinoline core with aromatic substitution on C3 (Figure 4.1). In addition, phenotypic analysis along with assessment of effects on shoot gravitropism of quinoline carboxamide and carboxylate AEX analogs suggested that the quinoline core could be the effective principle (Table S4.5; Figure S4.8). However, this was not supported by analog G which was inactive. Therefore, it can be concluded that AEX is largely stable and acts as such *in planta*.

Given that AEX issued from a screen for altered triple response characteristics, initial experiments were directed towards its possible role in ethylene biosynthesis or signaling. AEX triggered triple response-like characteristics or exacerbated the triple response in ethylene biosynthesis and signaling mutants, as well as in the wild type in the presence of the ethylene perception inhibitor $AgNO_3$ (Figure 4.5b), reminiscent of the phenotype of WT seedlings treated with AEX or the combination of AEX and ACC (Figure 4.1b). Hence, it was concluded that AEX acts downstream or independent of ethylene signaling. Further confirmation was provided by a kinetic study on apical hook development of *hls1-1*, in which AEX triggered a hook structure, suggesting AEX action downstream of HLS1 (Figure 4.6a,c). The partial hook was similar to the restored hook curvature in the *HLS1 suppressor* mutant (*hss1)/arf2*, with the auxin responsive transcription factor *ARF2* acting downstream of *HLS1*, a putative N-acetyltransferase (Li *et al.*, 2004). When combining ACC with AEX, the dynamics of *hls1-1* hook development was very similar to that observed in AEX-treated seedlings (Figure 4.6c), indicative for an ethylene-independent action of AEX. Ethylene independence was further suggested by analysis of the *EBS::GUS* reporter, in which AEX did not substantially affect expression (Figure S4.2b).

Analysis of cellular effects of AEX indicated similarities and differences of ethylene and AEX targets. AEX induced elongation, but not lateral expansion of the hypocotyl as ethylene does (Figure 4.3a-d). Furthermore, AEX strongly inhibited root meristematic activity (Figure S4.2a), resulting in a short meristem (Figure 4.4a-d), as well as inhibited cell size in the elongation zone, while ethylene had a limited effect on the meristem, but affected cell elongation similarly to AEX (Figure 4.4e,f). Moreover, AEX resulted in suppressed ACC/ethylene-induced lateral expansion (Figure 4.3a-d). In addition, AEX inhibited root hair emergence and outgrowth as opposed to the induction typically seen for ethylene (Figure 4.4g,h). Together, these results support the contention that AEX acts in parallel to the ethylene pathway rather than downstream of it.

AEX has biological properties reminiscent of auxin-like herbicides

Quinoline derivatives have very different biological properties in several kingdoms, including antibacterial (Shivaraj *et al.*, 2013), antimalarial (Raynes *et al.*, 1996; Narayan Acharya *et al.*, 2008), antitumor (Isaacs *et al.*, 2006), and herbicidal (Grossmann & Kwiatkowski, 1995; Grossmann & Scheltrup, 1998) action. One of the most important auxin herbicide families is based on quinoline carboxylic acid, exemplified by quinmerac (7-chloro-3-methylquinoline-8-carboxylic acid) and quinclorac (3,7-dichloroquinoline-8-carboxylic acid) (Grossmann & Kwiatkowski, 1995; Grossmann & Scheltrup, 1998), which share strong structural similarity with the quinoline backbone of AEX. Similar to other auxin herbicides and IAA at supra-optimal concentrations in dicot plants, quinoline carboxylic acid derivatives stimulate ethylene production in the light via the induction of ACS (Grossmann & Kwiatkowski, 1995; Grossmann & Scheltrup, 1998). Ethylene leads to leaf epinasty, tissue swelling and senescence (Grossmann, 2003). These ethylene-associated phenotypes were observed in AEX-treated light grown plants (Figure S4.7). In line with the herbicidal action of other quinoline carboxylates, AEX also triggered vitrification and senescence in light-grown plants (Figure S4.7).

AEX interferes with auxin metabolism at different levels

Analysis of *pCYCB1;1::DB-GUS* expression revealed an opposite effect of AEX on the root apex versus the apical hook (Figure S4.2a), suggesting that AEX differentially controls cell cycle activity, probably depending on the impact on IAA homeostasis. A similar case of spatial differences in cell cycle control was found in heavy metal exposed roots, in which meristematic activity in the main root was inhibited, but the cell division activity leading to new lateral roots was induced (Pasternak *et al.*, 2005a; Pasternak *et al.*, 2005b). These changes in root patterning suggested an auxin redistribution. Likewise, AEX is proposed to have an impact on auxin homeostasis, primarily acting at the shoot, and affecting the root as a consequence thereof.

The concentration of auxin within a plant cell is regulated both by the rate of its metabolism (synthesis, conjugation, catabolism) and the capacity and rate of its transport, together regulating cellular auxin homeostasis. Essentially the above-mentioned observations, together with the fact that AEX acts downstream of HLS1, suggest either an enhanced auxin catabolism or an interference with auxin efflux transport. The latter was supported by a dose-

dependent accumulation of [^{3}H]NAA in tobacco BY-2 cells, indicating that AEX can block auxin export (Figure 4.8). Furthermore, by analyzing IAA, IAA conjugates, and the major IAA catabolites in AEX-treated etiolated seedlings, we hypothesized that AEX limited movement of free IAA produced in meristems since its final catabolite oxIAA-GE largely accumulated there (Figure 4.9; Figure S4.6). The elevated production of oxIAA-GE suggested enhanced oxidative activity triggered by AEX. Since auxin catabolites are not transported across the plasma membrane (Pencik *et al.*, 2013), the very high amount of ox-IAA-GE indicated that only a small portion of IAA is transported to the hypocotyl. The altered auxin metabolism in the shoot could consequently lead to a distorted auxin homeostasis in the root, because of the minimized basipetal transport of active auxins. Recently, ROS were shown to induce the oxidation of IAA to oxIAA, in order to remove high levels of active auxin from the root apex to attenuate auxin signaling and maintain auxin homeostasis (Peer *et al.*, 2013; Pencik *et al.*, 2013). The link between AEX and ROS was largely supported by our microarray data and NBT/DAB stains. From the microarray analysis, indirect support was offered by more than one-third of overlap with H_2O_2 induced transcripts in the AEX up-regulated gene set (Figure 4.10a). Direct evidence for induction of ROS by AEX came from the NBT/DAB stains, where an enhanced accumulation of O_2^- was observed in the apical regions of hypocotyl and root and an enhanced accumulation of H_2O_2 above the meristem towards the root differentiation zone (Figure 4.11). Studies have shown that auxin-type herbicides might act through induction of H_2O_2 (Grossmann *et al*., 2001; Peer *et al*., 2013). Greatly increased ROS accumulation induced by AEX could disrupt the redox homeostasis, further oxidize IAA, hence, lower the IAA level, and ultimately diminish the meristematic cell activity as reported in the tomato *(Solanum lycopersicum) diageotropica (dgt)* mutant (Ivanchenko *et al.*, 2013). It was proposed that once the ratio of H_2O_2 to O_2^- reaches its maximal level, cell proliferation ceases, and cells differentiate (Tsukagoshi *et al.*, 2010). The reduced meristem size might result from reduction in cell wall extensibility of developing root cells, resulting from ROS accumulation (Büntemeyer *et al.*, 1998). In the microarray dataset, a group of cell wall proteins whose activity directly enhances cell wall extensibility, such as PROLINE RICH PROTEIN 3 (PRP3), LEUCINE-RICH REPEAT/EXTENSIN 1 (LRX1) and expansins (Cosgrove, 2005) were downregulated (Table S4.4). Particularly interesting is that in the AEX downregulated gene set, more than one-third of the genes overlapped with root-specific UPBEAT1 (UPB1) downregulated transcripts, including a large set of peroxidases (Tsukagoshi *et al.*, 2010) (Figure 4.10b). In addition, ectopic UPB1 expression conferred shortening of root meristem and overall length as well as significant decrease in cortex cell number, phenotypes mimicked by AEX. Conversely, ectopic UPB1 expression resulted in enhanced H_2O_2 accumulation above the root meristem accompanied with a decreased O_2^- in the meristem to maintain ROS homeostasis, whereas AEX induced H_2O_2 and O_2^- above and in the meristem, respectively. Therefore, despite the striking overlap in expression patterns, UPB1 does not seem to be the target of AEX.

Based on the above-mentioned findings we propose a model in which AEX interferes with auxin transport from its major biosynthesis sites, particularly the SAM and cotyledons. This is either the direct consequence of poor basipetal IAA transport from the meristematic region, or indirectly linked to excessive IAA oxidation. The auxin transporters affected by AEX could

be PIN-FORMED (PIN)1 and ATP-BINDING CASSETTE B/P-GLYCOPROTEIN/MULTIDRUG RESISTANCE (ABCB/PGP/MDR)19, primary mediators of shoot basipetal polar auxin transport (PAT) (Gälweiler *et al.*, 1998; Noh *et al.*, 2001). Given the central role of PAT, with the major auxin flux directed from shoot to root, a distortion of auxin homeostasis in the shoot is expected to have severe consequences in the root. This was reflected by enhanced ROS staining in the root tip, probably related to an imbalance in auxin (Figure 4.11). Microarray data supported accumulation of ROS in AEX-treated seedlings (Figure 4.10a,b). On the other hand, NADPH oxidases such as RbohD, were linked to auxin-induced ROS production (Peer *et al.*, 2013). In the root tip, auxin accumulation is resulting from PAT from the shoot and auxin synthesis at the root meristem (Ljung *et al.*, 2005). The strongly reduced stelar auxin flux toward the root tip probably results in a local increase in auxin synthesis and subsequent ROS accumulation, known to limit the size of the root meristem (Tsukagoshi *et al.*, 2010; Ivanchenko *et al.*, 2013), as seen upon AEX treatment (Figure 4.4c,d). Both basipetal transport and lateral distribution of auxin, mediated by the auxin transport facilitators PIN2, PIN3, and PIN7, are critical for controlling cell division and root meristem size (Blilou *et al.*, 2005). PIN(s) could be the candidate auxin transporters affected by AEX; however, effects of AEX on ABCB(s) transporters or their interactions with PIN(s) cannot be excluded (Blakeslee *et al.*, 2007; Mravec *et al.*, 2008). The inhibitory effects on root hair initiation and growth triggered by AEX (Figure 4.4g,h) could result from a transiently suppressed auxin signal caused by increased ROS production (Blomster *et al.*, 2011). A recent study also suggests that the impaired root hair growth in multiple *pin* loss-of-function mutants is most likely resulting from the imbalance in auxin homeostasis (Rigas *et al.*, 2013).

Distorted auxin accumulation was also reflected in altered gravitropism triggered upon AEX treatment and may be related to an alteration in endomembrane trafficking, affecting auxin transport. A successful example is the identification of Gravicin as a gravitropism and vacuolar transport inhibitor from a chemical genetics screen, which linked the altered gravity response phenotype with vesicular trafficking. ABCB19 was identified as a target for Gravicin (Surpin *et al.*, 2005; Rojas-Pierce *et al.*, 2007). The link of AEX triggered hypocotyl gravitropic response with endomembrane trafficking, could be tested with tonoplast-specific markers, such as GFP: γ-TIP and GFP: δ-TIP (Cutler *et al.*, 2000).

Further investigation of AEX can help to resolve issues linking ROS and auxin homeostasis in plant development. In order to gain insight into the auxin transporters that are affected by AEX, inhibitory effects of AEX on auxin transport mediated by recombinant PIN(s) and ABCB(s) expressed in *Schizosaccharomyces pomb*e could be screened for (Yang & Murphy, 2009). Current work is focusing on the identification of AEX targets using a forward genetics screen to identify mutants with reduced or enhanced sensitivity to AEX.

Materials and methods

Plant Materials

eto2-1 and *etr1-1* were from the Nottingham *Arabidopsis* Stock Centre. *ctr1-1* was from *Arabidopsis* Biological Resource Center. *ein2-1 and ein3-1 eil1-1* were a kind gift from J. Ecker (The Salk Institute, San Diego, USA). Further details are included in Supplemental information.

Growth conditions

Surface-sterilized seeds were sown on half-strength MS (Duchefa) medium (1% sucrose (pH5.7), 0.8% agar (LAMB)). Compound ACCERBATIN (AEX) (ID: 6527749) was procured from ChemBridge^{TM} (www.hit2lead.com) and a stock solution was prepared in DMSO (Dimethyl sulfoxide, Sigma-Aldrich) at 100 mM. The final concentrations of the screened compounds, 1-aminocyclopropane-1-carboxylic acid (ACC, Sigma-Aldrich, dissolved in deionized water (diH_2O)) and N-(1-naphtyl)phtalamic acid (NPA, Sigma-Aldrich, in DMSO) are indicated in the respective results sections. In all treatments and in the untreated control, DMSO was supplied in the same final concentration. For assays in darkness, seeds were stratified at 4°C for 2 days, exposed to light for 6 hours to stimulate germination, and returned to darkness (22°C) for desired time.

For ethylene exposure, plants were flushed continuously with 5 ppm ethylene in air (Air Liquide) in a sealed 5L jar. A control was performed with ethylene-free air.

Quantification of phenotypes

The angle of hook curvature was measured as defined previously; 180° minus or plus the angle between the tangential to the apical part and the axis of the lower part of the hypocotyl for normal and exaggerated hooks, respectively (Vandenbussche *et al.*, 2010). The number of cells along the apical-basal axis of the hypocotyl were obtained by counting a cortex cell file at the outer side of the hook. The apical hook region was defined starting from the first cell at the bifurcation of the vascular bundle below the cotyledons until the first obviously elongated cell.

The number of cells in the root meristematic zone was obtained by counting cells showing no signs of rapid elongation within a cortex cell file (Beemster & Baskin, 1998). Patterning of the root developmental zones was based on (Verbelen *et al.*, 2006).

The length and angle were measured by ImageJ (National Institute of Health).

Measurement of ethylene emanation

Ethylene emanation was measured with a photo-acoustic detector (ETD-300 ethylene detector, Sensor Sense, The Netherlands) as described in (Ellison *et al.*, 2011). Approximately 100 Col-0 seeds were sown in a 10 mL chromatography vial containing 5 mL of growth medium supplied with desired compounds. 24 hours before the measurement, the vial was sealed in

darkness with a rubber plug and a snap-cap (Chromacol) to allow ethylene accumulation. The output data were calculated using OriginPro 7.5 (OriginLab).

Dynamic imaging

For kinetic analysis of apical hook development and analysis of gravitropic effects, time-lapse images were taken in the dark using an infrared imaging system (Smet *et al.*, 2014).

Determination of the effects of AEX on gravitropism

The gravitropism assay was performed as described previously (Vandenbussche *et al.*, 2011) with reorientation of 3-day old seedlings and subsequent analysis after 24 hours.

Auxin accumulation assays in tobacco BY-2 suspension cells

Tobacco BY-2 cells (*Nicotiana tabacum* L., cv. Bright Yellow-2; (Nagata *et al.*, 1992) were cultivated as described previously (Petrášek *et al.*, 2003). Auxin efflux was measured by cellular changes in accumulation of radioactively labeled 1-Naphthaleneacetic acid (NAA) ([^{3}H]NAA) (Petrášek and Zažímalová, 2006). The accumulation of 2 nM [^{3}H]NAA (American Radiolabeled Chemicals, Inc.) in cells treated with AEX or ACC were determined by liquid scintillation counting (Packard Tri-Carb 2900TR scintillation counter; PerkinElmer). Cell surface radioactivity was corrected by subtracting counts of aliquots collected immediately after addition of [^{3}H]NAA. Counts were converted to pmols of [^{3}H]NAA per 1 million cells.

Determination of endogenous auxin and auxin metabolites

Cotyledons (with SAMs) and hypocotyls (60-80 pieces) of 4-day-old *Arabidopsis* seedlings grown in darkness were separated in darkness to prevent stimulation of photomorphogenesis. Pieces were collected in 300 ml methanol. The cutting positions are illustrated in Figure S4.9. After overnight extraction at –20°C, tissue debris was separated by centrifugation (10,000 *g*) and extracts were evaporated to dryness. Quantification of auxin and auxin metabolites was performed according to (Dobrev & Vankova, 2012).

Statistics

The quantitative data in figures were represented as mean ± SD. Statistical analysis was performed in R 3.2.3. (R Foundation for Statistical Computing, Vienna, Austria; https://www.R-project.org/). Comparison of means among three or more groups was done with Analysis Of Variance. Normality of the residuals and homoscedasticity were verified with quantile-quantile plots and boxplots, respectively. In most cases, large differences between the means of different groups correlated with large differences in variances. Therefore the non-parametric Kruskal-Wallis rank sum test was applied in the case of one categoric variable, while the Scheirer-Ray-Hare extension was applied for two categoric variables. Post-hoc Wilcoxon rank sum tests ($P < 0.05$) were performed for multiple pairwise comparisons and P-values were adjusted with Bonferroni correction to correct for multiple testing. Wilcoxon rank sum tests were also applied to test for differences between the

distributions of only two groups. Output of the statistical analyses is shown in the legends and can be found in supplementary Table S4.6. Effect size r was calculated as Z/sqrt (N) (with N = total number of samples; Z = absolute value of Z score, which is calculated from the Wilcoxon W statistic).

Microarray hybridization and analysis

Sample preparation was as described under 'Short term AEX treatment in liquid medium' (Supplemental information). 3 independent experiments were performed. RNA isolation was done using an RNeasy Mini Kit (Qiagen). For each sample, more than 1 µg RNA was sent to the Affy Gene Chip Service (NASC) for analysis on the *Arabidopsis* ATH1 Genome Array (Affymetrix). The Affymetrix data were provided as CEL files. Quality assessment, normalization and statistical analysis of microarray data were done with Robin software (Lohse *et al.*, 2010) (details in Supplemental information).

Detection of reactive oxygen species (ROS)

Staining for hydrogen peroxide with diaminobenzidine (DAB) and for superoxide with nitroblue tetrazolium (NBT) was essentially performed according to (He *et al.*, 2012). 1 mg/mL 3,3′-diaminobenzidine tetrahydrochloride dihydrate (DAB, Sigma-Aldrich) was prepared in diH_2O, and adjusted to pH 3.8 with Tris-HCL buffer (pH 7.5). For the NBT (Sigma-Aldrich) staining, 2 mM NBT solution was prepared in 20 mM phosphate buffer (pH 6.1). Incubation in DAB solution was 8 hours and 3 hours in NBT solution 3 hours, in darkness.

Accession Numbers

Sequence data from this article can be found in the EMBL/GenBank data libraries under accession numbers AT1G19020, AT1G05340, AT2G21640, AT1G57630, PRP3 (AT3G62680), LRX1 (AT1G12040), EXPA7 (AT1G12560), EXPA18 (AT1G62980) and UPB1 (AT2G47270).

Supplemental Data

S4.1 ACCERBATIN (AEX) stability*in vivo*, as determined by liquid chromatography–mass spectrometry (LC-MS) profiling

All chromatograms were processed, integrated and aligned as published before (Morreel et al., 2014). In total, this yielded 5692 m/z features that could be putatively assigned to 822 compounds following the "peak grouping" algorithm previously described (Morreel et al., 2014). Besides the AEX compound itself, only one other "peak group" (called AEXfrg) was observed to be solely present in those samples that were fed with the AEX compound. Following MS data for AEX and AEXfrg were obtained (relative abundance versus the base peak is given between parentheses for each product ion): Compound AEX. m/z 471.05251 [M-H+]- ($C_{23}H_{18}O_2N_2{}^{79}BrF_2^-$, Δppm = -0.019). MS2 (collision energy 35%): 295 (45), 315 (100), 451 (79). MS3 of first product ion at m/z 315 (collision energy 35%): 295 (100). MS3 of first product ion at m/z 451 (collision energy 35%): 295 (3), 369 (1), 407 (2), 423 (22), 433

(29), 451 (100). MS4 of second product ion at m/z 295 derived from the first product ion at m/z 315 (collision energy 35%): 223 (1), 253 (2), 259 (1), 267 (2), 275 (9), 277 (15), 280 (2), 293 (1), 295 (100). Compound AEXfrg. m/z 370.04467 [M-H+]- ($C_{19}H_{17}O_2N_1{}^{79}Br^-$, Δppm = -0.039). MS2 (collision energy 35%): 196 (2), 212 (1), 214 (100), 342 (1), 370 (64). MS3 of first product ion at m/z 214 (collision energy 35%): 134 (3), 160 (5), 172 (7), 178 (3), 186 (21), 196 (100), 199 (16). MS4 of second product ion at m/z 196 (collision energy 35%): 178 (100). The loss of both fluorines and one nitrogen in the chemical formulae of AEXfrg as compared to that of AEX indicates that AEXfrg is formed via cleavage of the amide bond in AEX. However, such cleavage would also have resulted in the loss of 6 carbons and 4 hydrogens which cannot be deduced by comparing both chemical formula. Clearly, the reaction proceeded with the addition of an ethylene moiety.

S4.2 AEX stability in vitro determined by Nuclear magnetic resonance (NMR)

The aim of the NMR analysis was to explore whether the fragmentation event observed in the MS analysis could be reproduced in vitro and whether the fragmentation product could be identified. Considering the fact that the original samples were already dissolved in protonated methanol, the baseline of several spectra was distorted due to the intensity of the two methanol signals. In addition, overlap of these signals with some signals of the molecule of interest cannot be excluded: as seen in Figure S4.1b, all the resonances could be assigned except for proton n° 14, which is expected to be located around 4.7 ppm (chemical shift prediction ChemDraw Ultra 13, numbering corresponds with the numbering in Figure S4.1a) and is believed to be overlapping with the second very intense methanol signal residing at 4.80 ppm. The assignment of the molecule itself could be performed almost solely on the basis of chemical shift and integral values, except for the amine n°10 and amide n°8 where none of the two could be assigned unambiguously. In addition, as can be seen in Figure S4.1b, the integral values are in agreement with the number of protons assigned to each 1H signal. It has to be noted that when the signal is situated closer to one of the methanol signals, the integral will start to deviate from the correct value due to the partial overlap of the large background of these solvent signals with the signal of interest (e.g. n°13 should correspond with 2 protons, where the integral corresponds with 2.8). Regarding the first comparison of the three different samples in Figure S4.1c, measured at room temperature under identical conditions, it can be noted that there are no significant differences in the signals of interest: both sets of aromatic signals are present and no new signals compared to signals of the AEX component are visible. During the temperature study, several 1D1H measurements were performed at regular intervals of ±30min. Figure S4.1d shows three spectra, one at the start of the temperature study and two spectra measured after 6 hours and 12 hours of heating at 50°C. As can be seen clearly, no changes whatsoever could be noticed throughout the experiments. Of special interest, highlighted in the three spectra, the aromatic signals remained identical. As a last type of experiment, two samples were subjected to a pH study: both the reference sample which wasn't heated as the sample prior heated at 80°C, were measured at pH ±5 and ±4. As can be seen from Figure S4.1e and S4.1f, no notable differences concerning the signals of interest, neither any new signals could be observed. Considering the fact that both the temperature as the pH study don not show notable differences before and after heating/pH

adjustment, it can be concluded the AEX compound is both thermal and pH stable. Should the fragmentation product detected by MS analysis be present, this clearly is below the NMR detection limit.

Supplemental Experimental Procedures

Additional plant materials

pCYCB1;1::DB-GUS was provided by L. De Veylder (Flemish Institute of Biotechnology, Ghent, Belgium). *EBS::GUS* 1-11 lines were from J. Ecker (The Salk Institute, San Diego, USA). DR5::GUS line was offered by T. Guilfoyle (University of Missouri, USA). *aux1lax3* and *aux1lax1lax2lax3* were from M. Bennett (The University of Nottingham, UK). *pin3-3* was from O.Tietz (Albert-Ludwigs-Universität, Germany). *pid salk, wag1, wag2, wag1wag2pid* were kindly provided by Remko Offringa (Leiden University, the Netherlands). *arf2-6, nph4-1arf19-1, aux1-7,* 35S::PIN1, *rcn1-1, pgp4-1, abcb1abcb19, axr3-1* were purchased from NASC.

Screened compounds

Compound ACCERBATIN (AEX) (6527749) was procured from ChemBridge™. Compounds 6640029, 6520852 and 6514196 are analogs of AEX and were obtained from a ChemBridge™ analog search using AEX as search term (www.hit2lead.com). Compounds LAT014C06, LAT013C04, LAT007H11, LAT010G08 and LAT024E02 were selected from the LATCA library (cutlerlab.blogspot.com/2008/05/latca.html). The latter were originally obtained from ChemBridge™ (ChemBridge ID 5601004, 5707885, 5473152, 5617132 and 5712036, respectively). All stock solutions were prepared in DMSO (Dimethyl sulfoxide, Sigma-Aldrich) at 100 mM.

Short term ACCERBATIN (AEX) treatment in liquid medium

1) Seed sterilization:

Seeds were sterilized using chlorine gas (http://www.plantpath.wisc.edu/fac/afb/vapster.html). The seeds were put in a labeled microcentrifuge tube with open lid, placed in a rack inside the dessicator jar in a fume hood. A beaker containing 100 mL bleach (4.5% active chlorine, Glorix, Unilever) was placed in the dessicator jar next to the rack. Prior to sealing the jar, 3 ml concentrated hydrochloric acid (HCl, 37%, Merck) were carefully added to the bleach and mixed. The seeds were left in the chlorine fumes for 5 hours.

2) Growth medium:

Freshly prepared MS/2 containing 1% sucrose adjusted with KOH to pH 5.7 was used as liquid plant growth medium.
The medium was supplemented with AEX to a final concentration of 100 μM or with an equivalent volume of DMSO as a control.

3) Growth condition and treatment:

Approximately 800 Col-0 seeds were sown on pre-cut sterilized filter paper (Whatman), fitting the dimensions of 145/20 mm Petri dishes (Greiner Bio-One), and kept on the agar containing growth medium in the Petri dishes. After stratification in darkness at 4°C for 2 days, the Petri dishes were exposed to cool-white fluorescent light for 6 hours at 22°C to stimulate the germination, wrapped in two layers of aluminum foil and left in a growth chamber at 22°C for 60 hours.

All treatments were done under the green safety light. 45 mL of liquid medium containing 100 µM AE or an equivalent amount of DMSO were poured in the 145/20 mm petri dishes. Afterwards, the filter paper with seeds was transferred from the solid to the liquid medium, submerged, and left to float for 6 hours until harvesting.

Microarray analysis using Robin software and data processing of online available transcriptomics resources

The original Compound Document Format (CDF) file (Arabidopsis ATH1-121501.CDF) was downloaded from NASC Arrays (NASC) (http://affy.arabidopsis.info/link_to_iplant.shtml) and imported together with the CEL files into Robin. The Robust Multichip Average (RMA) algorithm was applied to create an expression matrix (Irizarry et al., 2003), the false discovery rate (FDR) was chosen for p-value correction (Benjamini et al., 2001). The significance cut-off was defined as a log2 fold change in expression less than 1 (i.e. less than 2-fold up- or down regulation) and genes showing a p-value greater than 0.05 (i.e. 5% false discovery rate) were chosen. The gene annotation search was done in TAIR (http://www.arabidopsis.org/tools/bulk/microarray/). The overrepresentation of Gene Ontology groups on sets of differentially expressed genes was studied with BiNGO software (Maere et al., 2005).

Table S4.3a, b, c and d represent the overlap of AEX regulated genes with gene sets from H_2O_2 (Davletova et al., 2005), UPB1 arrays (Tsukagoshi et al., 2010), genes commonly regulated in auxin arrays (Zhao *et al.*, 2003; Okushima *et al.*, 2005b; Nemhauser *et al.*, 2006), and genes commonly regulated in ethylene arrays (Alonso et al., 2003; Olmedo et al., 2006). For auxin-related genes, data from Okushima et al. (2005b) were derived from the Gene Expression Omnibus (GEO) database (http://www.ncbi.nlm.nih.gov/geo/) with accession number GSE627 (using samples GSM9620 and GSM9624 to GSM9628); for ethylene-related genes, data from Olmedo et al. (2006) with accession number GSE5174 (samples GSM116733 to GSM116736) were used. False discovery rates were computed from P-values using the Benjamini-Hochberg procedure, auto-detect was applied to the log transformation to the data (log2 fold change in expression less than 1) and calculated by GEO2R (http://www.ncbi.nlm.nih.gov/geo/geo2r/).

Static imaging

A photograph of dark-grown seedlings was taken after transfer from the growth media to an agar plate without disturbing the plant's shape. A digital single-lens reflex (SLR) CCD camera (EOS 550D, Canon) mounted on a binocular (Stemi SV11, Carl Zeiss), controlled by DSLR REMOTE PRO 1.9.1 software (Breeze systems) was used.

To take close-up photos, seedlings were mounted on a microscope slide in a solution containing 2.5g of chloral hydrate (Acros) in 1mL of 30% glycerol (Sigma-Aldrich). Differential interference contrast (DIC) microscopy images were captured with an AxioCam ICc3 camera attached to a Zeiss Axiovert 200 microscope using AxioVision Rel. 4.6 software (Carl Zeiss). A Plan Apochromat 20x objective was used.

Histochemical analysis of GUS expression

Seedlings of GUS reporter lines were treated with 90% ice-cold acetone for 30 minutes after removal of the liquid medium, washed with 0.1 M phosphate buffer (pH 7.2) for 15 minutes at room temperature and incubated at 37ºC overnight in GUS staining buffer, containing 2mM 5-bromo-4-chloro-3-indolyl-glucuronide (X-gluc, Duchefa, The Netherlands), 0.1M sodium phosphate buffer (pH 7.2), 0.5 mM potassium ferricyanide and 0.5 mM potassium ferrocyanide. Seedlings were kept in 70% ethanol for further DIC microscopy analysis.

Liquid chromatography–mass spectrometry (LC-MS) profiling

All samples were profiled via reversed phase ultrahigh performance liquid chromatography (RP-UHPLC) hyphenated to a Fourier transform-ion cyclotron resonance-mass spectrometer (FT-ICR-MS) using the instruments and essentially the same method as previously published (Morreel et al., 2014). Modifications included the column type (Acquity UPLC BEH C18; 150 mm x 2.1 mm, 1.8 μm; Waters, Milford, MA) and the use of atmospheric pressure chemical ionization (APCI). Here, a gradient from 95% aqueous formic acid to 100% acetonitrile was performed in 35 min at a column temperature of 80° C. The APCI source was operated using 3.5 μA, 200° C, 300° C, 40 (arbitrary units, arb) and 20 (arb) for the source current, capillary temperature, vaporizer temperature, sheath gas and auxiliary gas flow rates, respectively. Full MS spectra in the range m/z 120-650 were recorded in the negative ionization mode.

Nuclear magnetic resonance (NMR) spectrometry

All NMR spectra were measured on an Avance II Bruker Spectrometer operating at a ^{1}H frequency of 500 MHz and equipped with a $^{1}H/^{13}C/^{31}P$ TXI-z probe. Three samples were provided, each of which containing 0.5mg of product dissolved in 53µl of protonated MeOH. One standard, non-manipulated sample, and two other samples heated at 50°C for 30 min and 80°C for 1 hour respectively, were analyzed. Each sample was subsequently diluted to 600µl total sample volume using deuterated MeOH. All spectra were referenced to the protonated methyl solvent signal at 3,34 (1) ppm for the ^{1}H frequency. The experiments recorded on the samples included 1D ^{1}H spectra recorded at room temperature for each sample provided. In addition, a temperature stability study was performed with spectra recorded at regular intervals (30 min) at 50°C over a period of 12 hours. Finally, a small-scale pH stability study was performed where both the original reference sample as well as the sample which was heated at 80°C were measured at pH ±5 and ±4 (measured in MeOH). Small aliquots of diluted HCl in deuterated methanol were used to adjust the pH to the desired values. All spectra were processed using TOPSPIN 3.2 pl3 software (http://www.bruker.com/products/mr/nmr/nmr-software/software/topspin/overview.html).

Growth conditions of light grown plants

The growth chamber was set at 22˚C under a photoperiod of 16 h light followed by 8 h darkness.

Supplemental Figures

(a)

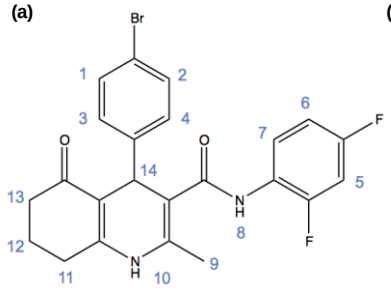

(b)

δ 1H (ppm)	multiplicity	Integral	# protons	Annotation
1,9/2,0	multiplet	1,13; 0,87	2	12
2,15	singlet	3,26	3	9
2,31	multiplet	2,37	2	11
2,54	multiplet	2,82	2	13
6,88	triplet	0,86	1	5
6,97	triplet of doublets	0,89	1	6
7,2	doublet	2,02	2	3 & 4
7,36	doublet	2	2	1 & 2
7,45	multiplet	0,89	1	7
8,75	broad singlet	0,61	1	8 or 10
9,12	broad singlet	0,64	1	8 or 10
		Total	18	

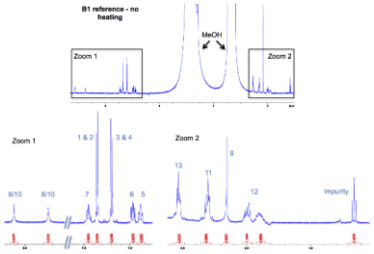

(c)

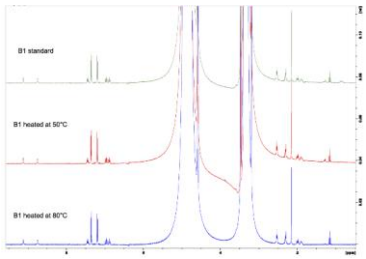

(d)

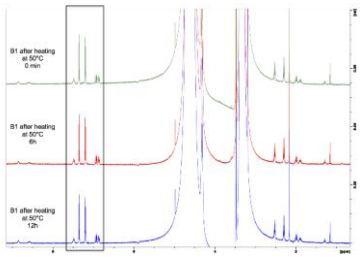

(e)

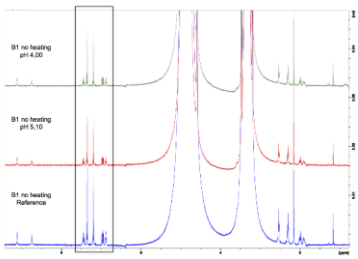

(f)

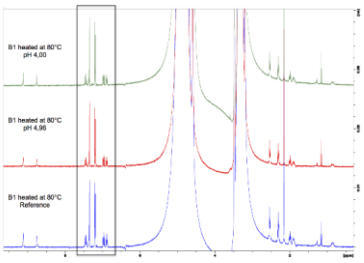

Figure S4.1 NMR Data (See Also Supplemental Data S2). **(a)** AEX structural formula and numbering used throughout the NMR assignment procedure. **(b)** Overview of the general 1D1H assignment of AEX (25°C, 500MHz). **(c)** Overview of the three samples measuredat room temperature (25°C, 500MHz). **(d)** Overview of the AEX temperature study at 50°C after 0, 6 and 12 hours time (500MHz). **(e)** Overview of the pH study on AEX (25°C, 500MHz). **(f)** Overview of the pH study on AEX prior heated at 80°C (25°C, 500MHz).

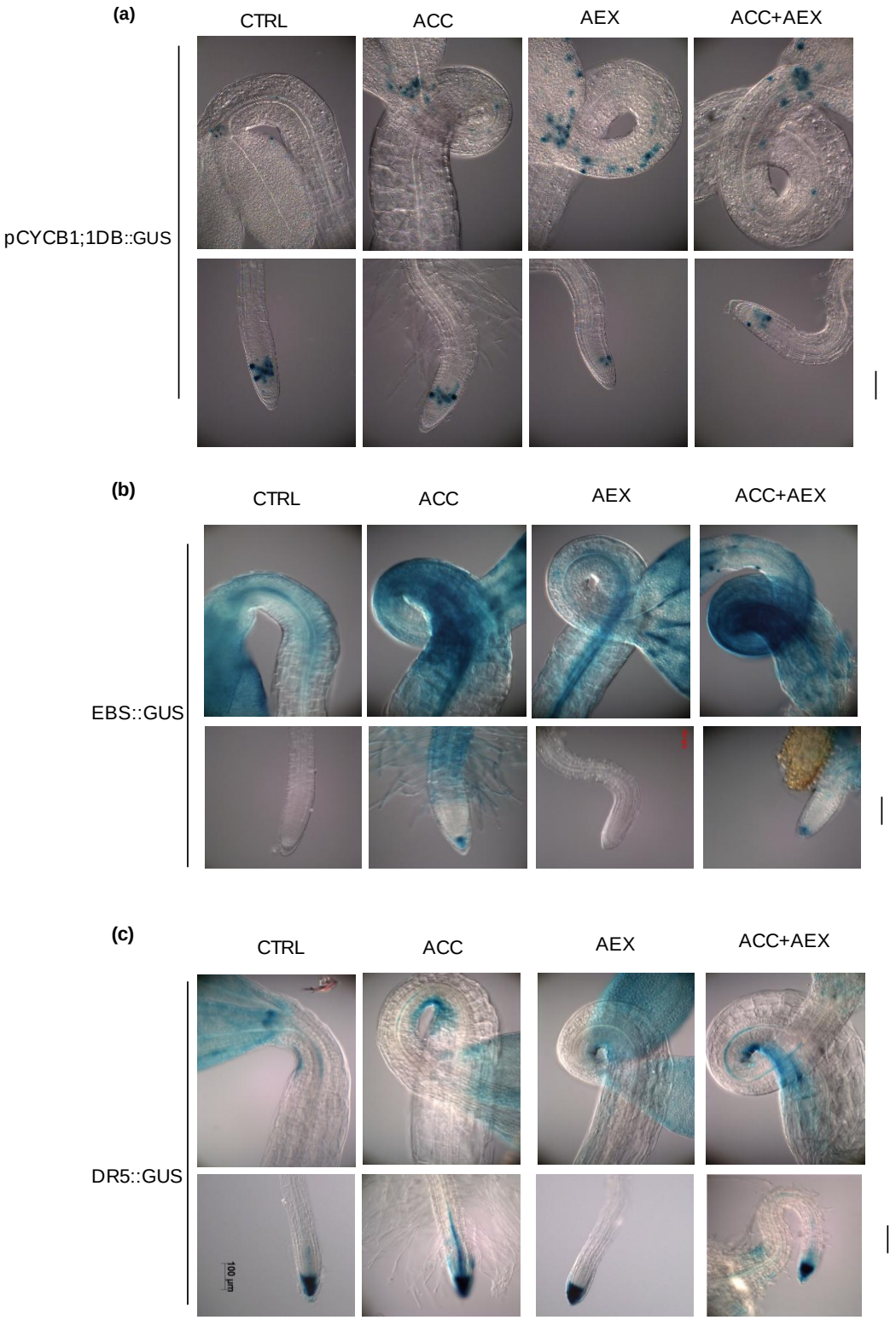

Figure S4.2 Histochemical Staining in 4-day Etiolated Seedlings of GUS-Reporter Lines. Seedingswere grown on horizontally standing plates with 1/2 MS medium containing 1% sucrose supplemented with 0.05% DMSO (CTRL), 10 µM ACC, 50 µM AEX or/and 10 µM ACC. All treatments contained 0.05% DMSO. **(a)** pCYCB1;1::DB::GUS; **(b)** EBS::GUS; **(c)** DR5::GUS. Scale bar = 100 µm.

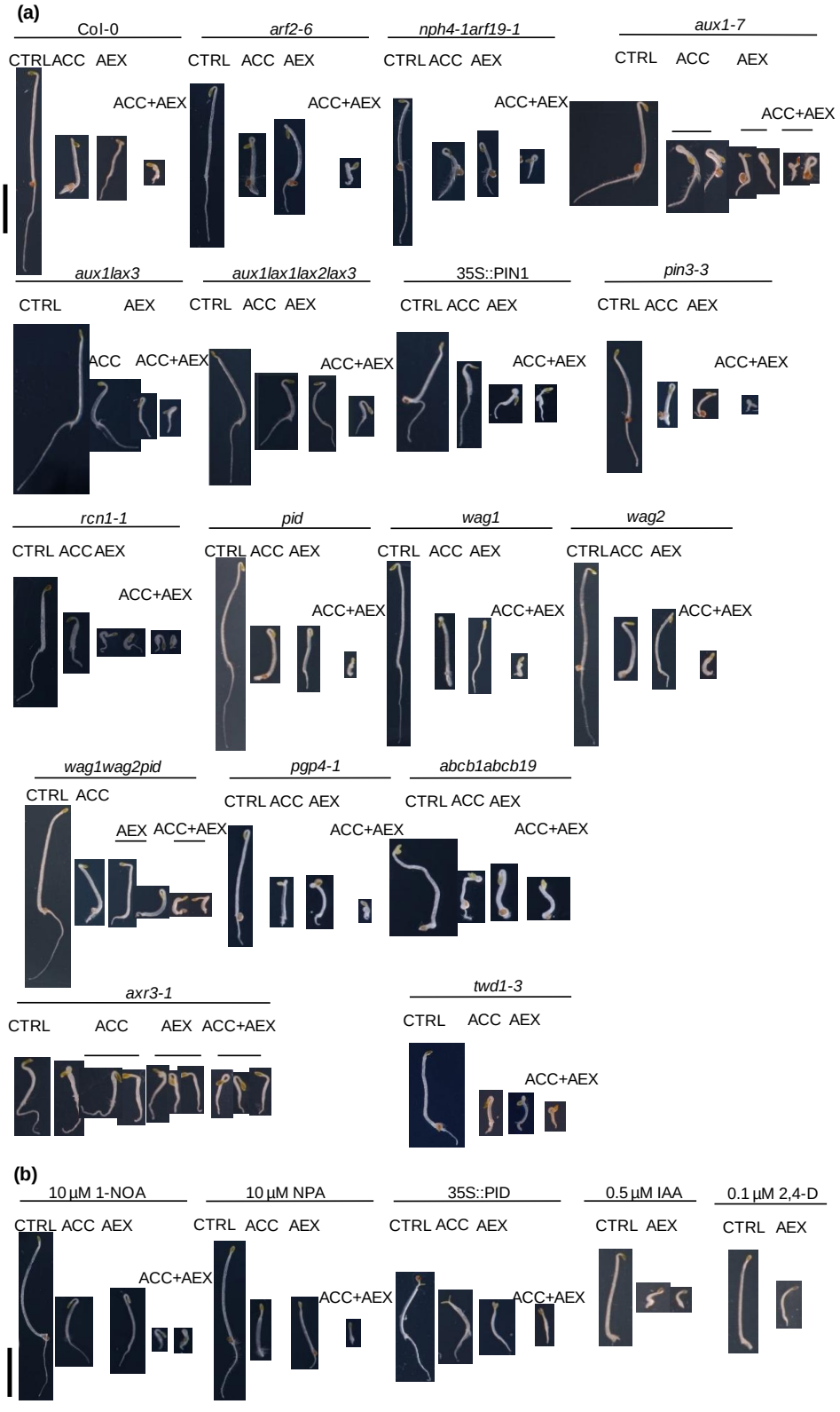

Figure S4.3 Phenotypic Effects of AEX on Auxin Mutants and of AEX in Combination with Auxins and Auxin Transport Inhibitors on the Wild Type. (a) Phenotypes of selected auxin mutants in the presence of 50 µM AEX. Auxin signaling mutants: *arf2-6*, *nph4-1arf19-1* and *axr3-1*; auxin transport mutants: *aux(s)lax3*, *aux1-7*, *35S::PIN1*, *pin3-3*, *rcn1-1*, *pid(s)*, *wag(s)*, *pgp4-1* and *abcb1abcb19*. **(b)** Phenotypes of Col-0 in the presence of 50 µM AEX and 0.5 µM IAA, 0.1 µM 2,4-D, 10 µM 1-NOA or 10 µM NPA. Seedlings were grown on horizontally standing plates.

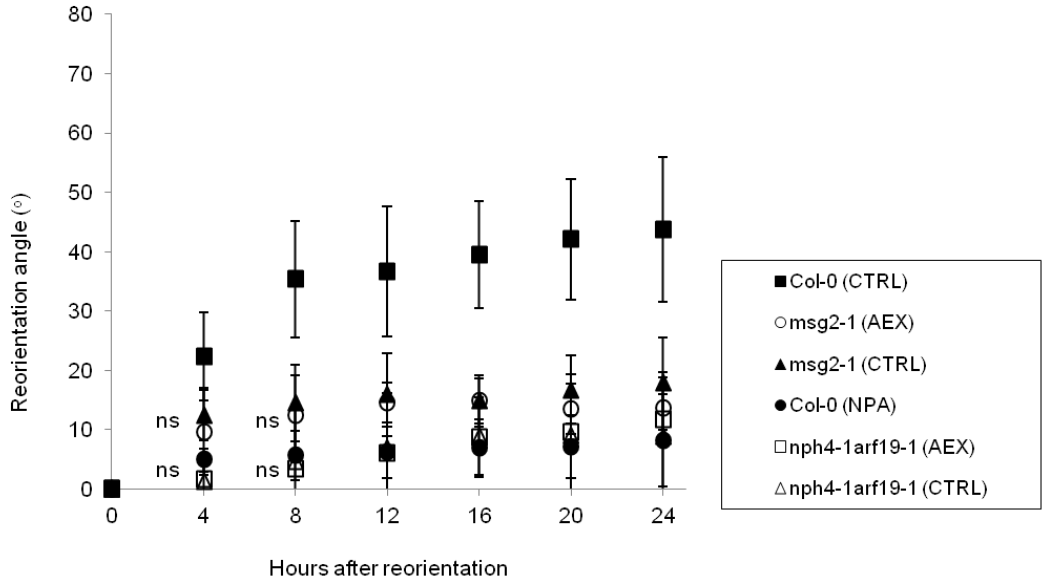

Figure S4.4 Response of Col-0, *msg2-1* and *nph4-1arf19-1* after Growth and Reorientation on Vertically Standing Platesin Darkness. On day 2 after germination, plates were rotated and the average reorientation angle of the hypocotyl was calculated. Data are mean values of at least 6 seedlings. Seedlings were grown on 1/2 MS medium containing 1% sucrose in the presence of 0.05% DMSO (CTRL), 10 µM ACC, 50 µM AEX or 10 µM NPA. All treatments contained 0.05% DMSO. 90°corresponds with the new direction of the gravity vector. Data are presented as mean ± SD. Mean angles of AEX-treated *msg2-1* and *nph4-1arf19-1* were compared with their untreated equivalents at 4 hours and 8 hours after reorientation (Wilcoxon rank sum test with $W(20) = 126{,}5$; $P = 0{,}1109$ (4 hours) and $W(20) = 119$; $P = 0{,}305$ (8 hours) for *msg2-1;* $W(20) = 101$; $P = 0{,}7649$ (4 hours) and $W(20) = 116$; $P = 0{,}4051$ (8 hours) for *nph4-1arf19-1*).

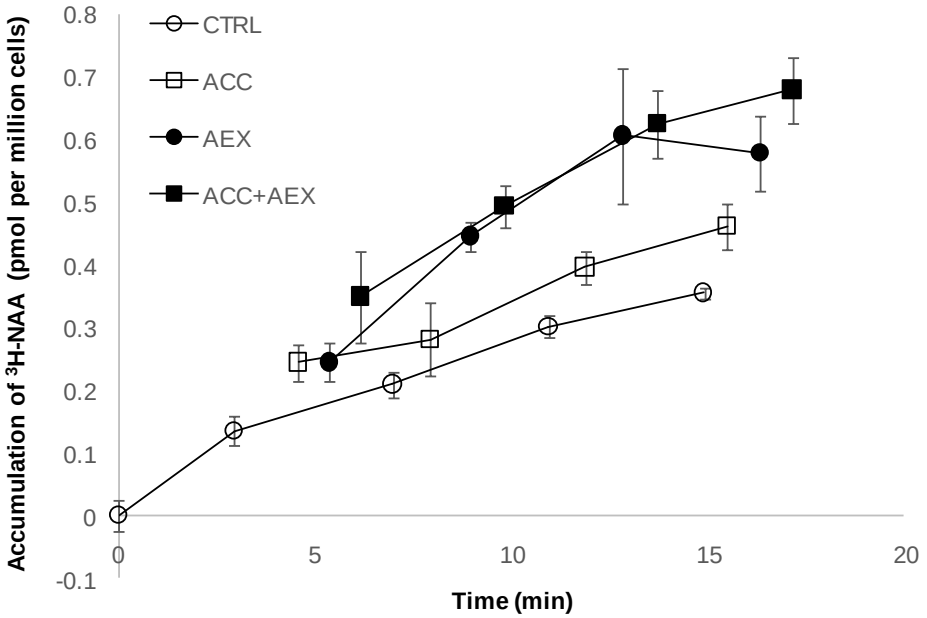

Figure S4.5 [^{3}H]NAA Accumulation Kinetics in Tobacco BY-2 Cells Upon 100 µM AEX or/and 100 µM ACC Treatments. All treatments contained 0.1% DMSO. Time of AEX/ACC Addition is Shown by the Arrow. Error bars indicate SD (n=4).

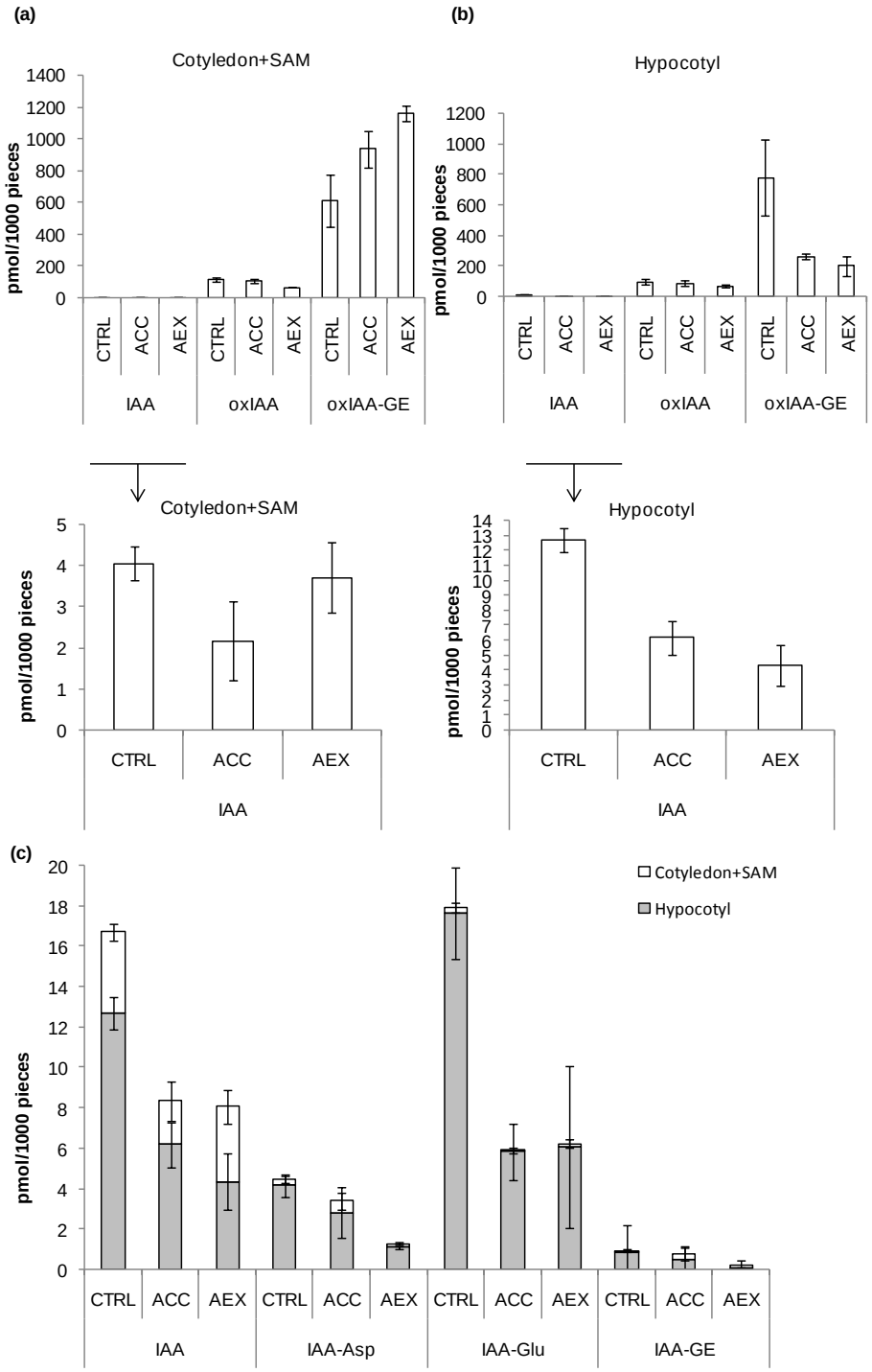

Figure S4.6 GC-MS/MS Determination of the Endogenous Content of IAA, IAA Catabolites and IAA Conjugates of 4-day Etiolated Seedlings Treated with AEX. IAA and oxIAA and oxIAA-GE content in **(a)** Cotyledons (including SAMs) and **(b)** Hypocotyls Treated; **(c)** Endogenous IAA or IAA Conjugate Contents in Cotyledons (including SAMs) and Hypocotyls. Contents are shown for Col-0 treated with 0.05% DMSO (CTRL), 10 µM ACC and 50 µM AEX. All treatments contained 0.05% DMSO. Error bars indicate SD. For **(c)** a three-way ANOVA ($F(23,51) = 69,35$; $P<0,001$) (Tukey's HSD, $P<0,05$; n=2~5) was performed to determine differences in the mean contents (measurement variable) of IAA and conjugates of hypocotyls or cotyledons (+SAM) between all treatments (nominal variables). Different letters represent means that are significantly different.

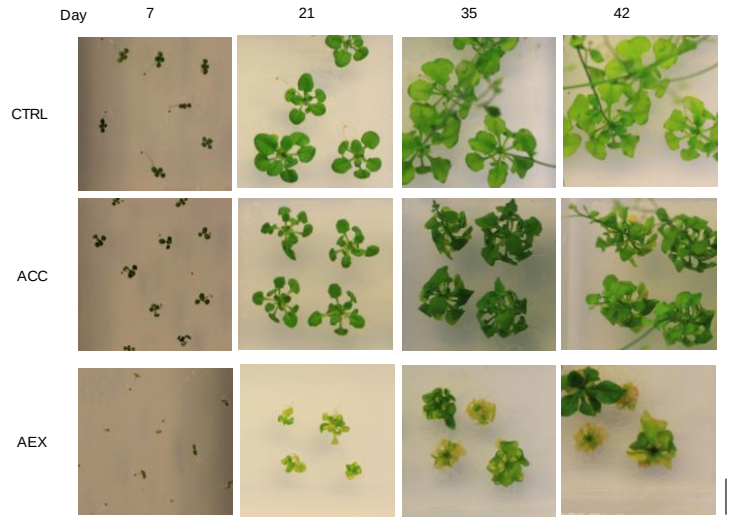

Figure S4.7 Phenotype of Light-Grown Plants. Plants were grown on 1/2 MS medium containing 1% sucrose in the presence of 0.05% DMSO (CTRL), 10 µM ACC, 50 µM AEX. All treatments contained 0.05% DMSO. Photographs were taken at day 7, 21, 35 and 42. Scale bar= 1 cm.

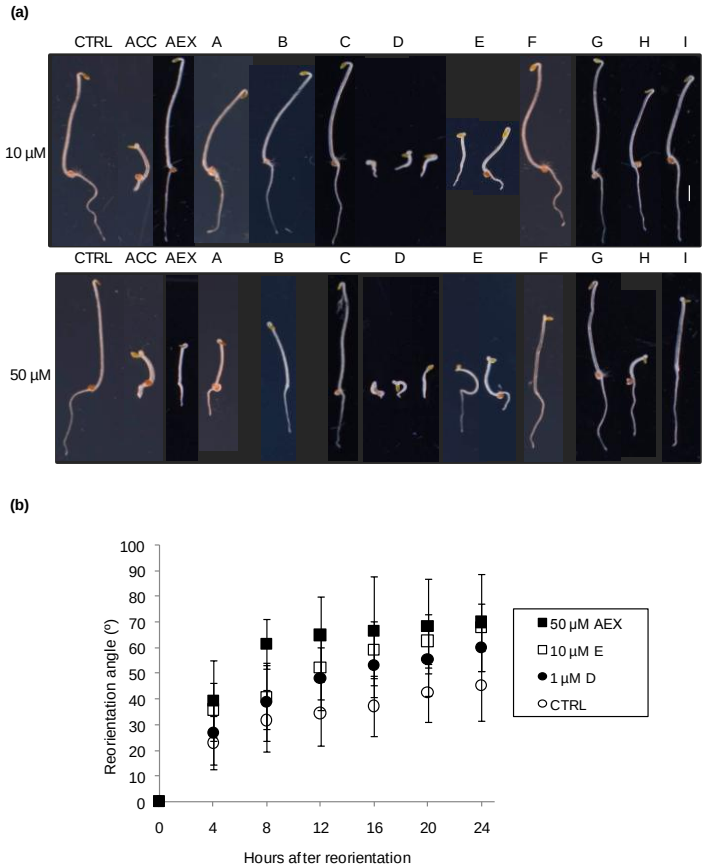

Figure S4.8 Effects of AEX and its analogs on phenotypes of etiolated seedlings and on the gravitropic response of hypocotyls. (a) Phenotypic effects of AEX and its analogs at 10 µM and 50 µM on 4-d dark grown seedlings. Chemical structures of analogs are listed in Table S4.5. The individual photographs were cropped without changing the scale; the black background was post-added. Scale bar = 1 mm. **(b)** Reorientation assay on 3-d-old dark-grown seedlings (2 days after germination, see details in legend of Figure 7). Col-0 were grown in the presence of AEX (50 µM) or E (10 µM) or D (1 µM) or mock treated (DMSO). The reorientation kinetics in the presence of 10 µM of E or 1 µM of D revealed an enhanced rate of reorientation visible at 12 hours. Data are presented as mean ± SD.

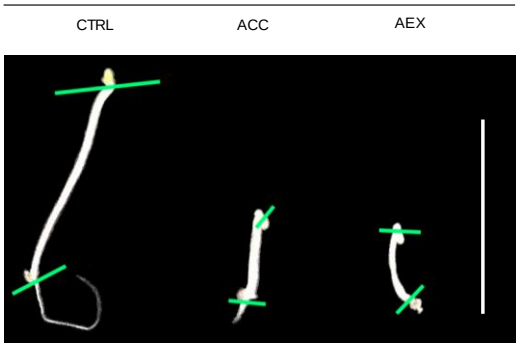

Figure S4.9 Sample Preparation for Determination of IAA, its Conjugates and Catabolites. Illustration of where the cotyledon (with SAM) and hypocotyl were separated. Etiolated seedlings were grown on 1/2 MS medium containing 1% sucrose supplemented with 0.05% DMSO (CTRL), 10 µM ACC and 50 µM AEX for 102-hour. All the treatments contained 0.05% DMSO. Scale bar = 1 cm.

Supplemental Tables

Table S4.1 Genes regulated by 6 hours AEX treatment.

S4.1.1 Genes upregulated by 6 hours AEX treatment compared to mock treated control

Fold change	Locus Identifier	Annotation
34.01	AT5G43450	2-oxoglutarate-dependent dioxygenase, putative
33.24	AT3G60140	DIN2 (DARK INDUCIBLE 2); hydrolase, hydrolyzing O-glycosyl compounds
29.96	AT1G05680	UDP-glucoronosyl/UDP-glucosyl transferase family protein
27.42	AT2G35980	YLS9 (YELLOW-LEAF-SPECIFIC GENE 9)
27.29	AT2G04050	MATE efflux family protein
26.83	AT1G71140	MATE efflux family protein
26.29	AT1G02530;AT1G02520	[AT1G02530, PGP12 (P-GLYCOPROTEIN 12); ATPase, coupled to transmembrane movement of substances];[AT1G02520, PGP11 (P-GLYCOPROTEIN 11); ATPase, coupled to transmembrane movement of substances]
26.18	AT1G26380	FAD-binding domain-containing protein
26.14	AT4G37370	CYP81D8 (cytochrome P450, family 81, subfamily D, polypeptide 8); oxygen binding
24.93	AT1G15520	ATPDR12/PDR12 (PLEIOTROPIC DRUG RESISTANCE 12); ATPase, coupled to transmembrane movement of substances
22.59	AT1G60750	pseudogene, aldo/keto reductase family, contains Pfam profile PF00248: oxidoreductase, aldo/keto reductase family; blastp match of 71% identity and 8.2e-127 P-value to GP|2606077|gb|AAB84222.1||AF030301 auxin-induced protein (Helianthus annuus)
13.25	AT5G62480	ATGSTU9 (GLUTATHIONE S-TRANSFERASE TAU 9); glutathione transferase
13.03	AT2G26560	PLP2 (PHOSPHOLIPASE A 2A); nutrient reservoir
12.76	AT1G05060	similar to hypothetical protein [Vitis vinifera] (GB:CAN75913.1)
12.60	AT1G19020	similar to unknown protein [Arabidopsis thaliana] (TAIR:AT3G48180.1); similar to unnamed protein product [Vitis vinifera] (GB:CAO40966.1)
12.45	AT1G05560	UGT1 (UDP-glucosyl transferase 75B1); UDP-glycosyltransferase/ transferase, transferring glycosyl groups
12.43	AT3G01970	WRKY45 (WRKY DNA-binding protein 45); transcription factor
12.34	AT1G17180	ATGSTU25 (Arabidopsis thaliana Glutathione S-transferase (class tau) 25); glutathione transferase
12.33	AT5G20230	ATBCB (ARABIDOPSIS BLUE-COPPER-BINDING PROTEIN); copper ion binding
12.07	AT2G41730	similar to unknown protein [Arabidopsis thaliana] (TAIR:AT5G24640.1); similar to unnamed protein product [Vitis vinifera] (GB:CAO14635.1)
11.91	AT2G36800;AT2G36790	[AT2G36800, DOGT1 (DON-GLUCOSYLTRANSFERASE); UDP-glycosyltransferase/ transferase, transferring glycosyl groups];[AT2G36790, UGT73C6 (UDP-GLUCOSYL TRANSFERASE 73C6); UDP-glucosyltransferase/ UDP-glycosyltransferase/ transferase, transferring glycosyl groups]
11.55	AT1G17170	ATGSTU24 (ARABIDOPSIS THALIANA GLUTATHIONE S-TRANSFERASE (CLASS TAU) 24); glutathione transferase
11.02	AT3G55090	ATPase, coupled to transmembrane movement of substances
10.84	AT1G66690;AT1G66700	[AT1G66690, S-adenosyl-L-methionine:carboxyl methyltransferase family protein];[AT1G66700, PXMT1; S-adenosylmethionine-dependent methyltransferase]
10.45	AT3G47780	ATATH6 (ABC2 homolog 6); ATPase, coupled to transmembrane movement of substances
10.28	AT5G09570	similar to unknown protein [Arabidopsis thaliana] (TAIR:AT5G64400.1); similar to unknown [Populus trichocarpa] (GB:ABK94558.1); contains InterPro domain CHCH (InterPro:IPR010625)
10.04	AT3G50970	LTI30 (LOW TEMPERATURE-INDUCED 30)
9.99	AT2G32020	GCN5-related N-acetyltransferase (GNAT) family protein
9.85	AT1G67980	CCoAMT (caffeoyl-CoA 3-O-methyltransferase); caffeoyl-CoA O-methyltransferase
9.79	AT2G47520	AP2 domain-containing transcription factor, putative
9.68	AT3G54520	similar to unknown protein [Arabidopsis thaliana] (TAIR:AT3G54530.1)
9.32	AT2G15490	UGT73B4; UDP-glycosyltransferase/ transferase, transferring glycosyl groups
9.02	AT5G02780	In2-1 protein, putative
8.98	AT5G12420	similar to unknown protein [Arabidopsis thaliana] (TAIR:AT5G16350.1); similar to unnamed protein product [Vitis vinifera] (GB:CAO48523.1); contains InterPro domain Protein of unknown function UPF0089 (InterPro:IPR004255); contains InterPro domain Protein of unknown function DUF1298 (InterPro:IPR009721)
8.92	AT1G32940	ATSBT3.5; subtilase
8.88	AT2G47890	zinc finger (B-box type) family protein
8.86	AT2G04070	transporter
8.68	AT2G29460	ATGSTU4 (GLUTATHIONE S-TRANSFERASE 22); glutathione transferase
8.28	AT5G27420	zinc finger (C3HC4-type RING finger) family protein
8.14	AT4G33666	unknown protein
7.98	AT3G09410	pectinacetylesterase family protein
7.95	AT4G36610	hydrolase, alpha/beta fold family protein
7.83	AT1G05340	similar to unknown protein [Arabidopsis thaliana] (TAIR:AT2G32210.1)
7.64	AT1G64900	CYP89A2 (CYTOCHROME P450 89A2); oxygen binding
7.53	AT1G33110	MATE efflux family protein

7.42	AT3G27880	similar to unknown protein [Arabidopsis thaliana] (TAIR:AT1G23710.1); similar to hypothetical protein [Vitis vinifera] (GB:CAN61665.1); similar to unnamed protein product [Vitis vinifera] (GB:CAO14763.1); contains InterPro domain Protein of unknown function DUF1645 (InterPro:IPR012442)
7.35	AT2G04040	ATDTX1; antiporter/ multidrug efflux pump/ multidrug transporter/ transporter
7.35	AT2G15480	UGT73B5 (UDP-GLUCOSYL TRANSFERASE 73B5); UDP-glycosyltransferase/ transferase, transferring glycosyl groups
7.25	AT1G69930	ATGSTU11 (Arabidopsis thaliana Glutathione S-transferase (class tau) 11); glutathione transferase
7.23	AT1G78340	ATGSTU22 (Arabidopsis thaliana Glutathione S-transferase (class tau) 22); glutathione transferase
7.19	AT5G13200	GRAM domain-containing protein / ABA-responsive protein-related
7.14	AT3G25250	AGC2-1 (OXIDATIVE SIGNAL-INDUCIBLE1); kinase
7.09	AT5G05410	DREB2A (DRE-BINDING PROTEIN 2A); DNA binding / transcription activator/ transcription factor
7.07	AT2G43000	ANAC042 (Arabidopsis NAC domain containing protein 42); transcription factor
7.01	AT3G25610	haloacid dehalogenase-like hydrolase family protein
6.99	AT5G66650	similar to unknown protein [Arabidopsis thaliana] (TAIR:AT2G23790.1); similar to unnamed protein product [Vitis vinifera] (GB:CAO22909.1); contains InterPro domain Protein of unknown function DUF607 (InterPro:IPR006769)
6.97	AT5G40690	similar to unknown protein [Arabidopsis thaliana] (TAIR:AT2G41730.1); similar to unnamed protein product [Vitis vinifera] (GB:CAO14635.1)
6.97	AT2G02000;AT2G02010	[AT2G02000, GAD3 (GLUTAMATE DECARBOXYLASE 3); calmodulin binding];[AT2G02010, GAD4 (GLUTAMATE DECARBOXYLASE 4); calmodulin binding]
6.92	AT5G57220	CYP81F2 (cytochrome P450, family 81, subfamily F, polypeptide 2); oxygen binding
6.86	AT2G03760	ST (steroid sulfotransferase); sulfotransferase
6.78	AT2G21640	similar to unknown protein [Arabidopsis thaliana] (TAIR:AT3G05570.1); similar to unknown protein [Arabidopsis thaliana] (TAIR:AT4G39235.1); similar to hypothetical protein OsI_027197 [Oryza sativa (indica cultivar-group)] (GB:EAZ05965.1)
6.66	AT2G18690	similar to unknown protein [Arabidopsis thaliana] (TAIR:AT2G18680.1); similar to hypothetical protein OsI_029427 [Oryza sativa (indica cultivar-group)] (GB:EAZ08195.1)
6.62	AT4G36430	peroxidase, putative
6.52	AT3G28210	PMZ; zinc ion binding
6.38	AT5G38900	DSBA oxidoreductase family protein
6.36	AT1G70420	similar to unknown protein [Arabidopsis thaliana] (TAIR:AT1G23710.1); similar to unnamed protein product [Vitis vinifera] (GB:CAO66069.1); contains InterPro domain Protein of unknown function DUF1645 (InterPro:IPR012442)
6.33	AT5G25930	leucine-rich repeat family protein / protein kinase family protein
6.33	AT5G14730	similar to unknown protein [Arabidopsis thaliana] (TAIR:AT3G01513.1); similar to unnamed protein product [Vitis vinifera] (GB:CAO64332.1); similar to hypothetical protein [Vitis vinifera] (GB:CAN65788.1)
6.16	AT3G22370	AOX1A (alternative oxidase 1A); alternative oxidase
6.07	AT1G07180	ATNDI1/NDA1 (ALTERNATIVE NAD(P)H DEHYDROGENASE 1); NADH dehydrogenase
6.00	AT1G72290	trypsin and protease inhibitor family protein / Kunitz family protein
5.80	AT5G48540	33 kDa secretory protein-related
5.79	AT3G53150	UGT73D1 (UDP-GLUCOSYL TRANSFERASE 73D1); UDP-glycosyltransferase
5.70	AT3G50770	calmodulin-related protein, putative
5.69	AT4G15120	VQ motif-containing protein
5.69	AT2G30750	CYP71A12 (CYTOCHROME P450, FAMILY 71, SUBFAMILY A, POLYPEPTIDE 12); oxygen binding
5.65	AT2G32190;AT2G32210	[AT2G32190, similar to unknown protein [Arabidopsis thaliana] (TAIR:AT2G32210.1); similar to unknown [Populus trichocarpa] (GB:ABK92801.1); contains domain PD188784 (PD188784)];[AT2G32210, similar to unknown protein [Arabidopsis thaliana] (TAIR:AT2G32190.1); similar to unknown [Populus trichocarpa] (GB:ABK92801.1); contains domain PD188784 (PD188784)]
5.64	AT3G49780	ATPSK4 (PHYTOSULFOKINE 4 PRECURSOR); growth factor
5.63	AT4G28460	unknown protein
5.62	AT5G59820	RHL41 (RESPONSIVE TO HIGH LIGHT 41); nucleic acid binding / transcription factor/ zinc ion binding
5.60	AT2G39400	hydrolase, alpha/beta fold family protein
5.49	AT3G22910	calcium-transporting ATPase, plasma membrane-type, putative / Ca(2+)-ATPase, putative (ACA13)
5.41	AT3G14690	CYP72A15 (cytochrome P450, family 72, subfamily A, polypeptide 15); oxygen binding
5.37	AT5G40010	AATP1 (AAA-ATPASE 1); ATP binding / ATPase
5.36	AT1G30700	FAD-binding domain-containing protein
5.31	AT2G40340;AT2G40350	[AT2G40340, AP2 domain-containing transcription factor, putative (DRE2B)];[AT2G40350, DNA binding / transcription factor]
5.30	AT1G33030	O-methyltransferase family 2 protein
5.28	AT4G37290	similar to unknown protein [Arabidopsis thaliana] (TAIR:AT2G23270.1); similar to hypothetical protein [Vitis vinifera] (GB:CAN62855.1)
5.27	AT2G45170	AtATG8e (AUTOPHAGY 8E); microtubule binding
5.26	AT3G50930	AAA-type ATPase family protein
5.26	AT5G22300	NIT4 (NITRILASE 4)
5.22	AT2G31945	similar to unknown protein [Arabidopsis thaliana] (TAIR:AT1G05575.1); similar to unnamed protein product [Vitis vinifera] (GB:CAO22015.1); similar to hypothetical protein [Vitis vinifera] (GB:CAN61524.1); similar to hypothetical protein [Vitis vinifera] (GB:CAN71356.1)
5.19	AT5G14470	GHMP kinase-related
5.19	AT3G16530	legume lectin family protein
5.13	AT1G26420	FAD-binding domain-containing protein
5.11	AT5G17860	CAX7 (CALCIUM EXCHANGER 7); calcium:sodium antiporter/ cation:cation antiporter
5.08	AT3G04640	glycine-rich protein
5.01	AT5G20830	SUS1 (SUCROSE SYNTHASE 1); UDP-glycosyltransferase/ sucrose synthase
4.88	AT2G43500	RWP-RK domain-containing protein
4.85	AT5G54490	PBP1 (PINOID-BINDING PROTEIN 1); calcium ion binding
4.85	AT5G13750	ZIFL1 (ZINC INDUCED FACILITATOR-LIKE 1); tetracycline:hydrogen antiporter/ transporter
4.84	AT5G64510	similar to unnamed protein product [Vitis vinifera] (GB:CAO49799.1)
4.84	AT1G32870	ANAC013 (Arabidopsis NAC domain containing protein 13); transcription factor
4.82	AT1G76690;AT1G76680	[AT1G76690, OPR2 (12-oxophytodienoate reductase 2); 12-oxophytodienoate reductase];[AT1G76680, OPR1 (12-oxophytodienoate reductase 1); 12-oxophytodienoate reductase]
4.79	AT1G65690	harpin-induced protein-related / HIN1-related / harpin-responsive protein-related
4.78	AT4G34131;AT4G34135	[AT4G34131, UGT73B3 (UDP-GLUCOSYL TRANSFERASE 73B3); UDP-glycosyltransferase/ abscisic acid glucosyltransferase/ transferase, transferring hexosyl groups];[AT4G34135, UGT73B2; UDP-glucosyltransferase/ UDP-glycosyltransferase/ flavonol 3-O-glucosyltransferase]
4.77	AT4G01870	tolB protein-related
4.75	AT5G39050	transferase family protein
4.75	AT1G43910	AAA-type ATPase family protein
4.74	AT1G59590	ZCF37
4.73	AT5G10695	similar to unknown protein [Arabidopsis thaliana] (TAIR:AT5G57123.1); similar to unknown [Picea sitchensis] (GB:ABK22689.1)
4.72	AT1G68620	hydrolase
4.72	AT5G09420	ATTOC64-V/MTOM64 (ARABIDOPSIS THALIANA TRANSLOCON AT THE OUTER MEMBRANE OF CHLOROPLASTS 64-V); amidase
4.71	AT1G23550	SRO2 (SIMILAR TO RCD ONE 2); NAD+ ADP-ribosyltransferase
4.70	AT1G02930;AT1G02920	[AT1G02930, ATGSTF6 (EARLY RESPONSIVE TO DEHYDRATION 11); glutathione transferase];[AT1G02920, ATGSTF7 (GLUTATHIONE S-TRANSFERASE 11); glutathione transferase]
4.69	AT5G64250	2-nitropropane dioxygenase family / NPD family
4.68	AT3G50260	ATERF#011/CEJ1 (COOPERATIVELY REGULATED BY ETHYLENE AND JASMONATE 1); DNA binding / transcription factor
4.66	AT3G49160	pyruvate kinase family protein
4.66	AT2G34500	CYP710A1 (cytochrome P450, family 710, subfamily A, polypeptide 1); C-22 sterol desaturase/ oxygen binding
4.65	ATMG00160	cytochrome c oxidase subunit 2

4.57	AT1G10170	ATNFXL1; transcription factor
4.57	AT5G59490	haloacid dehalogenase-like hydrolase family protein
4.54	AT3G02800	phosphoprotein phosphatase
4.50	AT4G20860	FAD-binding domain-containing protein
4.48	AT3G10500	ANAC053 (Arabidopsis NAC domain containing protein 53); transcription factor
4.45	AT1G26390	FAD-binding domain-containing protein
4.39	AT3G28740	cytochrome P450 family protein
4.38	AT2G36220	similar to unknown protein [Arabidopsis thaliana] (TAIR:AT3G52710.1); similar to unnamed protein product [Vitis vinifera] (GB:CAO15901.1)
4.37	AT1G03660	similar to ankyrin repeat family protein [Arabidopsis thaliana] (TAIR:AT1G03670.1); similar to unnamed protein product [Vitis vinifera] (GB:CAO23951.1); contains domain ANK REPEAT-CONTAINING (PTHR18958:SF80); contains domain ANKYRIN REPEAT-CONTAINING (PTHR18958)
4.37	AT3G47340	ASN1 (DARK INDUCIBLE 6)
4.34	AT2G34660	ATMRP2 (MULTIDRUG RESISTANCE-ASSOCIATED PROTEIN 2); ATPase, coupled to transmembrane movement of substances
4.29	AT2G35730	heavy-metal-associated domain-containing protein
4.26	AT3G13310	DNAJ heat shock N-terminal domain-containing protein
4.25	AT5G51440	23.5 kDa mitochondrial small heat shock protein (HSP23.5-M)
4.19	AT5G13580	ABC transporter family protein
4.17	AT3G44190	pyridine nucleotide-disulphide oxidoreductase family protein
4.16	AT1G76600	similar to unknown protein [Arabidopsis thaliana] (TAIR:AT1G21010.1); similar to hypothetical protein [Vitis vinifera] (GB:CAN67638.1)
4.15	AT3G63380	calcium-transporting ATPase, plasma membrane-type, putative / Ca(2+)-ATPase, putative (ACA12)
4.14	AT5G06730	peroxidase, putative
4.13	AT4G15610	integral membrane family protein
4.08	AT5G51830	pfkB-type carbohydrate kinase family protein
4.06	AT2G16900	similar to unknown protein [Arabidopsis thaliana] (TAIR:AT4G35110.2); similar to unknown protein [Arabidopsis thaliana] (TAIR:AT4G35110.3); similar to unknown protein [Arabidopsis thaliana] (TAIR:AT4G35110.4); similar to hypothetical protein [Vitis vinifera] (GB:CAN73143.1); contains InterPro domain Phospholipase-like, arabidopsis (InterPro:IPR007942)
4.05	AT4G12120	SEC1B; protein transporter
4.01	AT3G53230	cell division cycle protein 48, putative / CDC48, putative
4.00	AT4G18050	PGP9 (P-GLYCOPROTEIN 9); ATPase, coupled to transmembrane movement of substances
3.99	AT4G26270	phosphofructokinase family protein
3.99	AT1G76520	auxin efflux carrier family protein
3.97	AT4G18880	AT-HSFA4A (Arabidopsis thaliana heat shock transcription factor A4A); DNA binding / transcription factor
3.94	AT3G18250	contains domain PROKAR_LIPOPROTEIN (PS51257)
3.93	AT3G08970	DNAJ heat shock N-terminal domain-containing protein
3.91	AT1G08050	zinc finger (C3HC4-type RING finger) family protein
3.84	AT4G33070	pyruvate decarboxylase, putative
3.83	AT4G38060	similar to unknown protein [Arabidopsis thaliana] (TAIR:AT5G65480.1); similar to unknown [Lycopersicon esculentum] (GB:AAK84476.1)
3.78	AT2G44460	glycosyl hydrolase family 1 protein
3.77	AT4G20070	ATAAH (ARABIDOPSIS THALIANA ALLANTOATE AMIDOHYDROLASE); allantoate deiminase/ metallopeptidase
3.76	AT1G02850	glycosyl hydrolase family 1 protein
3.76	AT2G23270	similar to unknown protein [Arabidopsis thaliana] (TAIR:AT4G37290.1); similar to hypothetical protein [Vitis vinifera] (GB:CAN62855.1)
3.76	AT5G61820	similar to MtN19-like protein [Pisum sativum] (GB:AAU14999.2); contains InterPro domain Stress up-regulated Nod 19 (InterPro:IPR011692)
3.74	AT3G03640	GLUC (Beta-glucosidase homolog); hydrolase, hydrolyzing O-glycosyl compounds
3.72	AT2G29490	ATGSTU1 (GLUTATHIONE S-TRANSFERASE 19); glutathione transferase
3.68	AT1G60730	aldo/keto reductase family protein
3.67	AT3G48520	CYP94B3 (cytochrome P450, family 94, subfamily B, polypeptide 3); oxygen binding
3.67	AT5G04120	phosphoglycerate/bisphosphoglycerate mutase family protein
3.63	AT4G23700	ATCHX17 (CATION/H+ EXCHANGER 17); monovalent cation:proton antiporter
3.61	AT1G02750	zinc ion binding
3.59	AT3G26830	PAD3 (PHYTOALEXIN DEFICIENT 3); oxygen binding
3.59	AT1G63720	similar to hydroxyproline-rich glycoprotein family protein [Arabidopsis thaliana] (TAIR:AT5G52430.1); similar to unknown [Thellungiella halophila] (GB:ABJ98061.1)
3.58	ATMG00040; AT2G07671;ATMG01080	[ATMG00040, hypothetical protein];[AT2G07671, H+-transporting two-sector ATPase, C subunit family protein];[ATMG01080, subunit 9 of mitochondrial F0-ATPase]
3.58	AT5G18470	curculin-like (mannose-binding) lectin family protein
3.57	AT5G09530	hydroxyproline-rich glycoprotein family protein
3.56	AT2G47000	MDR4/PGP4 (P-GLYCOPROTEIN4); ATPase, coupled to transmembrane movement of substances / xenobiotic-transporting ATPase
3.56	AT4G27585;AT5G54100	[AT4G27585, band 7 family protein];[AT5G54100, band 7 family protein]
3.55	AT4G15490	UGT84A3; UDP-glycosyltransferase/ sinapate 1-glucosyltransferase/ transferase, transferring glycosyl groups
3.52	AT4G18950	ankyrin protein kinase, putative
3.52	AT1G57630	disease resistance protein (TIR class), putative
3.51	AT2G41380	embryo-abundant protein-related
3.50	AT4G09110	zinc finger (C3HC4-type RING finger) family protein
3.49	AT3G14620	CYP72A8 (cytochrome P450, family 72, subfamily A, polypeptide 8); oxygen binding
3.48	AT5G13080	WRKY75 (WRKY DNA-BINDING PROTEIN 75); transcription factor
3.46	AT5G03030	DNAJ heat shock N-terminal domain-containing protein
3.43	AT2G30250	WRKY25 (WRKY DNA-binding protein 25); transcription factor
3.43	AT3G62150	PGP21 (P-GLYCOPROTEIN 21); ATPase, coupled to transmembrane movement of substances
3.42	AT2G41230	unknown protein
3.41	AT3G06500	beta-fructofuranosidase, putative / invertase, putative / saccharase, putative / beta-fructosidase, putative
3.41	AT2G20800	NDB4 (NAD(P)H DEHYDROGENASE B4); NADH dehydrogenase
3.41	AT1G23730	carbonic anhydrase, putative / carbonate dehydratase, putative
3.39	AT3G59820	calcium-binding mitochondrial protein-related
3.38	AT4G20830	FAD-binding domain-containing protein
3.38	AT1G13340	similar to unknown protein [Arabidopsis thaliana] (TAIR:AT1G34220.2); similar to unknown [Carica papaya] (GB:ABS01355.1); contains InterPro domain Protein of unknown function DUF292, eukaryotic (InterPro:IPR005061)
3.37	AT3G47730	ATATH1 (ABC2 homolog 1); ATPase, coupled to transmembrane movement of substances
3.36	AT3G14660	CYP72A13 (cytochrome P450, family 72, subfamily A, polypeptide 13); oxygen binding
3.36	AT1G32350	AOX1D (ALTERNATIVE OXIDASE 1D); alternative oxidase
3.36	AT1G68850	peroxidase, putative
3.35	AT5G42830	transferase family protein
3.30	AT4G17215	similar to unknown protein [Arabidopsis thaliana] (TAIR:AT5G47635.1); similar to hypothetical protein 40.t00006 [Brassica oleracea] (GB:ABD65131.1)
3.29	AT2G29420	ATGSTU7 (GLUTATHIONE S-TRANSFERASE 25); glutathione transferase
3.29	AT3G16150	L-asparaginase, putative / L-asparagine amidohydrolase, putative
3.28	AT5G49690	UDP-glucoronosyl/UDP-glucosyl transferase family protein

3.25	AT2G30140	UDP-glucoronosyl/UDP-glucosyl transferase family protein
3.24	AT1G13990	similar to unnamed protein product [Vitis vinifera] (GB:CAO68469.1)
3.23	AT5G55970	zinc finger (C3HC4-type RING finger) family protein
3.22	AT1G09080	BIP3; ATP binding
3.20	AT5G07440	GDH2 (GLUTAMATE DEHYDROGENASE 2); oxidoreductase
3.20	AT5G06860	PGIP1 (POLYGALACTURONASE INHIBITING PROTEIN 1); protein binding
3.20	AT3G26740	CCL (CCR-LIKE)
3.19	AT3G26470	similar to ADR1-L1 (ADR1-LIKE 1), ATP binding / protein binding [Arabidopsis thaliana] (TAIR:AT4G33300.2); similar to ADR1-L1 (ADR1-LIKE 1), ATP binding / protein binding [Arabidopsis thaliana] (TAIR:AT4G33300.1); similar to unnamed protein product [Vitis vinifera] (GB:CAO61278.1); contains InterPro domain Disease resistance, plant (InterPro:IPR014011)
3.18	AT2G05940	protein kinase, putative
3.18	AT1G61560	MLO6 (MILDEW RESISTANCE LOCUS O 6); calmodulin binding
3.18	AT4G11600	ATGPX6 (GLUTATHIONE PEROXIDASE 6); glutathione peroxidase
3.16	AT2G38250	DNA-binding protein-related
3.15	AT1G55850	ATCSLE1 (Cellulose synthase-like E1); cellulose synthase/ transferase, transferring glycosyl groups
3.15	AT2G44130	kelch repeat-containing F-box family protein
3.14	AT5G13900	protease inhibitor/seed storage/lipid transfer protein (LTP) family protein
3.13	AT3G10930	similar to unknown protein [Arabidopsis thaliana] (TAIR:AT5G05300.1)
3.13	AT4G22070	WRKY31 (WRKY DNA-binding protein 31); transcription factor
3.13	AT5G57910	similar to unknown protein [Arabidopsis thaliana] (TAIR:AT4G30630.1); similar to unnamed protein product [Vitis vinifera] (GB:CAO66657.1)
3.12	AT2G02930;AT4G02520	[AT2G02930, ATGSTF3 (GLUTATHIONE S-TRANSFERASE 16); glutathione transferase];[AT4G02520, ATGSTF2 (Arabidopsis thaliana Glutathione S-transferase (class phi) 2); glutathione transferase]
3.11	AT4G03320	TIC20-IV (TRANSLOCON AT THE INNER ENVELOPE MEMBRANE OF CHLOROPLASTS 20-IV); P-P-bond-hydrolysis-driven protein transmembrane transporter
3.11	AT5G35735	auxin-responsive family protein
3.10	AT2G29470	ATGSTU3 (GLUTATHIONE S-TRANSFERASE 21); glutathione transferase
3.10	AT1G70170	MMP (MATRIX METALLOPROTEINASE); metalloendopeptidase
3.10	AT5G52640	HSP81-1 (HEAT SHOCK PROTEIN 81-1); ATP binding / unfolded protein binding
3.07	AT2G38470	WRKY33 (WRKY DNA-binding protein 33); transcription factor
3.07	AT5G24800	ATBZIP9/BZO2H2 (BASIC LEUCINE ZIPPER O2 HOMOLOG 2); DNA binding / protein heterodimerization/ transcription factor
3.04	AT4G25390	protein kinase family protein
3.03	AT1G02220	ANAC003 (Arabidopsis NAC domain containing protein 3); transcription factor
3.02	AT3G54150	embryo-abundant protein-related
3.02	AT3G46660	UDP-glucoronosyl/UDP-glucosyl transferase family protein
3.01	AT4G05020	NDB2 (NAD(P)H DEHYDROGENASE B2); disulfide oxidoreductase
3.00	AT2G39350	ABC transporter family protein
2.99	AT5G44580	similar to unknown protein [Arabidopsis thaliana] (TAIR:AT5G44582.1)
2.98	AT5G58210	hydroxyproline-rich glycoprotein family protein
2.98	AT5G63790	ANAC102 (Arabidopsis NAC domain containing protein 102); transcription factor
2.98	AT1G15040	glutamine amidotransferase-related
2.97	AT5G25260;AT5G25250	[AT5G25260, similar to unknown protein [Arabidopsis thaliana] (TAIR:AT5G25250.1); similar to unknown protein [Arabidopsis thaliana] (TAIR:AT5G64870.1); similar to unnamed protein product [Vitis vinifera] (GB:CAO44306.1); similar to hypothetical protein [Vitis vinifera] (GB:CAN77054.1); similar to 80C09_16 [Brassica rapa subsp. pekinensis] (GB:AAZ41827.1); contains domain PTHR13806:SF3 (PTHR13806:SF3); contains domain PTHR13806 (PTHR13806)];[AT5G25250, similar to unknown protein [Arabidopsis thaliana] (TAIR:AT5G64870.1); similar to unknown protein [Arabidopsis thaliana] (TAIR:AT5G25260.1); similar to unnamed protein product [Vitis vinifera] (GB:CAO44306.1); similar to 80C09_16 [Brassica rapa subsp. pekinensis] (GB:AAZ41827.1); similar to nodulin [Glycine max] (GB:AAC72337.1); contains domain PTHR13806:SF3 (PTHR13806:SF3); contains domain PTHR13806 (PTHR13806)]
2.97	AT5G49450;AT5G49448	[AT5G49450, ATBZIP1 (ARABIDOPSIS THALIANA BASIC LEUCINE-ZIPPER 1); DNA binding / protein heterodimerization/ transcription factor];[AT5G49448, CPuORF4 (Conserved peptide upstream open reading frame 4)]
2.96	AT4G36040	DNAJ heat shock N-terminal domain-containing protein (J11)
2.96	AT1G62570	flavin-containing monooxygenase family protein / FMO family protein
2.95	AT5G66780	similar to unknown [Ammopiptanthus mongolicus] (GB:AAW33981.1)
2.94	AT5G59510	DVL18/RTFL5 (ROTUNDIFOLIA LIKE 5)
2.93	AT2G27830	similar to pentatricopeptide (PPR) repeat-containing protein [Arabidopsis thaliana] (TAIR:AT4G22760.1); similar to hypothetical protein [Catharanthus roseus] (GB:CAC09928.1)
2.93	AT4G37010	caltractin, putative / centrin, putative
2.92	AT3G49580	similar to unknown protein [Arabidopsis thaliana] (TAIR:AT3G49570.1); similar to unknown protein [Brassica rapa subsp. pekinensis] (GB:AAQ92331.1)
2.92	AT5G59530	2-oxoglutarate-dependent dioxygenase, putative
2.91	AT1G66880	serine/threonine protein kinase family protein
2.91	AT3G50910	similar to unknown protein [Arabidopsis thaliana] (TAIR:AT5G66480.1); similar to hypothetical protein [Thellungiella halophila] (GB:ABB45854.1)
2.89	AT1G30420;AT1G30410	[AT1G30420, ATMRP12 (Arabidopsis thaliana multidrug resistance-associated protein 12)];[AT1G30410, ATMRP13 (Arabidopsis thaliana multidrug resistance-associated protein 13)]
2.88	AT5G55200	co-chaperone grpE protein, putative
2.88	AT2G43820	GT/UGT74F2 (UDP-GLUCOSYLTRANSFERASE 74F2); UDP-glucosyltransferase/ UDP-glycosyltransferase/ transferase, transferring glycosyl groups / transferase, transferring hexosyl groups
2.87	AT2G33710	AP2 domain-containing transcription factor family protein
2.86	AT1G74360	leucine-rich repeat transmembrane protein kinase, putative
2.85	AT3G56710	SIB1 (SIGMA FACTOR BINDING PROTEIN 1); binding
2.85	AT1G77450	ANAC032 (Arabidopsis NAC domain containing protein 32); transcription factor
2.83	AT5G58070	lipocalin, putative
2.83	AT5G56630	phosphofructokinase family protein
2.81	AT3G14990	4-methyl-5(b-hydroxyethyl)-thiazole monophosphate biosynthesis protein, putative
2.81	AT1G14540	anionic peroxidase, putative
2.81	AT2G01300	similar to unknown protein [Arabidopsis thaliana] (TAIR:AT1G15010.1); similar to unnamed protein product [Vitis vinifera] (GB:CAO42242.1)
2.80	AT4G27830	glycosyl hydrolase family 1 protein
2.80	AT1G56060	similar to unknown protein [Arabidopsis thaliana] (TAIR:AT2G32190.1); similar to unnamed protein product [Vitis vinifera] (GB:CAO68639.1); contains domain PD188784 (PD188784)
2.80	AT1G14550	anionic peroxidase, putative
2.80	AT3G07870	F-box family protein
2.79	AT4G38540	monooxygenase, putative (MO2)
2.78	AT4G15530	PPDK (PYRUVATE ORTHOPHOSPHATE DIKINASE); kinase/ pyruvate, phosphate dikinase
2.76	AT4G31860	protein phosphatase 2C, putative / PP2C, putative
2.75	AT3G14680	CYP72A14 (cytochrome P450, family 72, subfamily A, polypeptide 14); oxygen binding
2.75	AT3G25830;AT3G25820	[AT3G25830, ATTPS-CIN (TERPENE SYNTHASE-LIKE SEQUENCE-1,8-CINEOLE); myrcene/(E)-beta-ocimene synthase];[AT3G25820, ATTPS-CIN (TERPENE SYNTHASE-LIKE SEQUENCE-1,8-CINEOLE); myrcene/(E)-beta-ocimene synthase]
2.75	AT1G71530	protein kinase family protein
2.75	AT3G30775	ERD5 (EARLY RESPONSIVE TO DEHYDRATION 5); proline dehydrogenase
2.74	AT4G16190	cysteine proteinase, putative
2.74	AT3G16330	similar to unknown protein [Arabidopsis thaliana] (TAIR:AT1G52140.1); similar to hypothetical protein [Vitis vinifera] (GB:CAN64915.1)

2.73	AT5G20400	oxidoreductase, 2OG-Fe(II) oxygenase family protein
2.72	AT2G38340	AP2 domain-containing transcription factor, putative (DRE2B)
2.71	AT2G18150;AT2G18140	[AT2G18150, peroxidase, putative];[AT2G18140, peroxidase, putative]
2.71	AT5G47230	ERF5 (ETHYLENE RESPONSIVE ELEMENT BINDING FACTOR 5); DNA binding / transcription activator/ transcription factor
2.70	AT2G41100	TCH3 (TOUCH 3)
2.70	AT1G73480	hydrolase, alpha/beta fold family protein
2.69	AT4G19880	similar to unknown protein [Arabidopsis thaliana] (TAIR:AT5G45020.1); similar to Intracellular chloride channel [Medicago truncatula] (GB:ABC75353.2); contains InterPro domain Thioredoxin-like fold (InterPro:IPR012336); contains InterPro domain Glutathione S-transferase, C-terminal-like (InterPro:IPR010987); contains InterPro domain Glutathione S-transferase, C-terminal (InterPro:IPR004046); contains InterPro domain Glutathione S-transferase, predicted (InterPro:IPR016639)
2.69	AT2G18700	ATTPS11 (Arabidopsis thaliana trehalose phosphatase/synthase 11); transferase, transferring glycosyl groups
2.67	AT3G45730	unknown protein
2.67	AT4G17490	ATERF6 (ETHYLENE RESPONSIVE ELEMENT BINDING FACTOR 6); DNA binding / transcription factor
2.66	AT2G24500	FZF; transcription factor
2.65	AT3G13330	binding
2.65	AT3G61630	CRF6 (CYTOKININ RESPONSE FACTOR 6); DNA binding / transcription factor
2.64	AT3G57380	similar to unknown protein [Arabidopsis thaliana] (TAIR:AT2G41640.1); similar to glycosyltransferase [Medicago truncatula] (GB:CAI30145.1); contains InterPro domain Protein of unknown function DUF563 (InterPro:IPR007657)
2.64	AT4G39740	electron transport SCO1/SenC family protein
2.63	AT2G29480	ATGSTU2 (GLUTATHIONE S-TRANSFERASE 20); glutathione transferase
2.63	AT4G36580	AAA-type ATPase family protein
2.63	AT3G48850	mitochondrial phosphate transporter, putative
2.62	ATMG01190; AT2G07698	[ATMG01190, ATPase subunit 1];[AT2G07698, ATP synthase alpha chain, mitochondrial, putative]
2.62	AT1G51420	sucrose-phosphatase, putative
2.61	AT2G23320	WRKY15 (WRKY DNA-binding protein 15); transcription factor
2.59	AT4G27940	mitochondrial substrate carrier family protein
2.59	AT5G05600	oxidoreductase, 2OG-Fe(II) oxygenase family protein
2.59	AT5G04340	C2H2 (ZINC FINGER OF ARABIDOPSIS THALIANA 6); nucleic acid binding / transcription factor/ zinc ion binding
2.57	AT1G07160	protein phosphatase 2C, putative / PP2C, putative
2.57	AT1G74590	ATGSTU10 (Arabidopsis thaliana Glutathione S-transferase (class tau) 10); glutathione transferase
2.57	AT5G23190	CYP86B1 (cytochrome P450, family 86, subfamily B, polypeptide 1); oxygen binding
2.57	AT5G07870	transferase family protein
2.56	AT2G35770	SCPL28 (serine carboxypeptidase-like 28); serine carboxypeptidase
2.56	AT1G72900	disease resistance protein (TIR-NBS class), putative
2.56	AT3G57090	BIGYIN; binding
2.56	AT5G39040	ATTAP2 (Arabidopsis thaliana transporter associated with antigen processing protein 2); ATPase, coupled to transmembrane movement of substances
2.56	AT5G07860	transferase family protein
2.55	AT1G01720	ATAF1 (Arabidopsis NAC domain containing protein 2); transcription factor
2.54	AT5G06300	carboxy-lyase
2.54	AT3G01650	RGLG1 (RING DOMAIN LIGASE1); protein binding / zinc ion binding
2.53	AT5G64260	phosphate-responsive protein, putative
2.52	AT4G24160	hydrolase, alpha/beta fold family protein
2.52	AT4G39670	glycolipid binding / glycolipid transporter
2.52	AT2G43570	chitinase, putative
2.52	AT1G08940	phosphoglycerate/bisphosphoglycerate mutase family protein
2.52	AT1G22985	AP2 domain-containing transcription factor, putative
2.52	AT5G41080	glycerophosphoryl diester phosphodiesterase family protein
2.51	AT5G59680	leucine-rich repeat protein kinase, putative
2.50	AT2G22880	VQ motif-containing protein
2.49	AT1G76070	Identical to Uncharacterized protein At1g76070 [Arabidopsis Thaliana] (GB:Q9SGS5;GB:Q8LAC9;GB:Q9LQR1); similar to unknown protein [Arabidopsis thaliana] (TAIR:AT1G20310.1); similar to hypothetical protein [Vitis vinifera] (GB:CAN83887.1)
2.49	AT1G76970	VHS domain-containing protein / GAT domain-containing protein
2.49	AT1G25400	similar to unknown protein [Arabidopsis thaliana] (TAIR:AT1G68440.1); similar to unnamed protein product [Vitis vinifera] (GB:CAO42150.1)
2.49	AT1G10990	unknown protein
2.49	AT2G35480	similar to unknown protein [Arabidopsis thaliana] (TAIR:AT1G32260.1); similar to unnamed protein product [Vitis vinifera] (GB:CAO63339.1)
2.48	AT3G25655	unknown protein
2.48	AT5G27760	hypoxia-responsive family protein
2.48	AT3G02840	immediate-early fungal elicitor family protein
2.46	AT5G41610	ATCHX18 (cation/hydrogen exchanger 18); monovalent cation:proton antiporter
2.46	AT5G17760	AAA-type ATPase family protein
2.46	AT5G08250	cytochrome P450 family protein
2.45	AT2G29990	NDA2 (ALTERNATIVE NAD(P)H DEHYDROGENASE 2); NADH dehydrogenase
2.45	AT3G54420	ATEP3 (Arabidopsis thaliana chitinase class IV); chitinase
2.44	AT4G23190	CRK11 (CYSTEINE-RICH RLK11); kinase
2.44	AT3G11430	ATGPAT5/GPAT5 (GLYCEROL-3-PHOSPHATE ACYLTRANSFERASE 5); 1-acylglycerol-3-phosphate O-acyltransferase/ acyltransferase/ organic anion transmembrane transporter
2.43	AT1G24090	RNase H domain-containing protein
2.43	AT3G29035	ANAC059/ATNAC3 (Arabidopsis NAC domain containing protein 59); protein heterodimerization/ transcription factor
2.42	AT5G54500	FQR1 (FLAVODOXIN-LIKE QUINONE REDUCTASE 1)
2.42	AT5G15870	glycosyl hydrolase family 81 protein
2.42	AT5G51130	similar to unnamed protein product [Vitis vinifera] (GB:CAO65480.1); contains InterPro domain Methyltransferase type 12 (InterPro:IPR013217); contains InterPro domain Bicoid-interacting 3 (InterPro:IPR010675)
2.41	AT4G17260	L-lactate dehydrogenase, putative
2.41	AT1G51760;AT1G51780	[AT1G51760, IAR3 (IAA-ALANINE RESISTANT 3); metallopeptidase];[AT1G51780, ILL5 (IAA-leucine resistant (ILR)-like gene 5); metallopeptidase]
2.41	AT2G40140	CZF1/ZFAR1; transcription factor
2.40	AT1G22160	senescence-associated protein-related
2.40	AT5G67600	unknown protein
2.40	AT5G39610	ANAC092/ATNAC2/ATNAC6 (Arabidopsis NAC domain containing protein 92); protein heterodimerization/ protein homodimerization/ transcription factor
2.40	AT1G35670	ATCDPK2 (CALCIUM-DEPENDENT PROTEIN KINASE 2); calmodulin-dependent protein kinase/ kinase
2.39	AT3G05360	disease resistance family protein / LRR family protein
2.39	AT5G20910	zinc finger (C3HC4-type RING finger) family protein
2.37	AT2G42280	basic helix-loop-helix (bHLH) family protein
2.37	AT1G64110	AAA-type ATPase family protein
2.37	AT3G08590	2,3-biphosphoglycerate-independent phosphoglycerate mutase, putative / phosphoglyceromutase, putative
2.36	AT3G15500	ATNAC3 (ARABIDOPSIS NAC DOMAIN CONTAINING PROTEIN 55); transcription factor
2.36	AT2G37770	aldo/keto reductase family protein
2.36	AT3G61390	U-box domain-containing protein
2.36	AT2G48140	EDA4 (embryo sac development arrest 4); lipid binding

2.35	AT5G10510	AIL6 (AINTEGUMENTA-LIKE 6); DNA binding / transcription factor
2.34	AT1G56300	DNAJ heat shock N-terminal domain-containing protein
2.34	AT1G72680	cinnamyl-alcohol dehydrogenase, putative
2.34	AT4G30960	CIPK6 (CBL-INTERACTING PROTEIN KINASE 6); kinase
2.34	AT1G21680	similar to unknown protein [Arabidopsis thaliana] (TAIR:AT1G21670.1); similar to hypothetical protein [Vitis vinifera] (GB:CAN73514.1); similar to unnamed protein product [Vitis vinifera] (GB:CAO61906.1); similar to hypothetical protein OsJ_012725 [Oryza sativa (japonica cultivar-group)] (GB:EAZ29242.1); contains InterPro domain WD40-like Beta Propeller (InterPro:IPR011659); contains InterPro domain Six-bladed beta-propeller, TolB-like (InterPro:IPR011042)
2.33	AT1G69490	NAP (NAC-LIKE, ACTIVATED BY AP3/PI); transcription factor
2.33	AT5G13190	similar to unknown [Populus trichocarpa] (GB:ABK93196.1); contains InterPro domain LPS-induced tumor necrosis factor alpha factor (InterPro:IPR006629)
2.33	AT5G59930	DC1 domain-containing protein / UV-B light-insensitive protein, putative
2.32	AT2G41640	similar to unknown protein [Arabidopsis thaliana] (TAIR:AT3G57380.1); similar to glycosyltransferase [Medicago truncatula] (GB:CAI30145.1); contains InterPro domain Protein of unknown function DUF563 (InterPro:IPR007657)
2.32	AT3G57520	ATSIP2 (ARABIDOPSIS THALIANA SEED IMBIBITION 2); hydrolase, hydrolyzing O-glycosyl compounds
2.32	AT5G33290	XGD1 (XYLOGALACTURONAN DEFICIENT 1); catalytic
2.32	ATMG00080; ATMG00090	[ATMG00080, encodes a mitochondrial ribosomal protein L16, which is a constituent of the large ribosomal subunit];[ATMG00090, ribosomal protein S3]
2.31	AT4G17840	similar to unknown protein [Arabidopsis thaliana] (TAIR:AT2G35260.1); similar to hypothetical protein 40.t00061 [Brassica oleracea] (GB:ABD65174.1)
2.30	AT2G44750;AT1G02880	[AT2G44750, TPK2 (THIAMIN PYROPHOSPHOKINASE 2); thiamin diphosphokinase];[AT1G02880, TPK1 (THIAMIN PYROPHOSPHOKINASE1); thiamin diphosphokinase]
2.30	AT1G66090	disease resistance protein (TIR-NBS class), putative
2.30	AT3G53160	UGT73C7 (UDP-GLUCOSYL TRANSFERASE 73C7); UDP-glycosyltransferase/ transferase, transferring glycosyl groups
2.29	AT4G15550	IAGLU (INDOLE-3-ACETATE BETA-D-GLUCOSYLTRANSFERASE); UDP-glycosyltransferase/ transferase, transferring glycosyl groups
2.29	AT2G16365	F-box family protein
2.28	AT1G74750	pentatricopeptide (PPR) repeat-containing protein
2.28	AT1G15330	CBS domain-containing protein
2.28	AT1G18570	MYB51 (MYB DOMAIN PROTEIN 51); DNA binding / transcription factor
2.27	AT5G42050	similar to unknown protein [Arabidopsis thaliana] (TAIR:AT3G27090.1); similar to unknown [Populus trichocarpa] (GB:ABK95892.1); contains InterPro domain Kelch related (InterPro:IPR013089); contains InterPro domain Development and cell death (InterPro:IPR013989)
2.27	AT1G17860	trypsin and protease inhibitor family protein / Kunitz family protein
2.27	AT4G02880	similar to unknown protein [Arabidopsis thaliana] (TAIR:AT1G03290.1); similar to unnamed protein product [Vitis vinifera] (GB:CAO22500.1)
2.27	AT2G40000	similar to unknown protein [Arabidopsis thaliana] (TAIR:AT3G55840.1); similar to unnamed protein product [Vitis vinifera] (GB:CAO41329.1); contains InterPro domain Hs1pro-1, C-terminal (InterPro:IPR009743); contains InterPro domain Hs1pro-1, N-terminal (InterPro:IPR009869)
2.27	AT1G12200	flavin-containing monooxygenase family protein / FMO family protein
2.27	AT3G08760	ATSIK; kinase
2.27	AT2G32030	GCN5-related N-acetyltransferase (GNAT) family protein
2.27	AT1G74055	unknown protein
2.27	AT1G36640	similar to unknown protein [Arabidopsis thaliana] (TAIR:AT1G36622.1)
2.26	AT5G01550	lectin protein kinase, putative
2.26	AT2G36950	heavy-metal-associated domain-containing protein
2.26	AT1G69790	protein kinase, putative
2.26	AT1G51890	leucine-rich repeat protein kinase, putative
2.26	AT4G39235	similar to unknown protein [Arabidopsis thaliana] (TAIR:AT3G05570.1); similar to unknown [Populus trichocarpa] (GB:ABK93095.1)
2.26	AT5G59540	oxidoreductase, 2OG-Fe(II) oxygenase family protein
2.26	AT3G19920	similar to unknown protein [Arabidopsis thaliana] (TAIR:AT5G64230.1); similar to unnamed protein product [Vitis vinifera] (GB:CAO44392.1)
2.26	AT4G35770	SEN1 (DARK INDUCIBLE 1)
2.25	AT2G25140	CLPB-M/CLPB4/HSP98.7 (HEAT SHOCK PROTEIN 98.7); ATP binding / ATPase
2.25	AT3G10985	SAG20 (WOUND-INDUCED PROTEIN 12)
2.25	AT5G16010	3-oxo-5-alpha-steroid 4-dehydrogenase family protein / steroid 5-alpha-reductase family protein
2.24	AT4G34710	ADC2 (ARGININE DECARBOXYLASE 2)
2.24	AT5G17650	glycine/proline-rich protein
2.23	AT3G09270	ATGSTU8 (Arabidopsis thaliana Glutathione S-transferase (class tau) 8); glutathione transferase
2.23	AT3G51895	SULTR3;1 (SULFATE TRANSPORTER 1); sulfate transmembrane transporter
2.22	AT5G65110	ACX2 (ACYL-COA OXIDASE 2); acyl-CoA oxidase
2.22	AT5G65300	unknown protein
2.22	AT5G16980	NADP-dependent oxidoreductase, putative
2.22	AT5G63970	copine-related
2.22	AT1G26410	FAD-binding domain-containing protein
2.21	AT5G19440	cinnamyl-alcohol dehydrogenase, putative (CAD)
2.21	AT3G26910	hydroxyproline-rich glycoprotein family protein
2.21	AT1G21450	SCL1 (SCARECROW-LIKE 1); transcription factor
2.21	AT5G49520	WRKY48 (WRKY DNA-binding protein 48); transcription factor
2.21	AT1G78290	serine/threonine protein kinase, putative
2.20	AT1G68450	VQ motif-containing protein
2.19	AT2G31260	APG9 (AUTOPHAGY 9)
2.19	AT3G15770	similar to unknown protein [Arabidopsis thaliana] (TAIR:AT5G25360.1); similar to unknown [Populus trichocarpa] (GB:ABK94402.1)
2.19	AT5G24270	SOS3 (SALT OVERLY SENSITIVE 3)
2.19	AT1G68690	pseudogene, protein kinase family, similar to protein kinase 1 GB:BAA94509 GI:7573596 from (Populus nigra); blastp match of 71% identity and 2.4e-104 P-value to GP|13486635|dbj|BAB39873.1||AP002882 putative protein kinase {Oryza sativa (japonica cultivar-group)}
2.18	AT5G05190	Identical to Uncharacterized protein At5g05190 (Y-1) [Arabidopsis Thaliana] (GB:Q9FHK4); similar to unknown protein [Arabidopsis thaliana] (TAIR:AT3G56410.1); similar to unknown protein [Arabidopsis thaliana] (TAIR:AT3G56410.2); similar to unnamed protein product [Vitis vinifera] (GB:CAO41531.1); similar to hypothetical protein [Vitis vinifera] (GB:CAN78033.1)
2.18	AT5G67340	armadillo/beta-catenin repeat family protein / U-box domain-containing protein
2.18	AT1G30400	ATMRP1 (Arabidopsis thaliana multidrug resistance-associated protein 1); xenobiotic-transporting ATPase
2.18	AT4G23050	protein kinase, putative
2.17	AT1G78820;AT1G78830	[AT1G78820, curculin-like (mannose-binding) lectin family protein / PAN domain-containing protein];[AT1G78830, curculin-like (mannose-binding) lectin family protein]
2.16	AT5G10100	trehalose-6-phosphate phosphatase, putative
2.16	AT5G05140	transcription elongation factor-related
2.15	AT2G24180	CYP71B6 (CYTOCHROME P450 71B6); oxygen binding
2.15	AT1G69920	ATGSTU12 (Arabidopsis thaliana Glutathione S-transferase (class tau) 12); glutathione transferase
2.15	AT1G67970	AT-HSFA8 (Arabidopsis thaliana heat shock transcription factor A8); DNA binding / transcription factor
2.14	AT1G30040	ATGA2OX2; gibberellin 2-beta-dioxygenase
2.14	AT5G05390	LAC12 (laccase 12); copper ion binding / oxidoreductase
2.14	AT3G21250	ATMRP6 (Arabidopsis thaliana multidrug resistance-associated protein 6)
2.14	AT4G11360	RHA1B (RING-H2 finger A1B); protein binding / zinc ion binding

2.14	AT1G70590	F-box family protein
2.14	AT1G33590	disease resistance protein-related / LRR protein-related
2.13	AT1G03700	integral membrane family protein
2.13	AT4G17500	ATERF-1 (ETHYLENE RESPONSIVE ELEMENT BINDING FACTOR 1); DNA binding / transcription activator/ transcription factor
2.13	AT2G19450	TAG1 (TRIACYLGLYCEROL BIOSYNTHESIS DEFECT 1); diacylglycerol O-acyltransferase
2.13	AT1G18390	protein kinase family protein
2.13	ATCG00660	encodes a chloroplast ribosomal protein L20, a constituent of the large subunit of the ribosomal complex
2.12	AT5G47070	protein kinase, putative
2.12	AT1G17960	threonyl-tRNA synthetase, putative / threonine--tRNA ligase, putative
2.12	AT1G76590	zinc-binding family protein
2.12	AT4G28350	lectin protein kinase family protein
2.12	AT5G41040	transferase family protein
2.11	AT3G17700	CNBT1 (CYCLIC NUCLEOTIDE-BINDING TRANSPORTER 1); calmodulin binding / cyclic nucleotide binding / ion channel
2.11	AT5G48180	kelch repeat-containing protein
2.11	AT3G55620	EMB1624 (EMBRYO DEFECTIVE 1624); translation initiation factor
2.11	AT1G63440	HMA5 (HEAVY METAL ATPASE 5); ATPase, coupled to transmembrane movement of ions, phosphorylative mechanism
2.11	AT3G59700	ATHLECRK (ARABIDOPSIS THALIANA LECTIN-RECEPTOR KINASE); kinase
2.11	AT3G14770	nodulin MtN3 family protein
2.10	AT4G33920	protein phosphatase 2C family protein / PP2C family protein
2.10	AT2G37430	zinc finger (C2H2 type) family protein (ZAT11)
2.10	AT5G16930	AAA-type ATPase family protein
2.09	AT2G22540	SVP (SHORT VEGETATIVE PHASE); transcription factor
2.09	AT4G40080	epsin N-terminal homology (ENTH) domain-containing protein / clathrin assembly protein-related
2.09	AT3G45300	IVD (ISOVALERYL-COA-DEHYDROGENASE)
2.09	AT2G37970	SOUL-1; binding
2.09	AT1G01340	ATCNGC10 (CYCLIC NUCLEOTIDE GATED CHANNEL 10); calmodulin binding / cyclic nucleotide binding / ion channel
2.09	AT3G49530	ANAC062 (Arabidopsis NAC domain containing protein 62); transcription factor
2.09	AT3G60450	similar to unknown protein [Arabidopsis thaliana] (TAIR:AT3G60440.1); similar to unnamed protein product [Vitis vinifera] (GB:CAO70569.1); contains InterPro domain Phosphoglycerate mutase (InterPro:IPR013078); contains InterPro domain PRIB5 (InterPro:IPR012398)
2.08	AT5G61560	protein kinase family protein
2.08	AT5G04250	OTU-like cysteine protease family protein
2.08	ATCG00170	RNA polymerase beta' subunit-2
2.08	AT4G26200	ACS7 (1-Amino-cyclopropane-1-carboxylate synthase 7); 1-aminocyclopropane-1-carboxylate synthase
2.08	AT5G16970	AT-AER (ALKENAL REDUCTASE); 2-alkenal reductase
2.08	AT4G04790	similar to pentatricopeptide (PPR) repeat-containing protein [Arabidopsis thaliana] (TAIR:AT4G21880.1); similar to putative pentatricopeptide (PPR) repeat-containing protein [Oryza sativa (japonica cultivar-group)] (GB:BAD07992.1); contains InterPro domain Pentatricopeptide repeat (InterPro:IPR002885)
2.08	AT1G14130	2-oxoglutarate-dependent dioxygenase, putative
2.08	AT3G46600	scarecrow transcription factor family protein
2.08	AT4G37910	MTHSC70-1 (mitochondrial heat shock protein 70-1); ATP binding / unfolded protein binding
2.08	AT4G17670	senescence-associated protein-related
2.07	AT3G19390	cysteine proteinase, putative / thiol protease, putative
2.07	AT1G74460	GDSL-motif lipase/hydrolase family protein
2.07	AT3G15352	ATCOX17 (Arabidopsis thaliana cytochrome c oxidase 17)
2.07	AT2G01610	invertase/pectin methylesterase inhibitor family protein
2.07	AT5G44990	similar to unknown protein [Arabidopsis thaliana] (TAIR:AT4G19880.1); similar to Intracellular chloride channel [Medicago truncatula] (GB:ABC75353.2); contains InterPro domain Thioredoxin-like fold (InterPro:IPR012336); contains InterPro domain Glutathione S-transferase, C-terminal-like (InterPro:IPR010987); contains InterPro domain Glutathione S-transferase, predicted (InterPro:IPR016639)
2.07	AT5G04000	similar to hypothetical protein [Vitis vinifera] (GB:CAN76250.1)
2.07	AT3G20860	ATNEK5; kinase
2.06	AT3G49845	contains InterPro domain XYPPX repeat (InterPro:IPR006031)
2.06	AT3G18290	EMB2454 (EMBRYO DEFECTIVE 2454); protein binding / zinc ion binding
2.06	AT3G05200	ATL6 (Arabidopsis T?xicos en Levadura 6); protein binding / zinc ion binding
2.06	AT1G03905	ABC transporter family protein
2.05	AT1G67810	Fe-S metabolism associated domain-containing protein
2.05	AT5G54960	PDC2 (PYRUVATE DECARBOXYLASE-2); pyruvate decarboxylase
2.05	AT1G59700	ATGSTU16 (Arabidopsis thaliana Glutathione S-transferase (class tau) 16); glutathione transferase
2.05	AT1G54540	similar to harpin-induced protein-related / HIN1-related / harpin-responsive protein-related [Arabidopsis thaliana] (TAIR:AT1G65690.1); similar to unnamed protein product [Vitis vinifera] (GB:CAO62044.1); contains InterPro domain Harpin-induced 1 (InterPro:IPR010847)
2.05	AT4G33980	similar to unknown protein [Arabidopsis thaliana] (TAIR:AT5G42900.2); similar to unknown protein [Arabidopsis thaliana] (TAIR:AT5G42900.3); similar to unknown protein [Arabidopsis thaliana] (TAIR:AT5G42900.1); similar to hypothetical protein [Vitis vinifera] (GB:CAN64989.1)
2.05	AT2G32560	F-box family protein
2.05	AT2G38230;AT2G38210	[AT2G38230, ATPDX1.1 (PYRIDOXINE BIOSYNTHESIS 1.1); protein heterodimerization];[AT2G38210, PDX1L4 (PUTATIVE PDX1-LIKE PROTEIN 4)]
2.04	AT1G60610	protein binding / zinc ion binding
2.04	AT3G60420	similar to unknown protein [Arabidopsis thaliana] (TAIR:AT3G60450.1); similar to unnamed protein product [Vitis vinifera] (GB:CAO70569.1); contains InterPro domain Phosphoglycerate mutase (InterPro:IPR013078); contains InterPro domain PRIB5 (InterPro:IPR012398)
2.04	AT5G02020	similar to unknown protein [Arabidopsis thaliana] (TAIR:AT3G55646.1); similar to unknown protein [Arabidopsis thaliana] (TAIR:AT5G59080.1); similar to unnamed protein product [Vitis vinifera] (GB:CAO15731.1)
2.04	AT2G47730	ATGSTF8 (GLUTATHIONE S-TRANSFERASE 8); glutathione transferase
2.03	AT4G31610	REM1 (REPRODUCTIVE MERISTEM 1); DNA binding / transcription factor
2.03	AT4G02940	oxidoreductase, 2OG-Fe(II) oxygenase family protein
2.03	AT1G58030	CAT2 (CATIONIC AMINO ACID TRANSPORTER 2); amino acid transmembrane transporter
2.03	AT1G04310	ERS2 (ETHYLENE RESPONSE SENSOR 2); receptor
2.03	AT1G60940	SNRK2-10/SNRK2.10/SRK2B (SNF1-RELATED PROTEIN KINASE 2.10); kinase
2.03	AT5G50760	auxin-responsive family protein
2.03	AT3G51890	protein binding / protein transporter/ structural molecule
2.02	AT4G24690	ubiquitin-associated (UBA)/TS-N domain-containing protein / octicosapeptide/Phox/Bemp1 (PB1) domain-containing protein
2.02	AT1G21140	nodulin, putative
2.02	AT3G03470	CYP89A9 (cytochrome P450, family 87, subfamily A, polypeptide 9); oxygen binding
2.02	AT5G20250	DIN10 (DARK INDUCIBLE 10); hydrolase, hydrolyzing O-glycosyl compounds
2.02	AT1G33420	PHD finger family protein
2.02	AT3G11580	DNA-binding protein, putative
2.02	AT5G03240	UBQ3 (POLYUBIQUITIN 3); protein binding
2.02	AT4G15420	PRLI-interacting factor K
2.02	AT2G40880	FL3-27; cysteine protease inhibitor
2.02	AT5G48410	ATGLR1.3 (Arabidopsis thaliana glutamate receptor 1.3)
2.02	AT4G13180	short-chain dehydrogenase/reductase (SDR) family protein
2.02	AT3G12740	LEM3 (ligand-effect modulator 3) family protein / CDC50 family protein
2.01	AT5G03490	UDP-glucoronosyl/UDP-glucosyl transferase family protein

2.01	AT2G07727;ATMG00220	[AT2G07727, cytochrome b (MTCYB) (COB) (CYTB)];[ATMG00220, Mitochondrial apocytochrome b (cob) gene encodes a subunit of the ubiquinol-cytochrome c oxidoreductase and is part of a 5 kb transcript. The transcript also contains a pseudogene for ribosomal protein S14 called RPS15 and a tRNA(Ser) gene. Both the Cob and RPS15 genes are edited in the transcript.]
2.01	AT1G33600	leucine-rich repeat family protein
2.01	AT4G01250	WRKY22 (WRKY DNA-binding protein 22); transcription factor
2.01	AT5G15720	GLIP7 (GDSL-motif lipase 7); carboxylesterase
2.01	AT1G03290	similar to unknown protein [Arabidopsis thaliana] (TAIR:AT4G02880.1); similar to unnamed protein product [Vitis vinifera] (GB:CAO22500.1); contains InterPro domain UBA-like (InterPro:IPR009060)
2.01	AT3G19580	AZF2 (ARABIDOPSIS ZINC-FINGER PROTEIN 2); nucleic acid binding / transcription factor/ zinc ion binding
2.00	AT1G10050	glycosyl hydrolase family 10 protein / carbohydrate-binding domain-containing protein
2.00	AT4G37580	HLS1 (HOOKLESS 1); N-acetyltransferase

S4.1.2 Genes downregulated by 6 hours AEX treatment compared to mock treated control

Fold change	Locus Identifier	Annotation
18.12	AT5G04960	pectinesterase family protein
16.53	AT4G02270	pollen Ole e 1 allergen and extensin family protein
15.47	AT5G23020	IMS2/MAM-L/MAM3 (METHYLTHIOALKYMALATE SYNTHASE-LIKE); 2-isopropylmalate synthase/ methylthioalkylmalate synthase
14.98	AT1G01750	actin-depolymerizing factor, putative
13.27	AT3G49960	peroxidase, putative
13.14	AT3G01260	aldose 1-epimerase family protein
12.51	AT1G30870	cationic peroxidase, putative
12.30	AT4G00680	actin-depolymerizing factor, putative
11.22	AT5G57540	xyloglucan:xyloglucosyl transferase, putative / xyloglucan endotransglycosylase, putative / endo-xyloglucan transferase, putative
11.15	AT5G05500	pollen Ole e 1 allergen and extensin family protein
10.96	AT5G38940;AT5G38930	[AT5G38940, manganese ion binding / metal ion binding / nutrient reservoir];[AT5G38930, germin-like protein, putative]
10.88	AT1G62980	ATEXPA18 (ARABIDOPSIS THALIANA EXPANSIN A18)
10.78	AT2G32270	ZIP3 (ZINC TRANSPORTER 3 PRECURSOR); zinc ion transmembrane transporter
10.68	AT4G17340	DELTA-TIP2/TIP2;2 (tonoplast intrinsic protein 2;2); water channel
10.55	AT4G30170	peroxidase, putative
10.24	AT1G13300	myb family transcription factor
9.76	AT5G67400	peroxidase 73 (PER73) (P73) (PRXR11)
9.24	AT4G25790	allergen V5/Tpx-1-related family protein
9.08	AT5G47450	AtTIP2;3 (Arabidopsis thaliana tonoplast intrinsic protein 2;3); water channel
9.00	AT4G15390	transferase family protein
8.47	AT1G34510	peroxidase, putative
8.39	AT1G13420	sulfotransferase family protein
8.39	AT5G35190	proline-rich extensin-like family protein
8.38	AT5G04950	nicotianamine synthase, putative
8.24	AT5G22410	peroxidase, putative
8.21	AT2G21210	auxin-responsive protein, putative
8.12	AT5G57530	xyloglucan:xyloglucosyl transferase, putative / xyloglucan endotransglycosylase, putative / endo-xyloglucan transferase, putative
8.09	AT2G18980	peroxidase, putative
8.02	AT3G46280	protein kinase-related
8.00	AT1G12560	ATEXPA7 (ARABIDOPSIS THALIANA EXPANSIN A7)
7.82	AT5G10580	similar to unknown protein [Arabidopsis thaliana] (TAIR:AT4G31330.1); similar to hypothetical protein [Vitis vinifera] (GB:CAN79714.1); contains InterPro domain Protein of unknown function DUF599 (InterPro:IPR006747)
7.76	AT5G43350;AT5G43370	[AT5G43350, ATPT1 (PHOSPHATE TRANSPORTER 1); carbohydrate transmembrane transporter/ phosphate transmembrane transporter/ sugar:hydrogen ion symporter];[AT5G43370, APT1/PHT1;2/PHT2 (PHOSPHATE TRANSPORTER 2); carbohydrate transmembrane transporter/ inorgan
7.75	AT1G48930	ATGH9C1 (ARABIDOPSIS THALIANA GLYCOSYL HYDROLASE 9C1); hydrolase, hydrolyzing O-glycosyl compounds
7.61	AT4G39675	unknown protein
7.56	AT1G24280	G6PD3 (GLUCOSE-6-PHOSPHATE DEHYDROGENASE 3); glucose-6-phosphate dehydrogenase
7.50	AT1G54970	ATPRP1 (PROLINE-RICH PROTEIN 1); structural constituent of cell wall
7.31	AT5G05960	protease inhibitor/seed storage/lipid transfer protein (LTP) family protein
7.28	AT5G60520	late embryogenesis abundant protein-related / LEA protein-related
7.23	AT1G32450	proton-dependent oligopeptide transport (POT) family protein
7.13	AT2G47540	pollen Ole e 1 allergen and extensin family protein
7.10	AT4G28850	xyloglucan:xyloglucosyl transferase, putative / xyloglucan endotransglycosylase, putative / endo-xyloglucan transferase, putative
6.81	AT2G45220	pectinesterase family protein
6.73	AT2G37130	peroxidase 21 (PER21) (P21) (PRXR5)
6.66	AT1G73620	thaumatin-like protein, putative / pathogenesis-related protein, putative
6.65	AT3G62680	PRP3 (PROLINE-RICH PROTEIN 3); structural constituent of cell wall
6.56	AT1G72200	zinc finger (C3HC4-type RING finger) family protein
6.47	AT5G24313	unknown protein
6.47	AT4G12550	AIR1 (Auxin-Induced in Root cultures 1); lipid binding
6.41	AT5G62340	invertase/pectin methylesterase inhibitor family protein
6.40	AT3G54700;AT2G38940	[AT3G54700, carbohydrate transmembrane transporter/ phosphate transmembrane transporter/ sugar:hydrogen ion symporter];[AT2G38940, ATPT2 (PHOSPHATE TRANSPORTER 2); carbohydrate transmembrane transporter/ phosphate transmembrane transporter/ sugar:hydrogen
6.38	AT4G31320	auxin-responsive protein, putative / small auxin up RNA (SAUR_C)
6.32	AT1G06120;AT1G06090	[AT1G06120, fatty acid desaturase family protein];[AT1G06090, fatty acid desaturase family protein]
6.31	AT3G10710	pectinesterase family protein
6.15	AT2G38380;AT2G38390	[AT2G38380, peroxidase 22 (PER22) (P22) (PRXEA) / basic peroxidase E];[AT2G38390, peroxidase, putative]
6.15	AT5G53250	AGP22/ATAGP22 (ARABINOGALACTAN PROTEINS 22)
6.14	AT2G39040	peroxidase, putative
6.09	AT3G62040	hydrolase
6.09	AT4G40090	AGP3 (ARABINOGALACTAN-PROTEIN 3)
6.06	AT1G05250;AT1G05240	[AT1G05250, peroxidase, putative];[AT1G05240, peroxidase, putative]
6.03	AT3G01190	peroxidase 27 (PER27) (P27) (PRXR7)
5.96	AT1G22500	zinc finger (C3HC4-type RING finger) family protein
5.79	AT5G42500;AT5G42510	[AT5G42500, disease resistance-responsive family protein];[AT5G42510, disease resistance-responsive family protein]
5.67	AT1G33700	catalytic
5.67	AT4G30320	allergen V5/Tpx-1-related family protein
5.67	AT5G19890	peroxidase, putative
5.60	AT4G25250	invertase/pectin methylesterase inhibitor family protein
5.58	AT2G03720	MRH6 (morphogenesis of root hair 6)
5.57	AT2G25810	TIP4;1 (tonoplast intrinsic protein 4;1); water channel

5.49	AT4G26010	peroxidase, putative
5.45	AT4G16260	glycosyl hydrolase family 17 protein
5.39	AT1G54890	late embryogenesis abundant protein-related / LEA protein-related
5.34	AT1G49570	peroxidase, putative
5.31	AT5G18600	glutaredoxin family protein
5.25	AT3G29970	germination protein-related
5.12	AT3G19710	BCAT4 (BRANCHED-CHAIN AMINOTRANSFERASE4); catalytic/ methionine-oxo-acid transaminase
5.10	AT5G10130	pollen Ole e 1 allergen and extensin family protein
5.07	AT5G59780	MYB59 (myb domain protein 59); DNA binding / transcription factor
5.07	AT1G30760	FAD-binding domain-containing protein
5.05	AT4G11210	disease resistance-responsive family protein / dirigent family protein
4.99	AT3G43190	SUS4; UDP-glycosyltransferase/ sucrose synthase/ transferase, transferring glycosyl groups
4.91	AT4G25820	XTR9 (XYLOGLUCAN ENDOTRANSGLYCOSYLASE 9); hydrolase, acting on glycosyl bonds
4.85	AT3G45710	proton-dependent oligopeptide transport (POT) family protein
4.84	AT4G33730	pathogenesis-related protein, putative
4.83	AT1G52060	similar to jacalin lectin family protein [Arabidopsis thaliana] (TAIR:AT1G52070.1); similar to jasmonate inducible protein [Brassica napus] (GB:CAA72271.1); contains InterPro domain Mannose-binding lectin (InterPro:IPR001229)
4.80	AT2G41800	similar to unknown protein [Arabidopsis thaliana] (TAIR:AT2G41810.1); similar to unnamed protein product [Vitis vinifera] (GB:CAO23583.1); similar to hypothetical protein [Vitis vinifera] (GB:CAN80832.1); contains InterPro domain Protein of unknown functi
4.73	AT2G30930	similar to unknown protein [Arabidopsis thaliana] (TAIR:AT1G06540.1)
4.72	AT1G78000	SULTR1;2 (SULFATE TRANSPORTER 1;2); sulfate transmembrane transporter
4.67	AT5G47990	CYP705A5 (cytochrome P450, family 705, subfamily A, polypeptide 5); oxygen binding
4.66	AT1G14960	major latex protein-related / MLP-related
4.64	AT5G42590	CYP71A16 (cytochrome P450, family 71, subfamily A, polypeptide 16); oxygen binding
4.63	AT2G21880	AtRABG2/AtRab7A (Arabidopsis Rab GTPase homolog G2); GTP binding
4.62	AT2G20520	FLA6
4.57	AT4G34580	transporter
4.55	AT3G21770	peroxidase 30 (PER30) (P30) (PRXR9)
4.53	AT4G37160	SKS15 (SKU5 Similar 15); copper ion binding
4.53	AT4G26320	AGP13 (ARABINOGALACTAN PROTEIN 13)
4.50	AT2G29750	UDP-glucoronosyl/UDP-glucosyl transferase family protein
4.48	AT5G42180	peroxidase 64 (PER64) (P64) (PRXR4)
4.47	AT2G23620	esterase, putative
4.47	AT2G22860	ATPSK2 (PHYTOSULFOKINE 2 PRECURSOR); growth factor
4.46	AT3G22570	protease inhibitor/seed storage/lipid transfer protein (LTP) family protein
4.45	AT4G26220	caffeoyl-CoA 3-O-methyltransferase, putative
4.44	AT1G66280;AT1G66270	[AT1G66280, glycosyl hydrolase family 1 protein];[AT1G66270, beta-glucosidase (PSR3.2)]
4.43	AT5G44130	FLA13 (FASCICLIN-LIKE ARABINOGALACTAN PROTEIN 13 PRECURSOR)
4.43	AT5G24410	glucosamine/galactosamine-6-phosphate isomerase-related
4.41	AT3G61430	PIP1A (PLASMA MEMBRANE INTRINSIC PROTEIN 1A); water channel
4.41	AT1G30510	ATRFNR2 (ROOT FNR 2); oxidoreductase
4.38	AT5G56540	AGP14 (ARABINOGALACTAN PROTEIN 14)
4.36	AT2G01530	MLP329 (MLP-LIKE PROTEIN 329)
4.33	AT3G23190	lesion inducing protein-related
4.32	AT3G58990	aconitase C-terminal domain-containing protein
4.31	AT1G67110	CYP735A2 (cytochrome P450, family 735, subfamily A, polypeptide 2); oxygen binding
4.31	AT1G10550	XTH33 (xyloglucan:xyloglucosyl transferase 33); hydrolase, acting on glycosyl bonds
4.26	AT3G09940	ATMDAR3/MDHAR (MONODEHYDROASCORBATE REDUCTASE); monodehydroascorbate reductase (NADH)
4.26	AT5G48000	CYP708A2 (cytochrome P450, family 708, subfamily A, polypeptide 2); oxygen binding
4.25	AT1G12040	LRX1 (LEUCINE-RICH REPEAT/EXTENSIN 1); protein binding / structural constituent of cell wall
4.24	AT2G48080	oxidoreductase, 2OG-Fe(II) oxygenase family protein
4.11	AT3G04320;AT3G04330	[AT3G04320, endopeptidase inhibitor];[AT3G04330, trypsin and protease inhibitor family protein / Kunitz family protein]
4.11	AT4G18510	CLE2 (CLAVATA3/ESR-RELATED); receptor binding
4.11	AT4G01480	ATPPA5 (ARABIDOPSIS THALIANA PYROPHOSPHORYLASE 5); inorganic diphosphatase/ pyrophosphatase
4.09	AT4G09990	similar to unknown protein [Arabidopsis thaliana] (TAIR:AT1G33800.1); similar to unnamed protein product [Vitis vinifera] (GB:CAO16316.1); contains InterPro domain Protein of unknown function DUF579, plant (InterPro:IPR006514)
4.06	AT4G11460	protein kinase family protein
4.06	AT3G48100	ARR5 (ARABIDOPSIS RESPONSE REGULATOR 5); transcription regulator/ two-component response regulator
4.04	AT2G30210	LAC3 (laccase 3); copper ion binding / oxidoreductase
4.01	AT3G53980	protease inhibitor/seed storage/lipid transfer protein (LTP) family protein
4.00	AT5G17820	peroxidase 57 (PER57) (P57) (PRXR10)
3.95	AT1G44800	nodulin MtN21 family protein
3.93	AT1G19900	glyoxal oxidase-related
3.93	AT1G47600;AT1G51470	[AT1G47600, glycosyl hydrolase family 1 protein];[AT1G51470, glycosyl hydrolase family 1 protein]
3.90	AT2G45750	dehydration-responsive family protein
3.89	AT3G23430	PHO1 (PHOSPHATE 1)
3.88	AT5G60660	PIP2;4/PIP2F (plasma membrane intrinsic protein 2;4); water channel
3.87	AT3G06460	GNS1/SUR4 membrane family protein
3.86	AT5G60530	late embryogenesis abundant protein-related / LEA protein-related
3.85	AT2G44110	MLO15 (MILDEW RESISTANCE LOCUS O 15); calmodulin binding
3.84	AT2G41970	protein kinase, putative
3.82	AT1G52830	IAA6 (indoleacetic acid-induced protein 6); transcription factor
3.81	AT3G62280	carboxylesterase
3.81	AT4G21850	methionine sulfoxide reductase domain-containing protein / SeIR domain-containing protein
3.80	AT5G24140	SQP2 (Squalene monooxygenase 2); oxidoreductase
3.78	AT3G27170	CLC-B (chloride channel protein B); anion channel/ voltage-gated chloride channel
3.78	AT4G11190	disease resistance-responsive family protein / dirigent family protein
3.78	AT3G45970	ATEXLA1 (ARABIDOPSIS THALIANA EXPANSIN-LIKE A1)
3.77	AT1G49860	ATGSTF14 (Arabidopsis thaliana Glutathione S-transferase (class phi) 14); glutathione transferase
3.76	AT1G70850	MLP34 (MLP-LIKE PROTEIN 34)
3.75	AT5G18060	auxin-responsive protein, putative
3.75	AT1G33055	unknown protein
3.75	AT1G48750	protease inhibitor/seed storage/lipid transfer protein (LTP) family protein
3.73	AT4G04840	methionine sulfoxide reductase domain-containing protein / SeIR domain-containing protein
3.73	AT4G15340	ATPEN1 (Arabidopsis thaliana pentacyclic triterpene synthase 1); catalytic/ lyase
3.69	AT3G27690	LHCB2:4 (Photosystem II light harvesting complex gene 2.3); chlorophyll binding
3.69	AT2G47550	pectinesterase family protein
3.68	AT3G03840	auxin-responsive protein, putative
3.68	AT4G34760	auxin-responsive family protein
3.67	AT3G07070	protein kinase family protein
3.66	AT1G53680	ATGSTU28 (Arabidopsis thaliana Glutathione S-transferase (class tau) 28); glutathione transferase

3.65	AT2G05070;AT2G05100	[AT2G05070, LHCB2.2 (Photosystem II light harvesting complex gene 2.2); chlorophyll binding];[AT2G05100, LHCB2.1 (Photosystem II light harvesting complex gene 2.1); chlorophyll binding]
3.64	AT5G06200	integral membrane family protein
3.63	AT5G41670	6-phosphogluconate dehydrogenase family protein
3.63	AT4G22610	protease inhibitor/seed storage/lipid transfer protein (LTP) family protein
3.62	AT2G31110	similar to unknown protein [Arabidopsis thaliana] (TAIR:AT2G42570.1); similar to unnamed protein product [Vitis vinifera] (GB:CAO69853.1); contains InterPro domain Protein of unknown function DUF231, plant (InterPro:IPR004253)
3.61	AT2G39530	integral membrane protein, putative
3.59	AT1G56680	glycoside hydrolase family 19 protein
3.59	AT2G34080	cysteine proteinase, putative
3.58	AT3G54590	ATHRGP1; structural constituent of cell wall
3.57	AT1G22880	ATCEL5/ATGH9B4 (ARABIDOPSIS THALIANA GLYCOSYL HYDROLASE 9B4); hydrolase, hydrolyzing O-glycosyl compounds
3.55	AT1G30750	similar to Hypothetical protein CBG24759 [Caenorhabditis briggsae] (GB:CAE56916.1); contains InterPro domain Protein of unknown function DUF1720 (InterPro:IPR013182)
3.55	AT4G33790	acyl CoA reductase, putative
3.52	AT3G24290;AT3G24300	[AT3G24290, ammonium transporter, putative];[AT3G24300, AMT1;3/ATAMT1;3 (AMMONIUM TRANSPORTER 1;3); ammonium transmembrane transporter]
3.50	AT2G28780	similar to unknown protein [Arabidopsis thaliana] (TAIR:AT3G09450.1); similar to unnamed protein product [Vitis vinifera] (GB:CAO21693.1)
3.50	AT1G75580	auxin-responsive protein, putative
3.49	AT5G15830	ATBZIP3 (ARABIDOPSIS THALIANA BASIC LEUCINE-ZIPPER 3); DNA binding / transcription factor
3.44	AT1G78050	phosphoglycerate/bisphosphoglycerate mutase family protein
3.44	AT2G27370	integral membrane family protein
3.44	AT5G66815	unknown protein
3.44	AT5G19800	hydroxyproline-rich glycoprotein family protein
3.44	AT5G23830	MD-2-related lipid recognition domain-containing protein / ML domain-containing protein
3.44	AT5G19790	RAP2.11 (related to AP2 11); DNA binding / transcription factor
3.43	AT2G21020;AT1G31885	[AT2G21020, pseudogene, major intrinsic protein (MIP) family, contains Pfam profile: MIP PF00230; blastp match of 61% identity and 1.8e-40 P-value to PIR|S01444|S01444 nodulin-26 precursor - soybean];[AT1G31885, transporter]
3.43	AT5G59090	ATSBT4.12; subtilase
3.43	AT5G56320	ATEXPA14 (ARABIDOPSIS THALIANA EXPANSIN A14)
3.42	AT1G52050	jacalin lectin family protein
3.38	AT1G74670	gibberellin-responsive protein, putative
3.37	AT3G25930	universal stress protein (USP) family protein
3.36	AT5G40850	UPM1 (UROPHORPHYRIN METHYLASE 1); uroporphyrin-III C-methyltransferase
3.34	AT1G20070	unknown protein
3.33	AT2G47140	short-chain dehydrogenase/reductase (SDR) family protein
3.33	AT2G24980	proline-rich extensin-like family protein
3.31	AT3G18200	nodulin MtN21 family protein
3.30	AT4G25220	transporter, putative
3.29	AT1G61590	protein kinase, putative
3.28	AT4G13770	CYP83A1 (CYTOCHROME P450 83A1); oxygen binding
3.28	AT3G59370	contains domain PTHR22683 (PTHR22683)
3.28	AT1G67330	similar to unknown protein [Arabidopsis thaliana] (TAIR:AT1G27930.1); similar to unknown [Populus trichocarpa] (GB:ABK93495.1); contains InterPro domain Protein of unknown function DUF579, plant (InterPro:IPR006514)
3.26	AT3G14060	similar to unknown protein [Arabidopsis thaliana] (TAIR:AT1G54120.1); similar to unnamed protein product [Vitis vinifera] (GB:CAO45609.1)
3.25	AT1G22530	PATL2; transporter
3.25	AT2G39430	disease resistance-responsive protein-related / dirigent protein-related
3.24	AT4G37540	LBD39 (LOB DOMAIN-CONTAINING PROTEIN 39)
3.24	AT5G06630	proline-rich extensin-like family protein
3.24	AT2G02680	DC1 domain-containing protein
3.23	AT4G21830;AT4G21840	[AT4G21830, methionine sulfoxide reductase domain-containing protein / SeIR domain-containing protein];[AT4G21840, methionine sulfoxide reductase domain-containing protein / SelR domain-containing protein]
3.22	AT2G37180;AT2G37170	[AT2G37180, RD28 (plasma membrane intrinsic protein 2;3); water channel];[AT2G37170, PIP2B (plasma membrane intrinsic protein 2;2); water channel]
3.22	AT3G02850	SKOR (stelar K+ outward rectifier); cyclic nucleotide binding / outward rectifier potassium channel
3.22	AT1G14080	FUT6 (fucosyltransferase 6); fucosyltransferase/ transferase, transferring glycosyl groups
3.21	AT1G11580	ATPMEPCRA; pectinesterase
3.21	AT2G23630	SKS16 (SKU5 Similar 16); copper ion binding / pectinesterase
3.19	AT4G27140	2S seed storage protein 1 / 2S albumin storage protein / NWMU1-2S albumin 1
3.19	AT4G00080	UNE11 (unfertilized embryo sac 11); pectinesterase inhibitor
3.18	AT5G03120	similar to hypothetical protein [Vitis vinifera] (GB:CAN68657.1)
3.18	AT4G38840	auxin-responsive protein, putative
3.18	AT4G12510;AT4G12520	[AT4G12510, protease inhibitor/seed storage/lipid transfer protein (LTP) family protein];[AT4G12520, protease inhibitor/seed storage/lipid transfer protein (LTP) family protein]
3.18	AT4G07820	pathogenesis-related protein, putative
3.17	AT3G12110	ACT11 (ACTIN-11); structural constituent of cytoskeleton
3.15	AT1G14220	ribonuclease T2 family protein
3.15	AT4G19680	IRT2 (iron-responsive transporter 2); iron ion transmembrane transporter/ zinc ion transmembrane transporter
3.15	AT1G31950	terpene synthase/cyclase family protein
3.13	AT3G19430	late embryogenesis abundant protein-related / LEA protein-related
3.13	AT2G21220	auxin-responsive protein, putative
3.12	AT5G36270	pseudogene of dehydroascorbate reductase
3.12	AT1G73330	ATDR4 (Arabidopsis thaliana drought-repressed 4)
3.12	AT1G20160	ATSBT5.2; subtilase
3.10	AT4G30670	contains domain PROKAR_LIPOPROTEIN (PS51257)
3.10	AT3G50640	similar to unknown protein [Arabidopsis thaliana] (TAIR:AT5G66800.1); similar to hypothetical protein [Vitis vinifera] (GB:CAN61148.1)
3.09	AT1G51850	leucine-rich repeat protein kinase, putative
3.09	AT3G62270	anion exchange family protein
3.08	AT2G34910	similar to unknown protein [Arabidopsis thaliana] (TAIR:AT1G30850.1); similar to unnamed protein product [Vitis vinifera] (GB:CAO15288.1)
3.08	AT5G49270	COBL9/MRH4/SHV2 (COBRA-LIKE 9, SHAVEN 2); carbohydrate binding
3.07	AT5G54370	late embryogenesis abundant protein-related / LEA protein-related
3.07	AT3G05490	RALFL22 (RALF-LIKE 22)
3.07	AT1G57590	carboxylesterase
3.07	AT1G50560	CYP705A25 (cytochrome P450, family 705, subfamily A, polypeptide 25); oxygen binding
3.07	AT1G51860	leucine-rich repeat protein kinase, putative
3.07	AT5G14150	similar to unknown protein [Arabidopsis thaliana] (TAIR:AT5G11420.1); similar to hypothetical protein [Vitis vinifera] (GB:CAN70048.1); contains InterPro domain Protein of unknown function DUF642 (InterPro:IPR006946)
3.06	AT5G54040	DC1 domain-containing protein
3.06	AT4G36670	mannitol transporter, putative
3.06	AT1G30900	vacuolar sorting receptor, putative
3.04	AT5G62330	similar to invertase/pectin methylesterase inhibitor family protein [Arabidopsis thaliana] (TAIR:AT5G62340.1)

3.04	AT2G34430;AT2G34420	[AT2G34430, LHB1B1 (Photosystem II light harvesting complex gene 1.4); chlorophyll binding];[AT2G34420, LHB1B2 (Photosystem II light harvesting complex gene 1.5); chlorophyll binding]
3.03	AT4G34950	nodulin family protein
3.03	AT5G19970	similar to unnamed protein product [Vitis vinifera] (GB:CAO65601.1)
3.02	AT4G31470	pathogenesis-related protein, putative
3.02	AT3G19030	similar to unknown protein [Arabidopsis thaliana] (TAIR:AT1G49500.1)
3.01	AT4G02130	GATL6/LGT10; polygalacturonate 4-alpha-galacturonosyltransferase/ transferase, transferring glycosyl groups / transferase, transferring hexosyl groups
3.01	AT3G02910	Identical to UPF0131 protein At3g02910 [Arabidopsis Thaliana] (GB:Q9M8T3); similar to unknown protein [Arabidopsis thaliana] (TAIR:AT5G46720.1); similar to Os03g0854000 [Oryza sativa (japonica cultivar-group)] (GB:NP_001051934.1); similar to unknown [Pice
3.01	AT2G38170	CAX1 (CATION EXCHANGER 1); calcium ion transmembrane transporter/ calcium:hydrogen antiporter
3.00	AT2G36100	integral membrane family protein
3.00	AT1G69240	hydrolase, alpha/beta fold family protein
3.00	AT1G52070	jacalin lectin family protein
2.99	AT1G76090	SMT3 (S-adenosyl-methionine-sterol-C-methyltransferase 3); S-adenosylmethionine-dependent methyltransferase
2.97	AT3G54770	RNA recognition motif (RRM)-containing protein
2.97	AT4G31910	transferase family protein
2.96	AT1G05660;AT1G05650	[AT1G05660, polygalacturonase, putative / pectinase, putative];[AT1G05650, polygalacturonase, putative / pectinase, putative]
2.95	AT2G42870	HLH1/PAR1 (PHY RAPIDLY REGULATED 1); transcription regulator
2.95	AT5G47950	transferase family protein
2.94	AT1G75900	family II extracellular lipase 3 (EXL3)
2.93	AT2G17850	similar to unknown protein [Arabidopsis thaliana] (TAIR:AT5G66170.2); similar to unnamed protein product [Vitis vinifera] (GB:CAO48196.1); contains InterPro domain Rhodanese-like (InterPro:IPR001763)
2.92	AT4G20260	DREPP plasma membrane polypeptide family protein
2.92	AT5G46230	similar to unknown protein [Arabidopsis thaliana] (TAIR:AT1G09310.1); similar to unnamed protein product [Vitis vinifera] (GB:CAO14438.1); contains InterPro domain Protein of unknown function DUF538 (InterPro:IPR007493)
2.91	AT4G25090	respiratory burst oxidase, putative / NADPH oxidase, putative
2.91	AT1G70990	proline-rich family protein
2.91	AT4G35060	heavy-metal-associated domain-containing protein / copper chaperone (CCH)-related
2.90	AT5G45650	subtilase family protein
2.90	AT4G08410	proline-rich extensin-like family protein
2.90	AT1G29430;AT5G27780	[AT1G29430, auxin-responsive family protein];[AT5G27780, auxin-responsive family protein]
2.89	AT5G26200	mitochondrial substrate carrier family protein
2.88	AT1G06830	glutaredoxin family protein
2.88	AT5G20550	oxidoreductase, 2OG-Fe(II) oxygenase family protein
2.87	AT3G45700	proton-dependent oligopeptide transport (POT) family protein
2.86	AT1G49500	similar to unknown protein [Arabidopsis thaliana] (TAIR:AT3G19030.1)
2.85	AT1G78090	ATTPPB (TREHALOSE-6-PHOSPHATE PHOSPHATASE)
2.84	AT1G66800	cinnamyl-alcohol dehydrogenase family / CAD family
2.84	AT1G29500	auxin-responsive protein, putative
2.83	AT2G44380	DC1 domain-containing protein
2.83	AT1G19050	ARR7 (RESPONSE REGULATOR 7); transcription regulator/ two-component response regulator
2.83	AT5G10430	AGP4 (ARABINOGALACTAN-PROTEIN 4)
2.82	AT3G56230	speckle-type POZ protein-related
2.82	AT4G28780	GDSL-motif lipase/hydrolase family protein
2.81	AT5G15600	SP1L4 (SPIRAL1-LIKE4)
2.81	AT1G72430	auxin-responsive protein-related
2.81	AT5G46900;AT5G46890	[AT5G46900, protease inhibitor/seed storage/lipid transfer protein (LTP) family protein];[AT5G46890, protease inhibitor/seed storage/lipid transfer protein (LTP) family protein]
2.80	AT5G01870	lipid transfer protein, putative
2.80	AT2G21045	similar to unknown protein [Arabidopsis thaliana] (TAIR:AT5G66170.2); similar to putative senescence-associated protein [Oryza sativa (japonica cultivar-group)] (GB:BAD07813.1); contains InterPro domain Rhodanese-like (InterPro:IPR001763)
2.79	AT4G14980	DC1 domain-containing protein
2.79	AT2G15620	NIR1 (NITRITE REDUCTASE); ferredoxin-nitrate reductase
2.79	AT1G27140	ATGSTU14 (GLUTATHIONE S-TRANSFERASE 13); glutathione transferase
2.78	AT1G28130	GH3.17; indole-3-acetic acid amido synthetase
2.78	AT4G17030	ATEXLB1 (ARABIDOPSIS THALIANA EXPANSIN-LIKE B1)
2.78	AT1G66200	ATGSR2 (Arabidopsis thaliana glutamine synthase clone R2); glutamate-ammonia ligase
2.77	AT3G16440	ATMLP-300B (MYROSINASE-BINDING PROTEIN-LIKE PROTEIN-300B)
2.77	AT1G31770	ABC transporter family protein
2.77	AT3G11550	integral membrane family protein
2.77	AT5G62720	integral membrane HPP family protein
2.76	AT2G28630	beta-ketoacyl-CoA synthase family protein
2.75	AT5G06640	proline-rich extensin-like family protein
2.74	AT1G60680	AGD2 (ARF-GAP DOMAIN 2); aldo-keto reductase
2.74	AT2G01880	ATPAP7/PAP7 (purple acid phosphatase 7); acid phosphatase/ protein serine/threonine phosphatase
2.74	AT3G05900	neurofilament protein-related
2.73	AT2G36830	GAMMA-TIP (Tonoplast intrinsic protein (TIP) gamma); water channel
2.72	AT1G19540	isoflavone reductase, putative
2.72	AT3G23800	selenium-binding family protein
2.72	AT5G43180	similar to unknown protein [Arabidopsis thaliana] (TAIR:AT5G10580.1); similar to hypothetical protein [Vitis vinifera] (GB:CAN66486.1); contains InterPro domain Protein of unknown function DUF599 (InterPro:IPR006747)
2.71	AT2G04800	unknown protein
2.71	AT3G01730	unknown protein
2.70	AT2G45890	ATROPGEF4/ROPGEF4 (KINASE PARTNER PROTEIN-LIKE); Rho guanyl-nucleotide exchange factor/
2.70	AT5G56080	nicotianamine synthase, putative
2.70	AT5G59520	ZIP2 (ZINC TRANSPORTER 2 PRECURSOR); transferase, transferring glycosyl groups / zinc ion transmembrane transporter
2.69	AT2G43100	aconitase C-terminal domain-containing protein
2.69	AT1G61840	DC1 domain-containing protein
2.69	AT4G00700	C2 domain-containing protein
2.68	AT1G23205	invertase/pectin methylesterase inhibitor family protein
2.67	AT4G30460	glycine-rich protein
2.67	AT3G31415;AT3G32030	[AT3G31415, terpene synthase/cyclase family protein];[AT3G32030, terpene synthase/cyclase family protein]
2.65	AT2G24762	ATGDU4 (ARABIDOPSIS THALIANA GLUTAMINE DUMPER 4)
2.65	AT1G44050	DC1 domain-containing protein
2.65	AT4G38400	ATEXLA2 (ARABIDOPSIS THALIANA EXPANSIN-LIKE A2)
2.64	AT3G05730	Encodes a defensin-like (DEFL) family protein.
2.62	AT1G72230	plastocyanin-like domain-containing protein
2.61	AT1G13830	beta-1,3-glucanase-related
2.61	AT3G61380	similar to unknown protein [Arabidopsis thaliana] (TAIR:AT2G45900.1); similar to {, related [Medicago truncatula] (GB:ABD32828.1); contains domain PTHR21726:SF4 (PTHR21726:SF4); contains domain PTHR21726 (PTHR21726)

2.60	AT3G18450	similar to unknown protein [Arabidopsis thaliana] (TAIR:AT3G18460.1); similar to unnamed protein product [Vitis vinifera] (GB:CAO68031.1); contains InterPro domain Protein of unknown function Cys-rich (InterPro:IPR006461)
2.60	AT1G56430	nicotianamine synthase, putative
2.59	AT5G67450	AZF1 (ARABIDOPSIS ZINC-FINGER PROTEIN 1); nucleic acid binding / transcription factor/ zinc ion binding
2.59	AT3G57040	ARR9 (RESPONSE REACTOR 4); transcription regulator
2.58	AT1G44970	peroxidase, putative
2.57	AT1G63450	catalytic
2.57	AT4G40010	SNRK2-7/SNRK2.7/SRK2F (SNF1-RELATED PROTEIN KINASE 2.7); kinase
2.57	AT4G30450	glycine-rich protein
2.57	AT4G13580	disease resistance-responsive family protein
2.57	AT3G23090	similar to WDL1 (WVD2-LIKE 1) [Arabidopsis thaliana] (TAIR:AT3G04630.2); similar to WDL1 (WVD2-LIKE 1) [Arabidopsis thaliana] (TAIR:AT3G04630.3); similar to seed specific protein Bn15D14A [Brassica napus] (GB:AAP37969.1); contains InterPro domain Targetin
2.57	AT5G43520	DC1 domain-containing protein
2.57	AT5G47980	transferase family protein
2.56	AT3G16690	nodulin MtN3 family protein
2.56	AT3G21240	4CL2 (4-coumarate:CoA ligase 2); 4-coumarate-CoA ligase
2.55	AT3G29030	ATEXPA5 (ARABIDOPSIS THALIANA EXPANSIN A5)
2.54	AT1G29510	SAUR68 (SMALL AUXIN UPREGULATED 68)
2.54	AT4G36110	auxin-responsive protein, putative
2.54	AT1G02810	pectinesterase family protein
2.53	AT1G74090	sulfotransferase family protein
2.52	AT1G50060	pathogenesis-related protein, putative
2.52	AT4G10240	zinc finger (B-box type) family protein
2.52	AT1G65310	ATXTH17 (XYLOGLUCAN ENDOTRANSGLUCOSYLASE/HYDROLASE 17); hydrolase, acting on glycosyl bonds
2.51	AT1G71740	similar to unknown protein [Arabidopsis thaliana] (TAIR:AT3G18560.1); similar to hypothetical protein [Vitis vinifera] (GB:CAN60388.1)
2.51	AT1G77330	1-aminocyclopropane-1-carboxylate oxidase, putative / ACC oxidase, putative
2.50	AT1G07610	MT1C (metallothionein 1C)
2.50	AT1G12950	MATE efflux family protein
2.50	AT4G23400	PIP1;5/PIP1D (plasma membrane intrinsic protein 1;5); water channel
2.50	AT5G58784	dehydrodolichyl diphosphate synthase, putative / DEDOL-PP synthase, putative
2.47	AT2G47160	BOR1 (REQUIRES HIGH BORON 1); anion exchanger
2.47	AT4G39030	EDS5 (ENHANCED DISEASE SUSCEPTIBILITY 5); antiporter/ transporter
2.47	AT1G05570	CALS1 (CALLOSE SYNTHASE 1); transferase, transferring glycosyl groups
2.46	AT5G48010	pentacyclic triterpene synthase, putative
2.46	AT2G46690	auxin-responsive family protein
2.46	AT2G33790	pollen Ole e 1 allergen and extensin family protein
2.46	AT4G19030	NLM1 (NOD26-like intrinsic protein 1;1); water channel
2.45	AT3G19450	CAD4 (CINNAMYL ALCOHOL DEHYDROGENASE 4); cinnamyl-alcohol dehydrogenase
2.45	AT2G22930	glycosyltransferase family protein
2.45	AT5G66280	GMD1 (GDP-D-MANNOSE 4,6-DEHYDRATASE 1); GDP-mannose 4,6-dehydratase
2.45	AT4G22460	protease inhibitor/seed storage/lipid transfer protein (LTP) family protein
2.44	AT5G66490	similar to unknown protein [Arabidopsis thaliana] (TAIR:AT3G50900.1); similar to hypothetical protein [Thellungiella halophila] (GB:ABB45855.1)
2.43	AT2G25240	serine-type endopeptidase inhibitor
2.43	AT3G50570	hydroxyproline-rich glycoprotein family protein
2.43	AT1G68520	zinc finger (B-box type) family protein
2.43	AT1G23720	proline-rich extensin-like family protein
2.43	AT3G55150	ATEXO70H1 (exocyst subunit EXO70 family protein H1); protein binding
2.42	AT2G43880	polygalacturonase, putative / pectinase, putative
2.42	AT2G16660	nodulin family protein
2.42	AT1G72140	proton-dependent oligopeptide transport (POT) family protein
2.41	AT3G13760	DC1 domain-containing protein
2.41	AT3G54890	LHCA1; chlorophyll binding
2.41	AT1G03870	FLA9
2.41	AT5G15410	DND1 (DEFENSE NO DEATH 1); calcium channel/ calmodulin binding / cation channel/ cyclic nucleotide binding / inward rectifier potassium channel
2.41	AT3G49190	condensation domain-containing protein
2.40	AT2G24610	ATCNGC14 (cyclic nucleotide gated channel 14); calmodulin binding / cyclic nucleotide binding / ion channel
2.39	AT2G32300	UCC1 (UCLACYANIN 1); copper ion binding
2.39	AT3G27950	early nodule-specific protein, putative
2.39	AT1G05260	RCI3 (RARE COLD INDUCIBLE GENE 3); peroxidase
2.39	AT3G25780	AOC3 (ALLENE OXIDE CYCLASE 3)
2.39	AT5G07110	prenylated rab acceptor (PRA1) family protein
2.39	AT1G33800	similar to unknown protein [Arabidopsis thaliana] (TAIR:AT4G09990.1); similar to unknown [Populus trichocarpa] (GB:ABK93991.1); contains InterPro domain Protein of unknown function DUF579, plant (InterPro:IPR006514)
2.38	AT4G08300	nodulin MtN21 family protein
2.38	AT3G42800	similar to unknown protein [Arabidopsis thaliana] (TAIR:AT1G54200.1); similar to expressed protein [Olimarabidopsis pumila] (GB:ABA18092.1)
2.38	AT1G49030	similar to unknown protein [Arabidopsis thaliana] (TAIR:AT3G18460.1); similar to unnamed protein product [Vitis vinifera] (GB:CAO68031.1); contains InterPro domain Protein of unknown function Cys-rich (InterPro:IPR006461)
2.38	AT5G62920	ARR6 (RESPONSE REGULATOR 6); transcription regulator/ two-component response regulator
2.37	AT3G27220	kelch repeat-containing protein
2.37	AT2G17820	ATHK1 (HISTIDINE KINASE 1)
2.37	AT3G13980	similar to unknown protein [Arabidopsis thaliana] (TAIR:AT1G54200.1); similar to hypothetical protein [Vitis vinifera] (GB:CAN69469.1)
2.36	AT5G58010	basic helix-loop-helix (bHLH) family protein
2.36	AT1G18100	E12A11; phosphatidylethanolamine binding
2.36	AT1G70890	MLP43 (MLP-LIKE PROTEIN 43)
2.35	AT4G35320	similar to unknown protein [Arabidopsis thaliana] (TAIR:AT2G17300.1); similar to hypothetical protein [Vitis vinifera] (GB:CAN78386.1)
2.35	AT3G24670	pectate lyase family protein
2.35	AT1G29450	auxin-responsive protein, putative
2.35	AT5G04970	pectinesterase, putative
2.35	AT3G21230	4CL5 (4-COUMARATE:COA LIGASE 5); 4-coumarate-CoA ligase
2.35	AT4G13790	auxin-responsive protein, putative
2.34	AT4G01140	similar to unknown protein [Arabidopsis thaliana] (TAIR:AT3G08600.1); similar to unknown protein [Arabidopsis thaliana] (TAIR:AT4G23720.1); similar to unnamed protein product [Vitis vinifera] (GB:CAO45372.1); contains InterPro domain Protein of unknown fu
2.34	AT4G32650	ATKC1 (ARABIDOPSIS THALIANA K+ RECTIFYING CHANNEL 1); cyclic nucleotide binding / inward rectifier potassium channel
2.34	AT1G76240	similar to unknown protein [Arabidopsis thaliana] (TAIR:AT2G17080.1); similar to Os06g0725500 [Oryza sativa (japonica cultivar-group)] (GB:NP_001058623.1); similar to hypothetical protein OsI_023643 [Oryza sativa (indica cultivar-group)] (GB:EAZ02411.1);
2.34	AT3G16240	DELTA-TIP (delta tonoplast integral protein); water channel
2.34	AT5G46940	invertase/pectin methylesterase inhibitor family protein

2.33	AT1G74770	protein binding / zinc ion binding
2.33	AT1G48598;AT1G48600	[AT1G48598, CPuORF31 (Conserved peptide upstream open reading frame 31)];[AT1G48600, phosphoethanolamine N-methyltransferase 2, putative (NMT2)]
2.32	AT5G60860	AtRABA1f (Arabidopsis Rab GTPase homolog A1f); GTP binding
2.32	AT5G23750	remorin family protein
2.32	AT1G75450	CKX5 (CYTOKININ OXIDASE 5); cytokinin dehydrogenase
2.32	AT1G08500	plastocyanin-like domain-containing protein
2.31	AT5G24100	leucine-rich repeat transmembrane protein kinase, putative
2.31	AT4G00360	CYP86A2 (ABERRANT INDUCTION OF TYPE THREE GENES 1); oxygen binding
2.31	AT1G23120	major latex protein-related / MLP-related
2.31	AT1G43160	RAP2.6 (related to AP2 6); DNA binding / transcription factor
2.30	AT4G16980	arabinogalactan-protein family
2.29	AT1G18140	LAC1 (Laccase 1); copper ion binding / oxidoreductase
2.29	AT5G65530	protein kinase, putative
2.29	AT5G20150	SPX (SYG1/Pho81/XPR1) domain-containing protein
2.28	AT2G27840	HDT4 (histone deacetylase 13)
2.28	AT3G18560	similar to unknown protein [Arabidopsis thaliana] (TAIR:AT1G49000.1); similar to unnamed protein product [Vitis vinifera] (GB:CAO68009.1)
2.28	AT2G29330	TRI (TROPINONE REDUCTASE); oxidoreductase
2.28	AT2G18800	xyloglucan:xyloglucosyl transferase, putative / xyloglucan endotransglycosylase, putative / endo-xyloglucan transferase, putative
2.28	AT1G62440	LRX2 (LEUCINE-RICH REPEAT/EXTENSIN 2); protein binding / structural constituent of cell wall
2.27	AT3G14530;AT3G14550	[AT3G14530, geranylgeranyl pyrophosphate synthase, putative / GGPP synthetase, putative / farnesyltranstransferase, putative];[AT3G14550, GGPS3 (GERANYLGERANYL PYROPHOSPHATE SYNTHASE 3); farnesyltranstransferase]
2.26	AT1G01600	CYP86A4 (cytochrome P450, family 86, subfamily A, polypeptide 4); oxygen binding
2.26	AT3G18280	protease inhibitor/seed storage/lipid transfer protein (LTP) family protein
2.26	AT4G22080;AT4G22090	[AT4G22080, pectate lyase family protein];[AT4G22090, pectate lyase family protein]
2.26	AT3G12830	auxin-responsive family protein
2.26	AT1G70230	similar to unknown protein [Arabidopsis thaliana] (TAIR:AT1G01430.1); similar to Os09g0375300 [Oryza sativa (japonica cultivar-group)] (GB:NP_001063036.1); similar to Os06g0235200 [Oryza sativa (japonica cultivar-group)] (GB:NP_001057240.1); similar to le
2.26	AT4G37450	AGP18 (Arabinogalactan protein 18)
2.25	AT2G27510	ATFD3 (FERREDOXIN 3); electron carrier
2.25	AT2G42850	CYP718 (cytochrome P450, family 718); oxygen binding
2.25	AT1G74660	MIF1 (MINI ZINC FINGER 1); DNA binding / transcription factor
2.25	AT1G43800	acyl-(acyl-carrier-protein) desaturase, putative / stearoyl-ACP desaturase, putative
2.25	AT1G61667	similar to unknown protein [Arabidopsis thaliana] (TAIR:AT5G54530.1); similar to unnamed protein product [Vitis vinifera] (GB:CAO64729.1); contains InterPro domain Protein of unknown function DUF538 (InterPro:IPR007493)
2.25	AT5G46050	ATPTR3/PTR3 (PEPTIDE TRANSPORTER PROTEIN 3); transporter
2.24	AT5G64620	C/VIF2 (CELL WALL / VACUOLAR INHIBITOR OF FRUCTOSIDASE 2); pectinesterase inhibitor
2.24	AT3G23480;AT3G23470	[AT3G23480, cyclopropane fatty acid synthase-related];[AT3G23470, cyclopropane-fatty-acyl-phospholipid synthase]
2.24	AT3G17790	ATACP5 (acid phosphatase 5); acid phosphatase/ protein serine/threonine phosphatase
2.24	AT4G38860	auxin-responsive protein, putative
2.23	AT1G69040	ACR4 (ACT REPEAT 4); amino acid binding
2.23	AT4G31250	leucine-rich repeat transmembrane protein kinase, putative
2.22	AT5G64100	peroxidase, putative
2.22	AT1G30850	similar to unknown protein [Arabidopsis thaliana] (TAIR:AT2G34910.1); similar to unnamed protein product [Vitis vinifera] (GB:CAO15288.1)
2.22	AT1G16370	ATOCT6; carbohydrate transmembrane transporter/ sugar:hydrogen ion symporter
2.21	AT3G29780	RALFL27 (RALF-LIKE 27)
2.21	AT3G12540	similar to unknown protein [Arabidopsis thaliana] (TAIR:AT2G39690.1); similar to At3g12540-like protein [Boechera stricta] (GB:ABB89771.1); contains InterPro domain Protein of unknown function DUF547 (InterPro:IPR006869)
2.21	AT1G47480	hydrolase
2.21	AT4G33560	unknown protein
2.20	AT4G15290	ATCSLB05 (Cellulose synthase-like B5); transferase/ transferase, transferring glycosyl groups
2.20	AT5G15180	peroxidase, putative
2.20	AT4G21960	PRXR1 (peroxidase 42); peroxidase
2.20	AT5G15290	integral membrane family protein
2.19	AT3G06770	glycoside hydrolase family 28 protein / polygalacturonase (pectinase) family protein
2.19	AT1G80830	NRAMP1 (NRAMP metal ion transporter 1); manganese ion transmembrane transporter/ metal ion transmembrane transporter
2.19	AT4G10270	wound-responsive family protein
2.19	AT3G24450	copper-binding family protein
2.19	AT5G44020	acid phosphatase class B family protein
2.19	AT2G45210	auxin-responsive protein-related
2.19	AT4G20460	NAD-dependent epimerase/dehydratase family protein
2.18	AT2G43600	glycoside hydrolase family 19 protein
2.17	AT4G34770	auxin-responsive family protein
2.17	AT1G72150	PATL1 (PATELLIN 1); transporter
2.16	AT5G51460	ATTPPA (Arabidopsis thaliana trehalose-6-phosphate phosphatase); trehalose-phosphatase
2.16	AT1G21500	similar to hypothetical protein OsI_030994 [Oryza sativa (indica cultivar-group)] (GB:EAZ09762.1); similar to Os09g0517000 [Oryza sativa (japonica cultivar-group)] (GB:NP_001063677.1); similar to unknown protein [Oryza sativa (japonica cultivar-group)] (G
2.16	AT3G47380	invertase/pectin methylesterase inhibitor family protein
2.15	AT1G07740;AT1G07730	[AT1G07740, pentatricopeptide (PPR) repeat-containing protein];[AT1G07730, disease resistance-responsive family protein]
2.15	AT3G18170	similar to unknown protein [Arabidopsis thaliana] (TAIR:AT3G18180.1); similar to unnamed protein product [Vitis vinifera] (GB:CAO68130.1); contains InterPro domain Protein of unknown function DUF563 (InterPro:IPR007657)
2.15	AT1G75620	glyoxal oxidase-related
2.15	AT3G21510	AHP1 (HISTIDINE-CONTAINING PHOSPHOTRANSMITTER 3); histidine phosphotransfer kinase
2.15	AT5G23030	TET12 (TETRASPANIN12)
2.15	AT2G01830	WOL (WOODEN LEG)
2.14	AT4G02090	similar to unnamed protein product [Vitis vinifera] (GB:CAO40099.1)
2.14	AT3G59670	similar to unknown protein [Arabidopsis thaliana] (TAIR:AT4G37440.2); similar to unknown protein [Arabidopsis thaliana] (TAIR:AT4G37440.1); similar to unnamed protein product [Vitis vinifera] (GB:CAO46283.1)
2.14	AT1G16390	ATOCT3 (ARABIDOPSIS THALIANA ORGANIC CATION/CARNITINE TRANSPORTER2); carbohydrate transmembrane transporter/ sugar:hydrogen ion symporter
2.14	AT5G38550;AT5G38540	[AT5G38550, jacalin lectin family protein];[AT5G38540, jacalin lectin family protein]
2.13	AT1G08650	PPCK1 (PHOSPHOENOLPYRUVATE CARBOXYLASE KINASE); kinase
2.13	AT2G30540	glutaredoxin family protein
2.13	AT1G29660	GDSL-motif lipase/hydrolase family protein
2.13	AT1G29440	auxin-responsive family protein
2.13	AT3G46270	receptor protein kinase-related
2.13	AT1G72240	similar to unknown protein [Arabidopsis thaliana] (TAIR:AT1G22470.1)
2.12	AT3G11280	myb family transcription factor

2.12	AT2G23600;AT2G23590	[AT2G23600, ACL (ACETONE-CYANOHYDRIN LYASE); hydrolase];[AT2G23590, hydrolase, alpha/beta fold family protein]
2.12	AT4G34750	auxin-responsive protein, putative / small auxin up RNA (SAUR_E)
2.12	AT5G54160	ATOMT1 (O-METHYLTRANSFERASE 1)
2.12	AT4G28940	catalytic
2.11	AT4G11820	MVA1 (HYDROXYMETHYLGLUTARYL-COA SYNTHASE); acetyl-CoA C-acetyltransferase/ hydroxymethylglutaryl-CoA synthase
2.11	AT5G22555	unknown protein
2.11	AT5G07080	transferase family protein
2.11	AT1G48300	similar to hypothetical protein [Vitis vinifera] (GB:CAN81152.1); contains InterPro domain Thioredoxin-like fold (InterPro:IPR012336)
2.11	AT4G13390	proline-rich extensin-like family protein
2.11	AT3G45660;AT3G45650	[AT3G45660, proton-dependent oligopeptide transport (POT) family protein];[AT3G45650, NAXT1 (NITRATE EXCRETION TRANSPORTER1); nitrate efflux transmembrane transporter/ transporter]
2.11	AT2G20750	ATEXPB1 (ARABIDOPSIS THALIANA EXPANSIN B1)
2.11	AT2G35000	zinc finger (C3HC4-type RING finger) family protein
2.10	AT1G64780	ATAMT1;2 (AMMONIUM TRANSPORTER 1;2); ammonium transmembrane transporter
2.10	AT2G18010	auxin-responsive family protein
2.09	AT5G55170	SUM3 (SMALL UBIQUITIN-LIKE MODIFIER 3)
2.09	AT5G54270	LHCB3 (LIGHT-HARVESTING CHLOROPHYLL BINDING PROTEIN 3)
2.09	AT2G05540	glycine-rich protein
2.09	AT5G65390	AGP7 (Arabinogalactan protein 7)
2.09	AT1G53830	ATPME2 (Arabidopsis thaliana pectin methylesterase 2)
2.08	AT5G44550	integral membrane family protein
2.08	AT1G22650	beta-fructofuranosidase, putative / invertase, putative / saccharase, putative / beta-fructosidase, putative
2.08	AT5G39860	PRE1 (PACLOBUTRAZOL RESISTANCE1); DNA binding / transcription factor
2.08	AT3G25110	ATFATA (ARABIDOPSIS FATA ACYL-ACP THIOESTERASE); acyl carrier/ acyl-ACP thioesterase
2.07	AT1G69570	Dof-type zinc finger domain-containing protein
2.07	AT2G21200	auxin-responsive protein, putative
2.07	AT1G22740	RAB7 (Ras-related protein 7); GTP binding
2.07	AT3G56360	similar to unknown protein [Arabidopsis thaliana] (TAIR:AT5G05250.1); similar to unnamed protein product [Vitis vinifera] (GB:CAO41488.1)
2.07	AT1G22330	RNA binding
2.07	AT3G45530	DC1 domain-containing protein
2.07	AT5G38010;AT5G37950	[AT5G38010, UDP-glucoronosyl/UDP-glucosyl transferase family protein];[AT5G37950, transferase, transferring hexosyl groups]
2.07	AT1G11545	xyloglucan:xyloglucosyl transferase, putative / xyloglucan endotransglycosylase, putative / endo-xyloglucan transferase, putative
2.06	AT1G19450	integral membrane protein, putative / sugar transporter family protein
2.06	AT5G55050	GDSL-motif lipase/hydrolase family protein
2.06	AT1G78260	RNA recognition motif (RRM)-containing protein
2.06	AT3G48940	remorin family protein
2.06	AT3G51330	aspartyl protease family protein
2.06	AT4G10380	NIP5;1/NLM6/NLM8 (NOD26-like intrinsic protein 5;1); boron transporter/ water channel
2.06	AT4G15400	transferase family protein
2.05	AT2G32380	similar to unknown protein [Arabidopsis thaliana] (TAIR:AT1G05210.1); similar to unnamed protein product [Vitis vinifera] (GB:CAO24140.1); contains InterPro domain Transmembrane protein 97, predicted (InterPro:IPR016964)
2.05	AT3G45070;AT3G45080	[AT3G45070, sulfotransferase family protein];[AT3G45080, sulfotransferase family protein]
2.05	AT5G23840	MD-2-related lipid recognition domain-containing protein / ML domain-containing protein
2.05	AT5G16590	leucine-rich repeat transmembrane protein kinase, putative
2.04	AT3G25790	myb family transcription factor
2.04	AT3G04720	PR4 (PATHOGENESIS-RELATED 4)
2.04	AT2G41290	strictosidine synthase family protein
2.04	AT5G40510	similar to unknown protein [Arabidopsis thaliana] (TAIR:AT3G27570.1); similar to unnamed protein product [Vitis vinifera] (GB:CAO14698.1); contains InterPro domain Thioredoxin-like fold (InterPro:IPR012336); contains InterPro domain Thioredoxin fold (Inte
2.04	AT5G05790	myb family transcription factor
2.04	AT5G07680	ANAC079/ANAC080/ATNAC4 (Arabidopsis NAC domain containing protein 79, Arabidopsis NAC domain containing protein 80); transcription factor
2.04	AT4G01430	nodulin MtN21 family protein
2.04	AT2G28200	nucleic acid binding / transcription factor/ zinc ion binding
2.03	AT5G54020	zinc ion binding
2.03	AT4G32870	similar to unknown protein [Arabidopsis thaliana] (TAIR:AT2G25770.2); similar to unknown protein [Arabidopsis thaliana] (TAIR:AT2G25770.1); similar to unknown [Populus trichocarpa x Populus deltoides] (GB:ABK96434.1); contains domain SSF55961 (SSF55961)
2.03	AT4G22212	Encodes a defensin-like (DEFL) family protein.
2.03	AT4G02850	phenazine biosynthesis PhzC/PhzF family protein
2.03	AT4G24780	pectate lyase family protein
2.02	AT3G57490	40S ribosomal protein S2 (RPS2D)
2.02	AT4G16350	CBL6 (CALCINEURIN B-LIKE PROTEIN 6)
2.02	AT3G03830	auxin-responsive protein, putative
2.02	AT5G01050;AT5G01040	[AT5G01050, laccase family protein / diphenol oxidase family protein];[AT5G01040, LAC8 (laccase 8); copper ion binding / oxidoreductase]
2.02	AT5G60490	FLA12 (fasciclin-like arabinogalactan-protein 12)
2.02	AT1G06640	2-oxoglutarate-dependent dioxygenase, putative
2.02	AT5G35940	jacalin lectin family protein
2.01	AT5G15350	plastocyanin-like domain-containing protein
2.01	AT3G53420	PIP2A (PLASMA MEMBRANE INTRINSIC PROTEIN 2A); water channel
2.01	AT4G12030	bile acid:sodium symporter family protein
2.00	AT1G18940	nodulin family protein
2.00	AT4G16780	ATHB-2 (ARABIDOPSIS THALIANA HOMEOBOX PROTEIN 2); DNA binding / transcription factor
2.00	AT1G62800	ASP4 (ASPARTATE AMINOTRANSFERASE 4); catalytic/ pyridoxal phosphate binding / transaminase/ transferase, transferring nitrogenous groups

Table S4.2 Gene Ontology of AEX regulated genes.

S4.2.1 Gene Ontology of AEX upregulated genes.

Overrepresentation
Selected statistical test : Hypergeometric test
Selected correction : Benjamini & Hochberg False Discovery Rate (FDR) correction
Selected significance level : 0.05
Testing option : Test cluster versus whole annotation
Number of annotated genes in selection : 407

Number of annotated genes in network/whole annotation : 22304

GO-ID	p-value	corr p-value	x	n	Description
50896	0.0000%	0.0000%	130	31.9	response to stimulus
6950	0.0000%	0.0000%	85	20.9	response to stress
42221	0.0000%	0.0000%	82	20.1	response to chemical stimulus
9628	0.0000%	0.0000%	51	12.5	response to abiotic stimulus
10033	0.0000%	0.0023%	43	10.6	response to organic substance
19748	0.0000%	0.0000%	37	9.1	secondary metabolic process
9056	0.0000%	0.0001%	35	8.6	catabolic process
51704	0.0000%	0.0010%	34	8.4	multi-organism process
9607	0.0000%	0.0000%	33	8.1	response to biotic stimulus
51707	0.0000%	0.0000%	32	7.9	response to other organism
44248	0.0000%	0.0001%	30	7.4	cellular catabolic process
6952	0.0002%	0.0099%	30	7.4	defense response
6355	0.0997%	1.6560%	28	6.9	regulation of transcription, DNA-dependent
51252	0.1054%	1.6996%	28	6.9	regulation of RNA metabolic process
9266	0.0000%	0.0000%	26	6.4	response to temperature stimulus
9743	0.0000%	0.0000%	22	5.4	response to carbohydrate stimulus
6970	0.0003%	0.0119%	22	5.4	response to osmotic stress
9651	0.0003%	0.0123%	21	5.2	response to salt stress
10035	0.0055%	0.1623%	21	5.2	response to inorganic substance
10200	0.0000%	0.0000%	20	4.9	response to chitin
6979	0.0000%	0.0002%	20	4.9	response to oxidative stress
6725	0.0001%	0.0026%	20	4.9	cellular aromatic compound metabolic process
9404	0.0000%	0.0000%	19	4.7	toxin metabolic process
9407	0.0000%	0.0000%	19	4.7	toxin catabolic process
10038	0.0026%	0.0854%	19	4.7	response to metal ion
6519	0.1530%	2.2773%	19	4.7	cellular amino acid and derivative metabolic process
46483	0.0188%	0.4219%	17	4.2	heterocycle metabolic process
9409	0.0010%	0.0337%	16	3.9	response to cold
9617	0.0010%	0.0337%	16	3.9	response to bacterium
46686	0.0205%	0.4401%	15	3.7	response to cadmium ion
42742	0.0058%	0.1623%	13	3.2	defense response to bacterium
2376	0.2222%	2.9150%	13	3.2	immune system process
19438	0.0105%	0.2772%	12	2.9	aromatic compound biosynthetic process
6575	0.1164%	1.8393%	12	2.9	cellular amino acid derivative metabolic process
9408	0.0029%	0.0904%	11	2.7	response to heat
6790	0.0246%	0.5144%	11	2.7	sulfur metabolic process
42398	0.1224%	1.8950%	10	2.5	cellular amino acid derivative biosynthetic process
34637	0.1336%	2.0277%	10	2.5	cellular carbohydrate biosynthetic process
9698	0.0764%	1.4426%	9	2.2	phenylpropanoid metabolic process
7568	0.0126%	0.2954%	8	2.0	aging
16137	0.0191%	0.4219%	8	2.0	glycoside metabolic process
9699	0.0643%	1.2445%	8	2.0	phenylpropanoid biosynthetic process
9611	0.3104%	3.8752%	8	2.0	response to wounding
16138	0.0107%	0.2772%	7	1.7	glycoside biosynthetic process
6767	0.0287%	0.5844%	6	1.5	water-soluble vitamin metabolic process
6766	0.1006%	1.6560%	6	1.5	vitamin metabolic process
70482	0.0511%	1.0145%	4	1.0	response to oxygen levels
10150	0.1581%	2.3093%	4	1.0	leaf senescence
10260	0.1808%	2.5917%	4	1.0	organ senescence
46351	0.2328%	3.0027%	4	1.0	disaccharide biosynthetic process
9312	0.3658%	4.4238%	4	1.0	oligosaccharide biosynthetic process
10345	0.0059%	0.1623%	3	0.7	suberin biosynthetic process
6772	0.0116%	0.2801%	3	0.7	thiamin metabolic process
42723	0.0116%	0.2801%	3	0.7	thiamin and derivative metabolic process
6536	0.1890%	2.5958%	3	0.7	glutamate metabolic process
9646	0.1890%	2.5958%	3	0.7	response to absence of light
10286	0.2831%	3.5914%	3	0.7	heat acclimation
9636	0.3391%	4.1659%	3	0.7	response to toxin
46655	0.0984%	1.6560%	2	0.5	folic acid metabolic process
16098	0.0984%	1.6560%	2	0.5	monoterpenoid metabolic process
16099	0.0984%	1.6560%	2	0.5	monoterpenoid biosynthetic process
46482	0.0984%	1.6560%	2	0.5	para-aminobenzoic acid metabolic process
52546	0.1945%	2.5958%	2	0.5	cell wall pectin metabolic process
9759	0.1945%	2.5958%	2	0.5	indole glucosinolate biosynthetic process

S4.2.2 Gene Ontology of AEX downregulated genes.

GO-ID	p-value	corr p-value	x	n	Description
42221	6,62E-18	4,41E-15	94	1710,0	response to chemical stimulus
50896	1,66E-17	5,53E-15	139	3207,0	response to stimulus
71555	1,44E-15	3,19E-13	26	165,0	cell wall organization
9733	7,43E-14	1,24E-11	31	282,0	response to auxin stimulus
71554	3,33E-13	4,43E-11	29	260,0	cell wall organization or biogenesis
9664	5,10E-13	5,66E-11	17	78,0	plant-type cell wall organization
9725	6,93E-12	6,59E-10	49	767,0	response to hormone stimulus
9719	1,31E-11	1,09E-09	51	835,0	response to endogenous stimulus
42545	2,42E-10	1,79E-08	18	128,0	cell wall modification
10033	1,14E-09	7,62E-08	54	1037,0	response to organic substance
6810	2,44E-09	1,48E-07	68	1502,0	transport
71669	2,71E-09	1,50E-07	17	131,0	plant-type cell wall organization or biogenesis
51234	3,37E-09	1,73E-07	68	1514,0	establishment of localization
15698	4,90E-09	2,33E-07	11	49,0	inorganic anion transport
19748	1,11E-08	4,95E-07	26	330,0	secondary metabolic process
51179	1,30E-08	5,41E-07	68	1566,0	localization
6820	1,50E-08	5,88E-07	12	67,0	anion transport
6979	1,70E-08	6,30E-07	22	247,0	response to oxidative stress
10683	2,00E-07	7,00E-06	4	4,0	tricyclic triterpenoid metabolic process
6950	3,79E-07	1,26E-05	72	1853,0	response to stress
6811	4,14E-07	1,31E-05	24	345,0	ion transport
9827	4,41E-07	1,34E-05	9	46,0	plant-type cell wall modification
9828	5,49E-07	1,59E-05	8	35,0	plant-type cell wall loosening
6833	9,69E-07	2,58E-05	5	10,0	water transport
42044	9,69E-07	2,58E-05	5	10,0	fluid transport
6869	1,35E-06	3,46E-05	14	137,0	lipid transport

9735	2,77E-06	6,83E-05	10	72,0	response to cytokinin stimulus
10876	5,01E-06	1,19E-04	14	153,0	lipid localization
6817	7,18E-06	1,65E-04	5	14,0	phosphate transport
80003	9,48E-06	2,08E-04	3	3,0	thalianol metabolic process
6575	9,70E-06	2,08E-04	17	231,0	cellular amino acid derivative metabolic process
9698	2,72E-05	5,66E-04	12	133,0	phenylpropanoid metabolic process
9826	3,00E-05	5,88E-04	14	179,0	unidimensional cell growth
60560	3,00E-05	5,88E-04	14	179,0	developmental growth involved in morphogenesis
30418	3,73E-05	6,75E-04	3	4,0	nicotianamine biosynthetic process
30417	3,73E-05	6,75E-04	3	4,0	nicotianamine metabolic process
16138	3,75E-05	6,75E-04	8	60,0	glycoside biosynthetic process
16049	5,86E-05	1,03E-03	16	240,0	cell growth
15695	9,18E-05	1,53E-03	3	5,0	organic cation transport
15696	9,18E-05	1,53E-03	3	5,0	ammonium transport
16137	9,54E-05	1,55E-03	9	87,0	glycoside metabolic process
8361	1,14E-04	1,77E-03	16	254,0	regulation of cell size
48589	1,17E-04	1,77E-03	14	203,0	developmental growth
32535	1,19E-04	1,77E-03	16	255,0	regulation of cellular component size
90066	1,19E-04	1,77E-03	16	255,0	regulation of anatomical structure size
44262	1,35E-04	1,96E-03	22	428,0	cellular carbohydrate metabolic process
9736	1,59E-04	2,20E-03	6	39,0	cytokinin mediated signaling pathway
71368	1,59E-04	2,20E-03	6	39,0	cellular response to cytokinin stimulus
6722	1,69E-04	2,29E-03	4	14,0	triterpenoid metabolic process
902	1,84E-04	2,45E-03	15	238,0	cell morphogenesis
9831	1,91E-04	2,50E-03	5	26,0	plant-type cell wall modification involved in multidimensional cell growth
6970	2,60E-04	3,33E-03	20	388,0	response to osmotic stress
42547	2,76E-04	3,47E-03	5	28,0	cell wall modification involved in multidimensional cell growth
42398	3,03E-04	3,73E-03	12	171,0	cellular amino acid derivative biosynthetic process
9808	3,14E-04	3,80E-03	6	44,0	lignin metabolic process
40007	3,31E-04	3,94E-03	16	279,0	growth
16143	3,56E-04	4,02E-03	6	45,0	S-glycoside metabolic process
19757	3,56E-04	4,02E-03	6	45,0	glycosinolate metabolic process
19760	3,56E-04	4,02E-03	6	45,0	glucosinolate metabolic process
16144	3,86E-04	4,15E-03	5	30,0	S-glycoside biosynthetic process
19758	3,86E-04	4,15E-03	5	30,0	glycosinolate biosynthetic process
19761	3,86E-04	4,15E-03	5	30,0	glucosinolate biosynthetic process
9769	4,49E-04	4,67E-03	2	2,0	photosynthesis, light harvesting in photosystem II
10263	4,49E-04	4,67E-03	2	2,0	tricyclic triterpenoid biosynthetic process
32989	4,73E-04	4,84E-03	15	260,0	cellular component morphogenesis
15833	5,86E-04	5,83E-03	7	68,0	peptide transport
6857	5,86E-04	5,83E-03	7	68,0	oligopeptide transport
6725	6,31E-04	6,18E-03	16	296,0	cellular aromatic compound metabolic process
9098	7,24E-04	6,99E-03	3	9,0	leucine biosynthetic process
9651	7,41E-04	7,05E-03	18	360,0	response to salt stress
9765	8,97E-04	8,42E-03	4	21,0	photosynthesis, light harvesting
48869	1,09E-03	1,01E-02	20	435,0	cellular developmental process
15700	1,33E-03	1,18E-02	2	3,0	arsenite transport
22622	1,33E-03	1,18E-02	13	230,0	root system development
48364	1,33E-03	1,18E-02	13	230,0	root development
9696	1,38E-03	1,21E-02	3	11,0	salicylic acid metabolic process
6519	1,64E-03	1,42E-02	21	483,0	cellular amino acid and derivative metabolic process
10218	1,68E-03	1,42E-02	5	41,0	response to far red light
9699	1,68E-03	1,42E-02	8	104,0	phenylpropanoid biosynthetic process
46271	1,81E-03	1,49E-02	3	12,0	phenylpropanoid catabolic process
46274	1,81E-03	1,49E-02	3	12,0	lignin catabolic process
9628	2,03E-03	1,65E-02	40	1168,0	response to abiotic stimulus
6073	2,14E-03	1,71E-02	8	108,0	cellular glucan metabolic process
9639	2,15E-03	1,71E-02	10	159,0	response to red or far red light
10054	2,31E-03	1,75E-02	5	44,0	trichoblast differentiation
6551	2,31E-03	1,75E-02	3	13,0	leucine metabolic process
9082	2,31E-03	1,75E-02	3	13,0	branched chain family amino acid biosynthetic process
6829	2,31E-03	1,75E-02	3	13,0	zinc ion transport
44042	2,54E-03	1,89E-02	8	111,0	glucan metabolic process
65008	2,57E-03	1,89E-02	23	569,0	regulation of biological quality
46713	2,62E-03	1,89E-02	2	4,0	boron transport
15840	2,62E-03	1,89E-02	2	4,0	urea transport
9825	2,81E-03	2,02E-02	5	46,0	multidimensional cell growth
31669	2,99E-03	2,12E-02	8	114,0	cellular response to nutrient levels
34637	3,95E-03	2,77E-02	10	173,0	cellular carbohydrate biosynthetic process
41	4,06E-03	2,82E-02	5	50,0	transition metal ion transport
42886	4,30E-03	2,91E-02	2	5,0	amide transport
9806	4,32E-03	2,91E-02	3	16,0	lignan metabolic process
9807	4,32E-03	2,91E-02	3	16,0	lignan biosynthetic process
10015	5,15E-03	3,39E-02	7	99,0	root morphogenesis
5975	5,15E-03	3,39E-02	28	782,0	carbohydrate metabolic process
10053	5,22E-03	3,41E-02	5	53,0	root epidermal cell differentiation
9267	5,44E-03	3,51E-02	7	100,0	cellular response to starvation
31667	5,49E-03	3,51E-02	8	126,0	response to nutrient levels
10114	5,66E-03	3,59E-02	5	54,0	response to red light
71496	6,03E-03	3,75E-02	8	128,0	cellular response to external stimulus
31668	6,03E-03	3,75E-02	8	128,0	cellular response to extracellular stimulus
55071	6,36E-03	3,92E-02	2	6,0	manganese ion homeostasis
16036	7,06E-03	4,32E-02	6	80,0	cellular response to phosphate starvation
19439	7,13E-03	4,32E-02	3	19,0	aromatic compound catabolic process
9653	7,29E-03	4,38E-02	20	515,0	anatomical structure morphogenesis
42594	7,43E-03	4,42E-02	7	106,0	response to starvation
30001	8,16E-03	4,81E-02	9	163,0	metal ion transport
10167	8,26E-03	4,83E-02	3	20,0	response to nitrate

Table S4.3a Common genes regulated by H_2O_2 (Davletova et al., 2005) and AEX arrays.

Both up		Both down		H_2O_2 up; AEX down		H_2O_2 down; AEX up	
Locus Identifier	Fold change by AEX	Locus Identifier	Fold change by AEX	Locus Identifier	Fold change by AEX	Locus Identifier	Fold change by AEX
AT5G43450	34,00805	AT5G15410	2,409806	AT2G47140	3,33	AT3G03640	3,74
AT1G05680	29,96288	AT5G35190	8,393576				
AT1G26380	26,17857	AT5G67400	9,761633				
AT4G37370	26,13531	AT5G57530	8,120114				
AT2G26560	13,02983	AT5G17820	3,996951				
AT1G19020	12,60482	AT5G05500	11,14788				
AT1G05560	12,45354	AT3G62680	6,651526				
AT1G17180	12,33943	AT3G49960	13,27241				
AT5G20230	12,32844	AT4G40090	6,087381				
AT2G41730	12,06707	AT4G38840	3,184381				
AT2G36790	11,91	AT4G34760	3,678905				
AT1G17170	11,54628	AT4G28780	2,815687				
AT2G15490	9,321896	AT4G26010	5,488444				
AT5G27420	8,279529	AT4G25820	4,91226				
AT1G33110	7,533786	AT4G02270	16,53492				
AT2G04040	7,348355	AT4G01480	4,110563				
AT2G15480	7,345507	AT3G27170	3,78134				
AT1G69930	7,251075	AT3G21770	4,552816				
AT5G05410	7,086321	AT3G29030	2,549143				
AT3G25610	7,011341	AT3G25930	3,372421				
AT5G66650	6,987357	AT3G23430	3,888098				
AT2G02010	6,97	AT3G16440	2,774661				
AT5G57220	6,922949	AT1G28130	2,78437				
AT2G18690	6,655359	AT1G29510	2,541249				
AT3G28210	6,517797	AT1G29660	2,1308				
AT1G70420	6,359554	AT5G27780	2,897972				
AT5G25930	6,334515	AT1G32450	7,226766				
AT5G14730	6,329206	AT1G01750	14,9789				
AT3G22370	6,162165	AT1G70850	3,755229				
AT5G48540	5,802389	AT1G47600	3,92764				
AT2G32210	7,83	AT1G05570	2,46618				
AT5G59820	5,6249	AT2G21210	8,208314				
AT2G39400	5,601517	AT1G05240	6,058548				
AT3G14690	5,410565	AT1G52050	3,422557				
AT1G30700	5,35801	AT1G52070	2,995116				
AT2G40350	5,308155	AT1G30870	12,50819				
AT3G50930	5,26329	AT2G46690	2,460113				
AT5G22300	5,258777						
AT2G31945	5,222011						
AT5G14470	5,189917						
AT3G16530	5,187019						
AT5G17860	5,106164						
AT3G04640	5,077563						
AT5G54490	4,85172						
AT5G13750	4,84879						
AT5G64510	4,842711						
AT1G76690	4,823607						
AT4G34135	4,778615						
AT4G01870	4,766183						
AT5G39050	4,75355						
AT1G59590	4,742064						
AT5G10695	4,734571						
AT1G68620	4,72083						
AT1G02920	4,70						
AT5G64250	4,692004						
AT2G34500	4,659238						
AT1G10170	4,570101						
AT3G02800	4,537944						
AT3G10500	4,481702						
AT2G36220	4,37525						
AT3G47340	4,372833						
AT3G13310	4,26453						
AT5G51440	4,246348						
AT3G44190	4,16832						
AT1G76600	4,164876						
AT3G63380	4,151057						
AT5G51830	4,084656						
AT2G16900	4,063667						
AT4G18880	3,97117						
AT3G08970	3,926826						
AT1G08050	3,91131						
AT2G44460	3,776494						
AT5G61820	3,755391						
AT2G29490	3,716956						
AT1G60730	3,683736						
AT4G23700	3,625625						
AT1G63720	3,588413						
AT5G18470	3,577789						
AT4G18950	3,520979						
AT2G41380	3,509766						
AT2G41230	3,418452						
AT3G06500	3,414645						
AT4G20830	3,383598						
AT2G29420	3,290329						
AT5G49690	3,284615						
AT2G30140	3,248165						
AT5G55970	3,227115						
AT5G07440	3,204373						
AT5G06860	3,202393						
AT1G55850	3,154988						

AT3G10930	3,133563						
AT4G02520	3,12						
AT5G35735	3,112746						
AT5G52640	3,096245						
AT2G38470	3,074734						
AT3G54150	3,024353						
AT5G63790	2,977165						
AT1G15040	2,976601						
AT5G49450	2,97						
AT4G36040	2,964479						
AT2G27830	2,929859						
AT2G33710	2,86691						
AT3G56710	2,854434						
AT1G77450	2,849998						
AT3G14990	2,81379						
AT1G56060	2,801486						
AT4G15530	2,780025						
AT5G47230	2,71127						
AT2G41100	2,704244						
AT4G19880	2,691797						
AT2G18700	2,689123						
AT4G17490	2,668948						
AT2G24500	2,658216						
AT2G23320	2,611668						
AT5G04340	2,586615						
AT1G07160	2,571236						
AT5G07870	2,566933						
AT1G72900	2,561898						
AT1G01720	2,548682						
AT4G24160	2,524533						
AT4G39670	2,524076						
AT1G08940	2,523349						
AT2G22880	2,49898						
AT1G76070	2,493763						
AT1G25400	2,491211						
AT5G27760	2,483243						
AT3G02840	2,47593						
AT4G23190	2,442299						
AT5G54500	2,424111						
AT5G15870	2,42293						
AT2G40140	2,406077						
AT3G05360	2,386498						
AT3G15500	2,362982						
AT1G72680	2,34107						
AT1G21680	2,337223						
AT1G69490	2,334805						
AT5G13190	2,330748						
AT2G41640	2,32474						
AT2G44750	2,30						
AT1G66090	2,29856						
AT4G15550	2,294576						
AT1G18570	2,280284						
AT5G42050	2,274629						
AT1G17860	2,274435						
AT2G40000	2,273482						
AT1G12200	2,272505						
AT3G08760	2,271596						
AT2G32030	2,271274						
AT2G36950	2,261654						
AT5G59540	2,259682						
AT3G10985	2,246102						
AT4G34710	2,244024						
AT5G65300	2,219013						
AT3G26910	2,212026						
AT1G78820	2,166723						
AT1G69920	2,152149						
AT1G33590	2,136023						
AT4G17500	2,133662						
AT2G19450	2,129808						
AT1G18390	2,128038						
AT1G76590	2,117753						
AT5G48180	2,112867						
AT2G37430	2,10015						
AT4G40080	2,092187						
AT3G49530	2,088085						
AT5G16970	2,079199						
AT3G46600	2,076789						
AT3G18290	2,05978						
AT3G05200	2,057619						
AT1G03905	2,055657						
AT1G67810	2,054956						
AT3G60420	2,036224						
AT2G47730	2,035378						
AT3G51890	2,025061						
AT4G15420	2,01875						
AT4G13180	2,015187						
AT3G12740	2,015043						
AT1G33600	2,014029						
AT4G01250	2,011146						

Table S4.3b Common genes of UPB1 (Tsukagoshi et al., 2010) and AEX arrays.

Both up		Both down		UPB1 down; AEX up		UPB1 up; AEX down	
Locus Identifier	Fold change by AEX	Locus Identifier	Fold change by AEX	Locus Identifier	Fold change by AEX	Locus Identifier	Fold change by AEX
AT1G05680	299.629	AT5G60520	727.953	AT2G47890	8.880.054	AT5G04960	1.812.089
AT1G05560	124.535	AT1G73620	6.661.939	AT5G40690	6.974.673	AT4G02270	1.653.492
AT1G17170	115.463	AT5G10130	5.096.737	AT3G49780	5.643.116	AT1G01750	149.789
AT2G32020	999.172	AT1G49860	3.771.899	AT2G45170	5.267.826	AT3G49960	1.327.241
AT2G15490	93.219	AT5G01870	2.803.485	AT2G34500	4.659.238	AT1G30870	1.250.819
AT1G33110	753.379	AT5G56080	2.700.594	AT4G20860	4.499.038	AT4G00680	1.229.947
AT2G04040	734.835	AT1G56430	2.595.659	AT2G35730	4.286.918	AT5G57540	1.121.536
AT1G69930	725.108	AT1G05570	246.618	AT4G15610	4.134.974	AT5G05500	1.114.788
AT5G66650	698.736	AT3G27950	2.392.927	AT5G04120	3.674.614	AT1G62980	1.087.784
AT2G18690	665.536	AT2G29330	2.277.069	AT3G14660	3.361.632	AT2G32270	1.078.268
AT5G48540	580.239	AT3G12830	2.260.421	AT4G17215	3.297.463	AT4G17340	1.067.898
AT4G28460	562.801	AT1G80830	2.190.571	AT5G24800	3.070.696	AT4G30170	1.054.637
AT5G22300	525.878	AT2G43600	2.180.487	AT1G15040	2.976.601	AT1G13300	1.024.081
AT2G43500	488.362	AT3G47380	2.155.494	AT4G37010	2.926.215	AT5G67400	9.761.633
AT5G54490	485.172	AT3G56360	2.071.636	AT2G43820	2.875.695	AT5G47450	9.075.362
AT5G13750	484.879	AT2G41290	2.04	AT2G33710	286.691	AT1G13420	8.394.669
AT4G01870	476.618	AT3G57490	2.02	AT3G07870	279.956	AT5G35190	8.393.576
AT5G39050	475.355			AT1G71530	2.749.549	AT5G22410	8.236.645
AT1G59590	474.206			AT5G05600	2.588.657	AT5G57530	8.120.114
AT5G64250	4.692			AT1G76070	2.493.763	AT2G18980	8.092.067
AT1G76600	416.488			AT3G25655	248.342	AT3G46280	8.016.825
AT5G51830	408.466			AT1G56300	2.342.804	AT1G12560	799.871
AT1G76520	398.868			AT2G16365	2.285.803	AT1G48930	7.749.719
AT4G33070	383.604			AT1G74055	2.269.884	AT1G54970	7.495.222
AT4G20070	376.846			AT3G10985	2.246.102	AT2G47540	7.133.414
AT1G02850	376.287			AT4G11360	2.139.897	AT2G45220	6.806.489
AT2G29490	371.696			AT5G41040	2.115.533	AT2G37130	6.728.649
AT3G16150	32.858			AT3G19390	2.074.089	AT3G62680	6.651.526
AT2G30140	324.817			AT5G54960	2.054.854	AT1G72200	6.555.094
AT1G55850	315.499			AT4G33980	2.048.472	AT5G24313	6.470.893
AT3G10930	313.356			AT1G60940	203.054	AT4G12550	6.467.085
AT4G03320	311.326			AT5G03240	2.018.854	AT4G31320	6.381.686
AT1G02220	302.522					AT3G10710	6.310.711
AT2G39350	299.964					AT5G53250	6.146.939
AT1G30420;AT 1G30410	2.89					AT2G39040	6.136.227
AT5G20400	272.982					AT4G40090	6.087.381
AT2G41100	270.424					AT3G01190	6.026.537
AT4G36580	26.281					AT1G22500	596.161
AT2G23320	261.167					AT1G33700	5.673.796
AT4G27940	259.233					AT4G30320	5.667.317
AT5G07860	255.667					AT4G25250	5.603.762
AT5G51130	242.034					AT2G03720	5.577.829
AT1G72680	234.107					AT2G25810	5.573.719
AT4G15550	229.458					AT4G26010	5.488.444
AT1G74750	228.329					AT4G11210	5.050.452
AT5G19440	221.262					AT4G25820	491.226
AT5G24270	21.881					AT3G45710	4.851.185
AT2G24180	215.366					AT4G33730	4.840.618
AT5G48180	211.287					AT2G30930	4.733.776
AT5G16930	209.915					AT1G14960	4.657.646
AT1G67810	205.496					AT5G42590	4.638.857
AT1G33420	202.124					AT2G21880	4.629.297
AT5G03490	201.471					AT4G34580	4.573.425

Table S4.3c Common genes of IAA (global analysis of Zhao et al., 2003; Okushima et al., 2005b and Nemhauser et al., 2006)and AEX arrays.

Both up		Both down		IAA down; AEX up		IAA up; AEX down	
Locus Identifier	Fold change by AEX	Locus Identifier	Fold change by AEX	Locus Identifier	Fold change by AEX	Locus Identifier	Fold change by AEX
AT5G43450	3.400.805	AT3G01260	131.395	AT2G44130	3.15	AT2G18980	8.092.067
AT1G26380	2.617.857	AT5G47450	9.075.362			AT1G30760	5.068.457
AT2G26560	1.302.983	AT1G13420	8.394.669			AT1G10550	4.309.986
AT1G19020	1.260.482	AT5G35190	8.393.576			AT1G52830	381.517
AT3G01970	1.243.396	AT5G60520	727.953			AT5G18060	3.754.601
AT1G17180	1.233.943	AT1G32450	7.226.766			AT2G47550	3.690.508
AT2G41730	1.206.707	AT1G72200	6.555.094			AT3G03840	3.682.571
AT1G17170	1.154.628	AT5G53250	6.146.939			AT4G34760	3.678.905
AT2G32020	9.991.721	AT3G01190	6.026.537			AT1G22880	3.573.156
AT2G15490	9.321.896	AT2G30930	4.733.776			AT2G47140	3.329.463
AT5G27420	8.279.529	AT2G21880	4.629.297			AT3G14060	326.159
AT2G32210	7.831.177	AT1G66270	4.440.609			AT2G21220	3.127.905
AT1G69930	7.251.075	AT1G66280	4.440.609			AT1G29430	2.897.972
AT5G57220	6.922.949	AT5G56540	4.376.875			AT5G27780	2.897.972
AT2G18690	6.655.359	AT1G67110	4.311.062			AT1G29500	2.840.505
AT5G25930	6.334.515	AT5G60660	3.879.964			AT1G19540	2.722.075
AT2G32190	5.647.832	AT3G06460	3.869.924			AT1G72230	2.622.228
AT5G59820	56.249	AT1G53680	3.663.585			AT1G29510	2.541.249
AT1G30700	535.801	AT2G39530	3.606.226			AT4G36110	2.539.438

AT4G37290	5.279.267	AT3G24290	3.518.609			AT1G65310	2.517.426
AT3G50930	526.329	AT3G24300	3.518.609			AT3G25780	2.391.739
AT5G54490	485.172	AT2G28780	3.502.798			AT3G42800	2.378.962
AT1G43910	4.746.699	AT5G15830	3.492.437			AT1G29450	2.348.078
AT5G10695	4.734.571	AT1G14220	3.151.278			AT3G18560	2.280.118
AT1G68620	472.083	AT5G46890	2.809.393			AT1G74660	2.250.574
AT1G02920	4.699.092	AT5G46900	2.809.393			AT3G23470	2.243.092
AT1G02930	4.699.092	AT1G31770	2.773.907			AT4G38860	2.235.151
AT5G64250	4.692.004	AT1G23205	2.681.152			AT5G64100	2.222.898
AT2G36220	437.525	AT3G29030	2.549.143			AT3G24450	2.188.762
AT2G41380	3.509.766	AT1G68520	2.430.204			AT4G34770	2.173.531
AT2G41230	3.418.452	AT1G76240	2.337.793			AT1G29660	21.308
AT1G23730	3.407.029	AT2G42850	225.157			AT1G29440	2.128.984
AT4G20830	3.383.598	AT4G15290	2.203.972			AT2G18010	2.101.789
AT2G30140	3.248.165	AT1G78260	2.063.815			AT1G69570	2.074.144
AT5G06860	3.202.393					AT2G21200	2.074.105
AT3G26470	3.189.936					AT1G11545	206.551
AT3G10930	3.133.563					AT5G55050	2.064.356
AT5G57910	3.125.789					AT3G03830	2.017.982
AT2G38470	3.074.734						
AT2G39350	2.999.644						
AT5G63790	2.977.165						
AT1G14540	281.319						
AT1G56060	2.801.486						
AT5G47230	271.127						
AT2G41100	2.704.244						
AT4G17490	2.668.948						
AT5G04340	2.586.615						
AT2G35770	2.564.779						
AT5G64260	2.525.542						
AT4G24160	2.524.533						
AT2G43570	2.523.606						
AT2G22880	249.898						
AT5G54500	2.424.111						
AT2G40140	2.406.077						
AT5G13190	2.330.748						
AT2G41640	232.474						
AT4G15550	2.294.576						
AT2G40000	2.273.482						
AT2G32030	2.271.274						
AT3G09270	2.232.383						
AT5G65300	2.219.013						
AT5G24270	2.188.097						
AT1G69920	2.152.149						
AT5G48180	2.112.867						
AT1G67810	2.054.956						
AT2G32560	2.046.579						
AT1G04310	2.030.635						
AT4G13180	2.015.187						

Table S4.3d Common genes of Ethylene (global analysis of Alonso et al., 2003 and Olmedo et al., 2006) and AEX arrays.

Both up		Both down		Ethylene down; AEX up		Ethylene up; AEX down	
Locus Identifier	Fold change by AEX	Locus Identifier	Fold change by AEX	Locus Identifier	Fold change by AEX	Locus Identifier	Fold change by AEX
AT5G54490	4.851719537	AT5G04950	8.375140426	AT3G55090	11.02282496	AT3G49960	13.27241391
AT4G01870	4.766183351	AT5G53250	6.146939171	AT5G12420	8.98360229	AT5G57540	11.21535956
AT4G23700	3.62562476	AT4G25250	5.603762411	AT4G36610	7.951773142	AT5G38930	10.96028331
AT5G18470	3.57778921	AT4G11210	5.050451742	AT5G13580	4.19388903	AT5G57530	8.12011366
AT5G49690	3.28461546	AT5G47990	4.667566745	AT5G04120	3.674613918	AT1G54970	7.495221831
AT5G44580	2.987395088	AT5G42590	4.638857123	AT5G09530	3.574452	AT5G19890	5.666868724
AT5G39610	2.398169845	AT4G26320	4.525000531	AT5G13900	3.138871693	AT4G26220	4.450488104
AT4G15550	2.294576012	AT5G48000	4.262218963	AT5G66780	2.947224221	AT1G19900	3.932319483
AT5G59540	2.259681796	AT4G21850	3.805914004	AT5G23190	2.570183859	AT2G47550	3.690508263
AT4G31610	2.034856759	AT5G18060	3.754600887	AT5G63970	2.215407906	AT4G19680	3.148607592
AT5G15720	2.009158718	AT4G04840	3.732700189	AT5G41040	2.11553295	AT1G18100	2.359285208
AT4G37580	2.000584207	AT4G34760	3.678905225			AT4G13390	2.10640546
		AT4G22610	3.630062182				
		AT4G33790	3.546849693				
		AT5G15830	3.49243656				
		AT3G59370	3.283120273				
		AT5G03120	3.184446687				
		AT4G38840	3.184380595				
		AT3G50640	3.096851947				
		AT5G19970	3.025821621				
		AT4G02130	3.014002687				
		AT5G47950	2.946772148				
		AT1G66800	2.843381694				

		AT3G31415	2.665287882				
		AT5G47980	2.565298716				
		AT5G48010	2.464730476				
		AT4G19030	2.458113648				
		AT4G01140	2.341043217				
		AT5G23750	2.32053352				
		AT5G24100	2.312452185				
		AT1G18140	2.292965182				
		AT4G15290	2.203971641				
		AT4G11820	2.114254318				
		AT5G39860	2.079331398				
		AT1G22330	2.069533413				
		AT3G45530	2.066954181				
		AT3G48940	2.063259087				
		AT4G01430	2.035198776				
		AT5G35940	2.015111871				

Table S4.4 Cell wall related genes which expression decreased by minimal 4-fold after 6 hours AEX treatment.

Classification and Locus Identifier	Description	Fold change
Class III peroxidase		
AT3G49960	peroxidase, putative	13,27
AT1G30870	cationic peroxidase, putative	12,51
AT4G30170	peroxidase, putative	10,55
AT5G67400	peroxidase 73 (PER73) (P73) (PRXR11)	9,76
AT1G34510	peroxidase, putative	8,47
AT5G22410	peroxidase, putative	8,24
AT2G18980	peroxidase, putative	8,09
AT2G37130	peroxidase 21 (PER21) (P21) (PRXR5)	6,73
AT2G38380;AT2G38390	[AT2G38380, peroxidase 22 (PER22) (P22) (PRXEA) / basic peroxidase E];[AT2G38390, peroxidase, putative]	6,15
AT2G39040	peroxidase, putative	6,14
AT1G05250;AT1G05240	[AT1G05250, peroxidase, putative];[AT1G05240, peroxidase, putative]	6,06
AT3G01190	peroxidase 27 (PER27) (P27) (PRXR7)	6,03
AT5G19890	peroxidase, putative	5,67
AT4G26010	peroxidase, putative	5,49
AT1G49570	peroxidase, putative	5,34
AT3G21770	peroxidase 30 (PER30) (P30) (PRXR9)	4,55
AT5G42180	peroxidase 64 (PER64) (P64) (PRXR4)	4,48
AT5G17820	peroxidase 57 (PER57) (P57) (PRXR10)	4,00
Cell wall enzymes		
Xyloglucan endotransglucosylase/hydrolase		
AT5G57540	xyloglucan:xyloglucosyl transferase, putative / xyloglucan endotransglycosylase, putative / endo-xyloglucan transferase, putative	11,22
AT5G57530	xyloglucan:xyloglucosyl transferase, putative / xyloglucan endotransglycosylase, putative / endo-xyloglucan transferase, putative	8,12
AT4G28850	xyloglucan:xyloglucosyl transferase, putative / xyloglucan endotransglycosylase, putative / endo-xyloglucan transferase, putative	7,10
AT4G25820	XTR9 (XYLOGLUCAN ENDOTRANSGLYCOSYLASE 9); hydrolase, acting on glycosyl bonds	4,91
AT1G10550	XTH33 (xyloglucan:xyloglucosyl transferase 33); hydrolase, acting on glycosyl bonds	4,31
Pectin methylesterase		
AT5G04960	pectinesterase family protein	18,12
AT2G45220	pectinesterase family protein	6,81
AT3G10710	pectinesterase family protein	6,31
AT5G62340	invertase/pectin methylesterase inhibitor family protein	6,41
AT4G25250	invertase/pectin methylesterase inhibitor family protein	5,60
Glycosyl Hydrolase		
AT1G48930	ATGH9C1 (ARABIDOPSIS THALIANA GLYCOSYL HYDROLASE 9C1); hydrolase, hydrolyzing O-glycosyl compounds	7,75
AT4G16260	glycosyl hydrolase family 17 protein	5,45
AT1G66280;AT1G66270	[AT1G66280, glycosyl hydrolase family 1 protein];[AT1G66270, beta-glucosidase (PSR3.2)]	4,44
Glycosyltransferase		
AT3G43190	SUS4; UDP-glycosyltransferase/ sucrose synthase/ transferase, transferring glycosyl groups	4,99
AT2G29750	UDP-glucoronosyl/UDP-glucosyl transferase family protein	4,50
Cell wall proteins		
Expansin		
AT1G62980	ATEXPA18 (ARABIDOPSIS THALIANA EXPANSIN A18)	10,88
AT1G12560	ATEXPA7 (ARABIDOPSIS THALIANA EXPANSIN A7)	8,00
Extensin		
AT1G12040	LRX1 (LEUCINE-RICH REPEAT/EXTENSIN 1); protein binding / structural constituent of cell wall	4,25
Proline-rich protein		
AT5G35190	proline-rich extensin-like family protein	8,39
AT1G54970	ATPRP1 (PROLINE-RICH PROTEIN 1); structural constituent of cell wall	7,50
AT3G62680	PRP3 (PROLINE-RICH PROTEIN 3); structural constituent of cell wall	6,65
AT4G02270	pollen Ole e 1 allergen and extensin family protein	16,53
AT5G05500	pollen Ole e 1 allergen and extensin family protein	11,15
AT2G47540	pollen Ole e 1 allergen and extensin family protein	7,13
AT5G10130	pollen Ole e 1 allergen and extensin family protein	5,10
Arabinogalactan-protein		
AT5G53250	AGP22/ATAGP22 (ARABINOGALACTAN PROTEINS 22)	6,15

AT4G40090	AGP3 (ARABINOGALACTAN-PROTEIN 3)	6,09
AT2G20520	FLA6	4,62
AT4G26320	AGP13 (ARABINOGALACTAN PROTEIN 13)	4,53
AT5G44130	FLA13 (FASCICLIN-LIKE ARABINOGALACTAN PROTEIN 13 PRECURSOR)	4,43
AT5G56540	AGP14 (ARABINOGALACTAN PROTEIN 14)	4,38
Others		
AT4G25790	allergen V5/Tpx-1-related family protein	9,24
AT1G24280	G6PD3 (GLUCOSE-6-PHOSPHATE DEHYDROGENASE 3); glucose-6-phosphate dehydrogenase	7,56
AT4G30320	allergen V5/Tpx-1-related family protein	5,67
AT5G24410	glucosamine/galactosamine-6-phosphate isomerase-related	4,43

Table S4.5 The minimal tested concentration (10 or 50 µM) of AEX analogs to induce the apical hook curvature.

Name	Chembridge ID	Chemical Structures	IUPAC	Conc. (µM)*
AEX	6527749	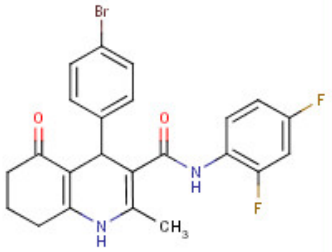	4-(4-bromophenyl)-N-(2,4-difluorophenyl)-2-methyl-5-oxo-1,4,5,6,7,8-hexahydro-3-quinolinecarboxamide	50
A	6514196	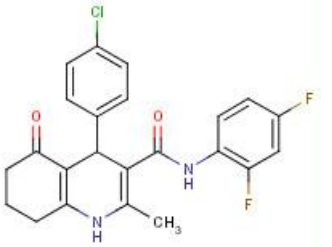	4-(4-chlorophenyl)-N-(2,4-difluorophenyl)-2-methyl-5-oxo-1,4,5,6,7,8-hexahydro-3-quinolinecarboxamide	50
B	6520852	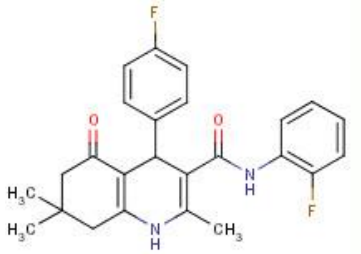	N-(2-fluorophenyl)-4-(4-fluorophenyl)-2,7,7-trimethyl-5-oxo-1,4,5,6,7,8-hexahydro-3-quinolinecarboxamide	50
C	6640029	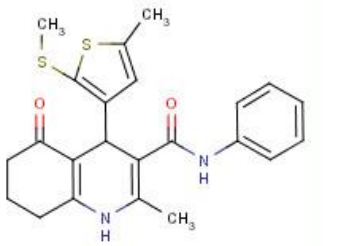	2-methyl-4-[5-methyl-2-(methylthio)-3-thienyl]-5-oxo-N-phenyl-1,4,5,6,7,8-hexahydro-3-quinolinecarboxamide	N/A
D	5754347	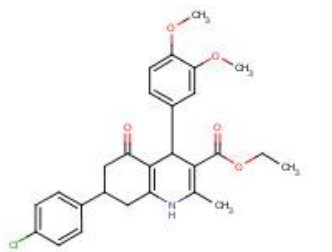	ethyl 7-(4-chlorophenyl)-4-(3,4-dimethoxyphenyl)-2-methyl-5-oxo-1,4,5,6,7,8-hexahydro-3-quinolinecarboxylate	10

E	5712036 (LATCA)	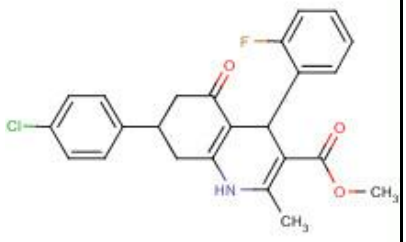	methyl 7-(4-chlorophenyl)-4-(2-fluorophenyl)-2-methyl-5-oxo-1,4,5,6,7,8-hexahydro-3-quinolinecarboxylate	10
F	5473152 (LATCA)	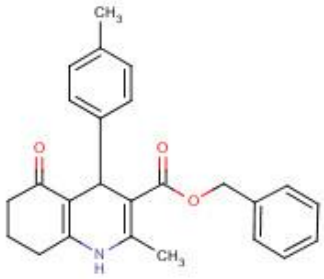	benzyl 2-methyl-4-(4-methylphenyl)-5-oxo-1,4,5,6,7,8-hexahydro-3-quinolinecarboxylate	50
G	5707885 (LATCA)	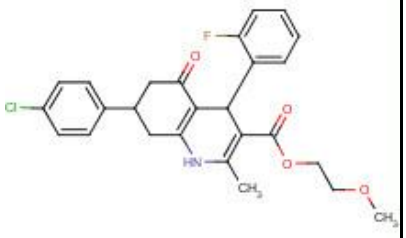	2-methoxyethyl 7-(4-chlorophenyl)-4-(2-fluorophenyl)-2-methyl-5-oxo-1,4,5,6,7,8-hexahydro-3-quinolinecarboxylate	N/A
H	5617132 (LATCA)	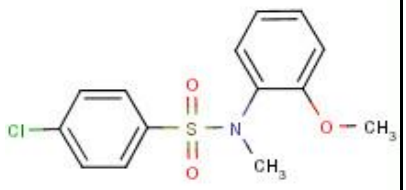	4-chloro-N-(2-methoxyphenyl)-N-methylbenzenesulfonamide	50
I	5601004 (LATCA)	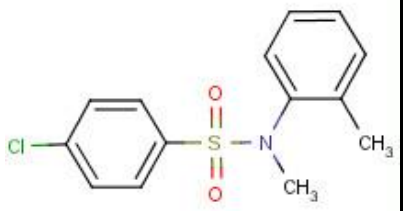	4-chloro-N-methyl-N-(2-methylphenyl)benzenesulfonamide	50

*: The minimal tested concentration (10 or 50 µM) which can induce the apical hook curvature compared to the Col-0 mock treated control

N/A: no effect detected

Table S4.6 Summary of statistical analysis

Figure 4.2a	**Analysis of variance**									
	Scheirer-Ray-Hare extension of Kruskal-Wallis test		**H=SS/MS$_{tot}$**	**df**	**P-value**	**N**				
	Dependent variable: apical hook curvature (ranked data)					256				
	Categorical variables:	Treatment	138.9936	1	4.42E-32					
		Concentration	62.08266	6	1.70E-11					
		Treatment*Concentration	0.008393938	6	1					
	Post-hoc Wilcoxon rank sum (91 pairwise comparisons)		**W statistic**	**P-value**	**Adjusted P-value**	N	**r**	**n_2**	**|Z| score**	**r**
	Group 1	**Group 2**								
	0 µM AEX	25 µM AEX	314	0.01135	1,00000	33	1	15	2.53	0.44
	0 µM AEX	35 µM AEX	264	0.00011	0.00967	29	1	12	3.88	0.72
	0 µM AEX	50 µM AEX	343	2.50E-06	0.00023	31	1	14	4.71	0.85
	ACC + 0 µM AEX	50 µM AEX	214	0.03968	1,00000	40	2	14	2.06	0.33
	ACC + 0 µM AEX	100 µM AEX	284	0.11993	1,00000	38	2	12	1.56	0.25
Figure 4.2a	**Analysis of variance**									
	Scheirer-Ray-Hare extension of Kruskal-Wallis test		**H=SS/MS$_{tot}$**	**df**	**P-value**	**N**				
	Dependent variable: hypocotyl length					353				
	Categorical variables:	Treatment	176.2712	1	3.16E-40					
		Concentration	140.5443	6	7.69E-28					
		Treatment*Concentration	0.520675	6	1.00					
	Post-hoc Wilcoxon rank sum (91 pairwise comparisons)		**W statistic**	**P-value**	**Adjusted P-value**	N	**r**	**n_2**	**|Z| score**	**r**
	Group 1	**Group 2**								
	0 µM AEX	15 µM AEX	556,5	0.02962	1,00000	72	5	20	2.18	0.26
	0 µM AEX	25 µM AEX	214	9.10E-11	8.30E-09	72	5	20	6.48	0.76
	0 µM AEX	50 µM AEX	465	6.20E-14	5.60E-12	82	5	30	7.50	0.83
	ACC + 0 µM AEX	50 µM AEX	941	0.1427	1,00000	70	4	30	1.47	0.18
Figure 4.2c	**Analysis of variance**									
	Scheirer-Ray-Hare extension of Kruskal-Wallis test		**H=SS/MS$_{tot}$**	**df**	**P-value**	**N**				
	Dependent variable: root length					353				
	Categorical variables:	Treatment	222.5015	1	2.57E-50					
		Concentration	95.11185	6	2.62E-18					
		Treatment*Concentration	0.5868523	6	1.00					
	Post-hoc Wilcoxon rank sum (91 pairwise comparisons)		**W statistic**	**P-value**	**Adjusted P-value**	**N**	**r**	**n_2**	**|Z| score**	**r**
	Group 1	**Group 2**								
	0 µM AEX	15 µM AEX	366.5	5.00E-06	0.0046	72	5	20	4.56	0.54
	0 µM AEX	25 µM AEX	210	6.50E-11	5.90E-09	72	5	20	6.53	0.77
	0 µM AEX	35 µM AEX	231	3.00E-11	2.70E-09	73	5	21	6.65	0.78
	0 µM AEX	50 µM AEX	465	6.20E-14	5.60E-12	82	5	20	7.50	0.83
	ACC + 0 µM AEX	50 µM AEX	1494.5	3.50E-07	3.20E-05	70	4	30	5.09	0.61
	ACC + 0 µM AEX	100 µM AEX	133	0.00048	0.04336	51	4	11	3.49	0.49
Figure 4.3a	**Analysis of variance**									
	Kruskal-Wallis rank sum test		**χ^2**	**df**	**P-value**	**N**				
	Dependent variable: hypocotyl length		79.293	3	2.20E-16	90				
	Categorical variable: treatment									
	Post-hoc Wilcoxon rank sum (6 pairwise comparisons)		**W statistic**	**P-value**	**Adjusted P-value**	**N**	**r**	**n_2**	**|Z| score**	**r**
	Group 1	**Group 2**								
	CTRL	ACC	684	8.20E-13	4.90E-12	45	1	26	5.66	0.84
	CTRL	AEX	665	2.00E-08	1.20E-07	44	1	25	5.62	0.85
	CTRL	ACC+AEX	570	1.00E-07	6.00E-07	39	1	20	5.33	0.85
	ACC	AEX	918.5	4.40E-07	2.70E-06	51	2	25	5.05	0.71
	ACC	ACC+AEX	210	8.90E-09	5.30E-08	46	2	20	5.75	0.85
	AEX	ACC+AEX	210	1.20E-08	7.20E-08	45	2	20	5.70	0.85
Figure 4.3b	**Analysis of variance**									
	Kruskal-Wallis rank sum test		**χ^2**	**df**	**P-value**	**N**				
	Dependent variable: cell length		47.082	3	3.34E-10	61				
	Categorical variable: treatment									
	Post-hoc Wilcoxon rank sum (6 pairwise comparisons)		**W statistic**	**P-value**	**Adjusted P-value**	**N**	**r**	**n_2**	**|Z| score**	**r**
	Group 1	**Group 2**								
	CTRL	ACC	196	5.30E-05	0,00032	28		20	4.04	0.76
	CTRL	AEX	143	0.00057	0,00339	22		14	3.45	0.74
	CTRL	ACC+AEX	188	6.10E-05	3.60E-04	27		19	4.01	0.77
	ACC	AEX	254	0.7661	1,00000	34	2	14	0.30	0.05
	ACC	ACC+AEX	190	1.00E-07	6.00E-07	39	2	19	5.32	0.85
	AEX	ACC+AEX	371	1.40E-06	8.30E-06	33	1	19	4.83	0.84
Figure 4.3c	**Analysis of variance**									
	Kruskal-Wallis rank sum test		**χ^2**	**df**	**P-value**	**N**				
	Dependent variable: diameter		21.29	3	9.162E-05	37				
	Categorical variable: treatment									
	Post-hoc Wilcoxon rank sum (6 pairwise comparisons)		**W statistic**	**P-value**	**Adjusted P-value**	**N**	**r**	**n_2**	**|Z| score**	**r**
	Group 1	**Group 2**								
	CTRL	ACC	28	0.0001	0,00062	17		10	3.37	0.82
	CTRL	AEX	70.5	0.75101	1,00000	18		11	0.32	0.07
	CTRL	ACC+AEX	45.5	0.1527	0,91623	16		9	1.43	0.36

	ACC	ACC+AEX	53.5	0.00327	0,01965	19	1	9	2.94	0.67
Figure 4.4a	**Analysis of variance**									
	Kruskal-Wallis rank sum test		**χ^2**	**df**	**P-value**	**N**				
	Dependent variable: root length		70.125	3	4.01E-15	95				
	Categorical variable: treatment									
	Post-hoc Wilcoxon rank sum (6 pairwise comparisons)		**W statistic**	**P-value**	**Adjusted P-value**	**N**	**r**	**n_2**	**|Z| score**	**r**
	Group 1	**Group 2**								
	CTRL	ACC	275	7.40E+05	0.00045	28	1	15	3.96	0.75
	CTRL	AEX	658	9.50E-08	5.70E-07	57	1	44	5.34	0.71
	CTRL	ACC+AEX	390	9.20E-07	5.50E-06	36	1	23	4.91	0.82
	ACC	AEX	694	2.20E-05	0.00013	59	1	44	4.24	0.55
	ACC	ACC+AEX	463	3.80E-07	2.30E-06	38	1	23	5.08	0.82
	AEX	ACC+AEX	337,5	4.50E-09	2.70E-08	67	4	23	5.86	0.72
Figure 4.4c	**Analysis of variance**									
	Kruskal-Wallis rank sum test		**χ^2**	**df**	**P-value**	**N**				
	Dependent variable: meristem length		35.107	3	1,157e-07	59				
	Categorical variable: treatment									
	Post-hoc Wilcoxon rank sum (6 pairwise comparisons)		**W statistic**	**P-value**	**Adjusted P-value**	**N**	**r**	**n_2**	**|Z| score**	**r**
	Group 1	**Group 2**								
	CTRL	ACC	258.5	0.63938	1.00000	33	1	17	0.47	0.08
	CTRL	AEX	108,5	0.00016	0.00097	29	1	13	3.77	0.70
	CTRL	ACC+AEX	103	6.00E-05	0.00036	29	1	13	4.01	0.75
	AEX	ACC+AEX	185.5	0.62601	1.00000	26	1	13	0.49	0.10
Figure 4.4d	**Analysis of variance**									
	Kruskal-Wallis rank sum test		**χ^2**	**df**	**P-value**	**N**				
	Dependent variable: meristem cell number		57.679	3	1.84E-12	76				
	Categorical variable: treatment									
	Post-hoc Wilcoxon rank sum (6 pairwise comparisons)		**W statistic**	**P-value**	**Adjusted P-value**	**N**	**r**	**n_2**	**|Z| score**	**r**
	Group 1	**Group 2**								
	CTRL	ACC	464	0.018	0.11	39	1	20	2.37	0.38
	CTRL	AEX	178	6.00E-07	3.60E-06	37	1	18	4.99	0.82
	CTRL	ACC+AEX	624.5	4.30E-08	2.60E-07	42	1	23	5.48	0.84
	AEX	ACC+AEX	343.5	0.364	1.00000	41	1	23	0.91	0.14
Figure 4.4f	**Analysis of variance**									
	Kruskal-Wallis rank sum test		**χ^2**	**df**	**P-value**	**N**				
	Dependent variable: epidermal cell length		16.017	3	0.001125	40				
	Categorical variable: treatment									
	Post-hoc Wilcoxon rank sum (6 pairwise comparisons)		**W statistic**	**P-value**	**Adjusted P-value**	**N**	**r**	**n_2**	**|Z| score**	**r**
	Group 1	**Group 2**								
	CTRL	ACC	203	0.0051	0.0304	26	1	15	2.80	0.55
	CTRL	AEX	63	0.0184	0.1106	20	1	9	2.36	0.53
	CTRL	ACC+AEX	51.5	0.0012	0.0074	20	1	9	3.23	0.72
	ACC	AEX	118	0.7654	1	24	1	9	0.30	0.06
Figure 4.4h	**Analysis of variance**									
	Kruskal-Wallis rank sum test		**χ^2**	**df**	**P-value**	**N**				
	Dependent variable: root hair number		28.609	2	53	6.13E-07				
	Categorical variable: treatment									
	Post-hoc Wilcoxon rank sum (3 pairwise comparisons)		**W statistic**	**P-value**	**Adjusted P-value**	**N**	**r**	**n_2**	**|Z| score**	**r**
	Group 1	**Group 2**								
	CTRL	AEX	136,5	3.20E-06	9.50E-06	38	2	15	4.66	0.76
	CTRL	ACC+AEX	180,5	0.00083	0.0025	38	2	15	3.34	0.54
	AEX	ACC+AEX	157	0.00174	0.0052	30	1	15	3.13	0.57
Figure 4.6c	**Wilcoxon rank sum test**		**W statistic**	**P-value**	**Adjusted P-value**	**N**	**r**	**n_2**	**|Z| score**	**r**
	Group 1	**Group 2**								
	hls1-1 (CTRL) at 24 hours	*hls1-1* (AEX) at 24 hours	78	0,004	0.004	16	1	6	2.87	0.72
Figure 4.7	**Wilcoxon rank sum test**		**W statistic**	**P-value**	**Adjusted P-value**	**N**	**r**	**n_2**	**|Z| score**	**r**
	Group 1	**Group 2**								
	CTRL at 4 hours	AEX at 4 hours	W = 50	0.0235	0.0235	18		10	2.27	0.53
Figure S4.4	**Wilcoxon rank sum test**		**W statistic**	**P-value**	**Adjusted P-value**	**N**	**r**	**n_2**	**|Z| score**	**r**
	Group 1	**Group 2**								
	msg2-1 (CTRL) at 4 hours	*msg2-1* (AEX) at 4 hours	126.5	0.1109	0.1109	20	1	10	1.59	0.50
	msg2-1 (CTRL) at 8 hours	*msg2-1* (AEX) at 8 hours	119	0.3055	0.3055	20	1	10	1.02	0.32
	nph4-1arf19-1 (CTRL) at 4 hours	*nph4-1arf19-1* (AEX) at 4 hours	101	0.7649	0.7649	20	1	10	0.30	0.09
	nph4-1arf19-1 (CTRL) at 8 hours	*nph4-1arf19-1* (AEX) at 8 hours	116	0,4051	0,4051	20	1	10	0.83	0.26

Note: Effect size given as r (|Z| value/sqrt(N) with N= total number of samples

Bonferroni corrected p-value is given as p-value*number of pairwise comparisons

Chapter 5

A forward genetics screen to investigate the mode of action of ACCERBATIN

Contribution:

Yuming Hu (YH) and Dominique Van Der Straeten (DVDS) **designed experiments**; YH, Magdalena Baltova and Thomas De Paepe (TDP) **performed experiments**; Figure 5.2, 5.3 and Table S5.1 was updated from version made by TDP; YH, TDP, Filip Vandenbussche and DVDS **wrote the chapter**.

Abstract

Previously, we identified a quinoline carboxamide, called ACCERBATIN (AEX), which partially mimicked the ethylene-induced triple response phenotype in dark-grown Arabidopsis seedlings, consisting of an exaggerated apical hook and a shortened hypocotyl and root, though lacking the typical radial expansion in the hypocotyl. Detailed analysis revealed that AEX acted downstream of, or in parallel with ethylene signaling and affected auxin metabolism, which was accompanied by the induction of oxidative stress in AEX-treated seedlings (Chapter 3). To unravel the mode of action of AEX in plants, we screened an M2 population of an ethyl methanesulfonate (EMS) mutagenized PIN3-GFP line. We identified 4 *Arabidopsis* mutants with reduced sensitivity to AEX: three showed partial restoration of the hypocotyl and root lengths on AEX; one showed a hookless phenotype and agravitropism regardless presence of AEX.

Introduction

Exogenous application of naturally occurring or synthetic chemicals has long been used to study fundamental research questions in plants and to explore agricultural applications. For instance, the auxin-resistant mutant *axr1* was isolated as resistant to a toxic level of the synthetic auxin 2,4-dichlorophenoxyacetic acid (2,4-D) (Estelle and Somerville, 1987); the *transport inhibitor response* mutants *tir(s)* were isolated as resistant to exogenous synthetic auxin transport inhibitors, N-1-naphthylphthalamic acid (NPA), 2-carboxyphenyl-3-phenylpropane-1,2-dione (CPD) and methyl-2-chloro-9-hydroxyfluorene-9-carboxylate (CFM) (Ruegger et al., 1997); the auxin resistant mutant *indole-3-acetic acid inducible 28-1* (*iaa28-1*) was isolated as resistant to exogenous Indole-3-acetic acid (IAA) conjugate IAA-alanine in inhibition of elongation (Rogg et al., 2001); the *brassinazole-resistant 1-1D* (*bzr1-1D*) mutant was isolated based on hypocotyl resistance to brassinazole (BRZ), a synthetic inhibitor of brassinolide biosynthesis (Asami et al., 2001; Wang et al., 2002). These examples illustrate the importance of hormone pathway inhibitors in mutant discovery as well as their value in exploring plant hormone functions. In addition, small chemical compounds may be useful to discover novel components in hormone pathway and crosstalk (Rigal et al., 2014).

Ethylene related mutants were characterized by forward genetics approaches involving external application of ethylene or its precursor 1-aminocyclopropane-1-carboxylic acid (ACC) to seedlings grown either in the light or in darkness (Guzman and Ecker, 1990). Most ethylene mutants were identified based on a change in the triple response in the presence of the signal, or an appearance of the triple response in the absence of the hormone or its precursor. The triple response includes an exaggeration of the apical hook, inhibition of hypocotyl and root elongation, and radial expansion of the hypocotyl of dark grown seedlings. Distinct loci were identified using different ranges of chemical concentrations. The strong ethylene insensitive mutant *ethylene insensitive 2-1* (*ein2-1)* was identified from the mutant screen in the presence of 10 µL/L of ethylene (Guzman and Ecker, 1990), while *ACC insensitive 1* (*ain1/ein5*) was isolated on a high concentration of ACC (500µM) (Van Der Straeten et al., 1993). Weak ethylene-insensitive mutants, *wei1-wei5*, were identified from screening for reduced sensitivity to a low concentration of ACC (0.5 µM) (Alonso et al.,

2003a). In contrast, enhanced ethylene response mutants, *enhanced ethylene response1* (*eer1*), *eer3-eer5* and *feronia-2* (*fer-2*), *suppressor of auxin resistance 1-7* (*sar1-7*) display a stronger hypocotyl shortening in the presence of ethylene or ACC in darkness, as compared to the wild type. *eer1* was isolated in the presence of ACC levels (0.1 µM) below those generating a visible phenotype in wild type seedlings (Larsen and Chang, 2001); *eer3-eer5*, *fer-2*, *sar1-7* were isolated in the presence of saturating levels of ethylene (100 µL/L) (Christians and Larsen, 2007; Christians et al., 2008; Deslauriers and Larsen, 2010; Robles et al., 2012; Robles et al., 2007). Moreover, aminoethoxyvinylglycine (AVG), α-aminoisobutyric acid (AIB), silver nitrate ($AgNO_3$) and trans-cyclooctene (TCO), characterized as ethylene biosynthesis (AVG and AIB) or signaling ($AgNO_3$ and TCO) inhibitors (Beyer, 1976b; Satoh and Esashi, 1980; Sisler, 1990; Yang and Hoffman, 1984), were used to distinguish the *constitutive triple response1* (*ctr1*) mutant from the phenotypically similar *ethylene overproducer* (*eto*) mutants in the absence of exogenous ethylene, since the triple response phenotype of *ctr1* can be reverted by the ethylene inhibitors while that of *eto(s*) cannot (Kieber et al., 1993). The mutants mentioned above have been contributing to our understanding of ethylene function and interactions between ethylene and other hormones. *eto2* and *eto3* are dominant mutations affecting the conserved C-terminal part in type 2 ACC synthases (ACS5 and ACS9) (Chae et al., 2003; Vogel et al., 1998). ETO1 interacts with Cullin3 (CUL3) thus participating in ACS5 ubiquitination causing subsequent degradation (Wang et al., 2004a). CTR1 and EIN2 are central components of ethylene signaling (Alonso et al., 1999; Kieber et al., 1993). Characterization of *wei5* confirms the role of EIL1 in the ethylene signaling cascade (Alonso et al., 2003b); *wei2*, *wei7* and *wei8* indicate crosstalk between ethylene response and auxin biosynthesis (Stepanova et al., 2005; Stepanova et al., 2008). Although it is not clear whether EER(s) are components of ethylene signaling or an alternative pathway dampening ethylene response, they confirm that the ethylene response is indeed modulated by interaction with other hormones. Characterization of *fer-2* illustrates the balance between ethylene responsiveness and brassinosteroid signaling (Deslauriers and Larsen, 2010); suppressor of auxin resistance1 (sar1-7) indicates the synergistic relationship between ethylene responsiveness and auxin signaling via ARF7 and ARF19 in hypocotyl elongation (Robles et al., 2012).

With the advent of combinatorial chemical synthesis and high throughput screening techniques, chemical biology became "omics-" based (Blackwell and Zhao, 2003; De Rybel et al., 2009a). The starting point is a high throughput screening of a chemical library, normally with diversity-oriented or target-based synthetic compounds. Because of the broad structural diversity which can be reached by combinatorial chemical synthesis, the range of phenotypes are broader, which can be associated with redundant or specific genes and their respective proteins (Hicks and Raikhel, 2012). Chemicals can overcome gene redundancy, based on their capacity to bind different protein isoforms encoded by a gene family (Hopkins and Groom, 2002), thus inducing phenotypes not revealed by loss-of-function mutation of a single locus due to redundancy. For instance, Bikinin is a non-selective inhibitor targeting BRASSINOSTEROID-INSENSITIVE 2 (BIN2) and multiple Glycogen synthase kinase 3 (GSK3) kinases, which prevents BES1 phosphorylation and thus triggers a complete brassinosteroid response (De Rybel et al., 2009b). In contrast, pyrabactin is a specific agonist,

activating PYRABACTIN RESISTANCE 1 (PYR1) which was identified as an abscisic acid (ABA) receptor; while ABA interacts with all PYR1-like homologs so that ABA phenotypes in a single mutant is masked (Park et al., 2009). Furthermore, the chemical can be applied and removed at any point during plant development in different doses, which could trigger gradient phenotypes in a controlled manner (Blackwell and Zhao, 2003). However, challenges remain on target identification. Phenotyping approaches to search for resistance in the presence of small molecules followed by a series of molecular and biochemical approaches, such as microarray analysis, enzymatic activity assays, phosphorylation and kinase assays, and protein binding assays have been used to discover the targets of bikinin and kynurenine, while prior knowledge of the pathway is required (De Rybel et al., 2009b; He et al., 2011). *In vivo* random mutagenesis is a commonly used method in whole-organism physiology with the aim of target identification (Wang et al., 2004b). Ethylmethane sulphonate (EMS) mutagenesis is widely used in *Arabidopsis* (Alonso and Ecker, 2006; Page and Grossniklaus, 2002); it can induce random point mutations of a single nucleotide change (C to T and G to A) throughout the genome by guanine alkylation (Greene et al., 2003; Kim et al., 2006). Causal mutations can be identified more rapidly and cost-effectively nowadays by the next-generation sequencing approach (Austin et al., 2011; Schneeberger et al., 2009).

Previously, we identified the chemical ACCERBATIN (AEX), which triggered an exaggerated apical hook curvature, shortening of the hypocotyl and root on etiolated *Arabidopsis* Col-0 seedlings, acted downstream of ethylene signaling and affects auxin metabolism, leading to the induction of oxidative stress. In this study, we applied the chemical to identify *Arabidopsis* mutants with reduced response to AEX by screening an EMS-mutagenized population.

Results and discussion

A forward genetic screen to identify mutants resistant to AEX

50 µM AEX triggered a triple-response mimicking phenotype consisting of an exaggerated apical hook curvature, inhibition of elongation of the hypocotyl and the root, but lacking the lateral expansion of the hypocotyl (Chapter 3, Figure 3.1 and 3.3). Based on a dose-response analysis (Chapter 3, Figure 3.2), this concentration was chosen to isolate resistant mutants. Col-0 harboring *PIN3::PIN3-GFP* had the same phenotype as the wild type, regardless of the presence of AEX (Figure 5.2). The primary screening was conducted as schematically shown in Figure 5.1. Approximately 106,800 M2 seeds from 4,777 self-fertilized EMS-mutagenized plants were germinated in the presence of 50 µM AEX. After 4 days of growth in the dark, the seedlings were scored for restoration of the AEX-induced phenotype on the apical hook, the hypocotyl and the root. 254 seedlings were selected as AEX resistant mutant candidates, which partially restored the untreated Col-0 or *PIN3::PIN3-GFP* phenotype, though none of them displayed complete AEX insensitivity. They were transferred to soil, and allowed to self-fertilize. The candidates were rescreened by browsing the images. 165 of them were reselected and classified into 4 phenotypic classes based on the following characteristics, as compared to AEX treated Col-0 and *PIN3::PIN3-GFP* seedlings: I) both hypocotyl and root are longer, but no complete opening of the apical hook (56 candidates); II) fully open apical

hook, with less pronounced changes in hypocotyl and root length (6 candidates); III) longer hypocotyl, but no difference in root length and no complete opening of the apical hook (85 candidates); IV) longer root, but no difference in hypocotyl length and no complete opening of the apical hook (18 candidates). Mutants from class I, which partially recovered the overall length reduced by AEX, as well as class II, which had apical hook-specific insensitivity upon AEX treatment were selected to be rescreened in the next generation (M3). Around 25 seedlings from each line were checked. Given the long-term interest of the Laboratory of Functional Plant Biology in seedling development, class III and IV seedlings, showing tissue-specific recovery, were stored for later work.

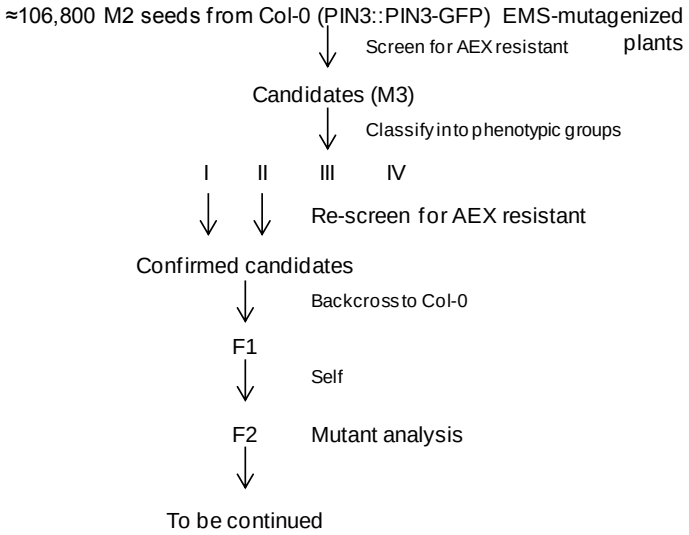

Figure 5.1 Screening approach for the isolation of AEX resistant mutants. For class I mutants, 6 candidates were confirmed showing partial restoration of the hypocotyl and root lengths on AEX; these were named M3 candidate (C)1- C6, though this trait was segregating in all lines (Figure 5.2, Table S5.1). For class II mutants, 1 candidate (named M3 C7) was confirmed showing a hookless phenotype, insensitive to AEX (Figure 5.2, Table S5.1). In addition, agravitropism was observed regardless presence of AEX. For each candidate line, 2-3 seedlings displaying the strongest phenotype upon AEX treatment (Figure 5.2)) were selected to be further grown and backcrossed (BC) to the parental ecotype, Col-0. 2-3 seeds from the resulting individual BCF1 plants were grown and their progeny (BCF2) was further analyzed. A parallel approach was conducted to self-fertilize M3 generation to generate purified M4 lines from the selected M3 mutants.

Table 5.1 Genetic analysis of BCF2 resistant mutants.

		Number of seedlings			
Cross	Generation	No AEX reversion	Partial AEX reversion	Ratio	χ^2
C1 x Col-0	F2	32	78	1:3	0,98
C3 x Col-0		73	77	1:1	
C4 x Col-0		62	15	3:1	1,25
C5 x Col-0		98	46	3:1	3,70
C7 x Col-0		53	159	1:3	1,10

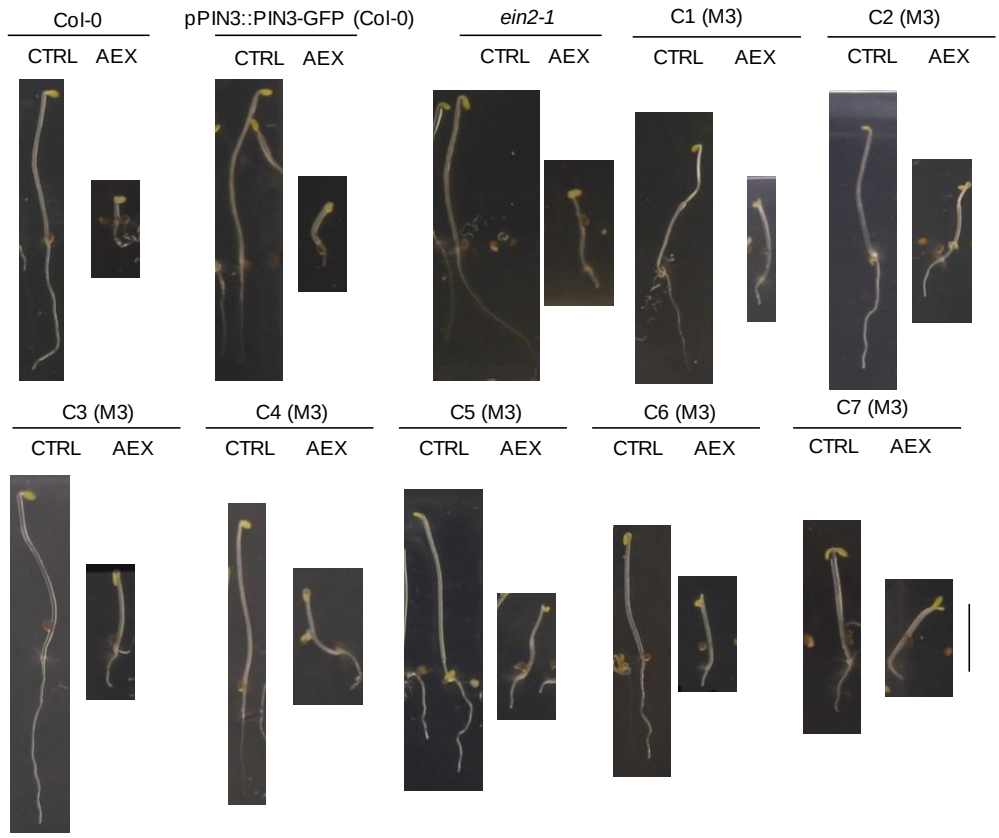

Figure 5.2 Phenotypes of selected resistant mutants in M3 generation.
Mutants (C1-C7, M3), controls of Col-0, pPIN3::PIN3-GFP (Col-0) and ein2-1 were grown in darkness for 4 days in the presence of 0.05% DMSO (CTRL), 50 µM AEX. For each candidate mutant, 2-3 seedlings displaying the strongest phenotype upon AEX treatment were grown for further analysis. Scale bar= 5 mm.

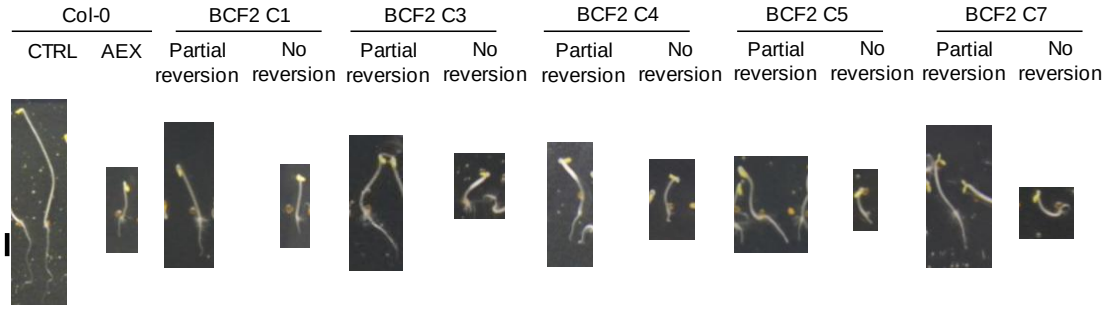

Figure 5.3 Phenotypes of representative resistant mutants in BCF2 generation.
Mutants (C1, C3-5 and C7, BCF2) and parental line of Col-0 were grown in darkness for 4 days in the presence of 0.05% DMSO (CTRL), 50 µM AEX. Scale bar= 2 mm.

Five out of 7 BCF2 lines, namely those derived from M3 C1, C3, C4, C5 and C7, were ready to be analyzed by the time stopping the experiments. Further genetic analysis was conducted on more than 100 BCF2 seeds from individual F2 plants for each candidate. These were based on whether they were resistant to AEX, in both shoot and root tissues or mainly in the apical hook. The representative mutants are shown in Figure 5.3. For mutants BCF2 C1, C3-5, the resistant phenotypes were scored based on partial reversion on both shoot and root; for mutants BCF2 C7, the resistant phenotypes were based on whether the seedlings were hookless and agravitropic or not. The numbers within different classes were analyzed by a

Chi-square ($\chi 2$) statistical test to determine whether a Mendelian segregation pattern was followed (Griffiths et al., 2000; Weigel and Glazebrook, 2008). Thus, mutants C1 and C7 were predicted as single dominant mutants with a ratio of 1:3 (WT: mutants) after backcross; mutants C4 and C5 were predicted as single recessive mutants with a ratio of 3:1 (WT: mutants) after backcross (Table 5.1). Seeds from selected BCF2 individuals with a mutant phenotype were used to follow segregation at the F3 generation to verify the inheritance of the mutation. If the analysis can be confirmed, a complementation test need to be performed on the recessive mutants C4 and C5, which showed similar partial resistant to AEX on hypocotyl and root, in order to exclude the possibility of which both mutations occur in the same gene. Inheritance of C3 cannot be easily determined because the phenotypic ratios deviated from the expected ratios according to Mendelian segregation. This may be due to reduced gametophytic transmission, to embryo lethality, or to the background mutations (Berná et al., 1999; Koornneef, 1994). Additional reciprocal backcrossing on C3 will be performed, in order to make decision on whether we go further analysis on it (Weigel and Glazebrook, 2008).

Perspectives

Based on the initial segregation analysis on 5 out of 7 available BCF2 mutant lines, we predicted that C1 and C7 are single dominant mutants, C4 and C5 are single recessive mutants (Table 5.1). However these data need verification in F3. Furthermore, the inheritance of C3 did not follow a Mendelian segregation pattern, and requires a second backcross. The segregation analysis also needs to be executed for mutants C2 and C6, which were not available by the time the experiments for this thesis were finalized. In addition, an allelism test will be necessary between mutants showing similar phenotypes, i.e. C4 and C5, to see whether they represent the same mutant allele. Isolation of mutants are possible only after transfer to non-AEX exposed conditions. A mapping population can be generated by outcrossing the homozygous AEX resistant mutants with the ecotype Landsberg (Ler). A population of 500 pooled F2 lines is recommended for ShoreMap (Schneeberger et al., 2009), which allows genome-wide genotyping and candidate-gene sequencing in a single step through deep sequencing analysis from a large pool of recombinants.

Notably, none of the 5 BCF2 mutants could fully restore the untreated phenotype. Partial AEX insensitivities were observed in the hypocotyl and the root of mutants C1, 3, 4 and 5, but not in the apical hook; while a hookless phenotype was observed in mutant C7. Given the conspicuous differences in phenotypes, which are not merely quantitative, the gene affected in mutant C7 is probably different from the other mutant loci. The fact that no full recovery of the wild type phenotype is found, indicates that the selected mutants could be weak alleles within particular loci. An example can be seen in the *ein2* alleles, in which *ein2-9* is the least severe one amongst fifteen *ein2* alleles (Alonso et al., 1999). Because of the complicity of AEX in auxin homeostasis (Chapter 3), AEX most likely targets a family of proteins rather than a single protein. This phenomenon is similar to synthetic molecule- pyrabactin, which was used to bypass the functional redundancy among PYR/PYL genes, masking ABA phenotypes in single mutants (Park et al., 2009). Thus, we expect that AEX could affect a protein family with high degree of functional redundancy. Redundancy leads to weak

phenotypes of single mutants, or to phenotypes limited to specific tissues, where a stronger gene specificity may occur. A good example is the PIN-FORMED (PIN) protein family of auxin transporters (Blilou et al., 2005; Friml et al., 2003; Vieten et al., 2005). For example, although *pin7* shows strong defects in early embryos, strong auxin-related defects in seedlings can only be seen in double, triple and quadruple combinations of *pin7* with *pin1*, *pin3* and *pin4*. However, the resistant screen could also lead to downstream components required to transport or activate the compound, for example, from the sirtinol-resistant screen, genes responsible for auxin signaling and conversion of sirtinol to an active auxin were identified (Dai et al., 2005). Nevertheless, it is interesting to identify the genes from the candidate mutants. Mutant C7 showing hookless and agravitropic phenotype, is probably related to PINOID (PID) protein serine/threonine kinase because the overexpression line of PID (PID-oex) showed AEX-resistant on the hook (Figure S3.3, Chapter 3) and PID-oex seedlings are agravitropic. AEX could also regulate PIN polarity in the process of endocytosis, transcytosis, and recycling as PID (Dhonukshe et al., 2008; Geldner et al., 2001; Kleine-Vehn et al., 2008). Mutants from class III and IV, showing tissue-specific recovery, are also interested to be identified.

Materials and methods

Plant materials and growth conditions

PIN3::PIN3-GFP in *Arabidopsis thaliana* (L.) Heynh. Col-0 background (Zadnikova et al., 2010) and its ethyl methanesulphonate (EMS)-mutagenized population of M2 seeds derived thereof were kindly provided by Jiri Friml (Institute of Science and Technology, Austria). The mutagenized population contained 4,777 M1 plants of EMS-mutagenized lines harvested into 178 pools, approximately 20-30 individuals per pool. Wild-type Col-0 and mutant ethylene insensitive *ein2-1* were from Nottingham Arabidopsis Stock Center. Half strength Murashige and Skoog (MS/2) (Duchefa) containing 1% sucrose, adjusted with 1 M of potassium hydroxide (KOH) to pH 5.7, and supplemented with 0.8% agar (for plant tissue culture, LABM) was used as plant growth medium. The additional chemicals were added after autoclaving the medium.

For the resistance screen, 50 µM of compound 6527749 (AEX, Chembridge) was used. Since dimethyl sulfoxide (DMSO) was used as a solvent of AEX, the untreated control was supplied with DMSO to the same final concentration. The same was done for 1-aminocyclopropane-1-carboxylic acid (ACC, final concentration 10 µM). DMSO and ACC were from Sigma-Aldrich. 45 mL medium was used in each square polystyrene petri dish (120 x 120 x 17 mm, Greiner bio-one).

The M2 seeds were sterilized with chlorine gas (Motte et al., 2013). To equally sow large amounts of seeds (≈600), the seeds were dispensed in 2-3 mL of 0.1% sterile agar, poured on the petri dish, and distributed with a Drigalski spatula (230mm, VWR). Small amounts of seeds (<100) were sterilized using liquid bleach, which was prepared using 5% NaOCl (Bleach water, Delhaize Group) and 0.05% Tween 20 (VWR). After 15 minutes of sterilization, the seeds were subsequently rinsed five times with sterilized water and sown using tweezers. The petri dishes were sealed using Micropore tape (3M). The seeds were then

stratified in darkness at 4°C for 2 days before being exposed to cool-white fluorescent light for 6 hours at 22°C to stimulate germination. Afterwards, the petri dishes were wrapped with two layers of aluminum foil to be protected from light and left in a growth chamber at 22°C for 4 days until analysis.

For propagation, seedlings from petri dishes were transferred to Jiffy pellets (Jiffy Products International) , and grown to maturity in a growth chamber set at 22˚C with a 16 hours (h) light/8 h dark photoperiod.

Screening mutants resistant to AEX

The initial screen was done using ≈106,800 M2 EMS-mutagenized seeds (around 600 M2 seeds from each pool). The seeds were sown on plates supplied with 50 µM AEX or 10 µM ACC or DMSO at a density of ≈1,200 per plate. The seedlings were examined after 4 days of growth in the dark on the horizontally oriented plates for their resistance to compound AEX. The selected mutants were propagated under the light by self-fertilization on soil. Harvested M3 seeds were subsequently re-examined for AEX resistance. The confirmed resistant mutants were further grown under the light and backcrossed to Col-0 plants. The F1 progenies were self-fertilized on soil to produce the F2 progeny. Genetic segregation analysis was performed on the F2 generation.

Supplemental information

Table S5.1 Phenotypic scores of AEX resistant mutants in the M3 generation. Phenotypes of apical hook, hypocotyl and root were compared to controls of Col-0 pPIN3::PIN3-GFP (Col-0) and ein2-1 in the presence of 50 µM AEX.

	Phenotypic categories*	Apical hook	Hypocotyl	Root	Pencentage (n≈25)
Col-0		-	-	-	
pPIN3::PIN3-GFP (Col-0)		-	-	-	
ein2-1		-	xxxx	xx	
C1	1	-	xxx	x	35
	2	-	-	-	65
C2	1	-	xxx	xxx	70
	2	-	xx	x	30
C3	1	-	xxx	xx	35
	2	-	x	xxx	35
	3	-	-	-	30
C4	1	-	xxx	xxx	60
	2	-	-	-	40
C5	1	-	xxx	xx	85
	2	-	-	-	15
C6	1	-	xx	x	35
	2	-	-	-	65
C7**	1	xxx	xxx	x	50
	2	xxx	-	-	50

xxx Strong insensitivity
xx Intermediate insensitivity
x Weak insensitivity
- No reversion of AEX
* Category "1" represents relative strong AEX insensitivity, which was selected for further studies; Categories "2" and "3" represent weaker or no reversion of AEX
** C7 shows agravitropic

Chapter 6

Conclusion and perspectives

Contribution: written by Yuming Hu

The initial goal of this work was to retrieve compounds that affect ethylene responses using a chemical genetics approach. Chemical genetics is the use of small molecules to study biological processes. It has been applied in the quest for herbicides for agrochemical use since the 1940s; and emerged into basic plant research due to the availability of broad structurally diversified chemical libraries and high-throughput screening methods. A number of applications have been proposed in reviews and research papers (Blackwell and Zhao, 2003; De Rybel et al., 2009; Hicks and Raikhel, 2009; Hicks and Raikhel, 2012; Hicks and Raikhel, 2014; Kaschani and van der Hoorn, 2007; Ma and Robert, 2013; Raikhel and Pirrung, 2005; Serrano et al., 2015; Walsh, 2007). In our work, we applied a library of 12,000 compounds with highly structural diversity on *Arabidopsis* seedlings grown in the dark in the presence of 1-aminocyclopropane-1-carboxylic acid (ACC) (Chapter 1); 1,313 (~11%) compounds altering ACC-induced triple response phenotype were selected and classified into phenotypic groups from the primary screen based on their effects on the apical hook curvature, the length and width of the hypocotyl and the root. A reporter line of Col-0 harboring *EIN3 BINDING SITE::β-GLUCURONIDASE (EBS::GUS)* was used here to evaluate ethylene response by visualization of GUS stained tissue as a reference factor (Chapter 3). In addition, we shared the screening data including the negative hits on our self-constructed web portal (https://chaos.ugent.be/WE15/), which is in line with the idea to share advances to the community as ChemMine (Backman et al., 2011).

Follow up studies of a quinoline carboxamide compound designated ACCERBATIN (AEX), that exacerbated the ACC-induced triple-response, and issued from the above-described library screening, were reported in Chapter 4 and 5. Applying AEX on ethylene-related mutants demonstrated that it acts downstream or independent of ethylene signaling. AEX effects on auxin pathways were chosen to be further studied because auxin plays a central role in plant growth and development (Ljung, 2013; Zažímalová et al., 2014) and has close interactions with ethylene in seedling and plant development (Chapter 2); besides, AEX-treated seedlings displayed some auxin traits, for instance the differential growth at the apical hook (Lehman et al., 1996). Therefore, we investigated AEX effects in combination with exogenous auxin and auxin inhibitors, as well as on auxin-related mutants; besides, interference with the hypocotyl gravitropic response suggested that AEX affects auxin homeostasis.

The distribution of auxin depends on both auxin metabolism and cellular auxin transport (Ljung, 2013; Mravec et al., 2009), therefore, auxin accumulation was measured in tobacco BY-2 cell system; auxin content and primary IAA metabolites were measured in seedlings. Radioactively labeled 1-Naphthaleneacetic acid ([^{3}H]NAA) accumulation indicated that AEX inhibited auxin efflux in the *in vitro* cultures. A drop of free IAA content in hypocotyl and an elevated level of OxIAA-GE in the shoot apical meristem indicated that AEX could lead to an enhanced oxidative activity coupled to an inhibitory effect on basipetal auxin transport from the shoot apical meristem (SAM) to the hypocotyl. The significant overlap between transcriptional profiles of AEX and hydrogen peroxide (H_2O_2), as well as between AEX and UPBEAT1 (UPB1), suggested an altered ROS homeostasis is triggered by AEX. A ROS accumulation in root tips triggered by AEX was visualized by the H_2O_2 and the superoxide

(O_2^-) staining (Chapter 4). Based on these observations, a model was proposed (Figure 6.1): AEX primarily blocks auxin transport to the hypocotyl from its major biosynthesis site in cotyledon and SAM through interfering with auxin transporters. The candidate auxin transporters could be PIN-FORMED PIN1 or/and ATP-BINDING CASSETTE subfamily B proteins/P-GLYCOPROTEIN/MULTIDRUG RESISTANCE (ABCB/PGP/MDR) ABCB19, because they express through the whole plant maintaining the main auxin stream from shoot to the root (Gälweiler et al., 1998; Noh et al., 2001); besides, they coordinately regulate auxin efflux in a heterologous system (Blakeslee et al., 2007; Titapiwatanakun et al., 2009). ABCB14 and ABCB15 could also be the candidates, because they mainly localize at the vascular tissues of the inflorescence stem and affect polar auxin transport (Kaneda et al., 2011). Moreover, the lack of auxin in the hypocotyl could also be the indirect consequence of excessive IAA oxidation at the meristematic region. A distortion of auxin homeostasis in the shoot is expected to have severe consequences in the root.

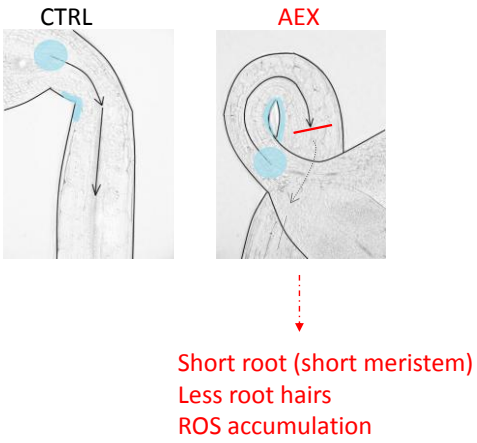

Figure 6.1 Model on AEX action. Without AEX as control (CTRL), there is an auxin flow from its major biosynthesis site in vicinity of the apical shoot meristem towards the roots. In the presence of AEX, the auxin transport from the meristematic region is blocked. This is either the direct consequence of poor basipetal IAA transport from the meristematic region, or indirectly linked to excessive IAA oxidation therein. The areas in blue indicate the auxin accumulation sites; the arrows in black indicate the direction of the auxin flow; the line in red indicates where the auxin flow blocked.

EXPLORING THE AUXIN CONNECTION

Whether AEX affects auxin transport directly, and which transport carriers were targeted remain a future scientific question to tackle.

Direct measurements of auxin transport in planta in the presence of AEX can be assessed using radiolabeled IAA (Lewis and Muday, 2009). AEX effects on the expression of major component of the auxin transport carrier proteins, fused to GFP of YFP under control of their endogenous promoters, can be monitored (Jeong et al., 2015). Alternatively, auxin export activity through these transport carriers can be measured in the presence of AEX in a yeast Schizosaccharomyces pombe system (Yang and Murphy, 2009). In addition to direct effects on auxin transport proteins, some chemicals can affect auxin transport via PIN vesicle trafficking, such as brefeldin A (BFA), 2,3,5-triiodobenzoic acid (TIBA) and 2-(1-pyrenoyl) benzoic acid (PBA) (Geldner et al., 2001). Gravacin (3-(5-[3,4-dichlorophenyl]-2-furyl)-

acrylic acid), an inhibitor of gravitropism through inhibition of auxin transporter carriers ATP-BINDING CASSETTE B/MULTI-DRUG RESISTANCE/P-GLYCOPROTEIN (ABCBs), found from a chemical genetics screen, can also inhibit endoplasmic reticulum (ER)-to-vacuole trafficking (Rojas-Pierce et al., 2007; Surpin et al., 2005). Therefore studying AEX in detail at the cell biological level may be in order. The endomembrane trafficking can be investigated by using endomembrane compartment markers and plasma membrane proteins (Drakakaki et al., 2011; Robert et al., 2008; Surpin et al., 2005).

We cannot exclude the possibility that AEX affects auxin signaling. An enhanced inhibitory effects on hypocotyl and root by AEX in the presence of 0.5 µM IAA (Figure S3, Chapter 4) suggested that AEX probably works as an auxin agonist. To test whether AEX affects auxin signaling via SCFTIR1/AFB mechanism, an auxin, TIR1/AFBs and proteasome activity dependent auxin signaling sensor DII-VENUS (Brunoud et al., 2012) can be monitored with different doses of AEX. Besides, a complementary experiment can be performed to compare AEX-treated seedlings to AEX+auxinole (α-[2,4-dimethylphenylethyl-2-oxo]-IAA). Auxinole is an auxin antagonist blocking TIR1-IAA-AUX/IAA through binding TIR1/AFB receptors (Hayashi et al., 2012). If AEX can complement the phenotypic effects triggered by auxinole, it means that AEX could act as auxin through TIR1/AFB receptors.

THE REACTIVE OXYGEN SPECIES (ROS) CONNECTION

Another outcome induced by AEX is the accumulation of ROS in root tips (Chapter 4), but the underlying mechanism remains unknown, and would be the focus of future research. A previous report indicated that a repression of cell division represented by CYCLIN-DEPENDENT PROTEIN KINASE B1;1 (CYCB1;1) was significant in roots of H_2O_2-treated plants coupled to a reduced meristem length (Tsukagoshi, 2012), which is similar to our observation on AEX-treated pCYCB1;1::DB-GUS line showing reduced expression in root. Scavenging H_2O_2 by potassium iodide (KI) (Dunand et al., 2007) in AEX-treated seedlings can be used to exam whether the inhibitory effects on cell division and elongation in root is directly linked to H_2O_2. O_2^- produced by NADPH oxidases has been shown to affect root growth and root hair development (Foreman et al., 2003). To investigate the role of O_2^- in AEX-treated seedling growth, diphenyleneiodonium (DPI), which primarily inhibits NADPH oxidase activities, can be applied.

THE AUXIN-ROS INTERCONNECTION

Although ROS-regulated root growth control can be auxin independent (Tsukagoshi et al., 2010), it is well possible that AEX affects plant growth through an auxin-redox (ROS-antioxidant) crosstalk because of the AEX-triggered alteration in auxin and ROS homeostasis as shown in Chapter 4 and published data (recently reviewed in (Krishnamurthy and Rathinasabapathi, 2013; Sharma et al., 2015; Tognetti et al., 2012)). For instance, apoplastic ROS can transiently decrease auxin signaling and cause stress-induced morphogenic response (SIMR) (Blomster et al., 2011). On the other hand, auxin-induced hydrogen peroxide (H_2O_2) mediates root gravitropism in maize (*Zea mays*) (Joo et al., 2001); auxin-induced ROS are involved in cell wall loosening during elongation growth of maize coleoptile (Schopfer, 2001; Schopfer et al., 2002).Therefore, ROS accumulation can be determined in the presence of

AEX and exogenous application of auxin or auxin inhibitors, or on auxin signaling mutants (e.g. *tir1afb2* (*TRANSPORT INHIBITOR RESPONSE1AUXIN SIGNALING F-BOX2*)) to investigate whether AEX effects is auxin-mediated. 3'-O-Acetyl-6'-O-pentafluorobenzenesulfonyl-2'-7'- difluorofluorescein (BES-H_2O_2-Ac) and dihydroethidium (DHE) can be applied simultaneous as a second indicator for H_2O_2 and O_2^-, respectively (Tsukagoshi et al., 2010). Studies can also be performed in mutants deficient in ROS production (e.g. *RESPIRATORY BURST OXIDASE HOMOLOGUESD* (*rbohD*), *rbohF* (Torres et al., 2002)).

Besides, AEX may affect enzymatic and non-enzymatic antioxidants that have been reported participating in auxin-mediated redox regulation in plant growth. For example, Ascorbate peroxidase 1 (APX1) is a cytosolic enzyme involved in H_2O_2 degradation, which can be denitrosylated and partially inhibited by auxin in *Arabidopsis* roots (Correa-Aragunde et al., 2013). Further study suggested that NADPH-dependent thioredoxin reductase (TrxR) is a key player in auxin-mediated denitrosylation process (Correa-Aragunde et al., 2015). Together with thioredoxin (TRX), glutathione (GSH) also plays an important role in auxin biosynthesis and transport, which was demonstrated by analyzing *ntra ntrb cad2*, a NADPH-dependent TrxR (*ntra ntrb*) and glutathione biosynthesis (*cad2*) triple mutant showing reduced root meristem size (Bashandy et al., 2010). Consistent herewith, GSH depletion caused root growth reduction through inhibition of auxin transport and PIN accumulation in root tips was also demonstrated by Koprivova et al. (Koprivova et al., 2010). Interestingly, AEX treated 4-day-old etiolated seedlings showed defective cell division in the root but not the shoot (Chapter 3), which was similar to the *root meristemless1* (*rml1*) mutant characterized by low GSH content (Vernoux et al., 2000). Remarkably, the cell cycle activity of the root meristem also depends on the auxin-mediated redox status (Jiang et al., 2003). Gao et al., showed that changes in glutathione redox status can also mediate crosstalk between auxin and H_2O_2 in catalase mutants (*cat2*) (Gao et al., 2013). Therefore, the redox intermediates (GSH, ascorbate) and the enzymes associated with their synthesis and metabolism of AEX treated seedlings can be measured to exam their involvement in AEX effects (Tyburski et al., 2007). ROS production can be measured in tobacco cell culture with supplementation of purified enzymes in the presence of AEX (Kawano and Muto, 2000). Within the enzymatic antioxidants, the focus would be on peroxidases because a number of peroxidases (Chapter 4) were downregulated by AEX within 6 hours.

In addition, ROS overproduction may be the mode of action of auxin-type herbicide (Pazmiño et al., 2011; ROMERO‐PUERTAS et al., 2004). On the other hand, exogenously applied auxin was responsible for the irreversible accumulation of an inactive auxin 2-oxindole-3-acetic acid (oxIAA) and the production of ROS in roots (Peer et al., 2013; Pěnčík et al., 2013), which was partially through NADPH oxidases *Respiratory burst oxidase homologues D* (*RbohD*) (Peer et al., 2013). Notably, none of the *Rboh* were induced by 6 hours AEX treatment, which may have happened at earlier time points and could be confirmed by real-time quantitative PCR (qPCR). Besides, it is possible that Rboh gene expression is very different in shoots versus roots. From that point of view, checking the gene expression pattern from separated tissues could explain the differences in shoots and roots.

Moreover, the auxin accumulation assay in tobacco BY-2 cells showed an enhanced auxin accumulation upon AEX treatment (Chapter 4). This is in contrast to a decreased auxin accumulation seen upon H_2O_2 treatment of BY-2 cells (Křeček, 2011). It is likely that a positive feedback loop exists.

TARGET IDENTIFICATION

Understanding the function of a chemical requires knowledge of the actual target(s) and the complex interactions between multiple signals. An effective way to identify the targets of a chemical in *Arabidopsis* research is to search for mutants with reduced or enhanced sensitivity to the chemical (Chen et al., 2013; De Rybel et al., 2012; Rojas-Pierce et al., 2007; Walsh et al., 2006; Zhao et al., 2003), which is our current focus (Chapter 5). Based on the initial segregation analysis on available mutant candidates after backcrossed and selfed (BCF2), three candidates showing partial reversion on both shoot and root were isolated, in which two were predicted as single recessive mutant and one was predicted as single dominant mutant; besides, one candidate showing hookless and agravitropism was isolated and predicted as single dominant mutant. The causal mutations in the selected mutants can be identified bynext-generation sequencing method followed by SHOREmap with bulked recombinants (Schneeberger et al., 2009), which has proven to speed up the progress in the forward genetics screen. Other alleles can be retrieved from additional screening on T-DNA collections or a full-length cDNA overexpressing gene (FOX) hunting system (Alonso et al., 2003; Ichikawa et al., 2006), which would be studied together with the first identified ones.

In addition, affinity-based approach is a major approach within the field of chemical genetics to identify potential targets of a compound (Dejonghe and Russinova, 2014). This approach requires a thorough structure-activity analysis (SAR) to identify functional groups that can be used to modify the compound or to optimize the effect of the compound. Thus, before the use of affinity-based approach, relevant derivatives of AEX should be tested to ensure the functional group can undergo addition of a linker molecule without affecting bioactivity. The success of using this approach also depends on the affinity between target protein and the compound as well as the abundance of the target (Overvoorde and Audenaert, 2013). Alternatively, the label-free approach, such as drug affinity responsive target stability (DARTS) might be used to detect small molecule interactors, which can prevent modification of the compound through compound labeling. This approach was based on the principle that small molecule binding to a target site can stabilize some proteins from proteolytic degradation, while non-target proteins are digested away (Lomenick et al., 2009). It has been used to confirm the target of Endosidin2 in plant system (Zhang et al., 2015).

POSSIBLE APPLICATION OF THE COMPOUND

Since AEX eventually led to plant death, a detailed, more applied study of AEX and its analogs may lead to the discovery of alternative herbicides or be part as an enhancer of herbicides. Taking the advantages of chemical genetics approach, chemicals can be easily applied in other plant species. Thus, the sensitivity test of AEX and its analogs on different crops and weeds can be easily performed.

The enhanced expression of a large of group of peroxidases and accumulation of H_2O_2 by AEX resembles the role of salicylic acid (SA) at higher concentration in plant death. Since SA can induce plant defense system at an intermediate concentration (War et al., 2011), the antioxidative enzyme activities triggered by AEX at lower concentration without disrupting the plant growth can be tested to see whether AEX can also induce the plant defense. Induced resistance can be exploited for developing components for sustainable crop production.

FINAL REMARKS

By analyzing AEX effects, we may obtain more insight into the crosstalk between auxin and stress signaling.

The initial aim of this work was to investigate ethylene responses using a chemical genetics approach. Although a lot of this work was focused on a compound dependent on auxin-stress crosstalk rather than being directly related to ethylene signaling, it appears linked to downstream effects of ethylene. Further work aims at understanding the action of a number of other chemicals showing enhanced or reduced ethylene triggered triple response, identified through the same high-throughput screen. Last but not least, researchers in the plant community, interested in chemicals affecting ethylene responses or related developmental effects can access the chemical library with basic chemical and phenotype information (Chapter 3).

References

Abbas, M., Alabadi, D., and Blazquez, M.A. (2013). Differential growth at the apical hook: all roads lead to auxin. Frontiers in plant science 4:441.

Abel, S., and Theologis, A. (1996). Early genes and auxin action. Plant physiology 111:9-17.

Abeles, F., Morgan, P., and Saltveit, M. (1992). Ethylene in plant biology.

Alonso, J.M., and Ecker, J.R. (2006). Moving forward in reverse: genetic technologies to enable genome-wide phenomic screens in Arabidopsis. Nature reviews. Genetics 7:524-536.

Alonso, J.M., Hirayama, T., Roman, G., Nourizadeh, S., and Ecker, J.R. (1999). EIN2, a bifunctional transducer of ethylene and stress responses in Arabidopsis. Science 284:2148-2152.

Alonso, J.M., and Stepanova, A.N. (2003). T-DNA mutagenesis in Arabidopsis. In: Plant Functional Genomics: Springer. 177-187.

Alonso, J.M., Stepanova, A.N., Leisse, T.J., Kim, C.J., Chen, H., Shinn, P., Stevenson, D.K., Zimmerman, J., Barajas, P., Cheuk, R., et al. (2003a). Genome-wide insertional mutagenesis of Arabidopsis thaliana. Science 301:653-657.

Alonso, J.M., Stepanova, A.N., Solano, R., Wisman, E., Ferrari, S., Ausubel, F.M., and Ecker, J.R. (2003b). Five components of the ethylene-response pathway identified in a screen for weak ethylene-insensitive mutants in Arabidopsis. Proc Natl Acad Sci U S A 100:2992-2997.

Amrhein, N., Schneebeck, D., Skorupka, H., Tophof, S., and Stöckigt, J. (1981). Identification of a major metabolite of the ethylene precursor 1-aminocyclopropane-1-carboxylic acid in higher plants. Naturwissenschaften 68:619-620.

An, F., Zhang, X., Zhu, Z., Ji, Y., He, W., Jiang, Z., Li, M., and Guo, H. (2012). Coordinated regulation of apical hook development by gibberellins and ethylene in etiolated Arabidopsis seedlings. Cell research 22:915-927.

Asami, T., Mizutani, M., Fujioka, S., Goda, H., Min, Y.K., Shimada, Y., Nakano, T., Takatsuto, S., Matsuyama, T., Nagata, N., et al. (2001). Selective interaction of triazole derivatives with DWF4, a cytochrome P450 monooxygenase of the brassinosteroid biosynthetic pathway, correlates with brassinosteroid deficiency in planta. J Biol Chem 276:25687-25691.

Austin, R.S., Vidaurre, D., Stamatiou, G., Breit, R., Provart, N.J., Bonetta, D., Zhang, J., Fung, P., Gong, Y., Wang, P.W., et al. (2011). Next-generation mapping of Arabidopsis genes. The Plant journal : for cell and molecular biology 67:715-725.

Backman, T.W.H., Cao, Y.Q., and Girke, T. (2011). ChemMine tools: an online service for analyzing and clustering small molecules. Nucleic Acids Res 39:W486-W491.

Bailly, A., Sovero, V., Vincenzetti, V., Santelia, D., Bartnik, D., Koenig, B.W., Mancuso, S., Martinoia, E., and Geisler, M. (2008). Modulation of P-glycoproteins by auxin transport inhibitors is mediated by interaction with immunophilins. J Biol Chem 283:21817-21826.

Bak, S., Tax, F.E., Feldmann, K.A., Galbraith, D.W., and Feyereisen, R. (2001). CYP83B1, a cytochrome P450 at the metabolic branch point in auxin and indole glucosinolate biosynthesis in Arabidopsis. The Plant Cell 13:101-111.

Baker, J.E., Anderson, J.D., Adams, D.O., Apelbaum, A., and Lieberman, M. (1982). Biosynthesis of Ethylene from Methionine in Aminoethoxyvinylglycine-Resistant Avocado Tissue. Plant physiology 69:93-97.

Baluska, F., Parker, J.S., and Barlow, P.W. (1992). Specific patterns of cortical and endoplasmic microtubules associated with cell growth and tissue differentiation in roots of maize (Zea mays L.). Journal of Cell Science 103:191-200.

Barbez, E., and Kleine-Vehn, J. (2013). Divide Et Impera--cellular auxin compartmentalization. Current opinion in plant biology 16:78-84.

Bashandy, T., Guilleminot, J., Vernoux, T., Caparros-Ruiz, D., Ljung, K., Meyer, Y., and Reichheld, J.P. (2010). Interplay between the NADP-linked thioredoxin and glutathione systems in Arabidopsis auxin signaling. Plant Cell 22:376-391.

Baskin, T.I. (2015). Auxin inhibits expansion rate independently of cortical microtubules. Trends in plant science 20:471-472.

Beemster, G.T., and Baskin, T.I. (1998). Analysis of cell division and elongation underlying the developmental acceleration of root growth in Arabidopsis thaliana. Plant physiology 116:1515-1526.

Benjamini, Y., Drai, D., Elmer, G., Kafkafi, N., and Golani, I. (2001). Controlling the false discovery rate in behavior genetics research. Behavioural brain research 125:279-284.

Bennett, M.J., Marchant, A., Green, H.G., May, S.T., Ward, S.P., Millner, P.A., Walker, A.R., Schulz, B., and Feldmann, K.A. (1996). Arabidopsis AUX1 gene: a permease-like regulator of root gravitropism. Science 273:948-950.

Berná, G., Robles, P., and Micol, J.L. (1999). A mutational analysis of leaf morphogenesis in Arabidopsis thaliana. Genetics 152:729-742.

Beyer, E. (1976a). Silver - Potent Antiethylene Agent. Plant physiology 57:98-98.

Beyer, E.M. (1976b). A potent inhibitor of ethylene action in plants. Plant physiology 58:268-271.

Binder, B.M., Mortimore, L.A., Stepanova, A.N., Ecker, J.R., and Bleecker, A.B. (2004). Short-term growth responses to ethylene in Arabidopsis seedlings are EIN3/EIL1 independent. Plant physiology 136:2921-2927.

Binder, B.M., Rodriguez, F.I., Bleecker, A.B., and Patterson, S.E. (2007). The effects of Group 11 transition metals, including gold, on ethylene binding to the ETR1 receptor and growth of Arabidopsis thaliana. Febs Lett 581:5105-5109.

Blackwell, H.E., and Zhao, Y. (2003). Chemical genetic approaches to plant biology. Plant physiology 133:448-455.

Blakeslee, J.J., Bandyopadhyay, A., Lee, O.R., Mravec, J., Titapiwatanakun, B., Sauer, M., Makam, S.N., Cheng, Y., Bouchard, R., Adamec, J., et al. (2007). Interactions among PIN-FORMED and P-glycoprotein auxin transporters in Arabidopsis. Plant Cell 19:131-147.

Blakeslee, J.J., Bandyopadhyay, A., Peer, W.A., Makam, S.N., and Murphy, A.S. (2004). Relocalization of the PIN1 auxin efflux facilitator plays a role in phototropic responses. Plant physiology 134:28-31.

Bleecker, A.B., Estelle, M.A., Somerville, C., and Kende, H. (1988). Insensitivity to Ethylene Conferred by a Dominant Mutation in Arabidopsis thaliana. Science 241:1086-1089.

Blilou, I., Xu, J., Wildwater, M., Willemsen, V., Paponov, I., Friml, J., Heidstra, R., Aida, M., Palme, K., and Scheres, B. (2005). The PIN auxin efflux facilitator network controls growth and patterning in Arabidopsis roots. Nature 433:39-44.

Blomster, T., Salojarvi, J., Sipari, N., Brosche, M., Ahlfors, R., Keinanen, M., Overmyer, K., and Kangasjarvi, J. (2011). Apoplastic reactive oxygen species transiently decrease auxin signaling and cause stress-induced morphogenic response in Arabidopsis. Plant physiology 157:1866-1883.

Bocobza, S., Willmitzer, L., Raikhel, N.V., and Aharoni, A. (2012). Discovery of New Modules in Metabolic Biology Using ChemoMetabolomics. Plant physiology 160:1160-1163.

Boerjan, W., Cervera, M.T., Delarue, M., Beeckman, T., Dewitte, W., Bellini, C., Caboche, M., Van Onckelen, H., Van Montagu, M., and Inze, D. (1995). Superroot, a recessive mutation in Arabidopsis, confers auxin overproduction. Plant Cell 7:1405-1419.

Boller, T., Herner, R.C., and Kende, H. (1979). Assay for and Enzymatic Formation of an Ethylene Precursor, 1-Aminocyclopropane-1-Carboxylic Acid. Planta 145:293-303.

Bondad, N. (1976). Response of some tropical and subtropical fruits to pre-and post-harvest applications of ethephon. Economic Botany 30:67-80.
Boutte, Y., Jonsson, K., McFarlane, H.E., Johnson, E., Gendre, D., Swarup, R., Friml, J., Samuels, L., Robert, S., and Bhalerao, R.P. (2013). ECHIDNA-mediated post-Golgi trafficking of auxin carriers for differential cell elongation. Proc Natl Acad Sci U S A 110:16259-16264.
Bovy, A.G., Angenent, G.C., Dons, H.J.M., and van Altvorst, A.C. (1999). Heterologous expression of the Arabidopsis etr1-1 allele inhibits the senescence of carnation flowers. Mol Breeding 5:301-308.
Bradford, K.J., Hsiao, T.C., and Yang, S.F. (1982). Inhibition of ethylene synthesis in tomato plants subjected to anaerobic root stress. Plant physiology 70:1503-1507.
Bradford, K.J., and Yang, S.F. (1980). Stress-induced Ethylene Production in the Ethylene-requiring Tomato Mutant Diageotropica. Plant physiology 65:327-330.
Brady, S.M., Orlando, D.A., Lee, J.Y., Wang, J.Y., Koch, J., Dinneny, J.R., Mace, D., Ohler, U., and Benfey, P.N. (2007). A high-resolution root spatiotemporal map reveals dominant expression patterns. Science 318:801-806.
Brown, K.M. (1997). Ethylene and abscission. Physiol Plantarum 100:567-576.
Brunoud, G., Wells, D.M., Oliva, M., Larrieu, A., Mirabet, V., Burrow, A.H., Beeckman, T., Kepinski, S., Traas, J., Bennett, M.J., et al. (2012). A novel sensor to map auxin response and distribution at high spatio-temporal resolution. Nature 482:103-U132.
Buer, C.S., and Muday, G.K. (2004). The transparent testa4 mutation prevents flavonoid synthesis and alters auxin transport and the response of Arabidopsis roots to gravity and light. Plant Cell 16:1191-1205.
Buer, C.S., Sukumar, P., and Muday, G.K. (2006). Ethylene modulates flavonoid accumulation and gravitropic responses in roots of Arabidopsis. Plant physiology 140:1384-1396.
Bufler, G., and Streif, J. (1986). Ethylene Biosynthesis of Golden Delicious Apples Stored in Different Mixtures of Carbon-Dioxide and Oxygen. Sci Hortic-Amsterdam 30:177-185.
Büntemeyer, K., Lüthen, H., and Böttger, M. (1998). Auxin-induced changes in cell wall extensibility of maize roots. Planta 204:515-519.
Burg, S.P., and Burg, E.A. (1966). The interaction between auxin and ethylene and its role in plant growth. Proc Natl Acad Sci U S A 55:262-269.
Burg, S.P., and Burg, E.A. (1967). Molecular requirements for the biological activity of ethylene. Plant physiology 42:144-152.
Byers, R.E. (1997). Peach and nectarine fruit softening following aminoethoxyvinylglycine sprays and dips. Hortscience 32:86-88.
Caspar, T., and Pickard, B.G. (1989). Gravitropism in a starchless mutant of Arabidopsis : Implications for the starch-statolith theory of gravity sensing. Planta 177:185-197.
Catalá, C., Rose, J.K., and Bennett, A.B. (2000). Auxin-regulated genes encoding cell wall-modifying proteins are expressed during early tomato fruit growth. Plant physiology 122:527-534.
Chae, H.S., Faure, F., and Kieber, J.J. (2003). The eto1, eto2, and eto3 mutations and cytokinin treatment increase ethylene biosynthesis in Arabidopsis by increasing the stability of ACS protein. Plant Cell 15:545-559.
Chang, C., Kwok, S.F., Bleecker, A.B., and Meyerowitz, E.M. (1993). Arabidopsis ethylene-response gene ETR1: similarity of product to two-component regulators. Science 262:539-544.
Chang, K.N., Zhong, S., Weirauch, M.T., Hon, G., Pelizzola, M., Li, H., Huang, S.S., Schmitz, R.J., Urich, M.A., Kuo, D., et al. (2013). Temporal transcriptional response to ethylene gas drives growth hormone cross-regulation in Arabidopsis. eLife 2:e00675.
Chao, Q., Rothenberg, M., Solano, R., Roman, G., Terzaghi, W., and Ecker, J.R. (1997). Activation of the ethylene gas response pathway in Arabidopsis by the nuclear protein ETHYLENE-INSENSITIVE3 and related proteins. Cell 89:1133-1144.
Chen, I.J., Lo, W.S., Chuang, J.Y., Cheuh, C.M., Fan, Y.S., Lin, L.C., Wu, S.J., and Wang, L.C. (2013). A chemical genetics approach reveals a role of brassinolide and cellulose synthase in hypocotyl elongation of etiolated Arabidopsis seedlings. Plant science : an international journal of experimental plant biology 209:46-57.
Chen, Q., Dai, X., De-Paoli, H., Cheng, Y., Takebayashi, Y., Kasahara, H., Kamiya, Y., and Zhao, Y. (2014). Auxin overproduction in shoots cannot rescue auxin deficiencies in Arabidopsis roots. Plant Cell Physiol 55:1072-1079.
Chen, R., Hilson, P., Sedbrook, J., Rosen, E., Caspar, T., and Masson, P.H. (1998). The Arabidopsis thaliana AGRAVITROPIC 1 gene encodes a component of the polar-auxin-transport efflux carrier. Proc. Natl. Acad. Sci. 95:15112–15117.
Chen, R., Rosen, E., and Masson, P.H. (1999). Gravitropism in Higher Plants. Plant physiology 120:343-350
Christians, M.J., Gingerich, D.J., Hansen, M., Binder, B.M., Kieber, J.J., and Vierstra, R.D. (2009). The BTB ubiquitin ligases ETO1, EOL1 and EOL2 act collectively to regulate ethylene biosynthesis in Arabidopsis by controlling type-2 ACC synthase levels. Plant Journal 57:332-345.
Christians, M.J., and Larsen, P.B. (2007). Mutational loss of the prohibitin AtPHB3 results in an extreme constitutive ethylene response phenotype coupled with partial loss of ethylene-inducible gene expression in Arabidopsis seedlings. Journal of experimental botany 58:2237-2248.
Christians, M.J., Robles, L.M., Zeller, S.M., and Larsen, P.B. (2008). The eer5 mutation, which affects a novel proteasome-related subunit, indicates a prominent role for the COP9 signalosome in resetting the ethylene-signaling pathway in Arabidopsis. Plant Journal 55:467-477.
Cohen, J.D., Baldi, B.G., and Slovin, J.P. (1986). 13C6-[Benzene Ringj-Indole-3-Acetic Acid. Plant physiology 80:14-19.
Collett, C.E., Harberd, N.P., and Leyser, O. (2000). Hormonal interactions in the control of Arabidopsis hypocotyl elongation. Plant physiology 124:553-562.
Cong, F., Cheung, A.K., and Huang, S.M. (2012). Chemical genetics-based target identification in drug discovery. Annu Rev Pharmacol Toxicol 52:57-78.
Correa-Aragunde, N., Cejudo, F.J., and Lamattina, L. (2015). Nitric oxide is required for the auxin-induced activation of NADPH-dependent thioredoxin reductase and protein denitrosylation during root growth responses in arabidopsis. Ann Bot 116:695-702.
Correa-Aragunde, N., Foresi, N., Delledonne, M., and Lamattina, L. (2013). Auxin induces redox regulation of ascorbate peroxidase 1 activity by S-nitrosylation/denitrosylation balance resulting in changes of root growth pattern in Arabidopsis. Journal of experimental botany 64:3339-3349.
Cosgrove, D.J. (2005). Growth of the plant cell wall. Nature reviews. Molecular cell biology 6:850-861.
Čovanová, M., Sauer, M., Rychtář, J., Friml, J., Petrášek, J., and Zažímalová, E. (2013). Overexpression of the auxin binding protein1 modulates PIN-dependent auxin transport in tobacco cells. PloS one 8:e70050.
Cutler, S.R., Ehrhardt, D.W., Griffitts, J.S., and Somerville, C.R. (2000). Random GFP::cDNA fusions enable visualization of subcellular structures in cells of Arabidopsis at a high frequency. Proc Natl Acad Sci 97:3718–3723.
Dai, X.H., Hayashi, K., Nozaki, H., Cheng, Y.F., and Zhao, Y.D. (2005). Genetic and chemical analyses of the action mechanisms of sirtinol in Arabidopsis. P Natl Acad Sci USA 102:3129-3134.
De Cnodder, T., Vissenberg, K., Van Der Straeten, D., and Verbelen, J.P. (2005). Regulation of cell length in the Arabidopsis thaliana root by the ethylene precursor 1-aminocyclopropane- 1-carboxylic acid: a matter of apoplastic reactions. The New phytologist 168:541-550.

De Grauwe, L., Vandenbussche, F., Tietz, O., Palme, K., and Van Der Straeten, D. (2005). Auxin, ethylene and brassinosteroids: Tripartite control of growth in the Arabidopsis hypocotyl. Plant Cell Physiol 46:827-836.
De Paepe, A., Vuylsteke, M., Van Hummelen, P., Zabeau, M., and Van Der Straeten, D. (2004). Transcriptional profiling by cDNA-AFLP and microarray analysis reveals novel insights into the early response to ethylene in Arabidopsis. The Plant journal : for cell and molecular biology 39:537-559.
De Rybel, B., Audenaert, D., Beeckman, T., and Kepinski, S. (2009a). The past, present, and future of chemical biology in auxin research. ACS chemical biology 4:987-998.
De Rybel, B., Audenaert, D., Vert, G., Rozhon, W., Mayerhofer, J., Peelman, F., Coutuer, S., Denayer, T., Jansen, L., Nguyen, L., et al. (2009b). Chemical Inhibition of a Subset of Arabidopsis thaliana GSK3-like Kinases Activates Brassinosteroid Signaling. Chem Biol 16:594-604.
De Rybel, B., Audenaert, D., Xuan, W., Overvoorde, P., Strader, L.C., Kepinski, S., Hoye, R., Brisbois, R., Parizot, B., Vanneste, S., et al. (2012). A role for the root cap in root branching revealed by the non-auxin probe naxillin. Nat Chem Biol 8:798-805.
De Vleesschauwer, D., Xu, J., and Hofte, M. (2014). Making sense of hormone-mediated defense networking: from rice to Arabidopsis. Frontiers in plant science 5:611.
de Wild, H.P.J., Otma, E.C., and Peppelenbos, H.W. (2003). Carbon dioxide action on ethylene biosynthesis of preclimacteric and climacteric pear fruit. Journal of experimental botany 54:1537-1544.
de Wild, H.P.J., Woltering, E.J., and Peppelenbos, H.W. (1999). Carbon dioxide and 1-MCP inhibit ethylene production and respiration of pear fruit by different mechanisms. Journal of experimental botany 50:837-844.
Delarue, M., Prinsen, E., Onckelen, H.V., Caboche, M., and Bellini, C. (1998). Sur2 mutations of Arabidopsis thaliana define a new locus involved in the control of auxin homeostasis. The Plant journal : for cell and molecular biology 14:603-611.
Delbarre, A., Muller, P., and Guern, J. (1998). Short-lived and phosphorylated proteins contribute to carrier-mediated efflux, but not to influx, of auxin in suspension-cultured tobacco cells. Plant physiology 116:833-844.
Delbarre, A., Muller, P., Imhoff, V., and Guern, J. (1996). Comparison of mechanisms controlling uptake and accumulation of 2, 4-dichlorophenoxy acetic acid, naphthalene-1-acetic acid, and indole-3-acetic acid in suspension-cultured tobacco cells. Planta 198:532-541.
Deslauriers, S.D., and Larsen, P.B. (2010). FERONIA is a key modulator of brassinosteroid and ethylene responsiveness in Arabidopsis hypocotyls. Molecular plant 3:626-640.
Dharmasiri, N., Dharmasiri, S., Weijers, D., Lechner, E., Yamada, M., Hobbie, L., Ehrismann, J.S., Jurgens, G., and Estelle, M. (2005). Plant development is regulated by a family of auxin receptor F box proteins. Dev Cell 9:109-119.
Dhonukshe, P., Grigoriev, I., Fischer, R., Tominaga, M., Robinson, D.G., Hasek, J., Paciorek, T., Petrasek, J., Seifertova, D., Tejos, R., et al. (2008). Auxin transport inhibitors impair vesicle motility and actin cytoskeleton dynamics in diverse eukaryotes. P Natl Acad Sci USA 105:4489-4494.
Ding, Z., Galvan-Ampudia, C.S., Demarsy, E., Langowski, L., Kleine-Vehn, J., Fan, Y., Morita, M.T., Tasaka, M., Fankhauser, C., Offringa, R., et al. (2011). Light-mediated polarization of the PIN3 auxin transporter for the phototropic response in Arabidopsis. Nature cell biology 13:447-452.
Dobrev, P.I., and Vankova, R. (2012). Quantification of abscisic acid, cytokinin, and auxin content in salt-stressed plant tissues. In: Plant Salt Tolerance: Springer. 251-261.
Dobson, C.M. (2004). Chemical space and biology. Nature 432:824-828.
Doerner, P., Jorgensen, J.E., You, R., Steppuhn, J., and Lamb, C. (1996). Control of root growth and development by cyclin expression. Nature 380:520-523.
Dolan, L., Duckett, C.M., Grierson, C., Linstead, P., Schneider, K., Lawson, E., Dean, C., Poethig, S., and Roberts, K. (1994). Clonal Relationships and Cell Patterning in the Root Epidermis of Arabidopsis. Development 120:2465-2474.
Dolan, L., Janmaat, K., Willemsen, V., Linstead, P., Poethig, S., Roberts, K., and Scheres, B. (1993). Cellular organisation of the Arabidopsis thaliana root. Development 119:71-84.
Dong, C.H., Jang, M., Scharein, B., Malach, A., Rivarola, M., Liesch, J., Groth, G., Hwang, I., and Chang, C. (2010). Molecular association of the Arabidopsis ETR1 ethylene receptor and a regulator of ethylene signaling, RTE1. J Biol Chem 285:40706-40713.
Dong, C.H., Rivarola, M., Resnick, J.S., Maggin, B.D., and Chang, C. (2008). Subcellular co-localization of Arabidopsis RTE1 and ETR1 supports a regulatory role for RTE1 in ETR1 ethylene signaling. Plant Journal 53:275-286.
Drakakaki, G., Robert, S., Szatmari, A.M., Brown, M.Q., Nagawa, S., Van Damme, D., Leonard, M., Yang, Z., Girke, T., Schmid, S.L., et al. (2011). Clusters of bioactive compounds target dynamic endomembrane networks in vivo. Proc Natl Acad Sci U S A 108:17850-17855.
Dugardeyn, J., and Van der Straeten, D. (2008). Ethylene: Fine-tuning plant growth and development by stimulation and inhibition of elongation. Plant Sci 175:59-70.
Dunand, C., Crevecoeur, M., and Penel, C. (2007). Distribution of superoxide and hydrogen peroxide in Arabidopsis root and their influence on root development: possible interaction with peroxidases. The New phytologist 174:332-341.
Dunlap, J.R., Kresovich, S., and McGee, R.E. (1986). The effect of salt concentration on auxin stability in culture media. Plant physiology 81:934-936.
Edlund, A., Eklof, S., Sundberg, B., Moritz, T., and Sandberg, G. (1995). A Microscale Technique for Gas Chromatography-Mass Spectrometry Measurements of Picogram Amounts of Indole-3-Acetic Acid in Plant Tissues. Plant physiology 108: 1043-1041 1047.
Egan, A.N., Schlueter, J., and Spooner, D.M. (2012). Applications of next-generation sequencing in plant biology. American journal of botany 99:175-185.
Esmon, C.A., Tinsley, A.G., Ljung, K., Sandberg, G., Hearne, L.B., and Liscum, E. (2005). A gradient of auxin and auxin-dependent transcription precedes tropic growth responses. Proc Natl Acad Sci U S A 103:236-241.
Estelle, M.A., and Somerville, C.R. (1987). Auxin Resistant Mutants of Arabidopsis with an Altered Morphology. J Cell Biochem:19-19.
Foreman, J., Demidchik, V., Bothwell, J.H., Mylona, P., Miedema, H., Torres, M.A., Linstead, P., Costa, S., Brownlee, C., Jones, J.D., et al. (2003). Reactive oxygen species produced by NADPH oxidase regulate plant cell growth. Nature 422:442-446.
Friml, J., and Jones, A.R. (2010). Endoplasmic reticulum: the rising compartment in auxin biology. Plant physiology 154:458-462.
Friml, J., Vieten, A., Sauer, M., Weijers, D., Schwarz, H., Hamann, T., Offringa, R., and Jurgens, G. (2003). Efflux-dependent auxin gradients establish the apical-basal axis of Arabidopsis. Nature 426:147-153.
Friml, J., Wisniewska, J., Benkova, E., Mendgen, K., and Palme, K. (2002). Lateral relocation of auxin efflux regulator PIN3 mediates tropism in Arabidopsis. Nature 415:806-809.
Fukaki, H., Wysocka-Diller, J., Kato, T., Fujisawa, H., Benfey, P.N., and Tasaka, M. (1998). Genetic evidence that the endodermis is essential for shoot gravitropism in Arabidopsis thaliana. The Plant journal : for cell and molecular biology 14:425-430.

Gadjev, I., Vanderauwera, S., Gechev, T.S., Laloi, C., Minkov, I.N., Shulaev, V., Apel, K., Inze, D., Mittler, R., and Van Breusegem, F. (2006). Transcriptomic footprints disclose specificity of reactive oxygen species signaling in Arabidopsis. Plant physiology 141:436-445.
Gälweiler, L., Guan, C., Müller, A., Wisman, E., Mendgen, K., Yephremov, A., and Palme, K. (1998). Regulation of polar auxin transport by AtPIN1 in Arabidopsis vascular tissue. Science 282 2226-2230
Gao, X., Yuan, H.M., Hu, Y.Q., Li, J., and Lu, Y.T. (2013). Mutation of Arabidopsis CATALASE2 results in hyponastic leaves by changes of auxin levels. Plant, cell & environment.
Geisler, M., Wang, B., and Zhu, J. (2014). Auxin transport during root gravitropism: transporters and techniques. Plant biology 16 Suppl 1:50-57.
Geitmann, A., Hush, J.M., and Overall, R.L. (1997). Inhibition of ethylene biosynthesis does not block microtubule re-orientation in wounded pea roots. Protoplasma 198:135-142.
Geldner, N., Friml, J., Stierhof, Y.-D., Jürgens, G., and Palme, K. (2001). Auxin transport inhibitors block PIN1 cycling and vesicle trafficking. Nature 413:425-428.
Gendreau, E., Traas, J., Desnos, T., Grandjean, O., Caboche, M., and Hofte, H. (1997). Cellular basis of hypocotyl growth in arabidopsis thaliana. Plant physiology vol. 114:295-305.
Gendron, J.M., Haque, A., Gendron, N., Chang, T., Asami, T., and Wang, Z.Y. (2008). Chemical genetic dissection of brassinosteroid-ethylene interaction. Molecular plant 1:368-379.
Giovanelli, J., Mudd, S.H., and Datko, A.H. (1985). Quantitative analysis of pathways of methionine metabolism and their regulation in Lemna. Plant physiology 78:555-560.
Girke, T., Cheng, L.C., and Raikhel, N. (2005). ChemMine. A compound mining database for chemical genomics. Plant physiology 138:573-577.
Gomezlim, M.A., Valdeslopez, V., Cruzhernandez, A., and Saucedoarias, L.J. (1993). Isolation and Characterization of a Gene Involved in Ethylene Biosynthesis from Arabidopsis-Thaliana. Gene 134:217-221.
Gong, W., He, K., Covington, M., Dinesh-Kumar, S.P., Snyder, M., Harmer, S.L., Zhu, Y.X., and Deng, X.W. (2008). The development of protein microarrays and their applications in DNA-protein and protein-protein interaction analyses of Arabidopsis transcription factors. Molecular plant 1:27-41.
Gorny, J.R., and Kader, A.A. (1996). Regulation of ethylene biosynthesis in climacteric apple fruit by elevated CO2 and reduced O-2 atmospheres. Postharvest Biol Tec 9:311-323.
Grebe, M., Friml, J., Swarup, R., Ljung, K., Sandberg, G., Terlou, M., Palme, K., Bennett, M.J., and Scheres, B. (2002). Cell polarity signaling in Arabidopsis involves a BFA-sensitive auxin influx pathway. Current biology : CB 12:329-334.
Greene, E.A., Codomo, C.A., Taylor, N.E., Henikoff, J.G., Till, B.J., Reynolds, S.H., Enns, L.C., Burtner, C., Johnson, J.E., Odden, A.R., et al. (2003). Spectrum of chemically induced mutations from a large-scale reverse-genetic screen in Arabidopsis. Genetics 164:731-740.
Griffiths, A., Miller, J., and Suzuki, D. (2000). Chi-square test for linkage. In: An Introduction to Genetic Analysis New York: W. H. Freeman.
Grossmann, K. (2003). Mediation of Herbicide Effects by Hormone Interactions. Journal of plant growth regulation 22:109-122.
Grossmann, K., and Kwiatkowski, J. (1995). Evidence for a causative role of cyanide, derived from ethylene biosynthesis, in the herbicidal mode of action of Quinclorac in Barnyard grass. Pesticide biochemistry and physiology 51:150-160.
Grossmann, K., and Scheltrup, F. (1998). Studies on the mechanism of selectivity of the auxin herbicide quinmerac. Pesticide Science 52:111-118.
Grozinger, C.M., Chao, E.D., Blackwell, H.E., Moazed, D., and Schreiber, S.L. (2001). Identification of a class of small molecule inhibitors of the sirtuin family of NAD-dependent deacetylases by phenotypic screening. J Biol Chem 276:38837-38843.
Guzman, P., and Ecker, J.R. (1990). Exploiting the Triple Response of Arabidopsis to Identify Ethylene-Related Mutants. Plant Cell 2:513-523.
Hagen, G., and Guilfoyle, T. (2002). Auxin-responsive gene expression: genes, promoters and regulatory factors. Plant Mol Biol 49:373-385.
Haggarty, S.J., Mayer, T.U., Miyamoto, D.T., Fathi, R., King, R.W., Mitchison, T.J., and Schreiber, S.L. (2000). Dissecting cellular processes using small molecules: identification of colchicine-like, taxol-like and other small molecules that perturb mitosis. Chem Biol 7:275-286.
Harper, R.M., Stowe-Evans, E.L., Luesse, D.R., Muto, H., Tatematsu, K., Watahiki, M.K., Yamamoto, K., and Liscum, E. (2000). The NPH4 Locus Encodes the Auxin Response Factor ARF7, a Conditional Regulator of Differential Growth in Aerial Arabidopsis Tissue. The Plant Cell 12:757–770.
Hayashi, K.-I., and Overvoorde, P. (2013). Use of Chemical Biology to Understand Auxin Metabolism, Signaling, and Polar Transport. In: Plant Chemical Biology --Audenaert, D., and Overvoorde, P., eds.: John Wiley & Sons, Inc, Hoboken, New Jersey.
Hayashi, K. (2012). The interaction and integration of auxin signaling components. Plant Cell Physiol 53:965-975.
Hayashi, K., Nakamura, S., Fukunaga, S., Nishimura, T., Jenness, M.K., Murphy, A.S., Motose, H., Nozaki, H., Furutani, M., and Aoyama, T. (2014). Auxin transport sites are visualized in planta using fluorescent auxin analogs. Proc Natl Acad Sci U S A 111:11557-11562.
Hayashi, K., Neve, J., Hirose, M., Kuboki, A., Shimada, Y., Kepinski, S., and Nozaki, H. (2012). Rational design of an auxin antagonist of the SCF(TIR1) auxin receptor complex. ACS chemical biology 7:590-598.
Hayashi, K., Tan, X., Zheng, N., Hatate, T., Kimura, Y., Kepinski, S., and Nozaki, H. (2008). Small-molecule agonists and antagonists of F-box protein-substrate interactions in auxin perception and signaling. P Natl Acad Sci USA 105:5632-5637.
He, J., Duan, Y., Hua, D., Fan, G., Wang, L., Liu, Y., Chen, Z., Han, L., Qu, L.J., and Gong, Z. (2012). DEXH box RNA helicase-mediated mitochondrial reactive oxygen species production in Arabidopsis mediates crosstalk between abscisic acid and auxin signaling. Plant Cell 24:1815-1833.
He, W.R., Brumos, J., Li, H.J., Ji, Y.S., Ke, M., Gong, X.Q., Zeng, Q.L., Li, W.Y., Zhang, X.Y., An, F.Y., et al. (2011). A Small-Molecule Screen Identifies L-Kynurenine as a Competitive Inhibitor of TAA1/TAR Activity in Ethylene-Directed Auxin Biosynthesis and Root Growth in Arabidopsis. Plant Cell 23:3944-3960.
Henderson, J., Bauly, J.M., Ashford, D.A., Oliver, S.C., Hawes, C.R., Lazarus, C.M., Venis, M.A., and Napier, R.M. (1997). Retention of maize auxin-binding protein in the endoplasmic reticulum: quantifying escape and the role of auxin. Planta 202:313-323.
Hicks, G.R., and Raikhel, N.V. (2009). Opportunities and challenges in plant chemical biology. Nat Chem Biol 5:268-272.
Hicks, G.R., and Raikhel, N.V. (2012). Small molecules present large opportunities in plant biology. Annual review of plant biology 63:261-282.
Hicks, G.R., and Raikhel, N.V. (2014). Plant chemical biology: are we meeting the promise? Frontiers in plant science 5:455.
Hirayama, T., Kieber, J.J., Hirayama, N., Kogan, M., Guzman, P., Nourizadeh, S., Alonso, J.M., Dailey, W.P., Dancis, A., and Ecker, J.R. (1999). Responsive-to-antagonist1, a Menkes/Wilson disease-related copper transporter, is required for ethylene signaling in Arabidopsis. Cell 97:383-393.

Hopkins, A.L., and Groom, C.R. (2002). The druggable genome. Nat Rev Drug Discov 1:727-730.
Hošek, P., Kubeš, M., Laňková, M., Dobrev, P.I., Klíma, P., Kohoutová, M., Petrášek, J., Hoyerová, K., Jiřina, M., and Zažímalová, E. (2012). Auxin transport at cellular level: new insights supported by mathematical modelling. Journal of Experimental Botany, 63:3815-3827.
Hoson, T., Saito, Y., Soga, K., and Wakabayashi, K. (2005). Signal perception, transduction, and response in gravity resistance. Another graviresponse in plants. Advances in Space Research 36:1196-1202.
Hu, Y., Callebert, P., Vandemoortel, I., Nguyen, L., Audenaert, D., Verschraegen, L., Vandenbussche, F., and Van Der Straeten, D. (2014). TR-DB: an open-access database of compounds affecting the ethylene-induced triple response in Arabidopsis. Plant Physiology and Biochemistry 75:128-137.
Hu, Y., Vandenbussche, F., and Van Der Straeten, D. (2013). Chemical genetics as a tool to study ethylene biology in plants. Plant Chemical Biology:184.
Huang, J., Zhu, H., Haggarty, S.J., Spring, D.R., Hwang, H., Jin, F.L., Snyder, M., and Schreiber, S.L. (2004). Finding new components of the target of rapamycin (TOR) signaling network through chemical genetics and proteome chips. P Natl Acad Sci USA 101:16594-16599.
Ichikawa, T., Nakazawa, M., Kawashima, M., Iizumi, H., Kuroda, H., Kondou, Y., Tsuhara, Y., Suzuki, K., Ishikawa, A., Seki, M., et al. (2006). The FOX hunting system: an alternative gain-of-function gene hunting technique. The Plant journal : for cell and molecular biology 48:974-985.
Ikeda, Y., Men, S., Fischer, U., Stepanova, A.N., Alonso, J.M., Ljung, K., and Grebe, M. (2009). Local auxin biosynthesis modulates gradient-directed planar polarity in Arabidopsis. Nature cell biology 11:731-738.
Irizarry, R.A., Hobbs, B., Collin, F., Beazer-Barclay, Y.D., Antonellis, K.J., Scherf, U., and Speed, T.P. (2003). Exploration, normalization, and summaries of high density oligonucleotide array probe level data. Biostatistics 4:249-264.
Irwin, J.J. (2006). How good is your screening library? Curr Opin Chem Biol 10:352-356.
Isaacs, J.T., Pili, R., Qian, D.Z., Dalrymple, S.L., Garrison, J.B., Kyprianou, N., Bjork, A., Olsson, A., and Leanderson, T. (2006). Identification of ABR-215050 as lead second generation quinoline-3-carboxamide anti-angiogenic agent for the treatment of prostate cancer. The Prostate 66:1768-1778.
Ivanchenko, M.G., den Os, D., Monshausen, G.B., Dubrovsky, J.G., Bednarova, A., and Krishnan, N. (2013). Auxin increases the hydrogen peroxide (H2O2) concentration in tomato (Solanum lycopersicum) root tips while inhibiting root growth. Ann Bot 112:1107-1116.
Jaillais, Y., and Chory, J. (2010). Unraveling the paradoxes of plant hormone signaling integration. Nature structural & molecular biology 17:642-645.
Jensen, P.J., Hangarter, R.P., and Estelle, M. (1998). Auxin transport is required for hypocotyl elongation in light-grown but not dark-grown Arabidopsis. Plant physiology 116:455-462.
Jeong, S., Kim, J.-Y., Choi, H., Kim, H., Lee, I., Soh, M.-S., Nam, H.G., Chang, Y.-T., Lim, P.O., and Woo, H.R. (2015). Rootin, a compound that inhibits root development through modulating PIN-mediated auxin distribution. Plant Science 233:116-126.
Jiang, K., Meng, Y.L., and Feldman, L.J. (2003). Quiescent center formation in maize roots is associated with an auxin-regulated oxidizing environment. Development 130:1429-1438.
Jing, Y., Zhang, D., Wang, X., Tang, W., Wang, W., Huai, J., Xu, G., Chen, D., Li, Y., and Lin, R. (2013). Arabidopsis chromatin remodeling factor PICKLE interacts with transcription factor HY5 to regulate hypocotyl cell elongation. The Plant Cell 25:242-256.
Johnson, P.R., and Ecker, J.R. (1998). The ethylene gas signal transduction pathway: a molecular perspective. Annual review of genetics 32:227-254.
Jones, A.M., and Herman, E.M. (1993). KDEL-Containing Auxin-Binding Protein Is Secreted to the Plasma Membrane and Cell Wall. Plant physiology 101:595-606.
Joo, J.H., Bae, Y.S., and Lee, J.S. (2001). Role of auxin-induced reactive oxygen species in root gravitropism. Plant physiology 126:1055-1060.
Ju, C., Yoon, G.M., Shemansky, J.M., Lin, D.Y., Ying, Z.I., Chang, J., Garrett, W.M., Kessenbrock, M., Groth, G., Tucker, M.L., et al. (2012). CTR1 phosphorylates the central regulator EIN2 to control ethylene hormone signaling from the ER membrane to the nucleus in Arabidopsis. Proc Natl Acad Sci U S A 109:19486-19491.
Jurado, S., Abraham, Z., Manzano, C., Lopez-Torrejon, G., Pacios, L.F., and Del Pozo, J.C. (2010). The Arabidopsis cell cycle F-box protein SKP2A binds to auxin. Plant Cell 22:3891-3904.
Kai, K., Horita, J., Wakasa, K., and Miyagawa, H. (2007). Three oxidative metabolites of indole-3-acetic acid from Arabidopsis thaliana. Phytochemistry 68:1651-1663.
Kakei, Y., Yamazaki, C., Suzuki, M., Nakamura, A., Sato, A., Ishida, Y., Kikuchi, R., Higashi, S., Kokudo, Y., Ishii, T., et al. (2015). Small-molecule auxin inhibitors that target YUCCA are powerful tools for studying auxin function. The Plant journal : for cell and molecular biology.
Kaneda, M., Schuetz, M., Lin, B.S., Chanis, C., Hamberger, B., Western, T.L., Ehlting, J., and Samuels, A.L. (2011). ABC transporters coordinately expressed during lignification of Arabidopsis stems include a set of ABCBs associated with auxin transport. Journal of experimental botany 62:2063-2077.
Kapulnik, Y., Resnick, N., Mayzlish-Gati, E., Kaplan, Y., Wininger, S., Hershenhorn, J., and Koltai, H. (2011). Strigolactones interact with ethylene and auxin in regulating root-hair elongation in Arabidopsis. Journal of experimental botany 62:2915-2924.
Kaschani, F., and van der Hoorn, R. (2007). Small molecule approaches in plants. Curr Opin Chem Biol 11:88-98.
Kaschani, F., Verhelst, S.H.L., van Swieten, P.F., Verdoes, M., Wong, C.S., Wang, Z.M., Kaiser, M., Overkleeft, H.S., Bogyo, M., and van der Hoorn, R.A.L. (2009). Minitags for small molecules: detecting targets of reactive small molecules in living plant tissues using 'click chemistry'. Plant Journal 57:373-385.
Katoh, A., and Hashimoto, T. (2004). Molecular biology of pyridine nucleotide and nicotine biosynthesis. Front Biosci 9:1577-1586.
Kawano, T., and Muto, S. (2000). Mechanism of peroxidase actions for salicylic acid-induced generation of active oxygen species and an increase in cytosolic calcium in tobacco cell suspension culture. Journal of experimental botany 51:685-693.
Kazan, K. (2015). Diverse roles of jasmonates and ethylene in abiotic stress tolerance. Trends in plant science 20:219-229.
Kerbel, E.L., Kader, A.A., and Romani, R.J. (1988). Effects of Elevated Co2 Concentrations on Glycolysis in Intact Bartlett Pear Fruit. Plant physiology 86:1205-1209.
Kieber, J., Rothenberg, M., Roman, G., Feldmann, K., and Ecker, J. (1993). CTR1, a negative regulator of the ethylene response pathway in Arabidopsis, encodes a member of the raf family of protein kinases. Cell 72:427-441.
Kim, H.K., Choi, Y.H., and Verpoorte, R. (2010a). NMR-based metabolomic analysis of plants. Nat Protoc 5:536-549.
Kim, H.K., Choi, Y.H., and Verpoorte, R. (2011a). NMR-based plant metabolomics: where do we stand, where do we go? Trends in biotechnology 29:267-275.

Kim, J.Y., Henrichs, S., Bailly, A., Vincenzetti, V., Sovero, V., Mancuso, S., Pollmann, S., Kim, D., Geisler, M., and Nam, H.G. (2010b). Identification of an ABCB/P-glycoprotein-specific inhibitor of auxin transport by chemical genomics. J Biol Chem 285:23309-23317.
Kim, T.H., Hauser, F., Ha, T., Xue, S., Bohmer, M., Nishimura, N., Munemasa, S., Hubbard, K., Peine, N., Lee, B.H., et al. (2011b). Chemical genetics reveals negative regulation of abscisic acid signaling by a plant immune response pathway. Curr Biol 21:990-997.
Kim, Y., Schumaker, K.S., and Zhu, J.K. (2006). EMS mutagenesis of Arabidopsis. Methods in molecular biology 323:101-103.
Klee, H.J., and Giovannoni, J.J. (2011). Genetics and control of tomato fruit ripening and quality attributes. Annual review of genetics 45:41-59.
Kleine-Vehn, J., Langowski, L., Wisniewska, J., Dhonukshe, P., Brewer, P.B., and Friml, J. (2008). Cellular and molecular requirements for polar PIN targeting and transcytosis in plants. Molecular plant 1:1056-1066.
Kley, N. (2004). Chemical dimerizers and three-hybrid systems: Scanning the proteome for targets of organic small molecules. Chem Biol 11:599-608.
Knight, L., Rose, R., and Crocker, W. (1910). Effect of various gases and vapors upon etiolated seedlings of the sweet pea. Science 31:635-636.
Kolb, H.C. (2001). Application of Click chemistry to the generation of new chemical libraries for drug discovery. Abstr Pap Am Chem S 221:U174-U174.
Koornneef, M. (1994). 5 Arabidopsis Genetics. Cold Spring Harbor Monograph Archive 27:89-120.
Koprivova, A., Mugford, S.T., and Kopriva, S. (2010). Arabidopsis root growth dependence on glutathione is linked to auxin transport. Plant cell reports 29:1157-1167.
Korasick, D.A., Enders, T.A., and Strader, L.C. (2013). Auxin biosynthesis and storage forms. Journal of experimental botany 64:2541-2555.
Kowalczyk, M., and Sandberg, G. (2001). Quantitative analysis of indole-3-acetic acid metabolites in Arabidopsis. Plant physiology 127:1845-1853.
Koyama, T. (2014). The roles of ethylene and transcription factors in the regulation of onset of leaf senescence. Frontiers in plant science 5:650.
Křeček, P. (2011). Regulation of activity of auxin efflux transporters In: Department of Experimental Plant Biology Prague, Czech Republic: Charles University.
Krishnamurthy, A., and Rathinasabapathi, B. (2013). Oxidative stress tolerance in plants: Novel interplay between auxin and reactive oxygen species signaling. Plant signaling & behavior 8:e25761.
Kubes, M., Yang, H., Richter, G.L., Cheng, Y., Mlodzinska, E., Wang, X., Blakeslee, J.J., Carraro, N., Petrasek, J., Zazimalova, E., et al. (2012). The Arabidopsis concentration-dependent influx/efflux transporter ABCB4 regulates cellular auxin levels in the root epidermis. The Plant journal : for cell and molecular biology 69:640-654.
Larsen, P.B., and Chang, C. (2001). The Arabidopsis eer1 mutant has enhanced ethylene responses in the hypocotyl and stem. Plant physiology 125:1061-1073.
Lau, O.-L., and Yang, S.F. (1976). Inhibition of ethylene production by cobaltous ion. Plant physiology 58:114-117.
Lawton, K.A., Potter, S.L., Uknes, S., and Ryals, J. (1994). Acquired-Resistance Signal-Transduction in Arabidopsis Is Ethylene Independent. Plant Cell 6:581-588.
Le, J., Vandenbussche, F., Cnodder, T., Straeten, D., and Verbelen, J.-P. (2005). Cell Elongation and Microtubule Behavior in the Arabidopsis Hypocotyl: Responses to Ethylene and Auxin. Journal of plant growth regulation 24:166-178.
Le, J., Vandenbussche, F., Straeten, D.V.D., and Verbelen, J.-P. (2004). Position and cell type-dependent microtubule reorientation characterizes the early response of the Arabidopsis root epidermis to ethylene. Physiol Plantarum 121:513–519.
Le, J., Vandenbussche, F., Van Der Straeten, D., and Verbelen, J.P. (2001). In the early response of Arabidopsis roots to ethylene, cell elongation is up- and down-regulated and uncoupled from differentiation. Plant physiology 125:519-522.
Leblanc, A., Renault, H., Lecourt, J., Etienne, P., Deleu, C., and Le Deunff, E. (2008). Elongation changes of exploratory and root hair systems induced by aminocyclopropane carboxylic acid and aminoethoxyvinylglycine affect nitrate uptake and BnNrt2. 1 and BnNrt1. 1 transporter gene expression in oilseed rape. Plant physiology 146:1928-1940.
Lee, J.S., Chang, W.-K., and Evans, M.L. (1990). Effects of ethylene on the kinetics of curvature and auxin redistribution in gravistimulated roots of Zea mays. Plant physiology 94:1770–1775.
Lehman, A., Black, R., and Ecker, J.R. (1996). HOOKLESS1, an ethylene response gene, is required for differential cell elongation in the Arabidopsis hypocotyl. Cell 85:183-194.
Lewis, D.R., Miller, N.D., Splitt, B.L., Wu, G., and Spalding, E.P. (2007). Separating the roles of acropetal and basipetal auxin transport on gravitropism with mutations in two Arabidopsis multidrug resistance-like ABC transporter genes. Plant Cell 19:1838-1850.
Lewis, D.R., and Muday, G.K. (2009). Measurement of auxin transport in Arabidopsis thaliana. Nat Protoc 4:437-451.
Lewis, D.R., Ramirez, M.V., Miller, N.D., Vallabhaneni, P., Ray, W.K., Helm, R.F., Winkel, B.S., and Muday, G.K. (2011). Auxin and ethylene induce flavonol accumulation through distinct transcriptional networks. Plant physiology 156:144-164.
Leyser, H.M., Lincoln, C.A., Timpte, C., Lammer, D., Turner, J., and Estelle, M. (1993). Arabidopsis auxin-resistance gene AXR1 encodes a protein related to ubiquitin-activating enzyme E1. Nature 364:161-164.
Leyser, H.M., Pickett, F.B., Dharmasiri, S., and Estelle, M. (1996). Mutations in the AXR3 gene of Arabidopsis result in altered auxin response including ectopic expression from the SAUR-AC1 promoter. The Plant journal : for cell and molecular biology 10:403-413.
Li, H., Johnson, P., Stepanova, A., Alonso, J.M., and Ecker, J.R. (2004). Convergence of signaling of differential cell growth pathways in the control in Arabidopsis. Dev Cell 7:193-204.
Li, W., Ma, M., Feng, Y., Li, H., Wang, Y., Ma, Y., Li, M., An, F., and Guo, H. (2015). EIN2-directed translational regulation of ethylene signaling in Arabidopsis. Cell 163:670-683.
Liang, X., Wang, H., Mao, L., Hu, Y., Dong, T., Zhang, Y., Wang, X., and Bi, Y. (2012). Involvement of COP1 in ethylene-and light-regulated hypocotyl elongation. Planta 236:1791-1802.
Licitra, E.J., and Liu, J.O. (1996). A three-hybrid system for detecting small ligand-protein receptor interactions. Proc Natl Acad Sci U S A 93:12817-12821.
Lin, L.C., Hsu, J.H., and Wang, L.C. (2010). Identification of Novel Inhibitors of 1-Aminocyclopropane-1-carboxylic Acid Synthase by Chemical Screening in Arabidopsis thaliana. J Biol Chem 285:33445-33456.
Lincoln, C., Britton, J.H., and Estelle, M. (1990). Growth and development of the axr1 mutants of Arabidopsis. Plant Cell 2:1071-1080.
Linkies, A., and Leubner-Metzger, G. (2012). Beyond gibberellins and abscisic acid: how ethylene and jasmonates control seed germination. Plant cell reports 31:253-270.
Lipinski, C., and Hopkins, A. (2004). Navigating chemical space for biology and medicine. Nature 432:855-861.
Ljung, K. (2013). Auxin metabolism and homeostasis during plant development. Development 140:943-950.

Ljung, K., Hull, A.K., Celenza, J., Yamada, M., Estelle, M., Normanly, J., and Sandberg, G. (2005). Sites and regulation of auxin biosynthesis in Arabidopsis roots. Plant Cell 17:1090-1104.
Lohse, M., Nunes-Nesi, A., Kruger, P., Nagel, A., Hannemann, J., Giorgi, F.M., Childs, L., Osorio, S., Walther, D., Selbig, J., et al. (2010). Robin: an intuitive wizard application for R-based expression microarray quality assessment and analysis. Plant physiology 153:642-651.
Lomenick, B., Hao, R., Jonai, N., Chin, R.M., Aghajan, M., Warburton, S., Wang, J., Wu, R.P., Gomez, F., Loo, J.A., et al. (2009). Target identification using drug affinity responsive target stability (DARTS). Proc Natl Acad Sci U S A 106:21984-21989.
Ludwig-Muller, J. (2011). Auxin conjugates: their role for plant development and in the evolution of land plants. Journal of experimental botany 62:1757-1773.
Luschnig, C., Gaxiola, R.A., Grisafi, P., and Fink, G.R. (1998). EIR1, a root-specific protein involved in auxin transport, is required for gravitropism in Arabidopsis thaliana. Gene Dev 12:2175-2187.
Ma, Q., and Robert, S. (2013). Auxin biology revealed by small molecules. Physiol Plant.
Maere, S., Heymans, K., and Kuiper, M. (2005). BiNGO: a Cytoscape plugin to assess overrepresentation of gene ontology categories in biological networks. Bioinformatics 21:3448-3449.
Mano, Y., and Nemoto, K. (2012). The pathway of auxin biosynthesis in plants. Journal of experimental botany 63:2853-2872.
Marchant, A., Bhalerao, R., Casimiro, I., Eklof, J., Casero, P.J., Bennett, M., and Sandberg, G. (2002). AUX1 promotes lateral root formation by facilitating indole-3-acetic acid distribution between sink and source tissues in the Arabidopsis seedling. Plant Cell 14:589-597.
Marchant, A., Kargul, J., T.May, S., Muller, P., Delbarre, A., Perrot-Rechenmann, C., and J.Bennett, M. (1999). AUX1 regulates root gravitropism in Arabidopsis by facilitating auxin uptake within root apical tissues. The EMBO Journal 18:2066–2073.
Martin, M.N., Cohen, J.D., and Saftner, R.A. (1995). A new 1-aminocyclopropane-1-carboxylic acid-conjugating activity in tomato fruit. Plant physiology 109:917-926.
Mashiguchi, K., Tanaka, K., Sakai, T., Sugawara, S., Kawaide, H., Natsume, M., Hanada, A., Yaeno, T., Shirasu, K., Yao, H., et al. (2011). The main auxin biosynthesis pathway in Arabidopsis. PNAS 108:18512-18517.
Masucci, J.D., and Schiefelbein, J.W. (1994). The rhd6 Mutation of Arabidopsis thaliana Alters Root-Hair Initiation through an Auxin- and Ethylene-Associated Process. Plant physiology 106:1335-1346.
Masucci, J.D., and Schiefelbein, J.W. (1996). Hormones act downstream of TTG and GL2 to promote root hair outgrowth during epidermis development in the Arabidopsis root. The Plant Cell 8:1505-1517.
Mathooko, F.M., Tsunashima, Y., Owino, W.Z.O., Kubo, Y., and Inaba, A. (2001). Regulation of genes encoding ethylene biosynthetic enzymes in peach (Prunus persica L.) fruit by carbon dioxide and 1-methylcyclopropene. Postharvest Biol Tec 21:265-281.
Mathur, J., Molnar, G., Fujioka, S., Takatsuto, S., Sakurai, A., Yokota, T., Adam, G., Voigt, B., Nagy, F., Maas, C., et al. (1998). Transcription of the Arabidopsis CPD gene, encoding a steroidogenic cytochrome P450, is negatively controlled by brassinosteroids. Plant Journal 14:593-602.
Mazzella, M.A., Casal, J.J., Muschietti, J.P., and Fox, A.R. (2014). Hormonal networks involved in apical hook development in darkness and their response to light. Frontiers in plant science 5.
McDonnell, L., Plett, J.M., Andersson-Gunnerås, S., Kozela, C., Dugardeyn, J., Van Der Straeten, D., Glick, B.R., Sundberg, B., and Regan, S. (2009). Ethylene levels are regulated by a plant encoded 1-aminocyclopropane-1-carboxylic acid deaminase. Physiol Plantarum 136:94-109.
Mehta, P.K., Hale, T.I., and Christen, P. (1993). Aminotransferases - Demonstration of Homology and Division into Evolutionary Subgroups. Eur J Biochem 214:549-561.
Merchante, C., Brumos, J., Yun, J., Hu, Q., Spencer, K.R., Enriquez, P., Binder, B.M., Heber, S., Stepanova, A.N., and Alonso, J.M. (2015). Gene-specific translation regulation mediated by the hormone-signaling molecule EIN2. Cell 163:684-697.
Mhaske, S.B., and Argade, N.P. (2006). The chemistry of recently isolated naturally occurring quinazolinone alkaloids☆. Tetrahedron 62:9787-9826.
Mikkelsen, M.D., Naur, P., and Halkier, B.A. (2004). Arabidopsis mutants in the C-S lyase of glucosinolate biosynthesis establish a critical role for indole-3-acetaldoxime in auxin homeostasis. The Plant Journal 37:770–777.
Morreel, K., Saeys, Y., Dima, O., Lu, F., Van de Peer, Y., Vanholme, R., Ralph, J., Vanholme, B., and Boerjan, W. (2014). Systematic Structural Characterization of Metabolites in Arabidopsis via Candidate Substrate-Product Pair Networks. Plant Cell 26:929-945.
Motte, H., Galuszka, P., Spichal, L., Tarkowski, P., Plihal, O., Smehilova, M., Jaworek, P., Vereecke, D., Werbrouck, S., and Geelen, D. (2013). Phenyl-adenine, identified in a LIGHT-DEPENDENT SHORT HYPOCOTYLS4-assisted chemical screen, is a potent compound for shoot regeneration through the inhibition of CYTOKININ OXIDASE/DEHYDROGENASE activity. Plant physiology 161:1229-1241.
Mravec, J., Kubes, M., Bielach, A., Gaykova, V., Petrasek, J., Skupa, P., Chand, S., Benkova, E., Zazimalova, E., and Friml, J. (2008). Interaction of PIN and PGP transport mechanisms in auxin distribution-dependent development. Development 135:3345-3354.
Mravec, J., Skupa, P., Bailly, A., Hoyerova, K., Krecek, P., Bielach, A., Petrasek, J., Zhang, J., Gaykova, V., Stierhof, Y.D., et al. (2009). Subcellular homeostasis of phytohormone auxin is mediated by the ER-localized PIN5 transporter. Nature 459:1136-1140.
Muday, G.K., Brady, S.R., Argueso, C., Deruere, J., Kieber, J.J., and DeLong, A. (2006). RCN1-regulated phosphatase activity and EIN2 modulate hypocotyl gravitropism by a mechanism that does not require ethylene signaling. Plant physiology 141:1617-1629.
Muday, G.K., Rahman, A., and Binder, B.M. (2012). Auxin and ethylene: collaborators or competitors? Trends in plant science 17:181-195.
Muller, A., Guan, C.H., Galweiler, L., Tanzler, P., Huijser, P., Marchant, A., Parry, G., Bennett, M., Wisman, E., and Palme, K. (1998). AtPIN2 defines a locus of Arabidopsis for root gravitropism control. Embo J 17:6903-6911.
Nagashima, A., Uehara, Y., and Sakai, T. (2008). The ABC subfamily B auxin transporter AtABCB19 is involved in the inhibitory effects of N-1-naphthyphthalamic acid on the phototropic and gravitropic responses of Arabidopsis hypocotyls. Plant Cell Physiol 49:1250-1255.
Nagata, T., Nemoto, Y., and Hasezawa, S. (1992). Tobacco by-2 Cell-Line as the Hela-Cell in the Cell Biology of Higher-Plants. Int Rev Cytol 132:1-30.
Nakamoto, D., A, I., T, A., and KT, Y. (2006). Inhibition of Brassinosteroid Biosynthesis by Either a dwarf4 Mutation or a Brassinosteroid Biosynthesis Inhibitor Rescues Defects in Tropic Responses of Hypocotyls in the Arabidopsis Mutant nonphototropic hypocotyl 4. Plant physiology 141:456-464.
Narayan Acharya, B., Thavaselvam, D., and Parshad Kaushik, M. (2008). Synthesis and antimalarial evaluation of novel pyridine quinoline hybrids. Medicinal Chemistry Research 17:487-494.
Negi, S., Ivanchenko, M.G., and Muday, G.K. (2008). Ethylene regulates lateral root formation and auxin transport in Arabidopsis thaliana. The Plant journal : for cell and molecular biology 55:175-187.
Neljubov, D. (1901). Uber die horizontale Nutation der Stengel von Pisum sativum und einiger anderen Pflanzen. Beih. Bot. Centralbl. 10:128–139.

Nemhauser, J.L., Hong, F., and Chory, J. (2006). Different plant hormones regulate similar processes through largely nonoverlapping transcriptional responses. Cell 126:467-475.
Nemhauser, J.L., Mockler, T.C., and Chory, J. (2004). Interdependency of brassinosteroid and auxin signaling in Arabidopsis. PLoS biology 2:E258.
Nieuwland, J., Maughan, S., Dewitte, W., Scofield, S., Sanz, L., and Murray, J.A. (2009). The D-type cyclin CYCD4;1 modulates lateral root density in Arabidopsis by affecting the basal meristem region. Proc Natl Acad Sci U S A 106:22528-22533.
Noh, B., Bandyopadhyay, A., Peer, W.A., Spalding, E.P., and Murphy, A.S. (2003). Enhanced gravi- and phototropism in plant mdr mutants mislocalizing the auxin efflux protein PIN1. Nature 423:999-1002.
Noh, B., Murphy, A.S., and Spalding, E.P. (2001). Multidrug resistance-like genes of Arabidopsis required for auxin transport and auxin-mediated development. Plant Cell 13:2441-2454.
Norambuena, L., Hicks, G.R., and Raikhel, N.V. (2009). The use of chemical genomics to investigate pathways intersecting auxin-dependent responses and endomembrane trafficking in Arabidopsis thaliana. Methods in molecular biology 495:133-143.
Normanly, J., Cohen, J.D., and Fink, G.R. (1993). Arabidopsis thaliana auxotrophs reveal a tryptophan-independent biosynthetic pathway for indole-3-acetic acid. Proc Natl Acad Sci U S A 90:10355-10359.
Novak, O., Henykova, E., Sairanen, I., Kowalczyk, M., Pospisil, T., and Ljung, K. (2012). Tissue-specific profiling of the Arabidopsis thaliana auxin metabolome. The Plant journal : for cell and molecular biology 72:523-536.
Okada, K., and Shimura, Y. (1994). Genetic analyses of signalling in flower development using Arabidopsis. Plant Mol Biol 26:1357-1377.
Okushima, Y., Mitina, I., Quach, H.L., and Theologis, A. (2005a). AUXIN RESPONSE FACTOR 2 (ARF2): a pleiotropic developmental regulator. The Plant journal : for cell and molecular biology 43:29-46.
Okushima, Y., Overvoorde, P.J., Arima, K., Alonso, J.M., Chan, A., Chang, C., Ecker, J.R., Hughes, B., Lui, A., Nguyen, D., et al. (2005b). Functional genomic analysis of the AUXIN RESPONSE FACTOR gene family members in Arabidopsis thaliana: unique and overlapping functions of ARF7 and ARF19. Plant Cell 17:444-463.
Olmedo, G., Guo, H., Gregory, B.D., Nourizadeh, S.D., Aguilar-Henonin, L., Li, H., An, F., Guzman, P., and Ecker, J.R. (2006). ETHYLENE-INSENSITIVE5 encodes a 5'-->3' exoribonuclease required for regulation of the EIN3-targeting F-box proteins EBF1/2. Proc Natl Acad Sci U S A 103:13286-13293.
Osswald, W.F., Schütz, W., and Elstner, E.F. (1988). Indole-3-acetic Acid oxidation and crocin bleaching by horseradish peroxidase. Plant physiology 86:1310–1314.
Ostin, A., Kowalyczk, M., Bhalerao, R.P., and Sandberg, G. (1998). Metabolism of indole-3-acetic acid in Arabidopsis. Plant physiology 118:285-296.
Ouyang, J., Shao, X., and Li, J. (2000). Indole-3-glycerol phosphate, a branchpoint of indole-3-acetic acid biosynthesis from the tryptophan biosynthetic pathway in Arabidopsis thaliana. The Plant Journal 24:327–334.
Page, D.R., and Grossniklaus, U. (2002). The art and design of genetic screens: Arabidopsis thaliana. Nature reviews. Genetics 3:124-136.
Paredez, A.R., Somerville, C.R., and Ehrhardt, D.W. (2006). Visualization of cellulose synthase demonstrates functional association with microtubules. Science 312:1491-1495.
Park, S.Y., Fung, P., Nishimura, N., Jensen, D.R., Fujii, H., Zhao, Y., Lumba, S., Santiago, J., Rodrigues, A., Chow, T.F., et al. (2009). Abscisic acid inhibits type 2C protein phosphatases via the PYR/PYL family of START proteins. Science 324:1068-1071.
Parry, G., Delbarre, A., Marchant, A., Swarup, R., Napier, R., Perrot-Rechenmann, C., and Bennett, M.J. (2001). Novel auxin transport inhibitors phenocopy the auxin influx carrier mutation aux1. The Plant journal : for cell and molecular biology 25:399-406.
Passardi, F., Penel, C., and Dunand, C. (2004). Performing the paradoxical: how plant peroxidases modify the cell wall. Trends in plant science 9:534-540.
Pasternak, T., Potters, G., Caubergs, R., and Jansen, M.A. (2005a). Complementary interactions between oxidative stress and auxins control plant growth responses at plant, organ, and cellular level. Journal of experimental botany 56:1991-2001.
Pasternak, T., Rudas, V., Potters, G., and Jansen, M. (2005b). Morphogenic effects of abiotic stress: reorientation of growth in seedlings. Environmental and Experimental Botany 53:299-314.
Pazmiño, D.M., Rodriguez-Serrano, M., Romero-Puertas, M.C., Archilla-Ruiz, A., Del Rio, L.A., and Sandalio, L.M. (2011). Differential response of young and adult leaves to herbicide 2,4-dichlorophenoxyacetic acid in pea plants: role of reactive oxygen species. Plant, cell & environment 34:1874-1889.
Peer, W.A., Cheng, Y., and Murphy, A.S. (2013). Evidence of oxidative attenuation of auxin signalling. Journal of experimental botany 64:2629-2639.
Pěnčík, A., Simonovik, B., Petersson, S.V., Henykova, E., Simon, S., Greenham, K., Zhang, Y., Kowalczyk, M., Estelle, M., Zazimalova, E., et al. (2013). Regulation of auxin homeostasis and gradients in Arabidopsis roots through the formation of the indole-3-acetic acid catabolite 2-oxindole-3-acetic acid. Plant Cell 25:3858-3870.
Petrášek, J., Cerna, A., Schwarzerova, K., Elckner, M., Morris, D.A., and Zazimalova, E. (2003). Do phytotropins inhibit auxin efflux by impairing vesicle traffic? Plant physiology 131:254-263.
Petrášek, J., and Zažímalová, E. (2006). The BY-2 cell line as a tool to study auxin transport. In: Tobacco BY-2 cells: from cellular dynamics to omics: Springer. 107-117.
Pitts, R.J., Cernac, A., and Estelle, M. (1998). Auxin and ethylene promote root hair elongation in arabidopsis. The Plant Journal 16:553–560.
Potuschak, T., Lechner, E., Parmentier, Y., Yanagisawa, S., Grava, S., Koncz, C., and Genschik, P. (2003). EIN3-dependent regulation of plant ethylene hormone signaling by two Arabidopsis F box proteins: EBF1 and EBF2. Cell 115:679-689.
Qiao, H., Chang, K.N., Yazaki, J., and Ecker, J.R. (2009). Interplay between ethylene, ETP1/ETP2 F-box proteins, and degradation of EIN2 triggers ethylene responses in Arabidopsis. Gene Dev 23:512-521.
Qiao, H., Shen, Z.X., Huang, S.S.C., Schmitz, R.J., Urich, M.A., Briggs, S.P., and Ecker, J.R. (2012). Processing and Subcellular Trafficking of ER-Tethered EIN2 Control Response to Ethylene Gas. Science 338:390-393.
Rahman, A., Hosokawa, S., Oono, Y., Amakawa, T., Goto, N., and Tsurumi, S. (2002). Auxin and ethylene response interactions during Arabidopsis root hair development dissected by auxin influx modulators. Plant physiology 130:1908-1917.
Raikhel, N., and Pirrung, M. (2005). Adding precision tools to the plant biologists' toolbox with chemical genomics. Plant physiology 138:563-564.
Rakusova, H., Gallego-Bartolome, J., Vanstraelen, M., Robert, H.S., Alabadi, D., Blazquez, M.A., Benkova, E., and Friml, J. (2011). Polarization of PIN3-dependent auxin transport for hypocotyl gravitropic response in Arabidopsis thaliana. The Plant journal : for cell and molecular biology 67:817-826.
Rando, R.R. (1974). Irreversible Inhibition of Aspartate-Aminotransferase by 2-Amino-3-Butenoic-Acid Acid. Biochemistry-Us 13:3859-3863.
Rashotte, A.M., Brady, S.R., Reed, R.C., Ante, S.J., and Muday, G.K. (2000). Basipetal auxin transport is required for gravitropism in roots of arabidopsis. Plant physiology 122:481-490.

Rashotte, A.M., DeLong, A., and Muday, G.K. (2001). Genetic and chemical reductions in protein phosphatase activity alter auxin transport, gravity response, and lateral root growth. Plant Cell 13:1683-1697.
Raynes, K., Foley, M., Tilley, L., and Deady, L.W. (1996). Novel bisquinoline antimalarials: synthesis, antimalarial activity, and inhibition of haem polymerisation. Biochem Pharmacol 52:551-559.
Raz, V., and Ecker, J.R. (1999). Regulation of differential growth in the apical hook of Arabidopsis. Development 126:3661-3668.
Raz, V., and Koornneef, M. (2001). Cell division activity during apical hook development. Plant physiology 125:219-226.
Reed, R.C., Brady, S.R., and Muday, G.K. (1998). Inhibition of auxin movement from the shoot into the root inhibits lateral root development in Arabidopsis. Plant physiology 118:1369-1378.
Refregier, G., Pelletier, S., Jaillard, D., and Hofte, H. (2004). Interaction between wall deposition and cell elongation in dark-grown hypocotyl cells in Arabidopsis. Plant physiology 135:959-968.
Rigal, A., Ma, Q., and Robert, S. (2014). Unraveling plant hormone signaling through the use of small molecules. Frontiers in plant science 5:373.
Rigas, S., Ditengou, F.A., Ljung, K., Daras, G., Tietz, O., Palme, K., and Hatzopoulos, P. (2013). Root gravitropism and root hair development constitute coupled developmental responses regulated by auxin homeostasis in the Arabidopsis root apex. The New phytologist 197:1130-1141.
Robert, S., Chary, S.N., Drakakaki, G., Li, S.D., Yang, Z.B., Raikhel, N.V., and Hicks, G.R. (2008). Endosidin1 defines a compartment involved in endocytosis of the brassinosteroid receptor BRI1 and the auxin transporters PIN2 and AUX1. P Natl Acad Sci USA 105:8464-8469.
Robert, S., Kleine-Vehn, J., Barbez, E., Sauer, M., Paciorek, T., Baster, P., Vanneste, S., Zhang, J., Simon, S., Covanova, M., et al. (2010). ABP1 mediates auxin inhibition of clathrin-dependent endocytosis in Arabidopsis. Cell 143:111-121.
Robles, L.M., Deslauriers, S.D., Alvarez, A.A., and Larsen, P.B. (2012). A loss-of-function mutation in the nucleoporin AtNUP160 indicates that normal auxin signalling is required for a proper ethylene response in Arabidopsis. Journal of experimental botany 63:2231-2241.
Robles, L.M., Wampole, J.S., Christians, M.J., and Larsen, P.B. (2007). Arabidopsis enhanced ethylene response 4 encodes an EIN3-interacting TFIID transcription factor required for proper ethylene response, including ERF1 induction. Journal of experimental botany 58:2627-2639.
Rodriguespousada, R.A., Derycke, R., Dedonder, A., Vancaeneghem, W., Engler, G., Vanmontagu, M., and Vanderstraeten, D. (1993). The Arabidopsis 1-Aminocyclopropane-1-Carboxylate Synthase Gene-1 Is Expressed during Early Development. Plant Cell 5:897-911.
Rodriguez, F.I., Esch, J.J., Hall, A.E., Binder, B.M., Schaller, G.E., and Bleecker, A.B. (1999). A copper cofactor for the ethylene receptor ETR1 from Arabidopsis. Science 283:996-998.
Rogg, L.E., Lasswell, J., and Bartel, B. (2001). A gain-of-function mutation in IAA28 suppresses lateral root development. Plant Cell 13:465-480.
Rojas-Pierce, M., Titapiwatanakun, B., Sohn, E.J., Fang, F., Larive, C.K., Blakeslee, J., Cheng, Y., Cuttler, S., Peer, W.A., Murphy, A.S., et al. (2007). Arabidopsis P-glycoprotein19 participates in the inhibition of Gravitropism by gravacin. Chem Biol 14:1366-1376.
Rojas-Ruiz, F.A., Vargas-Mendez, L.Y., and Kouznetsov, V.V. (2011). Challenges and perspectives of chemical biology, a successful multidisciplinary field of natural sciences. Molecules 16:2672-2687.
ROMERO-PUERTAS, M., McCarthy, I., Gómez, M., Sandalio, L., Corpas, F., Del Rio, L., and Palma, J. (2004). Reactive oxygen species-mediated enzymatic systems involved in the oxidative action of 2, 4-dichlorophenoxyacetic acid. Plant, cell & environment 27:1135-1148.
Rothan, C., Duret, S., Chevalier, C., and Raymond, P. (1997). Suppression of ripening-associated gene expression in tomato fruits subjected to a high CO2 concentration. Plant physiology 114:255-263.
Ruegger, M., Dewey, E., Hobbie, L., Brown, D., Bernascon, P., Turner, O.J., Muday, G., and Estelle, M. (1997). Reduced Naphthylphthalamic Acid Binding in the tir3 Mutant of Arabidopsis Is Associated with a Reduction in Polar Auxin Transport and Diverse Morphological Defects. The Plant Cell 9:745-757.
Růžička, K., Ljung, K., Vanneste, S., Podhorská, R., Beeckman, T., Friml, J., and Benková, E. (2007). Ethylene regulates root growth through effects on auxin biosynthesis and transport-dependent auxin distribution. The Plant Cell 19:2197-2212.
Sabatini, S., Beis, D., Wolkenfelt, H., Murfett, J., Guilfoyle, T., Malamy, J., Benfey, P., Leyser, O., Bechtold, N., Weisbeek, P., et al. (1999). An Auxin-Dependent Distal Organizer of Pattern and Polarity in the Arabidopsis Root. Cell 99:463–472.
Sabatini, S., Heidstra, R., Wildwater, M., and Scheres, B. (2003). SCARECROW is involved in positioning the stem cell niche in the Arabidopsis root meristem. Genes Dev 17:354-358.
Sadhukhan, A., Sahoo, L., and Panda, S.K. (2012). Chemical Genomics in Plant Biology. Indian journal of biochemistry & biophysics 49:143-154.
Saftner, R.A., and Martin, M.N. (1993). Transport of 1-aminocyclopropane-1-carboxylic acid into isolated maize mesophyll vacuoles. Physiol Plantarum 87:535-543.
Saltveit, M.E. (2004). Effect of 1-methylcyclopropene on phenylpropanoid metabolism, the accumulation of phenolic compounds, and browning of whole and fresh-cut 'iceberg' lettuce. Postharvest Biol Tec 34:75-80.
Santisree, P., Nongmaithem, S., Sreelakshmi, Y., Ivanchenko, M., and Sharma, R. (2012). The root as a drill: an ethylene-auxin interaction facilitates root penetration in soil. Plant signaling & behavior 7:151-156.
Satoh, S., and Esashi, Y. (1980). Alpha-Aminoisobutyric-Acid - a Probable Competitive Inhibitor of Conversion of 1-Aminocyclopropane-1-Carboxylic Acid to Ethylene. Plant Cell Physiol 21:939-949.
Sauer, M., Robert, S., and Kleine-Vehn, J. (2013). Auxin: simply complicated. Journal of experimental botany 64:2565-2577.
Savaldi-Goldstein, S., Baiga, T.J., Pojer, F., Dabi, T., Butterfield, C., Parry, G., Santner, A., Dharmasiri, N., Tao, Y., Estelle, M., et al. (2008). New auxin analogs with growth-promoting effects in intact plants reveal a chemical strategy to improve hormone delivery. Proc Natl Acad Sci U S A 105:15190-15195.
Schneeberger, K., Ossowski, S., Lanz, C., Juul, T., Petersen, A.H., Nielsen, K.L., Jorgensen, J.E., Weigel, D., and Andersen, S.U. (2009). SHOREmap: simultaneous mapping and mutation identification by deep sequencing. Nature methods 6:550-551.
Schopfer, P. (2001). Hydroxyl radical-induced cell-wall loosening in vitro and in vivo: implications for the control of elongation growth. The Plant Journal 28:679-688.
Schopfer, P., Liszkay, A., Bechtold, M., Frahry, G., and Wagner, A. (2002). Evidence that hydroxyl radicals mediate auxin-induced extension growth. Planta 214:821-828.
Schreiber, K.J., Nasmith, C.G., Allard, G., Singh, J., Subramaniam, R., and Desveaux, D. (2011). Found in translation: high-throughput chemical screening in Arabidopsis thaliana identifies small molecules that reduce Fusarium head blight disease in wheat. Mol Plant Microbe In 24:640-648.
Schreiber, S.L. (2000). Target-oriented and diversity-oriented organic synthesis in drug discovery. Science 287:1964-1969.

Schwark, A., and Schierle, J. (1992). Interaction of Ethylene and Auxin in the Regulation of Hook Growth I The Role of Auxin in Different Growing Regions of the Hypocotyl Hook of Phaseolus vulgaris. J Plant Physiol 140:562-570.
Serrano, M., Kombrink, E., and Meesters, C. (2015). Considerations for designing chemical screening strategies in plant biology. Frontiers in plant science 6:131.
Sexton, R., Porter, A.E., Littlejohns, S., and Thain, S.C. (1995). Effects of Diazocyclopentadiene (Dacp) and Silver Thiosulfate (Sts) on Ethylene Regulated Abscission of Sweet-Pea Flowers (Lathyrus-Odoratus L). Ann Bot-London 75:337-342.
Sharma, E., Sharma, R., Borah, P., Jain, M., and Khurana, J.P. (2015). Emerging Roles of Auxin in Abiotic Stress Responses. In: Elucidation of Abiotic Stress Signaling in Plants: Springer. 299-328.
Shibaoka, H. (1994). Plant Hormone-Induced Changes in the Orientation of Cortical Microtubules: Alterations in the Cross-linking Between Microtubules and the Plasma Membrane. Annu Rev Plant Phys 45:527-544
Shivaraj, Y., Naveen, M.H., Vijayakumar, G.R., and Kumar, D.B.A. (2013). Design, Synthesis and Antibacterial Activity Studies of Novel Quinoline Carboxamide Derivatives. Journal of the Korean Chemical Society 57:241-245.
Simmons, S., Oelke, E., Wiersma, J., Lueschen, W., and Warnes, D. (1988). Spring wheat and barley responses to ethephon. Agron J 80:829-834.
Simon, S., and Petrasek, J. (2011). Why plants need more than one type of auxin. Plant science : an international journal of experimental plant biology 180:454-460.
Sisler, E. (1990). Ethylene-binding receptors: is there more than one? In: Plant growth substances 1988--Pharis RP, R.S., ed.: Springer. 192–200.
Sisler, E.C. (2006). The discovery and development of compounds counteracting ethylene at the receptor level. Biotechnol Adv 24:357-367.
Sisler, E.C., Blankenship, S.M., and Guest, M. (1990). Competition of Cyclooctenes and Cyclooctadienes for Ethylene Binding and Activity in Plants. Plant Growth Regul 9:157-164.
Sisler, E.C., and Serek, M. (1997). Inhibitors of ethylene responses in plants at the receptor level: Recent developments. Physiol Plantarum 100:577-582.
Skottke, K.R., Yoon, G.M., Kieber, J.J., and DeLong, A. (2011). Protein phosphatase 2A controls ethylene biosynthesis by differentially regulating the turnover of ACC synthase isoforms. PLoS genetics 7:e1001370.
Smalle, J., Haegman, M., Kurepa, J., VanMontagu, M., and VanderStraeten, D. (1997). Ethylene can stimulate Arabidopsis hypocotyl elongation in the light. P Natl Acad Sci USA 94:2756-2761.
Smet, D., Žádníková, P., Vandenbussche, F., Benková, E., and Van Der Straeten, D. (2014). Dynamic infrared imaging analysis of apical hook development in Arabidopsis: the case of brassinosteroids. New Phytologist 202:1398-1411.
Soeno, K., Goda, H., Ishii, T., Ogura, T., Tachikawa, T., Sasaki, E., Yoshida, S., Fujioka, S., Asami, T., and Shimada, Y. (2010). Auxin biosynthesis inhibitors, identified by a genomics-based approach, provide insights into auxin biosynthesis. Plant Cell Physiol 51:524-536.
Spartz, A.K., Lee, S.H., Wenger, J.P., Gonzalez, N., Itoh, H., Inze, D., Peer, W.A., Murphy, A.S., Overvoorde, P.J., and Gray, W.M. (2012). The SAUR19 subfamily of SMALL AUXIN UP RNA genes promote cell expansion. The Plant journal : for cell and molecular biology.
Staswick, P.E. (2009). The tryptophan conjugates of jasmonic and indole-3-acetic acids are endogenous auxin inhibitors. Plant physiology 150:1310-1321.
Staswick, P.E., and Tiryaki, I. (2004). The oxylipin signal jasmonic acid is activated by an enzyme that conjugates it to isoleucine in Arabidopsis. The Plant Cell 16:2117-2127.
Steen, D.A., and Chadwick, A.V. (1981). Ethylene effects in Pea stem tissue. Plant Physiol. 67:460-466.
Stepanova, A.N., Hoyt, J.M., Hamilton, A.A., and Alonso, J.M. (2005a). A Link between ethylene and auxin uncovered by the characterization of two root-specific ethylene-insensitive mutants in Arabidopsis. Plant Cell 17:2230-2242.
Stepanova, A.N., Robertson-Hoyt, J., Yun, J., Benavente, L.M., Xie, D.Y., DoleZal, K., Schlereth, A., Jurgens, G., and Alonso, J.M. (2008). TAA1-mediated auxin biosynthesis is essential for hormone crosstalk and plant development. Cell 133:177-191.
Stepanova, A.N., Yun, J., Likhacheva, A.V., and Alonso, J.M. (2007). Multilevel interactions between ethylene and auxin in Arabidopsis roots. The Plant Cell 19:2169-2185.
Stepanova, A.N., Yun, J., Robles, L.M., Novak, O., He, W., Guo, H., Ljung, K., and Alonso, J.M. (2011). The Arabidopsis YUCCA1 flavin monooxygenase functions in the indole-3-pyruvic acid branch of auxin biosynthesis. Plant Cell 23:3961-3973.
Stockwell, B.R. (2000). Chemical genetics: ligand-based discovery of gene function. Nature reviews. Genetics 1:116-125.
Strader, L.C., and Bartel, B. (2011). Transport and metabolism of the endogenous auxin precursor indole-3-butyric acid. Molecular plant 4:477-486.
Strader, L.C., Beisner, E.R., and Bartel, B. (2009). Silver Ions Increase Auxin Efflux Independently of Effects on Ethylene Response. The Plant Cell Online 21:3585-3590.
Strader, L.C., Chen, G.L., and Bartel, B. (2010). Ethylene directs auxin to control root cell expansion. The Plant journal : for cell and molecular biology 64:874-884.
Sugawara, S., Hishiyama, S., Jikumaru, Y., Hanada, A., Nishimura, T., Koshiba, T., Zhao, Y., Kamiya, Y., and Kasahara, H. (2009). Biochemical analyses of indole-3-acetaldoxime-dependent auxin biosynthesis in Arabidopsis. Proc Natl Acad Sci U S A 106:5430-5435.
Sukumar, P., Edwards, K.S., Rahman, A., Delong, A., and Muday, G.K. (2009). PINOID kinase regulates root gravitropism through modulation of PIN2-dependent basipetal auxin transport in Arabidopsis. Plant physiology 150:722-735.
Surpin, M., Rojas-Pierce, M., Carter, C., Hicks, G.R., Vasquez, J., and Raikhel, N.V. (2005). The power of chemical genomics to study the link between endomembrane system components and the gravitropic response. Proc Natl Acad Sci U S A 102:4902-4907.
Suttle, J.C. (1988). Effect of Ethylene Treatment on Polar IAA Transport, Net IAA Uptake and Specific Binding of N-1-Naphthylphthalamic Acid in Tissues and Microsomes Isolated from Etiolated Pea Epicotyls. Plant Physiol. 88:795–799.
Suzumori, N., Burns, K.H., Yan, W., and Matzuk, M.M. (2003). RFPL4 interacts with oocyte proteins of the ubiquitin-proteasome degradation pathway. Proc Natl Acad Sci U S A 100:550-555.
Swarup, K., Benkova, E., Swarup, R., Casimiro, I., Peret, B., Yang, Y., Parry, G., Nielsen, E., De Smet, I., Vanneste, S., et al. (2008). The auxin influx carrier LAX3 promotes lateral root emergence. Nature cell biology 10:946-954.
Swarup, R., Friml, J., Marchant, A., Ljung, K., Sandberg, G., Palme, K., and Bennett, M. (2001). Localization of the auxin permease AUX1 suggests two functionally distinct hormone transport pathways operate in the Arabidopsis root apex. Genes Dev 15:2648-2653.
Swarup, R., Perry, P., Hagenbeek, D., Van Der Straeten, D., Beemster, G.T., Sandberg, G., Bhalerao, R., Ljung, K., and Bennett, M.J. (2007). Ethylene upregulates auxin biosynthesis in Arabidopsis seedlings to enhance inhibition of root cell elongation. The Plant cell 19:2186-2196.
Szyjewicz, E., Rosner, N., and Kliewer, W.M. (1984). Ethephon ((2-Chloroethyl)Phosphonic Acid, Ethrel, Cepa) in Viticulture - a Review. Am J Enol Viticult 35:117-123.

Takahashi, F., Yoshida, R., Ichimura, K., Mizoguchi, T., Seo, S., Yonezawa, M., Maruyama, K., Yamaguchi-Shinozaki, K., and Shinozaki, K. (2007). The mitogen-activated protein kinase cascade MKK3-MPK6 is an important part of the jasmonate signal transduction pathway in Arabidopsis. Plant Cell 19:805-818.
Tam, Y.Y., Epstein, E., and Normanly, J. (2000). Characterization of auxin conjugates in Arabidopsis. Low steady-state levels of indole-3-acetyl-aspartate, indole-3-acetyl-glutamate, and indole-3-acetyl-glucose. Plant physiology 123:589-596.
Tan, X., Calderon-Villalobos, L.I.A., Sharon, M., Zheng, C.X., Robinson, C.V., Estelle, M., and Zheng, N. (2007). Mechanism of auxin perception by the TIR1 ubiquitin ligase. Nature 446:640-645.
Tanimoto, M., Roberts, K., and Dolan, L. (1995). Ethylene is a positive regulator of root hair development in Arabidopsis thaliana. The Plant journal : for cell and molecular biology 8:943-948.
Tao, Y., Ferrer, J.-L., Ljung, K., Pojer, F., Hong, F., Long, J.A., Li, L., Moreno, J.E., Bowman, M.E., Ivans, L.J., et al. (2008). Rapid synthesis of auxin via a new tryptophan-dependent pathway is required for shade avoidance in plants. Cell 133:164–176.
Tatematsu, K., Kumagai, S., Muto, H., Sato, A., Watahiki, M.K., Harper, R.M., Liscum, E., and Yamamoto, K.T. (2004). MASSUGU2 encodes Aux/IAA19, an auxin-regulated protein that functions together with the transcriptional activator NPH4/ARF7 to regulate differential growth responses of hypocotyl and formation of lateral roots in Arabidopsis thaliana. Plant Cell 16:379-393.
Thomson, K.-S., Hertel, R., Müller, S., and Tavares, J.E. (1973). 1-N-naphthylphthalamic acid and 2, 3, 5-triiodobenzoic acid. Planta 109:337-352.
Tian, Q., and Reed, J.W. (1999). Control of auxin-regulated root development by the Arabidopsis thaliana SHY2/IAA3 gene. Development 126:711-721.
Timpte, C., Lincoln, C., Pickett, F.B., Turner, J., and Estelle, M. (1995). The AXR1 and AUX1 genes of Arabidopsis function in separate auxin-response pathways. The Plant journal : for cell and molecular biology 8:561-569.
Titapiwatanakun, B., Blakeslee, J.J., Bandyopadhyay, A., Yang, H., Mravec, J., Sauer, M., Cheng, Y., Adamec, J., Nagashima, A., Geisler, M., et al. (2009). ABCB19/PGP19 stabilises PIN1 in membrane microdomains in Arabidopsis. The Plant journal : for cell and molecular biology 57:27-44.
Tivendale, N.D., Davies, N.W., Molesworth, P.P., Davidson, S.E., Smith, J.A., Lowe, E.K., Reid, J.B., and Ross, J.J. (2010). Reassessing the role of N-hydroxytryptamine in auxin biosynthesis. Plant physiology 154:1957-1965.
Tivendale, N.D., Ross, J.J., and Cohen, J.D. (2014). The shifting paradigms of auxin biosynthesis. Trends in plant science 19:44-51.
Tognetti, V.B., Muhlenbock, P., and Van Breusegem, F. (2012). Stress homeostasis - the redox and auxin perspective. Plant, cell & environment 35:321-333.
Tognolli, M., Penel, C., Greppin, H., and Simon, P. (2002). Analysis and expression of the class III peroxidase large gene family in Arabidopsis thaliana. Gene 288:129-138.
Torres, M.A., Dangl, J.L., and Jones, J.D. (2002). Arabidopsis gp91phox homologues AtrbohD and AtrbohF are required for accumulation of reactive oxygen intermediates in the plant defense response. Proc Natl Acad Sci U S A 99:517-522.
Toth, R., and van der Hoorn, R.A. (2010). Emerging principles in plant chemical genetics. Trends Plant Sci 15:81-88.
Tripathi, S.K., and Tuteja, N. (2007). Integrated signaling in flower senescence: an overview. Plant signaling & behavior 2:437-445.
Tsang, D.L., Edmond, C., Harrington, J.L., and Nuhse, T.S. (2011). Cell wall integrity controls root elongation via a general 1-aminocyclopropane-1-carboxylic acid-dependent, ethylene-independent pathway. Plant physiology 156:596-604.
Tsuchisaka, A., and Theologis, A. (2004). Unique and overlapping expression patterns among the Arabidopsis 1-amino-cyclopropane-1-carboxylate synthase gene family members. Plant physiology 136:2982-3000.
Tsuchisaka, A., Yu, G., Jin, H., Alonso, J.M., Ecker, J.R., Zhang, X., Gao, S., and Theologis, A. (2009). A Combinatorial Interplay Among the 1-Aminocyclopropane-1-Carboxylate Isoforms Regulates Ethylene Biosynthesis in Arabidopsis thaliana. Genetics 183:979-1003.
Tsuchiya, Y., Vidaurre, D., Toh, S., Hanada, A., Nambara, E., Kamiya, Y., Yamaguchi, S., and McCourt, P. (2010). A small-molecule screen identifies new functions for the plant hormone strigolactone. Nature chemical biology 6:741-749.
Tsukagoshi, H. (2012). Defective root growth triggered by oxidative stress is controlled through the expression of cell cycle-related genes. Plant science : an international journal of experimental plant biology 197:30-39.
Tsukagoshi, H., Busch, W., and Benfey, P.N. (2010). Transcriptional regulation of ROS controls transition from proliferation to differentiation in the root. Cell 143:606-616.
Tucker, Mark, and Chi-Kuang Wen. "Research Tool: Ethylene Preparation: Treatment with Ethylene and Its Replacements." Ethylene in Plants. Springer Netherlands, 2015. 245-261.
Tyburski, J., Krzemiński, Ł., and Tretyn, A. (2007). Exogenous auxin affects ascorbate metabolism in roots of tomato seedlings. Plant Growth Regul 54:203-215.
Ulmasov, T., Hagen, G., and Guilfoyle, T.J. (1997a). ARF1, a transcription factor that binds to auxin response elements. Science 276:1865-1868.
Ulmasov, T., Hagen, G., and Guilfoyle, T.J. (1997b). AuxREs and AuxRE transcription factors: a model for auxin-responsive gene expression. Plant physiology 114:1255-1255.
Ulmasov, T., Murfett, J., Hagen, G., and Guilfoyle, T.J. (1997c). Aux/IAA proteins repress expression of reporter genes containing natural and highly active synthetic auxin response elements. Plant Cell 9:1963-1971.
Van de Poel, B., Smet, D., and Van Der Straeten, D. (2015). Ethylene and Hormonal Cross Talk in Vegetative Growth and Development. Plant Physiol 169:61-72.
Van de Poel, B., and Van Der Straeten, D. (2014). 1-aminocyclopropane-1-carboxylic acid (ACC) in plants: more than just the precursor of ethylene! Frontiers in plant science 5:640.
Van Der Straeten, D., Djudzman, A., Vancaeneghem, W., Smalle, J., and Vanmontagu, M. (1993). Genetic and Physiological Analysis of a New Locus in Arabidopsis That Confers Resistance to 1-Aminocyclopropane-1-Carboxylic Acid and Ethylene and Specifically Affects the Ethylene Signal-Transduction Pathway. Plant physiology 102:401-408.
Vandenbussche, F., Callebert, P., Zadnikova, P., Benkova, E., and Van Der Straeten, D. (2013). Brassinosteroid control of shoot gravitropism interacts with ethylene and depends on auxin signaling components. American journal of botany 100:215-225.
Vandenbussche, F., Petrasek, J., Zadnikova, P., Hoyerova, K., Pesek, B., Raz, V., Swarup, R., Bennett, M., Zazimalova, E., Benkova, E., et al. (2010). The auxin influx carriers AUX1 and LAX3 are involved in auxin-ethylene interactions during apical hook development in Arabidopsis thaliana seedlings. Development 137:597-606.
Vandenbussche, F., Suslov, D., De Grauwe, L., Leroux, O., Vissenberg, K., and Van Der Straeten, D. (2011). The Role of Brassinosteroids in Shoot Gravitropism. Plant physiology 156:1331-1336.
Vandenbussche, F., Smalle, J., Le, J., Saibo, N.J.M., De Paepe, A., Chaerle, L., Tietz, O., Smets, R., Laarhoven, L.J.J., Harren, F.J.M., et al. (2003). The Arabidopsis mutant alh1 illustrates a cross talk between ethylene and auxin. Plant physiology 131:1228-1238.
Vandenbussche, F., Vaseva, I., Vissenberg, K., and Van Der Straeten, D. (2012). Ethylene in vegetative development: a tale with a riddle. The New phytologist.
Vanneste, S., and Friml, J. (2009). Auxin: a trigger for change in plant development. Cell 136:1005-1016.

Vatulescu, A.D., Fortunato, A.S., Sa, M.C., Amancio, S., Ricardo, C.P., and Jackson, P.A. (2004). Cloning and characterisation of a basic IAA oxidase associated with root induction in Vitis vinifera. Plant physiology and biochemistry : PPB / Societe francaise de physiologie vegetale 42:609-615.
Verbelen, J.P., De Cnodder, T., Le, J., Vissenberg, K., and Baluska, F. (2006). The Root Apex of Arabidopsis thaliana Consists of Four Distinct Zones of Growth Activities: Meristematic Zone, Transition Zone, Fast Elongation Zone and Growth Terminating Zone. Plant signaling & behavior 1:296-304.
Vernoux, T., Brunoud, G., Farcot, E., Morin, V., Van den Daele, H., Legrand, J., Oliva, M., Das, P., Larrieu, A., Wells, D., et al. (2011). The auxin signalling network translates dynamic input into robust patterning at the shoot apex. Molecular systems biology 7:508.
Vernoux, T., Wilson, R.C., Seeley, K.A., Reichheld, J.-P., Muroy, S., Brown, S., Maughan, S.C., Cobbett, C.S., Montagu, M.V., Inzé, D., et al. (2000). The ROOT MERISTEMLESS1/CADMIUM SENSITIVE2 Gene Defines a Glutathione-Dependent Pathway Involved in Initiation and Maintenance of Cell Division during Postembryonic Root Development. The Plant Cell 12:97-110.
Vieten, A., Vanneste, S., Wisniewska, J., Benkova, E., Benjamins, R., Beeckman, T., Luschnig, C., and Friml, J. (2005). Functional redundancy of PIN proteins is accompanied by auxin-dependent cross-regulation of PIN expression. Development 132:4521-4531.
Vogel, J.P., Woeste, K.E., Theologis, A., and Kieber, J.J. (1998). Recessive and dominant mutations in the ethylene biosynthetic gene ACS5 of Arabidopsis confer cytokinin insensitivity and ethylene overproduction, respectively. Proc Natl Acad Sci U S A 95:4766-4771.
Walsh, D.P., and Chang, Y.T. (2006). Chemical genetics. Chemical reviews 106:2476-2530.
Walsh, T.A. (2007). The emerging field of chemical genetics: potential applications for pesticide discovery. Pest management science 63:1165-1171.
Walsh, T.A., Neal, R., Merlo, A.O., Honma, M., Hicks, G.R., Wolff, K., Matsumura, W., and Davies, J.P. (2006). Mutations in an auxin receptor homolog AFB5 and in SGT1b confer resistance to synthetic picolinate auxins and not to 2,4-dichlorophenoxyacetic acid or indole-3-acetic acid in arabidopsis. Plant physiology 142:542-552.
Wang, K.L., Yoshida, H., Lurin, C., and Ecker, J.R. (2004a). Regulation of ethylene gas biosynthesis by the Arabidopsis ETO1 protein. Nature 428:945-950.
Wang, R., and Estelle, M. (2014). Diversity and specificity: auxin perception and signaling through the TIR1/AFB pathway. Current opinion in plant biology 21C:51-58.
Wang, S., Sim, T.B., Kim, Y.S., and Chang, Y.T. (2004b). Tools for target identification and validation. Curr Opin Chem Biol 8:371-377.
Wang, W.Y., Esch, J.J., Shiu, S.H., Agula, H., Binder, B.M., Chang, C., Patterson, S.E., and Bleecker, A.B. (2006). Identification of important regions for ethylene binding and signaling in the transmembrane domain of the ETR1 ethylene receptor of Arabidopsis. Plant Cell 18:3429-3442.
Wang, Z.Y., Nakano, T., Gendron, J., He, J., Chen, M., Vafeados, D., Yang, Y., Fujioka, S., Yoshida, S., Asami, T., et al. (2002). Nuclear-localized BZR1 mediates brassinosteroid-induced growth and feedback suppression of brassinosteroid biosynthesis. Dev Cell 2:505-513.
War, A.R., Paulraj, M.G., War, M.Y., and Ignacimuthu, S. (2011). Role of salicylic acid in induction of plant defense system in chickpea (Cicer arietinum L.). Plant signaling & behavior 6:1787-1792.
Wasteneys, G.O. (2004). Progress in understanding the role of microtubules in plant cells. Current opinion in plant biology 7:651-660.
Weigel, D., and Glazebrook, J. (2008). Genetic analysis of Arabidopsis mutants. CSH protocols 2008:pdb top35.
Wend, S., Dal Bosco, C., Kampf, M.M., Ren, F., Palme, K., Weber, W., Dovzhenko, A., and Zurbriggen, M.D. (2013). A quantitative ratiometric sensor for time-resolved analysis of auxin dynamics. Scientific reports 3:2052.
Went, F.W., and Thimann, K.V. (1937). Phytohormones. New York: The Macmillan Company.
Williams, M. (2010). Introduction to phytohormones. The Plant Cell 22:1-9.
Willige, B.C., Ogiso-Tanaka, E., Zourelidou, M., and Schwechheimer, C. (2012). WAG2 represses apical hook opening downstream from gibberellin and PHYTOCHROME INTERACTING FACTOR 5. Development 139:4020-4028.
Wilson, A.K., Pickett, F.B., Turner, J.C., and Estelle, M. (1990). A dominant mutation in Arabidopsis confers resistance to auxin, ethylene and abscisic acid. Molecular & general genetics : MGG 222:377-383.
Woeste, K.E., Ye, C., and Kieber, J.J. (1999). Two Arabidopsis Mutants That Overproduce Ethylene Are Affected in the Posttranscriptional Regulation of 1-Aminocyclopropane-1-Carboxylic Acid Synthase. Plant physiology 119:521–530.
Won, C., Shen, X., Mashiguchi, K., Zheng, Z., Dai, X., Cheng, Y., Kasahara, H., Kamiya, Y., Chory, J., and Zhao, Y. (2011). Conversion of tryptophan to indole-3-acetic acid by TRYPTOPHAN AMINOTRANSFERASES OF ARABIDOPSIS and YUCCAs in Arabidopsis. Proc Natl Acad Sci U S A 108:18518-18523.
Wu, G., Cameron, J.N., Ljung, K., and Spalding, E.P. (2010). A role for ABCB19-mediated polar auxin transport in seedling photomorphogenesis mediated by cryptochrome 1 and phytochrome B. The Plant journal : for cell and molecular biology 62:179-191.
Xie, D.X., Feys, B.F., James, S., Nieto-Rostro, M., and Turner, J.G. (1998). COI1: an Arabidopsis gene required for jasmonate-regulated defense and fertility. Science 280:1091-1094.
Xu, S.L., Rahman, A., Baskin, T.I., and Kieber, J.J. (2008). Two leucine-rich repeat receptor kinases mediate signaling, linking cell wall biosynthesis and ACC synthase in Arabidopsis. Plant Cell 20:3065-3079.
Yamaguchi-Shinozaki, K., and Shinozaki, K. (1994). A novel cis-acting element in an Arabidopsis gene is involved in responsiveness to drought, low-temperature, or high-salt stress. Plant Cell 6:251-264.
Yang, C., Lu, X., Ma, B., Chen, S.Y., and Zhang, J.S. (2015). Ethylene signaling in rice and Arabidopsis: conserved and diverged aspects. Molecular plant 8:495-505.
Yang, H., and Murphy, A.S. (2009). Functional expression and characterization of Arabidopsis ABCB, AUX 1 and PIN auxin transporters in Schizosaccharomyces pombe. The Plant journal : for cell and molecular biology 59:179-191.
Yang, S., and Hoffman, N. (1984). Ethylene Biosynthesis and its Regulation in Higher Plants. Annu Rev Plant Physiol 35:155-189.
Yang, X., Lee, S., So, J.H., Dharmasiri, S., Dharmasiri, N., Ge, L., Jensen, C., Hangarter, R., Hobbie, L., and Estelle, M. (2004). The IAA1 protein is encoded by AXR5 and is a substrate of SCF(TIR1). The Plant journal : for cell and molecular biology 40:772-782.
Yang, Y., Hammes, U.Z., Taylor, C.G., Schachtman, D.P., and Nielsen, E. (2006). High-affinity auxin transport by the AUX1 influx carrier protein. Current biology : CB 16:1123-1127.
Yu, Y., Wang, J., Zhang, Z., Quan, R., Zhang, H., Deng, X.W., Ma, L., and Huang, R. (2013). Ethylene promotes hypocotyl growth and HY5 degradation by enhancing the movement of COP1 to the nucleus in the light. PLoS genetics 9:e1004025.
Zadnikova, P., Petrasek, J., Marhavy, P., Raz, V., Vandenbussche, F., Ding, Z.J., Schwarzerova, K., Morita, M.T., Tasaka, M., Hejatko, J., et al. (2010). Role of PIN-mediated auxin efflux in apical hook development of Arabidopsis thaliana. Development 137:607-617.
Zadnikova, P., Smet, D., Zhu, Q., Van Der Straeten, D., and Benkova, E. (2015). Strategies of seedlings to overcome their sessile nature: auxin in mobility control. Frontiers in plant science 6:218.
Zažímalová, E., Petrasek, J., and Benková, E. (2014). Auxin and its role in plant development: Springer.

Zhang, C., Brown, M.Q., van de Ven, W., Zhang, Z.M., Wu, B., Young, M.C., Synek, L., Borchardt, D., Harrison, R., Pan, S., et al. (2015). Endosidin2 targets conserved exocyst complex subunit EXO70 to inhibit exocytosis. Proc Natl Acad Sci U S A.
Zhao, X.C., Qu, X., Mathews, D.E., and Schaller, G.E. (2002a). Effect of ethylene pathway mutations upon expression of the ethylene receptor ETR1 from Arabidopsis. Plant physiology 130:1983-1991.
Zhao, Y. (2010). Auxin biosynthesis and its role in plant development. Annual review of plant biology 61:49-64.
Zhao, Y. (2012). A chemical genetics method to uncover small molecules for dissecting the mechanism of ABA responses in Arabidopsis seed germination. Methods in molecular biology 876:107-116.
Zhao, Y. (2014). Auxin biosynthesis. The Arabidopsis book / American Society of Plant Biologists 12:e0173.
Zhao, Y., Christensen, S.K., Fankhauser, C., Cashman, J.R., Cohen, J.D., Weigel, D., and Chory, J. (2001). A role for flavin monooxygenase-like enzymes in auxin biosynthesis. Science 291:306-309.
Zhao, Y., Dai, X., Blackwell, H.E., Schreiber, S.L., and Chory, J. (2003). SIR1, an upstream component in auxin signaling identified by chemical genetics. Science 301:1107-1110.
Zhao, Y., Hull, A.K., Gupta, N.R., Goss, K.A., Alonso, J., Ecker, J.R., Normanly, J., Chory, J., and Celenza, J.L. (2002b). Trp-dependent auxin biosynthesis in Arabidopsis: involvement of cytochrome P450s CYP79B2 and CYP79B3. Genes Dev 16:3100-3112.
Zhao, Z., Andersen, S.U., Ljung, K., Dolezal, K., Miotk, A., Schultheiss, S.J., and Lohmann, J.U. (2010). Hormonal control of the shoot stem-cell niche. Nature 465:1089-U1154.
Zheng, X.S., Chan, T.-F., and Zhou, H.H. (2004). Genetic and genomic approaches to identify and study the targets of bioactive small molecules. Chem Biol 11:609-618.
Zheng, Y., and Zhu, Z. (2016). Relaying the Ethylene Signal: New Roles for EIN2. Trends in plant science 21:2-4.
Zheng, Z., Guo, Y., Novak, O., Dai, X., Zhao, Y., Ljung, K., Noel, J.P., and Chory, J. (2013). Coordination of auxin and ethylene biosynthesis by the aminotransferase VAS1. Nat Chem Biol 9:244-246.
Zhong, S., Shi, H., Xue, C., Wang, L., Xi, Y., Li, J., Quail, P.H., Deng, X.W., and Guo, H. (2012). A molecular framework of light-controlled phytohormone action in Arabidopsis. Current biology : CB 22:1530-1535.
Zolman, B.K., Yoder, A., and Bartel, B. (2000). Genetic analysis of indole-3-butyric acid responses in Arabidopsis thaliana reveals four mutant classes. Genetics 156:1323-1337.

Acknowledgement

At the end, I would like to express my gratitude to all the people who have helped me going through these years. Only with so much love and support, I could be brave enough to explore the scientific world step by step and finally end up with this thesis.

Throughout my PhD study, my first and utmost gratitude goes to the irreplaceable person, my promotor and supervisor: Prof. Van Der Straeten. I would like to thanks for all you have done for me over all these years, spending great efforts on my thesis even in your difficult situations. Without you, I cannot complete this task. I really have learnt a lot from you, not only in scientific world, but also in life, to face difficulties, to enjoy being a great mother and a daughter.

My greatest gratitude goes to my promotor and daily supervisor Prof. Vandenbussche. You are the person I spent the most time with during these four years living in Gent, even more than with my family. Thanks for your continuous guidance and encouragement throughout the up-and-down moments during my work and life. Moreover, I am really enjoying the family time with Carolina and your three adorable boys. Also I am thankful to Carolina for the help in my study.

To Prof. De Jaeger, Dr. Dominique Audenaert, Prof. Kris Audenaert, Prof. Cammue, Prof. Cuypers and Prof. Petrášek, it is my pleasure having you in my exam committee. Thanks a lot for your time. Your thoughtful comments gave me a lot of inspiration not only on this thesis, but also for my future career. To Dominique Audenaert, thank you very much for all the help when starting this project. Thanks a lot to Jan for all the discussion and efforts on the auxin aspect, which leads to crucial results for this study. Thanks Ann for the important comments on the oxidative stress.

A great deal of gratitude is owed to the external collaborators participating in this study: Long Nguyen from VIB in setting up the primary screening; Ilse Vandemoortel and Luc Verschraegen from Information and Communication Technology Department in creating the TR-DB website; Klara Hoyerova and Petr Klíma from Institute of Experimental Botany AS CR, v. v. i., Czech Republic in auxin assays; Kris Morreel and Wout Boerjan from VIB in performing metabolite profiling experiments; Dieter Buyst, Tim Courtin and José Martins from Department of Organic chemistry in NMR analysis; Sean Cutler from plant cell biology at the University of California, Riverside, Hana Rakusova and Jiri Friml from VIB in providing essential materials; Annemieke Madder and Johan Winne from Organic and Biomimetic Chemistry in suggestions on the organic compounds. I also enjoy precipitating in the project of rosette tracker with Jonas De Vylder; and with Amanda Rasmussen and Danny Geelen for their project.

I am so lucky having Magdalena, Dajo and Thomas joining in the project in the last stage of my study. They really gave the project great advance. Thomas will continue working on this topic. I believe with his intelligence and hard work, the action of (more) mysterious compounds will be identified. Thanks a lot to Pieter for the help from different aspects in addition to the project these years. Thanks Katrien and Mathias for the assistance in ethylene measurement for the project of Amanda, and for sure, much more. Thanks Griet for the recent help.

There are a lot of personal help from people cannot be neglected. Thanks Dieter for being in front over the years. Thanks Nuria, Vera, Jolien, Oana and Irina for being there all the time. It means a lot to me. Also to the people have been far away but will have lifelong connection: Yunlong, Qiang, Oscar, Liesbeth, Enas, Mike, Sabine, Bart…

Thanks to the friends I met in Gent: Jing, Ping, Yingjie, Ying, Yanlu, Wenjing, Chuan, Yueqi, Chenjing, Jisheng, Honghui, Kai, Yuanyuan, Xu, Kun, Lingxiang, Inês, Baldric… There are still many people not listed here, but will be remembered. I have been away from home for almost 12 years, I am also very thankful for the friends I met in Wageningen, Davis and Leiden.

Last but not least, thanks to my family, especially to my parents for their endless love. I have been so proud of them since childhood. Now, I am thankful for being a mom.